ISSN 1007-9327 (print)
ISSN 2219-2840 (online)

World Journal of *Gastroenterology*

World J Gastroenterol 2022 June 28; 28(24): 2636-2781

Published by Baishideng Publishing Group Inc

World Journal of Gastroenterology

Contents

Weekly Volume 28 Number 24 June 28, 2022

REVIEW

MINIREVIEWS

ORIGINAL ARTICLE

Basic Study

Clinical and Translational Research

Retrospective Cohort Study

Retrospective Study

Observational Study

LETTER TO THE EDITOR

ABOUT COVER

Editorial Board Member of *World Journal of Gastroenterology*, Vasiliy Ivanovich Reshetnyak, DSc, MD, Full Professor, Department of Propaedeutic of Internal Diseases and Gastroenterology, A.I. Yevdokimov Moscow State University of Medicine and Dentistry, p. 1, 20 Delegatskaya Street, Moscow 127473, Russia. vasiliy.reshetnyak@yandex.ru

AIMS AND SCOPE

The primary aim of *World Journal of Gastroenterology* (*WJG*, *World J Gastroenterol*) is to provide scholars and readers from various fields of gastroenterology and hepatology with a platform to publish high-quality basic and clinical research articles and communicate their research findings online. *WJG* mainly publishes articles reporting research results and findings obtained in the field of gastroenterology and hepatology and covering a wide range of topics including gastroenterology, hepatology, gastrointestinal endoscopy, gastrointestinal surgery, gastrointestinal oncology, and pediatric gastroenterology.

INDEXING/ABSTRACTING

The *WJG* is now indexed in Current Contents®/Clinical Medicine, Science Citation Index Expanded (also known as SciSearch®), Journal Citation Reports®, Index Medicus, MEDLINE, PubMed, PubMed Central, and Scopus. The 2021 edition of Journal Citation Report® cites the 2020 impact factor (IF) for *WJG* as 5.742; Journal Citation Indicator: 0.79; IF without journal self cites: 5.590; 5-year IF: 5.044; Ranking: 28 among 92 journals in gastroenterology and hepatology; and Quartile category: Q2. The *WJG*'s CiteScore for 2020 is 6.9 and Scopus CiteScore rank 2020: Gastroenterology is 19/136.

RESPONSIBLE EDITORS FOR THIS ISSUE

Production Editor: *Yu-Xi Chen*; **Production Department Director:** *Xu Guo*; **Editorial Office Director:** *Ze-Mao Gong*.

NAME OF JOURNAL
World Journal of Gastroenterology

ISSN
ISSN 1007-9327 (print) ISSN 2219-2840 (online)

LAUNCH DATE
October 1, 1995

FREQUENCY
Weekly

EDITORS-IN-CHIEF
Andrzej S Tarnawski

EDITORIAL BOARD MEMBERS
http://www.wjgnet.com/1007-9327/editorialboard.htm

PUBLICATION DATE
June 28, 2022

INSTRUCTIONS TO AUTHORS
https://www.wjgnet.com/bpg/gerinfo/204

GUIDELINES FOR ETHICS DOCUMENTS
https://www.wjgnet.com/bpg/GerInfo/287

GUIDELINES FOR NON-NATIVE SPEAKERS OF ENGLISH
https://www.wjgnet.com/bpg/gerinfo/240

PUBLICATION ETHICS
https://www.wjgnet.com/bpg/GerInfo/288

PUBLICATION MISCONDUCT
https://www.wjgnet.com/bpg/gerinfo/208

ARTICLE PROCESSING CHARGE
https://www.wjgnet.com/bpg/gerinfo/242

STEPS FOR SUBMITTING MANUSCRIPTS
https://www.wjgnet.com/bpg/GerInfo/239

ONLINE SUBMISSION
https://www.f6publishing.com

World Journal of Gastroenterology

Submit a Manuscript: https://www.f6publishing.com

World J Gastroenterol 2022 June 28; 28(24): 2636-2653

DOI: 10.3748/wjg.v28.i24.2636

ISSN 1007-9327 (print) ISSN 2219-2840 (online)

REVIEW

Patient-derived organoids for therapy personalization in inflammatory bowel diseases

Marianna Lucafò, Antonella Muzzo, Martina Marcuzzi, Lorenzo Giorio, Giuliana Decorti, Gabriele Stocco

Specialty type: Gastroenterology and hepatology

Provenance and peer review: Invited article; Externally peer reviewed.

Peer-review model: Single blind

Peer-review report's scientific quality classification

Grade A (Excellent): A, A
Grade B (Very good): 0
Grade C (Good): 0
Grade D (Fair): 0
Grade E (Poor): 0

P-Reviewer: Liu DY, China; Zhang Y, China
A-Editor: Maslennikov R

Received: January 17, 2022
Peer-review started: January 17, 2022
First decision: March 8, 2022
Revised: March 21, 2022
Accepted: May 17, 2022
Article in press: May 17, 2022
Published online: June 28, 2022

Marianna Lucafò, Giuliana Decorti, Gabriele Stocco, Advanced Translational Diagnostics Laboratory, Institute for Maternal and Child Health-IRCCS "Burlo Garofolo", Trieste 34137, Italy

Antonella Muzzo, Giuliana Decorti, Department of Medicine, Surgery and Health Sciences, University of Trieste, Trieste 34127, Italy

Martina Marcuzzi, Lorenzo Giorio, Gabriele Stocco, Department of Life Sciences, University of Trieste, Trieste 34127, Italy

Corresponding author: Giuliana Decorti, MD, Associated Professor, Advanced Translational Diagnostics Laboratory, Institute for Maternal and Child Health-IRCCS "Burlo Garofolo", Via dell'Istria 65/1, Trieste 34137, Italy. giuliana.decorti@burlo.trieste.it

Abstract

Inflammatory bowel diseases (IBDs) are chronic inflammatory disorders of the intestinal tract that have emerged as a growing problem in industrialized countries. Knowledge of IBD pathogenesis is still incomplete, and the most widely-accepted interpretation considers genetic factors, environmental stimuli, uncontrolled immune responses and altered intestinal microbiota composition as determinants of IBD, leading to dysfunction of the intestinal epithelial functions. *In vitro* models commonly used to study the intestinal barrier do not fully reflect the proper intestinal architecture. An important innovation is represented by organoids, 3D *in vitro* cell structures derived from stem cells that can self-organize into functional organ-specific structures. Organoids may be generated from induced pluripotent stem cells or adult intestinal stem cells of IBD patients and therefore retain their genetic and transcriptomic profile. These models are powerful pharmacological tools to better understand IBD pathogenesis, to study the mechanisms of action on the epithelial barrier of drugs already used in the treatment of IBD, and to evaluate novel target-directed molecules which could improve therapeutic strategies. The aim of this review is to illustrate the potential use of organoids for therapy personalization by focusing on the most significant advances in IBD research achieved through the use of adult stem cells-derived intestinal organoids.

Key Words: Inflammatory bowel disease; Organoids; Intestinal epithelium; 3D cell cultures; Personalized medicine

Core Tip: Intestinal organoids have helped to unveil knowledge about inflammatory bowel diseases pathogenesis, focusing on the genetic and epigenetic factors involved in the onset of these diseases, the altered intestinal epithelial cell (IEC) functions, and the interplay between IECs and other surrounding cells, including immune cells and the intestinal bacteria. Intestinal organoids are currently being evaluated in pre-clinical studies as pharmacological tools to better understand the specific mechanisms of action of already used drugs on the IECs and to identify novel pharmacological targets and approaches.

Citation: Lucafò M, Muzzo A, Marcuzzi M, Giorio L, Decorti G, Stocco G. Patient-derived organoids for therapy personalization in inflammatory bowel diseases. *World J Gastroenterol* 2022; 28(24): 2636-2653
URL: https://www.wjgnet.com/1007-9327/full/v28/i24/2636.htm
DOI: https://dx.doi.org/10.3748/wjg.v28.i24.2636

INTRODUCTION

Inflammatory bowel diseases (IBDs) are chronic inflammatory disorders of the gastrointestinal tract that have emerged as a growing problem in industrialized countries[1]. IBDs include Crohn's disease (CD) and ulcerative colitis (UC)[2], which can be distinguished by differences in genetic predisposition, clinical aspects, and risk factors[3], and by the location and nature of inflammation[4]. UC is restricted to the mucosal surface of the large intestine: It starts in the rectum and extends through the entire colon in a continuous manner[3]. The severity of symptoms depends on the intestinal areas involved in inflammation[4]: It usually occurs with bloody diarrhea with pus and mucus (often nocturnal and postprandial), fever, weight loss, abdominal pain, and signs of systemic inflammation[5]. CD is characterized by the involvement of both the small and large intestine; it most commonly affects the ileocecal region, the terminal ileum, the perianal area, and the colon, with segmental and transmural inflammation, fissuring ulcerations, non-caseating granulomas, strictures, abscesses, and fistulas[4,6,7]. The clinical presentation of CD depends on the location, extent, and severity of inflammation: Patients usually show postprandial abdominal pain, especially around the periumbilical area, bloody diarrhea, nausea, emesis, dysphagia, early satiety, and weight loss[7].

Although no curative treatment is available for these diseases, current therapeutic options aim at achieving an improvement in symptoms and can be divided in two different groups: The remission induction drugs, which are used to achieve clinical remission, and the maintenance drugs which sustain the clinical remission and prevent disease relapse[8]. Aminosalicylates are administered as first-line agents to treat mild to moderately active UC. They exert their anti-inflammatory activity by binding to the peroxisome proliferator-activated receptor[9]. Glucocorticoids are used for inducing remission; when bound to their receptor, they modulate the expression of inflammatory mediators and control inflammatory states[9,10]. The thiopurines azathioprine and mercaptopurine are efficacious for maintaining remission. Thiopurines are inactive prodrugs but their metabolites (thioguanine nucleotides) are responsible for causing immunosuppression, either by inhibiting the *de novo* purine synthesis or by incorporating into the DNA or RNA[9]. Infliximab and adalimumab, which bind the pro-inflammatory cytokine tumor necrosis factor (TNF), have been introduced both for inducing remission and for maintenance therapy[11]. Furthermore, other monoclonal antibodies such as vedolizumab, a selective α4β7 integrin inhibitor, and ustekinumab, an interleukin (IL)-12/23 p40 inhibitor, have been used as alternatives for patients who have failed or are intolerant to anti-TNF therapy[12]. Eventually, thalidomide, by selectively inhibiting TNF-α expression and suppressing TNF-α -induced nuclear factor-kappa B (NF-κB) activation, can be employed when patients do not respond to the standard therapies[9,13]. Despite the multiple therapeutic options, high interindividual variability in response to these drugs is evident, and genetic and epigenetic factors could play a key role in these differences[14,15].

IBDs are multi-etiological diseases: It is currently believed that uncontrolled immune response against intestinal microbiota, combined with environmental factors in genetically predisposed individuals, leads to bowel inflammation, perturbing the mucosal barrier and increasing intestinal epithelial cell (IEC) dysfunction[16,17]. However, even today, it is not completely understood which of these factors are the initiators of inflammation and which are contributors[18]. An altered intestinal architecture and abnormalities in the intestinal wall function have been associated with the onset of the disease[19].

The current models employed to study the intestinal barrier *in vitro* show many weaknesses: Stabilized cell lines, such as the human epithelial colorectal adenocarcinoma cells Caco2 or HT-29, do not reproduce the heterogeneous intestinal cell types[20-22] and do not represent IBD pathophysiology

[23]. Animal models are highly costly, require probands to be raised for weeks[5], and may not reflect human pathobiology, which may contribute to drug failure in clinical therapy[21,24]. Consequently, new models are necessary to better define the pathogenesis underlying IBDs and to find new clinical approaches in its treatment[25].

A major advancement in clinical research of human IECs is represented by the development of 3D organoid cultures, which re-create intestinal epithelial tissue *in vitro*[25] starting from adult stem cells (ASCs) or pluripotent stem cells (PSCs), such as embryonic stem cells or induced PSCs (iPSCs)[22]. These cells, grown under appropriate conditions and stimuli, self-organize and show the specific tissue structures, properties and functionality of the gastrointestinal tissue, forming a spheroid-like structure [26].

INTESTINAL ORGANOIDS

ASCs are located at the base of the intestinal crypts, which can be isolated from intestinal biopsies[27]. Intestinal crypts are embedded in a 3D membrane-like gel, such as matrigel, which mimics the extracellular matrix, and supplemented with an appropriate culture medium that is crucial for the development and expansion of ASCs, from which intestinal organoids can be obtained[5,28,29]. The organoids obtained *in vitro* with this method present only IECs (Paneth cells, goblet cells, enterocytes and enteroendocrine cells) derived from the crypt-based stem cells and are oriented with their apical side toward the lumen and their basolateral domain in contact with matrigel[25,28]. On the other hand, Spence *et al*[30], have demonstrated that it is possible to successfully generate intestinal organoids starting from iPSCs with a process that mimics organogenesis, and that this type of organoids may present not only epithelial cells but also mesenchymal cells, including myofibroblasts, and smooth muscle cells, thus providing a more accurate model[30,31]. This method is advantageous when it is necessary to generate organoids starting from tissues not easily accessible, reprogramming peripheral blood mononuclear cells or fibroblasts to a pluripotent state, thus obtaining iPSCs that can be differentiated to the tissue of interest by using dedicated protocols[29]. The reprogramming phase is complex and can be achieved using different methods. These methods are chosen according to efficiency, footprint (integration of viral vector sequences into reprogrammed cell genome), and type of somatic cells to be reprogrammed[32]. Subsequently, in order to obtain the different types of cells constituting the organ of interest, a microenvironment that mimics embryogenesis is required[33]. However, iPSC-derived intestinal organoids, unlike ASC-derived intestinal organoids, can acquire genetic and epigenetic variations. For example, mutations can occur during the reprogramming process or arise during the prolonged culture which can be conserved if they facilitate cell propagation[30,34,35].

After expansion, intestinal organoids can be employed in any experimental approach developed for cell lines, such as DNA-, RNA-, protein-based techniques, live imaging, drug screening and "omics" approaches (including single-cell RNA sequencing, MethylC sequencing, and mass spectrometry)[22]. For example, Yin *et al*[36] have combined genome-wide analysis of open chromatin by Omni Assay for Transposase-Accessible Chromatin-seq with the transcriptome data from RNA-seq. By correlating gene expression with open chromatin peaks, intestine-specific processes were identified. These results confirm the relevance of intestinal organoids to better define the genetic characteristics and, at the same time, to investigate crucial physiological and biochemical processes in the gut epithelium[36].

Organoid cultures are also a powerful model for genetic manipulation tools, such as transposon mutagenesis, siRNAs, and CRISPR-Cas (*e.g.*, knock-down, knock-out, knock-in, or overexpression)[29]. In particular CRISPR-Cas, along with transcription activator-like effector nuclease, and zinc finger nucleases technologies[37] allows the low frequency IBD-associated mutations to be gradually introduced into organoids derived from healthy patients, providing a better understanding of their effect on the epithelial cell functions[22,29]. In this way, intestinal organoids can be useful to explain in a more specific manner the effect of known genetic variants identified by genome-wide association studies[38] and can become crucial tools for IBD research, especially for the very early-onset IBD (VEO-IBD).

In addition, ASC-derived organoids can undergo extensive expansion in culture and maintain genome stability, which makes them suitable for biobanking[39].

In this review, we focus on the most significant advances in IBD research obtained using ASC-derived intestinal organoids (Figure 1).

Organoid models to study the genetic and epigenetic contribution on IBD epithelium

Several forms of IBD are polygenic and multiple susceptibility loci have been correlated to IBD onset [38]. Intestinal organoids retain the genetic and epigenetic signatures of the original tissue and can hence be employed for studying genetic and epigenetic-phenotypic profiles[22]. Moreover, the study of specific variants affecting the different cell types constituting the epithelium of IBD patients could identify sub-phenotypes of the disease that could help to understand their behavior and outcome[40].

Organoids also maintain the region-specific (duodenum/ileum/jejunum) gene expression of the gastrointestinal tract from which they derive[41]. Moreover, biopsies from IBD patients and derived

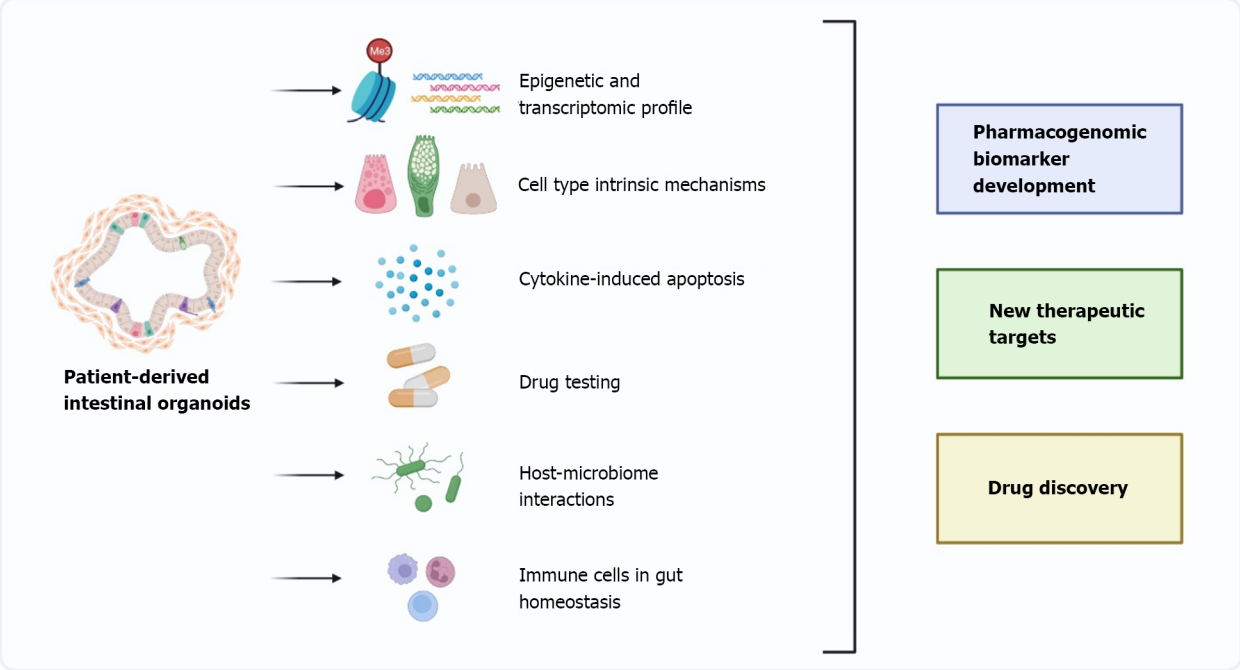

DOI: 10.3748/wjg.v28.i24.2636

Figure 1 Intestinal organoid in inflammatory bowel disease research: The future of precision medicine. Patient-derived intestinal organoids are three-dimensional *in vitro* cell structures derived from stem cells that differentiate and self-organize into functional intestinal epithelium-specific cell types. For this reason, this model is suitable for different research approaches useful to inflammatory bowel disease (IBD) modelling and to study current and new therapeutic options. By retaining the disease-specific phenotypic defects, intestinal organoids can be employed to study epigenetic and transcriptomic profiles. In addition, the ability of intestinal organoids to differentiate into all the different cell types present in the intestinal epithelium makes this model useful to discover new cell-specific disease mechanisms. Furthermore, organoids can be used to study cytokine-induced apoptosis and to test currently used drugs to better understand their mechanisms. Co-culturing intestinal organoids with either microbiota components or immune cells helps to investigate IBD pathogenesis. Thanks to all these research approaches new pharmacogenomic biomarkers, new therapeutic targets and new drugs could be discovered, enabling the development of precision medicine for IBD patients. The image was created with https://biorender.com/.

intestinal organoids show similar expression levels of several IBD-marker genes. Dotti *et al*[42] have identified a set of genes, including *LYZ*, *CLDN18,* and *HYAL1,* upregulated both in the mucosa of patients with active UC and in the derived organoids[42]. Accordingly, the expression levels of genes encoding junctional proteins, such as *ZO-1*, also known as *tight junction protein 1*, *OCLN* and *CTNNB*, were similar in intestinal crypts from CD-patients and derived organoids.

VEO-IBDs are a subset of pediatric patients with IBD diagnosed before the age of 6 years, and up to 15% of these patients may have a rare monogenic disorder. Several defects in genes responsible for the proper intestinal epithelial barrier functions have been discovered, including *NOX1*[43] and *TTC7A*[44]. To study the impact of these mutations on IECs, Schwerd *et al*[44] generated human colonic organoids of patients affected by IBD carrying a *NOX1* p.N122H mutation[44]. These organoids show significantly less production of constitutive superoxide than organoids derived from healthy patients. This defect could favor the crypt colonization by luminal microorganisms since superoxide has an anti-adhesive or anti-invasive effect on bacteria. On the other hand, biallelic missense mutations in the *TTC7A* gene have been found in VEO-IBD patients, resulting in the activation of RhoA-dependent proteins which regulate cytoskeletal architecture by altering cell polarization and proliferation, as demonstrated in organoid cultures[45].

Among the genetic variants associated with the risk of developing IBD, polymorphisms in *NOD-2*, involved in the microbial pathogens recognition[46], and *ATG16L1*[47] genes play an important role. However, their biological functions in the intestinal epithelium of IBD patients remain unclear[47,48].

Organoids generated from *NOD2* knockout (KO) mice show increased intracellular *Escherichia coli* (*E. coli*) following metabolic stress[48], while the number of Paneth cells, known to have antimicrobial activity in the intestinal epithelium, is not affected. *Atg16L1*-deficient intestinal organoids derived from mice present a higher activation of STING-dependent type I interferon (IFN) signaling after IL-22 stimulation, leading to transient endoplasmic reticulum (ER) stress[49]. No data on patient-derived organoids with variants already associated with the increased susceptibility to IBD have been published yet.

Kelsen *et al*[50] reported transcriptomic differences from RNA sequencing between organoids derived from pediatric IBD (VEO and older onset) and non-IBD patients[50]. One of the most upregulated genes in organoids generated from pediatric IBD patients is *LYZ*, encoding for the antimicrobial protein

lysozyme, confirming previous results by Dotti *et al*[42] conducted on adult IBD patient-derived organoids[42]. In addition, an upregulation of the antigen presentation genes *HLA-DRB1* and *HLA-DRA*, necessary for T-cell activation, was demonstrated[50]. Similar results have been obtained by McDonald and Jewell[51] in mucosal epithelial cells by histological and immunohistochemical analysis on colonic biopsy specimens[51]. It is therefore possible that, since these genes are upregulated, the continuous and pathological activation of T cells may lead to the development of IBD[50]. Moreover, the same authors have found that the most downregulated gene in IBD-derived organoids was *CD177*[50], a glycosylphosphatidylinositol-anchored glycoprotein expressed in neutrophils and colon crypt cells.

Looking at the role of epigenetic modifications in IBD, a recent study showed changes in DNA methylation profiles in purified IECs from IBD, compared to non-IBD pediatric patients, that were strictly correlated to IBD pathogenesis[40]. To assess whether these alterations are also preserved in 3D models, intestinal organoids have been developed from children newly diagnosed with IBD and from healthy controls. Differences in DNA methylation and transcription profiles have been found between pediatric patient-derived organoids and controls. This suggests that IBD-associated intestinal epithelial-specific epigenetic alterations can be preserved in organoid cultures. Moreover, it has been observed that these epigenetic alterations are stable over time and therefore can contribute to chronic relapsing inflammation due to impaired IEC function[40].

These data suggest that intestinal organoids can be a promising tool to assess the molecular and functional effects on the intestinal epithelium of genetic and epigenetic variations related to IBD.

Intestinal organoids to study the epithelial barrier

The intestinal epithelium, consisting of different cell types (enterocytes, enteroendocrine cells, goblet cells, and Paneth cells), plays a fundamental role in maintaining intestinal homeostasis, acting as a physical and chemical barrier against pathogens through the production of mucus and antimicrobial peptides. A defect of these activities is evident in IBD patients, but it is still not clear whether these are primary defects or secondary effects of the inflammatory state[52].

In particular, reduced levels of trefoil factor 3 in goblet cells of IBD patients have been observed, which results in a decreased viscosity of the intestinal mucus layer and, as a consequence, the invasion of several IBD-inducing microorganisms. In IBD patients, decreased goblet cells number, diminished mucin 2 (MUC2) production, reduced mucus sulfation, and decreased mucus barrier have been detected [53-55]. Moreover, a decreased expression of constitutive defensins by Paneth cells in IBD patients has also been observed: A low expression of the constitutive human ß-defensin 1 has been demonstrated in patients with UC, while a low expression of human ß-defensin 2 and human ß-defensin 3 was demonstrated in those affected by CD, allowing bacteria to enter the intestinal mucosa[56].

Intestinal organoids can be manipulated to induce differentiation to definite lineages, allowing the study of cell-type-specific functions/dysfunctions in the context of the intestinal epithelium as described in the study conducted by Treveil *et al*[57]. Intestinal organoids can be specifically differentiated towards goblet cell or Paneth cell lineages by specific small molecules, with improved representation of these cell types within the entire organoid cell population[57]. In particular, organoids enriched in Paneth cells can be obtained with the addition of DAPT, a small molecule inhibitor of Notch signaling, whereas the differentiation towards the goblet cell lineage can be induced through the addition of DAPT and IWP-2, which inhibits Wnt signaling[58]. To characterize the effect of cell type enrichment and to predict key molecular regulators involved in Paneth cell and goblet cell specific functions, authors have used mRNA, miRNA, and lncRNA profiles[57]. Thanks to this approach, they predicted key factors involved in differentiation or maintenance of Paneth cells and goblet cells, such as Cebpa, Jun, Nr1d1, and Rxra specific to Paneth cells, Gfi1b and Myc specific for goblet cells, and Ets1, Nr3c1 and Vdr shared between them. Interestingly, several predicted regulators are associated with inflammation and IBD, indicating that their dysregulation can contribute to IBD pathogenesis[57].

Organoids derived from a mouse model of colitis were established to investigate the relationship between the differentiation state and cytokine secretion in the intestinal epithelium[59]. Undifferentiated mouse-derived intestinal organoids showed expression levels of pro-inflammatory cytokines and other inflammatory mediators higher than those differentiated into secretory or absorptive lineages. This suggests that the differentiation state of the intestinal epithelium, regardless of bacteria and immune cells, promotes the release of immunomodulatory factors and has a crucial role in maintaining intestinal homeostasis[59].

In IBD, cytokines play an important role in the pathological process. In particular, TNF-α, which is produced by immune and non-immune cells, through the activation of different pathways including NF-kB, can stimulate the production of other pro-inflammatory cytokines by macrophages and induce the death of Paneth cells, epithelial cells, and T cells[60]. TNF-α has an accepted role in the continuous immune stimulation in intestinal organoids by triggering several signaling cascades which lead to cell activation, survival, and gene expression[61]. It has also been confirmed that high expression of the TNF-α induced protein 3 gene, which encodes A20, a ubiquitin-editing enzyme and negative feedback regulator of NF-kB, promotes TNF-α dependent IEC death[62]. Intestinal organoids from A20 transgenic mice, in which A20 expression is driven by the Villin promoter, were more susceptible to TNF-dependent death. Moreover, after TNF-α addition, A20 transgenic organoids showed a strong caspase 3 and 8 expression whereas control organoids were unaffected, indicating that immune cells or gut

microbiota are not necessary for TNF-induced apoptosis of A20-expressing cells[62]. The authors demonstrated that this effect depended on receptor-interacting protein kinase 1 with its proapoptotic activity, and A20 was found to associate with the death-inducing signaling ripoptosome complex, potentiating its ability to activate caspase-8[62].

Grabinger *et al*[63] have found that both TNF-α receptors, TNFR1 and TNFR2, are involved in cell death in intestinal organoid models, although TNFR1 is the predominant mediator[63]. Indeed, the authors showed an almost complete abrogation of TNF-induced cell death in TNFR1-deficient organoids while organoids from TNFR2-deficient mice showed reduced cell death following exposure to TNF[63].

Ferrer-Picón *et al*[64] have observed that TNF-α reduces the response to butyrate of the intestinal epithelium by decreasing its uptake, oxidation, and consumption[64]. The authors have used differentiated epithelial organoids from IBD patients, which mimic the phenotype of cells residing on the luminal side of the crypt and that are directly exposed to bacteria and their metabolites, and non-IBD controls treated with butyrate and TNF-α. The expression of the butyrate transporters monocarboxylate transporter 1 (encoded by *SLC16A1*), *ABCG2,* and the butyrate receptor *GPR43* was evaluated. After TNF-α treatment, they have found a downregulation of *SLC16A1* and *ABCG2* genes, as well as an increase of *GPR43* gene expression in both IBD and non-IBD derived organoids, indicating that the response to butyrate is not intrinsically altered in IBD patients and that inflammation affected butyrate uptake and oxidation[64].

TNF-α also contributes to barrier deterioration by activating the myosin light chain kinase, which alters tight-junctions (TJ), and, therefore, intestinal permeability[63]. TJ dislocation seems to be a crucial event in IBD pathogenesis as confirmed by Hall *et al*[65]. These authors have demonstrated that the downregulation of the creatine transporter (*SLC6A8*, also known as CRT), observed in IBD patients, is associated with alterations in TJ architecture[65]. In detail, CRT-KO intestinal organoids show a leaky TJ profile, a stressed metabolic phenotype, and a diminished epithelial barrier formation. This might be caused by a decreased creatine uptake, which is required by actin and myosin to regulate TJ structure and intestinal barrier integrity[65].

The role of inflammation in the intestinal epithelial barrier function has also been investigated by the FITC-dextran 4kDa (FD4) uptake assay, using murine intestinal organoids exposed *in vitro* to dextran sodium sulfate (DSS)[66]. DSS is a sulfated polysaccharide with variable molecular weights which causes UC-like pathologies due to its toxicity to colonic epithelial cells, which results in compromised mucosal barrier function. DSS caused a decline in the absorption ability of the inflamed-organoid intestinal barrier, confirmed by FD4 altered intestinal concentration and reduced translocation to the lumen. DSS also caused increased production of TNF-α, IL-6, and other important factors involved in the epithelial barrier disruption, including matrix metallopeptidases MMP10, MMP3, the chemokine ligand CXCL1, and the proteasome-dependent protein degradation ubiquitin D (UBD)[66].

Alteration in the autophagy process within different cellular compartments could potentially lead to an inflammatory response in the gut, increasing intestinal barrier dysfunction and IBD development [67]. Autophagy is a housekeeping process that maintains cellular homeostasis, allowing the degradation and recycling of cellular components[68,69]. Autophagy is also dysregulated in intestinal organoids from patients with IBDs and in mouse intestinal organoids lacking *ATG16L1*, which show decreased Paneth cell levels and increased ER stress-induced cell death, exacerbated when cultured with TNF-α[49,68]. Additionally, recent studies have suggested a novel process by which altered autophagy is associated with IBDs: As already observed in other autophagy-deficient cellular models, such as ATG5-/- and ATG16-/- mouse embryonic fibroblast cells, Atg7−/− autophagy-deficient mouse intestinal organoids show increased levels of argonaute 2, a crucial effector of miRNAs whose upregulation in patients with IBD results in the altered expression of genes implicated in IBD pathogenesis.

Different studies have also demonstrated a crucial relationship between unresolved ER stress, failing autophagy, and pro-inflammatory mediators in IECs during active IBD. For example, IL-22 potentiates the ER stress response caused by other cytokines *via* the activation of STAT3 and induces IEC apoptosis in synergy with IL-17A[49]. Moreover, IL-22 treatment reduces the LGR5+ intestinal stem cell (ISC) levels and amplifies the number of transit-amplifying (TA) cells, an undifferentiated population in transition between stem cells and differentiated cells, by inhibiting Wnt and Notch signaling pathways [70]. All these findings show that IL-22 decreases organoid survival by limiting ISC expansion and promoting TA progenitor proliferation[71].

Intestinal organoids to study the relationship between IECs and the surrounding cells, including immune cells and microbiota

IECs are involved in complex crosstalk with other cell types, including immune and mesenchymal cells. Intestinal organoids have been used for in-depth *ex vivo* analyses of interactions between the epithelium and lamina propria cells[29] and between the epithelium and the underlying immune cells[22].

Co-culturing intestinal organoids with other specific cell types may help to investigate IBD pathogenesis. For example, Ihara *et al*[72] have established a mouse organoid–mononuclear phagocyte (MP) co-culture to study how MPs, such as dendritic cells and macrophages, accumulate in the inflamed intestine causing an imbalance between intestinal immune responses and microbiota and mediating

several interactions with other intestinal cell types[72]. The authors have revealed that excessive E-cadherin, a cell adhesion molecule crucial in the formation of adherens junctions (AJs), expressed by MPs, mediates their adhesive interactions with the epithelium, activating Notch signaling and perturbing physiological IEC differentiation and epithelial homeostasis, with the promotion of goblet cell depletion, mucus layer disruption, dysbiosis, and gut inflammation[72].

Intestinal organoids are also useful to study the interactions between IECs and luminal bacteria, involved in intestinal inflammation: Abnormal growth of a specific microorganism leads to unbalance of the gut microbiota, which may initiate intestinal inflammatory diseases, including IBD[73]. Dysregulated immune responses towards the gut microbiota induce a tissue-damaging chronic inflammatory state, leading to barrier dysfunction, infections, and intestinal inflammation[74]. Therefore, the microbiota-epithelial interaction has been investigated to understand IBD pathogenesis. Intestinal organoid models have emerged as a helpful tool to study this crucial interaction *in vitro,* showing that differences in IEC behavior can contribute to the altered composition of the gut microbiome, barrier permeability, and microbiome interaction in IBD patients[75]. This has been confirmed by Leber *et al* [74], who have used mouse intestinal organoids to study the nucleotide-binding oligomerization domain, leucine-rich repeat containing X1 (NLRX1) as a regulator of gut homeostasis, involved in the control of the immune response, microbiota composition, and metabolism[74]. Intestinal organoids derived from NLRX1-deficient mice show an altered glutamine metabolism because of increased glutamate dehydrogenase activity compared to intestinal organoids obtained from WT mice. With this abnormal host glutamine metabolism, intestinal bacteria may be less exposed to amino acids, and this may lead to increased proliferation of microorganisms capable of amino acid production[75].

In addition, it has recently been found that organoids derived from mice with highly simplified microbiota are different from those derived from mice harboring complex-conventional microbiota[76]. For example, organoids derived from mice harboring limited bacterial species have an accelerated proliferation rate, are less subjected to cell death, and respond differently to pro-inflammatory stimuli, in particular TNF-α stimulation. The effects of different concentrations of TNF-α on these two organoids have been studied: ISC growth from mice with limited bacterial species was inhibited only by the lower concentration of TNF-α tested compared to that of mice with complex bacterial species, in which growth was inhibited by all concentrations tested. Moreover, with increased concentration of the cytokine, the inhibition decreases, and, conversely, growth of organoids from mice with limited bacterial species is promoted. These results suggest that the microenvironment, such as microbial composition, of the intestinal segment from which the organoids are originated could affect ISC replication and, as a consequence, organoid growth, and could also affect the response to different concentrations of cytokines, such as TNF-α[76].

Intestinal organoids can be employed to evaluate the contribution of luminal pathogens to IBD pathogenesis. For example, the cytotoxic effect of *Clostridioides difficile* toxins on the small intestinal epithelium was studied using a jejunal-derived intestinal organoid culture developed by Engevik *et al* [77]. These organoids show high expression of the toxin A and the binary toxin *C. difficile* transferase receptors, and as a result, are more sensitive to toxin A than to toxin B, the other toxin produced by *C. difficile*, developing mucosal damage and an altered permeability[77].

In consideration of the aforementioned data, organoid models must be implemented with the intestinal microbiota to determine the specific effect of bacteria on the epithelial barrier[22]. However, organoid cultures form a spheroid with an enclosed lumen and, therefore, pathogens introduction is difficult[78]. For this reason, different techniques have been generated to better introduce microorganisms into the intestinal organoids. For example, Saxena *et al*[79] have mechanically disrupted the organoids to promote bacterial exposure; however, polarization was lost and, consequently, both the apical and basolateral domains were in contact with bacteria[79]. Leslie *et al*[80] have developed microinjection techniques to introduce bacteria into organoids but these procedures are difficult to perform and to replicate[80]. According to several studies, the culture of intestinal organoids in monolayer could overcome these limits since it preserves the major properties and factors of intestinal epithelium *in vivo*; hence, 3D organoids have been mechanically disrupted and seeded on transwell membrane gels to form a selective and permeable layer, separating the apical and basal domain which are both directly accessible[29]. This important innovation shows the ability to manipulate the model system, introducing bacteria and viruses in the culture medium on the luminal side, and represents a powerful alternative to other 2D models of primary epithelial cells by mimicking *in vivo* physiology and providing a lumen (apical side) and a lamina propria (basal domain)[29,75]. It has been demonstrated that the monolayer system successfully reflects the properties of intestinal epithelium *in vivo*, including epithelial barrier formation, polarization, and gene expression profiles[75]. The monolayer also reflects the aberrant permeability caused by pro-inflammatory cytokines, such as TNF-α and IFN-γ, which cause a mislocalization of both TJs and AJs and reduce their mRNA levels[81]. Another successful use of the organoid-derived monolayer has been demonstrated by Sayed *et al*[82]: These authors demonstrated that detection of high concentrations of the engulfment and cell motility protein 1 in the epithelium could be a diagnostic marker of dysbiosis and gut inflammation since it is a crucial intestinal bacterial sensor[82]. In addition, a co-culture of human intestinal organoid-derived monolayer and macrophages shows how epithelial and innate immune cells respond to pathogens[83]. In this model, macrophages have the capability to sense and interact with *E. coli,* when added to the apical side of IECs, by

improving their adherence properties and by promoting the generation of cell membrane projections to capture the pathogen. This system has provided an important tool to evaluate the host defense towards organisms[83].

INTESTINAL ORGANOIDS TO STUDY CURRENT THERAPIES

Intestinal organoid cultures have recently been employed to study the molecular mechanisms of action of already approved drugs (Table 1).

In IBDs, mucosal healing has emerged as a key prognostic parameter and represents the therapeutic goal in the treatment of these diseases[84]. Indeed, healing means suppression of inflammation, improvement of intestinal barrier by a dynamic interaction of cell regeneration, differentiation, and migration[19] and, consequently, sustained clinical remission, reduced rate of surgery, and lower incidence of potential long term complications such as colorectal cancer[85,86]. However, although a number of therapies have become available in recent years, IBD heterogeneity makes it difficult to obtain complete mucosal healing in order to avoid relapse, and it is not yet clear which is the optimal therapy for a specific patient. A better comprehension of the mechanisms involved in mucosal healing may contribute to ameliorating the therapeutic and clinical approaches currently used. For example, IL-10 KO mouse intestinal organoids, which spontaneously develop enterocolitis, and WT mouse intestinal organoids have been established to understand the different molecular interactions between azathioprine, 5-aminosalicylic acid, and the intestinal epithelium and the mechanistic aspects of mucosal healing[19]. In detail, the researchers have treated with TNF-α the WT and IL-10 KO organoids with and without 5-aminosalicylic acid and azathioprine and have investigated the expression levels of E-cadherin and desmoglein-2, which are closely related to the regulation of the intestinal barrier. TNF-α-treated WT organoids showed internalization and abnormal disruption of E-cadherin, while treatment with 5-aminosalicylic acid and azathioprine restored E-cadherin levels on cell membranes. On the other side, untreated IL-10 KO organoids resulted in defective E-cadherin membrane expression and increased cytoplasmatic expression, which was not further altered by TNF-α treatment. However, it was observed in both models that the effects on E-cadherin were greater with 5-aminosalicylic acid than with azathioprine treatment. Western-blot analysis confirmed that the two drugs impact only the re-distribution of proteins on the intestinal surface. Desmoglein-2 levels were reduced by TNF-α administration in WT models and restored only by 5-aminosalicylic acid whereas, in IL-10 KO organoids, desmoglein-2 expression was increased in all treatment groups by the activation of p38 mitogen-activated protein kinase pathway, a crucial factor in the maintenance of epithelial barrier[19].

Intestinal organoids have also been employed to study the effects of the thiopurine thioguanine on the replication of rotavirus, a *Reoviridae* family virus that might play a role in the pathogenesis of IBD [87]. Although thioguanine is rarely used to treat IBD due to its adverse effects, it has been proposed in the treatment or prevention of rotavirus infection *via* Rac1 inactivation. Rac1 is a member of the Rho family of small GTPases, ubiquitously expressed, which mediates several cellular signaling pathways including actin reorganization, gene transcription, apoptosis, and redox signaling. Rac1 shows two conformational states, the inactive GDP-bound structure and the active GTP-bound form which exerts the biological functions. Several viruses use Rac1 in the active conformational form to infect cells, a process impaired by a loss-of-function of Rac1 by gene knockout or knockdown. It has been demonstrated that virus replication is interrupted after thioguanine treatment at a dose of 100 ng/mL in patient-derived rotavirus isolated from human intestinal organoids. This could be due to thioguanine metabolites, deoxy-6-thioguanosine phosphate and 6-thioguanosine phosphate, that can bind to Rac1, forming a complex and inhibiting the Rac1 activity[87].

Anti-TNF agents, in particular infliximab, have been established as the reference therapy to treat refractory IBD. However, whether anti-TNF agents have any direct effect on IECs remains unknown [53]. Recently it was demonstrated that treatment of organoids from UC patients with infliximab concurrently with TNF-α did not cause a clear effect on their viability or morphology but resulted in a significant reduction of UBD mRNA expression. UBD is a ubiquitin-like modifier involved in protein degradation that is upregulated in inflamed intestinal tissue. UBD mRNA expression pattern also correlated with protein levels, as confirmed by immunoblotting of organoid lysates[88].

Glucocorticoids have beneficial effects in restoring the epithelial barrier disrupted by cytokines. Xu *et al*[89] studied the epithelial barrier function of ASCs derived intestinal organoids of CD patients and the role of glucocorticoid treatment[89]. Using confocal microscopy, they evaluated the permeation of the FD4 marker, which is used to measure macromolecular paracellular permeability from the basal to the luminal side of organoids treated with a cytokine mixture. After an increase in intraluminal FD4 concentration compared to the untreated, the authors exposed the organoids to the glucocorticoid prednisolone, which significantly reduced intraluminal FD4 permeation. In addition, prednisolone restored CLDN2 expression that was upregulated by the cytokine mixture[89]. This is crucial because CLDN2 is one of the most represented TJ components, forming cation-selective pores that make the intestinal barrier more permeable to ions and molecules and its expression is increased in CD patients biopsies[90,91]. The authors also found that the administration of mifepristone, a glucocorticoid receptor

Table 1 Molecular target identified by treatment of intestinal organoids with current therapies for inflammatory bowel disease

Molecular target	Treatment effect	Drug	Species	Ref.
E-cadherin	Re-distribution of protein on intestinal surface restored correct permeability	5-aminosalycilic acid, azathioprine	Mouse (IL-10$^{-/-}$)	[19]
Desmoglein-2	Restored physiological desmoglein-2 expression levels	5-aminosalycilic acid	Mouse (IL-10$^{-/-}$)	[19]
UBD	Restored physiological UBD expression levels	Infliximab	Human (UC patients)	[88]
CLDN-2	Restored physiological CLDN-2 expression levels	Prednisolone, tofacitinib	Human (CD and CRC patients)	[89, 92]
ZO-1	Re-distribution of protein on intestinal surface restored correct permeability	Tofacitinib	Human (CRC patients)	[92]

CD: Crohn's disease; CLDN-2: Claudin-2; CRC: Colorectal cancer; IL-10: Interleukin-10; UBD: Ubiquitin D; UC: Ulcerative colitis; ZO-1: Zonula occludens.

antagonist, reduced the beneficial effect of prednisolone, confirming that the effect is glucocorticoid receptor dependent[89].

A recent study published by Sayoc-Becerra and collaborators employed human colonic organoids to understand how tofacitinib treatment restores TJ architecture and epithelial barrier functions, achieving healing[92]. In addition to CLDNs, OCLN and tricellulin are induced by different pro-inflammatory mediators, such as IFN-γ. These proteins are highly expressed in the intestinal epithelium and control the paracellular transport of solutes, while ZO-1 regulates and assembles TJ structure. Therefore, the proper localization of these proteins is essential in the maintenance of the epithelial barrier function. Several genes are involved in regulating the epithelial barrier function, including genes that control the Janus Kinase-signal transduction and transcription pathway [Janus kinase-signal transducer and activator of transcription (JAK-STAT)]. The activation of JAK-STAT signaling induces the triggering of JAK1 and JAK2 and the phosphorylation of their downstream targets STAT1 and STAT3 which are associated with the upregulation of CLDN2, and the consequent altered permeability across the intestinal epithelium. Therefore, targeting the JAK-STAT pathway has become a new therapeutic approach in IBD, and tofacitinib has been approved as a pan-JAK inhibitor. The drug binds to the adenosine triphosphate binding site in the catalytic cleft of the kinase domain of JAK and inhibits the activation of JAK-STAT pathway. Tofacitinib has a direct effect on IECs, rescuing the permeability altered by INF-γ. After IFN-γ treatment, FD4 influx increases approximately 4-fold into the organoids, and the addition of tofacitinib restores the FD4 physiological flux. To better understand the specific mechanism of tofacitinib on IECs, ZO-1 and OCLN levels were evaluated by western blotting in intestinal organoids, but were unaltered after IFN-γ and tofacitinib treatments. These results suggest that tofacitinib is able to counter damages caused by IFN-γ on epithelial permeability by re-localization of TJ proteins rather than by increasing their expression[92].

Lloyd *et al*[93] have recently demonstrated for the first time the potential use of macrolides, in particular clarithromycin, in the treatment of IBDs[93]. Using human intestinal organoids generated from patients without evidence of IBD, these authors have demonstrated that, in addition to its antibiotic properties, clarithromycin shows anti-inflammatory effects in the intestinal epithelia, suppressing the increase in NF-kB nuclear levels induced by TNF[93].

INTESTINAL ORGANOIDS AS A RESEARCH TOOL FOR NEW POSSIBLE THERAPEUTIC APPROACHES

Recently, studies have been performed using mouse and human intestinal organoids to identify novel therapeutic targets and approaches for IBD treatment[21] (Tables 2 and 3).

The liver receptor homolog 1 (LRH-1) is a nuclear receptor that has been found in the intestinal crypts, where it promotes epithelial renewal by activating Wnt/β catenin signaling[94]. The use of human intestinal organoids has demonstrated the fundamental role of LRH-1 in intestinal epithelial homeostasis and cell survival, confirming the results derived from humanized mouse intestinal organoids in which the mouse *Lrh-1* is deleted, and the human *LRH-1* is expressed. Intestinal organoids from both CD patients and healthy controls have shown that LRH-1 overexpression abrogates TNF-α-mediated cell death and improves epithelial resistance to the effects of fluorouracil, a chemotherapeutic agent with known intestinal toxicity which has been used to mimic damaged mucosa, reducing intestinal inflammation and epithelial wounds[94]. The activation of LRH-1 is ligand-dependent and is carried out by signaling phospholipids, such as phosphatidylinositol trisphosphate, which has been demonstrated to bind with high-affinity LRH-1[95]. It has been demonstrated that modeling

Table 2 Novel potential molecular targets identified using intestinal organoids

Potential molecular targets	Effect	Species	Ref.
LRH-1	Improved resistance to pro-inflammatory mediators and induced mucosal healing	Humanized mouse (Lrh-1$^{-/-}$ LRH-1$^{+/+}$) and Human	[94]
PXR	Reduced NF-kB activity	Human (IBD patients)	[97]
IL-22-pSTAT3 SP	Restored tissue damage and intestinal homeostasis	Mouse (ATF3$^{-/-}$)	[98]
TGF-β SP	Arrested inflammatory signals	Mouse	[104]
SIRT2	Regulated Wnt/β-catenin SP	Mouse (Sirt2$^{-/-}$)	[105]

ATF3: Activating transcription factor 3; IBD: Inflammatory bowel disease; IL: Interleukin; LRH-1: Liver receptor homolog 1; NF-kB: Nuclear factor-kappa B; PXR: Pregnane X receptor; SIRT2: Human sirtuin protein 2; SP: Signaling pathway; STAT: Signal transducer and activator of transcription; TGF-β: Transforming growth factor B.

Table 3 Potential therapeutic approaches for inflammatory bowel disease treatment identified using intestinal organoids

Potential therapeutic approaches	Effect	Species	Ref.
Sex hormones	Decreased expression of ER stress markers	Human (UC female patients)	[100]
Naltrexone	Reduced ER stress levels, increased the expression of endogenous encephalins and endorphins	Human (IBD patients)	[101]
Bacillus subtilis (RZ001)	Promoted intestinal mucosa repair	Mouse	[102]
Bacterial indoleacrylic acid	Promoted anti-inflammatory cytokines secretion while inducing goblet cells differentiation	Mouse	[103]
Hyaluronan 35 kDa	Promoted epithelial wound healing	Mouse	[106]

ER: Endoplasmic reticulum; IBD: Inflammatory bowel disease; UC: Ulcerative colitis.

hydrophobic residues in the binding site of the receptor prevents ligand binding[96], resulting in a failed rescue of TNF-α-mediated cell death. This finding suggests that targeting LRH-1 could improve resistance to pro-inflammatory mediators and induce mucosal healing in IBD patients[94].

Intriguingly, pregnane X receptor (PXR), the main signal transducer in the intestinal response to xenobiotic stress, has been shown to reduce NF-kB activity, whose contribution in IBD pathogenesis is undisputed[97]. Intestinal organoids derived from patients with IBD were pretreated with TNF-α and then with the antibiotic rifampicin, a known PXR ligand. PXR inhibits the expression of several pro-inflammatory genes, especially in the IEC compartment, compared to the stromal and immunological compartments, and reduces IL-8 and IL-1β levels, which are NF-kB target genes. Therefore, the stimulation of PXR by rifampicin or other PXR ligands might be of interest as a novel therapeutic approach in IBD management, especially in patients in which hyper-activation of NF-kB pathway occurs[97].

Moreover, a novel IL-22-induced signal in IECs has been observed thanks to the use of organoids. IL-22 activates its downstream target, the activating transcription factor 3 (ATF3) which is actively involved in the IL-22-pSTAT3 signaling pathway to restore tissue damage and intestinal homeostasis [98]. Stimulation of IECs by IL-22 initiates a signal cascade leading to phosphorylation and consequent activation of STAT3 *via* the involvement of ATF3. This protein has been identified as an essential factor for IEC proliferation by directly controlling crypt regeneration and recovering and maintaining epithelial barrier functionality. To confirm these data, colon organoids from WT and ATF3$^{-/-}$ mice have been implanted into DSS-treated ATF3$^{-/-}$ mice colon through intra-rectal injection. Only mice transplanted with WT organoids showed a reduction in the inflammatory state with increased cell survival, reduced disease activity, recovered epithelial injuries, and improved colon integrity. Most importantly, inducing the IL-22 pathway can promote host defense and wound restoration and can mitigate disease progression and perpetuation[98]. However, several studies have also reported a critical role of the STAT3 signaling pathway, demonstrating that it suppresses the autophagy processes, causing bacterial invasion and intestinal inflammation[99]. Indeed, the inhibition of this pathway protects the *Salmonella*-infected-intestinal mouse-organoid model from bacterial-induced injury, reducing the pro-inflammatory cytokine levels and restoring the autophagy processes. Interestingly, persistent alteration in autophagy processes could lead to chronic intestinal inflammation, exposing the

intestinal epithelium to bacteria and pathogens[99].

In addition to IL-22, IL-28 has also emerged as a novel therapeutic approach by promoting mucosal healing and wound repair *via* the phosphorylation and activation of STAT1. This has been confirmed by using organoids derived from WT, IL28RA$^{-/-}$, and STAT1-lacking mice. IL-28 controls proliferations of intestinal crypts in WT organoids by activating IL-28RA and STAT1 signaling pathways, and induces the overexpression of several genes implicated in crucial functions, including the positive regulation of cytokine production, immune response, and wound healing. This suggests that the epithelial STAT1 phosphorylation by IL-28 balances gut homeostasis.

Of note, some pro-inflammatory cytokines have also been found to be negatively modulated by high levels of progesterone and estrogen released during pregnancy in IBD patients[100]. To clarify the effect of sex hormones, van der Giessen *et al*[100] have established intestinal organoids from UC females and mimicked the tissue inflammation with tunicamycin, which results in an increased expression of ER stress markers, including the 78 kDa glucose-regulated protein 78 (GRP78), CCAAT-enhancer-binding protein homologous protein (CHOP), and phosphorylated inositol-requiring enzyme 1 (IRE1). Specifically, GRP78 expression is decreased after progesterone addition, the stress-downstream target CHOP is reduced with estrogen alone or in combination with progesterone, and IRE1 phosphorylation is decreased upon treatment with estrogen, progesterone, or with their combination. In addition, IL-8 and IL-6, which are highly expressed in inflamed intestine, are modulated by hormones only in tunicamycin-treated organoids, thus suggesting that estrogen and progesterone decrease the stress-induced cytokine production. Moreover, sex hormones positively modulate the intestinal barrier by ameliorating TJ dynamics *via* the upregulation of CLDN1, CLDN2, and OCLN. A limitation of this study is the hormone concentration used *in vitro*, that was significantly higher than the *in vivo* hormone levels during pregnancy. However, a new possible clinical approach in IBD, applying treatment with sex hormones could be proposed[100].

ER stress has also been significantly reduced by a low dose of naltrexone, an opioid antagonist that acts on the μ-opioid receptor (MOR)[101]. This has been confirmed using intestinal organoids from patients with IBD treated with LPS, which induces the expression of GRP78, an important ER stress marker. Treatment with naltrexone reduced ER stress levels and increased the expression of encephalins and endorphins, endogenous agonists of opioid receptors. Interestingly, low doses of naltrexone induced clinical improvement in 74.5% of patients with refractory IBD and long-lasting disease remission in 25.5%. In addition, it has been reported that naltrexone is safe in pediatric IBD patients. The molecular mechanism by which naltrexone is able to reduce ER stress is not entirely clear; however, the authors hypothesize that it could be due to the antagonism on MOR[101].

Organoid cultures have also been treated with several luminal bacteria to better comprehend their positive modulation of inflammatory flares during IBD. For example, the probiotic *Bacillus subtilis* RZ001 promotes intestinal mucosa repair in organoid models by upregulating the expression of MUC2 in the mucus layer[102]. On the other hand, Wlodarska *et al*[103] have evaluated the role of bacteria that are able to use mucins as an energy source as a new possible therapeutic approach by the release of the indoleacrylic acid (IA), a beneficial bioactive tryptophan metabolite[103]. Bacterial IA treatment does not change organoid growth or size but increases the expression of genes associated with goblet cell functions, such as MUC2, which is decreased during intestinal inflammation, and the expression of target genes in the NF-E2-related factor 2-mediated antioxidant pathway, which also suppresses pro-inflammatory pathways and activates aryl hydrocarbon receptor signaling. In fact, an upregulation of the aryl hydrocarbon receptor target gene *CYP1A1* was observed. In addition, IA increases MUC2 and IL-10 levels and decreases TNF expression in LPS-treated co-cultures of bone marrow-derived macrophages and murine intestinal organoids, thus suggesting that IA can simultaneously promote anti-inflammatory cytokines secretion while inducing goblet cells differentiation[103].

Another important anti-inflammatory function has been found for transforming growth factor β (TGF-β): TGF-β signaling pathway arrests inflammatory signals in the intestinal compartment through small mother against decapentaplegic (SMAD4) activation as downstream target[104]. After the binding to its receptors, TGF-β induces the phosphorylation and activation of receptor-SMADs, which consequently bind SMAD4, translocate into the nucleus, and regulate gene transcription, thus acting as transcriptional repressors or activators of genes. The anti-inflammatory effect of TGF-β has also been demonstrated using mouse intestinal organoids: In particular, it has been observed that exposure to TNF-α induces the expression of *CCL20*, that encodes for a chemokine that is up-regulated by inflammatory signaling pathways, and that, following the addition of TGF-β, this induction is interrupted [104].

The canonical Wnt signaling pathway plays a fundamental role in maintaining intestinal epithelium homeostasis, preserving the undifferentiated ISC profile, inducing proliferation and controlling differentiation[105]. The epithelial human sirtuin protein 2 (SIRT2) is also known to be involved in cell differentiation, growth, and autophagy. To better investigate the role that these factors play in IBD, Li *et al* [105] have used WT and SIRT2 KO mouse intestinal organoids. The inhibition of SIRT2 determines the activation of the Wnt/β-catenin signaling pathway and exhibits enhanced epithelial proliferation, which coincides with what has been seen *in vivo* on the mucosa of IBD patients. Furthermore, TNF treatment of WT organoids reduces SIRT2 expression, suggesting that TNF may induce Wnt/β-catenin signaling through repression of SIRT2 expression. In this way, the critical role of Wnt pathway and the beneficial

effect of SIRT2 in the intestinal epithelium was demonstrated[105]. More studies are required to understand the effective role of Wnt signals in the intestinal epithelium.

Kim *et al*[106] have demonstrated that oral treatment with hyaluronan 35 kDa (HA35) may be an effective therapy for IBD patients, promoting epithelial wound healing *via* the activation of RhoA/Rho-associated protein kinase signaling. The use of mouse intestinal organoids has confirmed that HA35, which is specifically internalized by the layilin receptor, induces ZO-1 expression, and restores the epithelial barrier, which is disrupted during active IBD[106].

In addition to all these possible therapeutic targets, Davoudi *et al*[107] have used mouse intestinal organoids to study novel drug-delivery strategies, including nanoparticles and microparticles-based therapies, to provide drug delivery at specific areas, thus reducing the disadvantages of systemic treatments that result in non-selective distribution of drugs and side effects[107]. Authors have inserted 5-aminosalicylic acid or rhodamine B, used as a tracer dye, into polylactic-co-glycolic acid nanoparticles and have loaded them into the lumen of intestinal organoids. By confocal fluorescent microscopy, it was shown that rhodamine B was released into the lumen and digested after 3 d, demonstrating the ability of the organoid to digest nanoparticles and confirming the adsorption of nanoparticles inside the lumen with no negative consequences on organoid growth. This is a trojan horse system in which the drug is concealed from the host cells, and could represent a new therapeutic approach for delivering drugs to the specific inflamed location, reducing adverse reactions[107].

LIMITATIONS OF INTESTINAL ORGANOID TECHNOLOGY

Although the future applications and clinical contributions of intestinal organoids seem to be very encouraging, there are still several issues to overcome. One of the limitations is that several components used to culture intestinal organoids, such as the matrigel and some growth factors, are derived from cell lines. Therefore, they might contain large amounts of xenogenic factors and unknown components that could potentially cause pathogen/immunogen transmission to organoid cultures, in addition to the large variability between the different production batches used. For these reasons, growth conditions must be further optimized and standardized[21]. For example, Wnt-conditioned medium might be replaced with commercial variants[58] and matrigel might be substituted by synthetic extracellular matrices, such as collagen and hydrogel. Yin *et al*[58] have used small molecules, including valproic acid and CHIR99021, a glycogen synthase kinase 3β inhibitor, as conditioned media to maintain self-renewal of mouse $Lgr5^+$ ISCs, resulting in homogeneous cultures[58]. Moreover, the current protocols used to isolate and culture intestinal organoids must be improved because it has been shown that the intestinal crypts isolated from actively inflamed segments often do not allow for correct growth of intestinal organoids due to the loss or disruption of the epithelial layer[21]. Another limit is that intestinal organoids lack other cell and tissue types, including nervous tissue, endothelium-lined blood vessels, and immune mediators, which are crucial for drug pharmacokinetic analyses and disease modeling; in addition, they lack the physiological intestinal and blood flow, the mechanical deformations similar to those seen in the contractions of peristalsis, and the gut microbiota[21,108]. For these reasons, the intestinal organoid technology still requires standardized methods to include the intestinal microbiota and immune cells of the lamina propria, which could allow for mechanistic studies of IBDs[29]. Moreover, ASC-derived intestinal organoids miss the mesenchymal structure in contrast to those derived from iPSCs[21,22].

CONCLUSION

The intestinal epithelium plays a pivotal role in the maintenance of intestinal homeostasis by controlling the microbial composition and lamina propria factors and its study is important to increase knowledge on IBD pathogenesis. Intestinal organoids provide advantages by better reflecting the *in vivo* physiology of intestinal epithelium and are thus becoming an important tool for IBD modeling.

Intestinal organoids demonstrated that IECs play an important role in promoting the inflammatory states, by releasing several pro-inflammatory cytokines; the contribution of the interplay with surrounding cells and with bacteria-host interactions, occurring in patients with IBDs, has also been explored. Furthermore, intestinal organoids have been used to better understand the mechanisms of already-approved drugs for the management of IBD and to comprehend their effects on the intestinal epithelium. In addition, since they can be generated from a specific patient, they could be used to test different drugs to optimize and personalize treatment, reducing therapy failure and the occurrence of adverse effects.

However, it is important to underline that this recent technology still needs to be improved and currently, in the literature, the data available are few and preliminary. Therefore, more studies are required to improve this technique and to better understand how to use intestinal organoids, especially in the context of personalized therapy and drug development for IBD.

FOOTNOTES

Author contributions: Lucafò M, Decorti G, and Stocco G contributed to the conceptualization; Lucafò M, Muzzo A, Marcuzzi M, and Giorio L wrote the original draft; Lucafò M, Decorti G, and Stocco G wrote the review and edited the review; all authors have read and agree to the published version of the manuscript.

Conflict-of-interest statement: All the authors report no relevant conflicts of interest for this article.

Country/Territory of origin: Italy

ORCID number: Marianna Lucafò 0000-0003-1355-3782; Antonella Muzzo 0000-0002-8759-7967; Martina Marcuzzi 0000-0001-9498-5063; Lorenzo Giorio 0000-0001-8490-0150; Giuliana Decorti 0000-0002-9714-6246; Gabriele Stocco 0000-0003-0964-5879.

S-Editor: Fan JR
L-Editor: Filipodia
P-Editor: Fan JR

REFERENCES

1 **Kaplan GG**. The global burden of IBD: from 2015 to 2025. *Nat Rev Gastroenterol Hepatol* 2015; **12**: 720-727 [PMID: 26323879 DOI: 10.1038/nrgastro.2015.150]
2 **Leppkes M**, Neurath MF. Cytokines in inflammatory bowel diseases - Update 2020. *Pharmacol Res* 2020; **158**: 104835 [PMID: 32416212 DOI: 10.1016/j.phrs.2020.104835]
3 **Ordás I**, Eckmann L, Talamini M, Baumgart DC, Sandborn WJ. Ulcerative colitis. *Lancet* 2012; **380**: 1606-1619 [PMID: 22914296 DOI: 10.1016/S0140-6736(12)60150-0]
4 **Yeshi K**, Ruscher R, Hunter L, Daly NL, Loukas A, Wangchuk P. Revisiting Inflammatory Bowel Disease: Pathology, Treatments, Challenges and Emerging Therapeutics Including Drug Leads from Natural Products. *J Clin Med* 2020; **9** [PMID: 32354192 DOI: 10.3390/jcm9051273]
5 **Schulte L**, Hohwieler M, Müller M, Klaus J. Intestinal Organoids as a Novel Complementary Model to Dissect Inflammatory Bowel Disease. *Stem Cells Int* 2019; **2019**: 8010645 [PMID: 31015842 DOI: 10.1155/2019/8010645]
6 **Abraham C**, Cho JH. Inflammatory bowel disease. *N Engl J Med* 2009; **361**: 2066-2078 [PMID: 19923578 DOI: 10.1056/NEJMra0804647]
7 **Hendrickson BA**, Gokhale R, Cho JH. Clinical aspects and pathophysiology of inflammatory bowel disease. *Clin Microbiol Rev* 2002; **15**: 79-94 [PMID: 11781268 DOI: 10.1128/cmr.15.1.79-94.2002]
8 **Ham M**, Moss AC. Mesalamine in the treatment and maintenance of remission of ulcerative colitis. *Expert Rev Clin Pharmacol* 2012; **5**: 113-123 [PMID: 22390554 DOI: 10.1586/ecp.12.2]
9 **Lucafò M**, Franca R, Selvestrel D, Curci D, Pugnetti L, Decorti G, Stocco G. Pharmacogenetics of treatments for inflammatory bowel disease. *Expert Opin Drug Metab Toxicol* 2018; **14**: 1209-1223 [PMID: 30465611 DOI: 10.1080/17425255.2018.1551876]
10 **Prantera C**, Marconi S. Glucocorticosteroids in the treatment of inflammatory bowel disease and approaches to minimizing systemic activity. *Therap Adv Gastroenterol* 2013; **6**: 137-156 [PMID: 23503968 DOI: 10.1177/1756283X12473675]
11 **Travassos WJ**, Cheifetz AS. Infliximab: Use in Inflammatory Bowel Disease. *Curr Treat Options Gastroenterol* 2005; **8**: 187-196 [PMID: 15913508 DOI: 10.1007/s11938-005-0011-2]
12 **Shim HH**, Chan PW, Chuah SW, Schwender BJ, Kong SC, Ling KL. A review of vedolizumab and ustekinumab for the treatment of inflammatory bowel diseases. *JGH Open* 2018; **2**: 223-234 [PMID: 30483594 DOI: 10.1002/jgh3.12065]
13 **Bramuzzo M**, Ventura A, Martelossi S, Lazzerini M. Thalidomide for inflammatory bowel disease: Systematic review. *Medicine (Baltimore)* 2016; **95**: e4239 [PMID: 27472695 DOI: 10.1097/MD.0000000000004239]
14 **Lucafò M**, Di Silvestre A, Romano M, Avian A, Antonelli R, Martelossi S, Naviglio S, Tommasini A, Stocco G, Ventura A, Decorti G, De Iudicibus S. Role of the Long Non-Coding RNA Growth Arrest-Specific 5 in Glucocorticoid Response in Children with Inflammatory Bowel Disease. *Basic Clin Pharmacol Toxicol* 2018; **122**: 87-93 [PMID: 28722800 DOI: 10.1111/bcpt.12851]
15 **De Iudicibus S**, Lucafò M, Vitulo N, Martelossi S, Zimbello R, De Pascale F, Forcato C, Naviglio S, Di Silvestre A, Gerdol M, Stocco G, Valle G, Ventura A, Bramuzzo M, Decorti G. High-Throughput Sequencing of microRNAs in Glucocorticoid Sensitive Paediatric Inflammatory Bowel Disease Patients. *Int J Mol Sci* 2018; **19** [PMID: 29738455 DOI: 10.3390/ijms19051399]
16 **Porter RJ**, Kalla R, Ho GT. Ulcerative colitis: Recent advances in the understanding of disease pathogenesis. *F1000Res* 2020; **9** [PMID: 32399194 DOI: 10.12688/f1000research.20805.1]
17 **Caër C**, Wick MJ. Human Intestinal Mononuclear Phagocytes in Health and Inflammatory Bowel Disease. *Front Immunol* 2020; **11**: 410 [PMID: 32256490 DOI: 10.3389/fimmu.2020.00410]

18 **Holleran G**, Lopetuso L, Petito V, Graziani C, Ianiro G, McNamara D, Gasbarrini A, Scaldaferri F. The Innate and Adaptive Immune System as Targets for Biologic Therapies in Inflammatory Bowel Disease. *Int J Mol Sci* 2017; **18** [PMID: 28934123 DOI: 10.3390/ijms18102020]

19 **Khare V**, Krnjic A, Frick A, Gmainer C, Asboth M, Jimenez K, Lang M, Baumgartner M, Evstatiev R, Gasche C. Mesalamine and azathioprine modulate junctional complexes and restore epithelial barrier function in intestinal inflammation. *Sci Rep* 2019; **9**: 2842 [PMID: 30809073 DOI: 10.1038/s41598-019-39401-0]

20 **Onozato D**, Akagawa T, Kida Y, Ogawa I, Hashita T, Iwao T, Matsunaga T. Application of Human Induced Pluripotent Stem Cell-Derived Intestinal Organoids as a Model of Epithelial Damage and Fibrosis in Inflammatory Bowel Disease. *Biol Pharm Bull* 2020; **43**: 1088-1095 [PMID: 32612071 DOI: 10.1248/bpb.b20-00088]

21 **Yoo JH**, Donowitz M. Intestinal enteroids/organoids: A novel platform for drug discovery in inflammatory bowel diseases. *World J Gastroenterol* 2019; **25**: 4125-4147 [PMID: 31435168 DOI: 10.3748/wjg.v25.i30.4125]

22 **Dotti I**, Salas A. Potential Use of Human Stem Cell-Derived Intestinal Organoids to Study Inflammatory Bowel Diseases. *Inflamm Bowel Dis* 2018; **24**: 2501-2509 [PMID: 30169820 DOI: 10.1093/ibd/izy275]

23 **Rodansky ES**, Johnson LA, Huang S, Spence JR, Higgins PD. Intestinal organoids: a model of intestinal fibrosis for evaluating anti-fibrotic drugs. *Exp Mol Pathol* 2015; **98**: 346-351 [PMID: 25828392 DOI: 10.1016/j.yexmp.2015.03.033]

24 **Chandra L**, Borcherding DC, Kingsbury D, Atherly T, Ambrosini YM, Bourgois-Mochel A, Yuan W, Kimber M, Qi Y, Wang Q, Wannemuehler M, Ellinwood NM, Snella E, Martin M, Skala M, Meyerholz D, Estes M, Fernandez-Zapico ME, Jergens AE, Mochel JP, Allenspach K. Derivation of adult canine intestinal organoids for translational research in gastroenterology. *BMC Biol* 2019; **17**: 33 [PMID: 30975131 DOI: 10.1186/s12915-019-0652-6]

25 **d'Aldebert E**, Quaranta M, Sébert M, Bonnet D, Kirzin S, Portier G, Duffas JP, Chabot S, Lluel P, Allart S, Ferrand A, Alric L, Racaud-Sultan C, Mas E, Deraison C, Vergnolle N. Characterization of Human Colon Organoids From Inflammatory Bowel Disease Patients. *Front Cell Dev Biol* 2020; **8**: 363 [PMID: 32582690 DOI: 10.3389/fcell.2020.00363]

26 **Zhang M**, Liu Y, Chen YG. Generation of 3D human gastrointestinal organoids: principle and applications. *Cell Regen* 2020; **9**: 6 [PMID: 32588198 DOI: 10.1186/s13619-020-00040-w]

27 **Sato T**, Vries RG, Snippert HJ, van de Wetering M, Barker N, Stange DE, van Es JH, Abo A, Kujala P, Peters PJ, Clevers H. Single Lgr5 stem cells build crypt-villus structures in vitro without a mesenchymal niche. *Nature* 2009; **459**: 262-265 [PMID: 19329995 DOI: 10.1038/nature07935]

28 **Zachos NC**, Kovbasnjuk O, Foulke-Abel J, In J, Blutt SE, de Jonge HR, Estes MK, Donowitz M. Human Enteroids/Colonoids and Intestinal Organoids Functionally Recapitulate Normal Intestinal Physiology and Pathophysiology. *J Biol Chem* 2016; **291**: 3759-3766 [PMID: 26677228 DOI: 10.1074/jbc.R114.635995]

29 **Angus HCK**, Butt AG, Schultz M, Kemp RA. Intestinal Organoids as a Tool for Inflammatory Bowel Disease Research. *Front Med (Lausanne)* 2019; **6**: 334 [PMID: 32010704 DOI: 10.3389/fmed.2019.00334]

30 **Spence JR**, Mayhew CN, Rankin SA, Kuhar MF, Vallance JE, Tolle K, Hoskins EE, Kalinichenko VV, Wells SI, Zorn AM, Shroyer NF, Wells JM. Directed differentiation of human pluripotent stem cells into intestinal tissue in vitro. *Nature* 2011; **470**: 105-109 [PMID: 21151107 DOI: 10.1038/nature09691]

31 **Workman MJ**, Mahe MM, Trisno S, Poling HM, Watson CL, Sundaram N, Chang CF, Schiesser J, Aubert P, Stanley EG, Elefanty AG, Miyaoka Y, Mandegar MA, Conklin BR, Neunlist M, Brugmann SA, Helmrath MA, Wells JM. Engineered human pluripotent-stem-cell-derived intestinal tissues with a functional enteric nervous system. *Nat Med* 2017; **23**: 49-59 [PMID: 27869805 DOI: 10.1038/nm.4233]

32 **Malik N**, Rao MS. A review of the methods for human iPSC derivation. *Methods Mol Biol* 2013; **997**: 23-33 [PMID: 23546745 DOI: 10.1007/978-1-62703-348-0_3]

33 **Li M**, Izpisua Belmonte JC. Organoids - Preclinical Models of Human Disease. *N Engl J Med* 2019; **380**: 569-579 [PMID: 30726695 DOI: 10.1056/NEJMra1806175]

34 **Liang G**, Zhang Y. Genetic and epigenetic variations in iPSCs: potential causes and implications for application. *Cell Stem Cell* 2013; **13**: 149-159 [PMID: 23910082 DOI: 10.1016/j.stem.2013.07.001]

35 **Tsuruta S**, Uchida H, Akutsu H. Intestinal Organoids Generated from Human Pluripotent Stem Cells. *JMA J* 2020; **3**: 9-19 [PMID: 33324771 DOI: 10.31662/jmaj.2019-0027]

36 **Yin S**, Ray G, Kerschner JL, Hao S, Perez A, Drumm ML, Browne JA, Leir SH, Longworth M, Harris A. Functional genomics analysis of human colon organoids identifies key transcription factors. *Physiol Genomics* 2020; **52**: 234-244 [PMID: 32390556 DOI: 10.1152/physiolgenomics.00113.2019]

37 **Shi Y**, Inoue H, Wu JC, Yamanaka S. Induced pluripotent stem cell technology: a decade of progress. *Nat Rev Drug Discov* 2017; **16**: 115-130 [PMID: 27980341 DOI: 10.1038/nrd.2016.245]

38 **de Lange KM**, Moutsianas L, Lee JC, Lamb CA, Luo Y, Kennedy NA, Jostins L, Rice DL, Gutierrez-Achury J, Ji SG, Heap G, Nimmo ER, Edwards C, Henderson P, Mowat C, Sanderson J, Satsangi J, Simmons A, Wilson DC, Tremelling M, Hart A, Mathew CG, Newman WG, Parkes M, Lees CW, Uhlig H, Hawkey C, Prescott NJ, Ahmad T, Mansfield JC, Anderson CA, Barrett JC. Genome-wide association study implicates immune activation of multiple integrin genes in inflammatory bowel disease. *Nat Genet* 2017; **49**: 256-261 [PMID: 28067908 DOI: 10.1038/ng.3760]

39 **van de Wetering M**, Francies HE, Francis JM, Bounova G, Iorio F, Pronk A, van Houdt W, van Gorp J, Taylor-Weiner A, Kester L, McLaren-Douglas A, Blokker J, Jaksani S, Bartfeld S, Volckman R, van Sluis P, Li VS, Seepo S, Sekhar Pedamallu C, Cibulskis K, Carter SL, McKenna A, Lawrence MS, Lichtenstein L, Stewart C, Koster J, Versteeg R, van Oudenaarden A, Saez-Rodriguez J, Vries RG, Getz G, Wessels L, Stratton MR, McDermott U, Meyerson M, Garnett MJ, Clevers H. Prospective derivation of a living organoid biobank of colorectal cancer patients. *Cell* 2015; **161**: 933-945 [PMID: 25957691 DOI: 10.1016/j.cell.2015.03.053]

40 **Howell KJ**, Kraiczy J, Nayak KM, Gasparetto M, Ross A, Lee C, Mak TN, Koo BK, Kumar N, Lawley T, Sinha A, Rosenstiel P, Heuschkel R, Stegle O, Zilbauer M. DNA Methylation and Transcription Patterns in Intestinal Epithelial Cells From Pediatric Patients With Inflammatory Bowel Diseases Differentiate Disease Subtypes and Associate With Outcome. *Gastroenterology* 2018; **154**: 585-598 [PMID: 29031501 DOI: 10.1053/j.gastro.2017.10.007]

41 **Middendorp S**, Schneeberger K, Wiegerinck CL, Mokry M, Akkerman RD, van Wijngaarden S, Clevers H, Nieuwenhuis EE. Adult stem cells in the small intestine are intrinsically programmed with their location-specific function. *Stem Cells* 2014; **32**: 1083-1091 [PMID: 24496776 DOI: 10.1002/stem.1655]

42 **Dotti I**, Mora-Buch R, Ferrer-Picón E, Planell N, Jung P, Masamunt MC, Leal RF, Martín de Carpi J, Llach J, Ordás I, Batlle E, Panés J, Salas A. Alterations in the epithelial stem cell compartment could contribute to permanent changes in the mucosa of patients with ulcerative colitis. *Gut* 2017; **66**: 2069-2079 [PMID: 27803115 DOI: 10.1136/gutjnl-2016-312609]

43 **Xu P**, Becker H, Elizalde M, Masclee A, Jonkers D. Intestinal organoid culture model is a valuable system to study epithelial barrier function in IBD. *Gut* 2018; **67**: 1905-1906 [PMID: 29208677 DOI: 10.1136/gutjnl-2017-315685]

44 **Schwerd T**, Bryant RV, Pandey S, Capitani M, Meran L, Cazier JB, Jung J, Mondal K, Parkes M, Mathew CG, Fiedler K, McCarthy DJ; WGS500 Consortium; Oxford IBD cohort study investigators; COLORS in IBD group investigators; UK IBD Genetics Consortium, Sullivan PB, Rodrigues A, Travis SPL, Moore C, Sambrook J, Ouwehand WH, Roberts DJ, Danesh J; INTERVAL Study, Russell RK, Wilson DC, Kelsen JR, Cornall R, Denson LA, Kugathasan S, Knaus UG, Serra EG, Anderson CA, Duerr RH, McGovern DP, Cho J, Powrie F, Li VS, Muise AM, Uhlig HH. NOX1 loss-of-function genetic variants in patients with inflammatory bowel disease. *Mucosal Immunol* 2018; **11**: 562-574 [PMID: 29091079 DOI: 10.1038/mi.2017.74]

45 **Lemoine R**, Pachlopnik-Schmid J, Farin HF, Bigorgne A, Debré M, Sepulveda F, Héritier S, Lemale J, Talbotec C, Rieux-Laucat F, Ruemmele F, Morali A, Cathebras P, Nitschke P, Bole-Feysot C, Blanche S, Brousse N, Picard C, Clevers H, Fischer A, de Saint Basile G. Immune deficiency-related enteropathy-lymphocytopenia-alopecia syndrome results from tetratricopeptide repeat domain 7A deficiency. *J Allergy Clin Immunol* 2014; **134**: 1354-1364.e6 [PMID: 25174867 DOI: 10.1016/j.jaci.2014.07.019]

46 **Hugot JP**, Chamaillard M, Zouali H, Lesage S, Cézard JP, Belaiche J, Almer S, Tysk C, O'Morain CA, Gassull M, Binder V, Finkel Y, Cortot A, Modigliani R, Laurent-Puig P, Gower-Rousseau C, Macry J, Colombel JF, Sahbatou M, Thomas G. Association of NOD2 leucine-rich repeat variants with susceptibility to Crohn's disease. *Nature* 2001; **411**: 599-603 [PMID: 11385576 DOI: 10.1038/35079107]

47 **Rioux JD**, Xavier RJ, Taylor KD, Silverberg MS, Goyette P, Huett A, Green T, Kuballa P, Barmada MM, Datta LW, Shugart YY, Griffiths AM, Targan SR, Ippoliti AF, Bernard EJ, Mei L, Nicolae DL, Regueiro M, Schumm LP, Steinhart AH, Rotter JI, Duerr RH, Cho JH, Daly MJ, Brant SR. Genome-wide association study identifies new susceptibility loci for Crohn disease and implicates autophagy in disease pathogenesis. *Nat Genet* 2007; **39**: 596-604 [PMID: 17435756 DOI: 10.1038/ng2032]

48 **Saxena A**, Lopes F, Poon KKH, McKay DM. Absence of the NOD2 protein renders epithelia more susceptible to barrier dysfunction due to mitochondrial dysfunction. *Am J Physiol Gastrointest Liver Physiol* 2017; **313**: G26-G38 [PMID: 28450277 DOI: 10.1152/ajpgi.00070.2017]

49 **Aden K**, Tran F, Ito G, Sheibani-Tezerji R, Lipinski S, Kuiper JW, Tschurtschenthaler M, Saveljeva S, Bhattacharyya J, Häsler R, Bartsch K, Luzius A, Jentzsch M, Falk-Paulsen M, Stengel ST, Welz L, Schwarzer R, Rabe B, Barchet W, Krautwald S, Hartmann G, Pasparakis M, Blumberg RS, Schreiber S, Kaser A, Rosenstiel P. ATG16L1 orchestrates interleukin-22 signaling in the intestinal epithelium *via* cGAS-STING. *J Exp Med* 2018; **215**: 2868-2886 [PMID: 30254094 DOI: 10.1084/jem.20171029]

50 **Kelsen JR**, Dawany N, Conrad MA, Karakasheva TA, Maurer K, Wei JM, Uman S, Dent MH, Behera R, Bryant LM, Ma X, Moreira L, Chatterji P, Shraim R, Merz A, Mizuno R, Simon LA, Muir AB, Giraudo C, Behrens EM, Whelan KA, Devoto M, Russo PA, Andres SF, Sullivan KE, Hamilton KE. Colonoids From Patients With Pediatric Inflammatory Bowel Disease Exhibit Decreased Growth Associated With Inflammation Severity and Durable Upregulation of Antigen Presentation Genes. *Inflamm Bowel Dis* 2021; **27**: 256-267 [PMID: 32556182 DOI: 10.1093/ibd/izaa145]

51 **McDonald GB**, Jewell DP. Class II antigen (HLA-DR) expression by intestinal epithelial cells in inflammatory diseases of colon. *J Clin Pathol* 1987; **40**: 312-317 [PMID: 3558865 DOI: 10.1136/jcp.40.3.312]

52 **Roda G**, Sartini A, Zambon E, Calafiore A, Marocchi M, Caponi A, Belluzzi A, Roda E. Intestinal epithelial cells in inflammatory bowel diseases. *World J Gastroenterol* 2010; **16**: 4264-4271 [PMID: 20818809 DOI: 10.3748/wjg.v16.i34.4264]

53 **Tytgat KM**, van der Wal JW, Einerhand AW, Büller HA, Dekker J. Quantitative analysis of MUC2 synthesis in ulcerative colitis. *Biochem Biophys Res Commun* 1996; **224**: 397-405 [PMID: 8702401 DOI: 10.1006/bbrc.1996.1039]

54 **Okamoto R**, Watanabe M. Role of epithelial cells in the pathogenesis and treatment of inflammatory bowel disease. *J Gastroenterol* 2016; **51**: 11-21 [PMID: 26138071 DOI: 10.1007/s00535-015-1098-4]

55 **Gersemann M**, Becker S, Kübler I, Koslowski M, Wang G, Herrlinger KR, Griger J, Fritz P, Fellermann K, Schwab M, Wehkamp J, Stange EF. Differences in goblet cell differentiation between Crohn's disease and ulcerative colitis. *Differentiation* 2009; **77**: 84-94 [PMID: 19281767 DOI: 10.1016/j.diff.2008.09.008]

56 **Wehkamp J**, Schmid M, Stange EF. Defensins and other antimicrobial peptides in inflammatory bowel disease. *Curr Opin Gastroenterol* 2007; **23**: 370-378 [PMID: 17545771 DOI: 10.1097/MOG.0b013e328136c580]

57 **Treveil A**, Sudhakar P, Matthews ZJ, Wrzesiński T, Jones EJ, Brooks J, Ölbei M, Hautefort I, Hall LJ, Carding SR, Mayer U, Powell PP, Wileman T, Di Palma F, Haerty W, Korcsmáros T. Regulatory network analysis of Paneth cell and goblet cell enriched gut organoids using transcriptomics approaches. *Mol Omics* 2020; **16**: 39-58 [PMID: 31819932 DOI: 10.1039/c9mo00130a]

58 **Yin X**, Farin HF, van Es JH, Clevers H, Langer R, Karp JM. Niche-independent high-purity cultures of Lgr5+ intestinal stem cells and their progeny. *Nat Methods* 2014; **11**: 106-112 [PMID: 24292484 DOI: 10.1038/nmeth.2737]

59 **Lyons J**, Ghazi PC, Starchenko A, Tovaglieri A, Baldwin KR, Poulin EJ, Gierut JJ, Genetti C, Yajnik V, Breault DT, Lauffenburger DA, Haigis KM. The colonic epithelium plays an active role in promoting colitis by shaping the tissue cytokine profile. *PLoS Biol* 2018; **16**: e2002417 [PMID: 29596476 DOI: 10.1371/journal.pbio.2002417]

60 **Marafini I**, Sedda S, Dinallo V, Monteleone G. Inflammatory cytokines: from discoveries to therapies in IBD. *Expert Opin Biol Ther* 2019; **19**: 1207-1217 [PMID: 31373244 DOI: 10.1080/14712598.2019.1652267]

61 **Wajant H**, Pfizenmaier K, Scheurich P. Tumor necrosis factor signaling. *Cell Death Differ* 2003; **10**: 45-65 [PMID:

12655295 DOI: 10.1038/sj.cdd.4401189]

62 **Garcia-Carbonell R**, Wong J, Kim JY, Close LA, Boland BS, Wong TL, Harris PA, Ho SB, Das S, Ernst PB, Sasik R, Sandborn WJ, Bertin J, Gough PJ, Chang JT, Kelliher M, Boone D, Guma M, Karin M. Elevated A20 promotes TNF-induced and RIPK1-dependent intestinal epithelial cell death. *Proc Natl Acad Sci U S A* 2018; **115**: E9192-E9200 [PMID: 30209212 DOI: 10.1073/pnas.1810584115]

63 **Grabinger T**, Bode KJ, Demgenski J, Seitz C, Delgado ME, Kostadinova F, Reinhold C, Etemadi N, Wilhelm S, Schweinlin M, Hänggi K, Knop J, Hauck C, Walles H, Silke J, Wajant H, Nachbur U, W Wei-Lynn W, Brunner T. Inhibitor of Apoptosis Protein-1 Regulates Tumor Necrosis Factor-Mediated Destruction of Intestinal Epithelial Cells. *Gastroenterology* 2017; **152**: 867-879 [PMID: 27889570 DOI: 10.1053/j.gastro.2016.11.019]

64 **Ferrer-Picón E**, Dotti I, Corraliza AM, Mayorgas A, Esteller M, Perales JC, Ricart E, Masamunt MC, Carrasco A, Tristán E, Esteve M, Salas A. Intestinal Inflammation Modulates the Epithelial Response to Butyrate in Patients With Inflammatory Bowel Disease. *Inflamm Bowel Dis* 2020; **26**: 43-55 [PMID: 31211831 DOI: 10.1093/ibd/izz119]

65 **Hall CHT**, Lee JS, Murphy EM, Gerich ME, Dran R, Glover LE, Abdulla ZI, Skelton MR, Colgan SP. Creatine Transporter, Reduced in Colon Tissues From Patients With Inflammatory Bowel Diseases, Regulates Energy Balance in Intestinal Epithelial Cells, Epithelial Integrity, and Barrier Function. *Gastroenterology* 2020; **159**: 984-998.e1 [PMID: 32433978 DOI: 10.1053/j.gastro.2020.05.033]

66 **Rallabandi HR**, Yang H, Oh KB, Lee HC, Byun SJ, Lee BR. Evaluation of Intestinal Epithelial Barrier Function in Inflammatory Bowel Diseases Using Murine Intestinal Organoids. *Tissue Eng Regen Med* 2020; **17**: 641-650 [PMID: 32594459 DOI: 10.1007/s13770-020-00278-0]

67 **Pott J**, Kabat AM, Maloy KJ. Intestinal Epithelial Cell Autophagy Is Required to Protect against TNF-Induced Apoptosis during Chronic Colitis in Mice. *Cell Host Microbe* 2018; **23**: 191-202.e4 [PMID: 29358084 DOI: 10.1016/j.chom.2017.12.017]

68 **Matsuzawa-Ishimoto Y**, Shono Y, Gomez LE, Hubbard-Lucey VM, Cammer M, Neil J, Dewan MZ, Lieberman SR, Lazrak A, Marinis JM, Beal A, Harris PA, Bertin J, Liu C, Ding Y, van den Brink MRM, Cadwell K. Autophagy protein ATG16L1 prevents necroptosis in the intestinal epithelium. *J Exp Med* 2017; **214**: 3687-3705 [PMID: 29089374 DOI: 10.1084/jem.20170558]

69 **Salem M**, Ammitzboell M, Nys K, Seidelin JB, Nielsen OH. ATG16L1: A multifunctional susceptibility factor in Crohn disease. *Autophagy* 2015; **11**: 585-594 [PMID: 25906181 DOI: 10.1080/15548627.2015.1017187]

70 **Rees WD**, Sly LM, Steiner TS. How do immune and mesenchymal cells influence the intestinal epithelial cell compartment in inflammatory bowel disease? *J Leukoc Biol* 2020; **108**: 309-321 [PMID: 32057139 DOI: 10.1002/JLB.3MIR0120-567R]

71 **Zwarycz B**, Gracz AD, Rivera KR, Williamson IA, Samsa LA, Starmer J, Daniele MA, Salter-Cid L, Zhao Q, Magness ST. IL22 Inhibits Epithelial Stem Cell Expansion in an Ileal Organoid Model. *Cell Mol Gastroenterol Hepatol* 2019; **7**: 1-17 [PMID: 30364840 DOI: 10.1016/j.jcmgh.2018.06.008]

72 **Ihara S**, Hirata Y, Hikiba Y, Yamashita A, Tsuboi M, Hata M, Konishi M, Suzuki N, Sakitani K, Kinoshita H, Hayakawa Y, Nakagawa H, Ijichi H, Tateishi K, Koike K. Adhesive Interactions between Mononuclear Phagocytes and Intestinal Epithelium Perturb Normal Epithelial Differentiation and Serve as a Therapeutic Target in Inflammatory Bowel Disease. *J Crohns Colitis* 2018; **12**: 1219-1231 [PMID: 29917067 DOI: 10.1093/ecco-jcc/jjy088]

73 **Putignani L**, Del Chierico F, Petrucca A, Vernocchi P, Dallapiccola B. The human gut microbiota: a dynamic interplay with the host from birth to senescence settled during childhood. *Pediatr Res* 2014; **76**: 2-10 [PMID: 24732106 DOI: 10.1038/pr.2014.49]

74 **Leber A**, Hontecillas R, Tubau-Juni N, Zoccoli-Rodriguez V, Abedi V, Bassaganya-Riera J. NLRX1 Modulates Immunometabolic Mechanisms Controlling the Host-Gut Microbiota Interactions during Inflammatory Bowel Disease. *Front Immunol* 2018; **9**: 363 [PMID: 29535731 DOI: 10.3389/fimmu.2018.00363]

75 **Roodsant T**, Navis M, Aknouch I, Renes IB, van Elburg RM, Pajkrt D, Wolthers KC, Schultsz C, van der Ark KCH, Sridhar A, Muncan V. A Human 2D Primary Organoid-Derived Epithelial Monolayer Model to Study Host-Pathogen Interaction in the Small Intestine. *Front Cell Infect Microbiol* 2020; **10**: 272 [PMID: 32656095 DOI: 10.3389/fcimb.2020.00272]

76 **Sun L**, Rollins D, Qi Y, Fredericks J, Mansell TJ, Jergens A, Phillips GJ, Wannemuehler M, Wang Q. TNFα regulates intestinal organoids from mice with both defined and conventional microbiota. *Int J Biol Macromol* 2020; **164**: 548-556 [PMID: 32693143 DOI: 10.1016/j.ijbiomac.2020.07.176]

77 **Engevik MA**, Danhof HA, Chang-Graham AL, Spinler JK, Engevik KA, Herrmann B, Endres BT, Garey KW, Hyser JM, Britton RA, Versalovic J. Human intestinal enteroids as a model of *Clostridioides difficile*-induced enteritis. *Am J Physiol Gastrointest Liver Physiol* 2020; **318**: G870-G888 [PMID: 32223302 DOI: 10.1152/ajpgi.00045.2020]

78 **Hares MF**, Tiffney EA, Johnston LJ, Luu L, Stewart CJ, Flynn RJ, Coombes JL. Stem cell-derived enteroid cultures as a tool for dissecting host-parasite interactions in the small intestinal epithelium. *Parasite Immunol* 2021; **43**: e12765 [PMID: 32564379 DOI: 10.1111/pim.12765]

79 **Saxena K**, Blutt SE, Ettayebi K, Zeng XL, Broughman JR, Crawford SE, Karandikar UC, Sastri NP, Conner ME, Opekun AR, Graham DY, Qureshi W, Sherman V, Foulke-Abel J, In J, Kovbasnjuk O, Zachos NC, Donowitz M, Estes MK. Human Intestinal Enteroids: a New Model To Study Human Rotavirus Infection, Host Restriction, and Pathophysiology. *J Virol* 2016; **90**: 43-56 [PMID: 26446608 DOI: 10.1128/JVI.01930-15]

80 **Leslie JL**, Huang S, Opp JS, Nagy MS, Kobayashi M, Young VB, Spence JR. Persistence and toxin production by Clostridium difficile within human intestinal organoids result in disruption of epithelial paracellular barrier function. *Infect Immun* 2015; **83**: 138-145 [PMID: 25312952 DOI: 10.1128/IAI.02561-14]

81 **Gleeson JP**, Estrada HQ, Yamashita M, Svendsen CN, Targan SR, Barrett RJ. Development of Physiologically Responsive Human iPSC-Derived Intestinal Epithelium to Study Barrier Dysfunction in IBD. *Int J Mol Sci* 2020; **21** [PMID: 32093254 DOI: 10.3390/ijms21041438]

82 **Sayed IM**, Suarez K, Lim E, Singh S, Pereira M, Ibeawuchi SR, Katkar G, Dunkel Y, Mittal Y, Chattopadhyay R, Guma M, Boland BS, Dulai PS, Sandborn WJ, Ghosh P, Das S. Host engulfment pathway controls inflammation in inflammatory

bowel disease. *FEBS J* 2020; **287**: 3967-3988 [PMID: 32003126 DOI: 10.1111/febs.15236]
83 **Noel G**, Baetz NW, Staab JF, Donowitz M, Kovbasnjuk O, Pasetti MF, Zachos NC. A primary human macrophage-enteroid co-culture model to investigate mucosal gut physiology and host-pathogen interactions. *Sci Rep* 2017; **7**: 45270 [PMID: 28345602 DOI: 10.1038/srep45270]
84 **Neurath MF**, Travis SP. Mucosal healing in inflammatory bowel diseases: a systematic review. *Gut* 2012; **61**: 1619-1635 [PMID: 22842618 DOI: 10.1136/gutjnl-2012-302830]
85 **Pickert G**, Neufert C, Leppkes M, Zheng Y, Wittkopf N, Warntjen M, Lehr HA, Hirth S, Weigmann B, Wirtz S, Ouyang W, Neurath MF, Becker C. STAT3 links IL-22 signaling in intestinal epithelial cells to mucosal wound healing. *J Exp Med* 2009; **206**: 1465-1472 [PMID: 19564350 DOI: 10.1084/jem.20082683]
86 **Pineton de Chambrun G**, Peyrin-Biroulet L, Lémann M, Colombel JF. Clinical implications of mucosal healing for the management of IBD. *Nat Rev Gastroenterol Hepatol* 2010; **7**: 15-29 [PMID: 19949430 DOI: 10.1038/nrgastro.2009.203]
87 **Yin Y**, Chen S, Hakim MS, Wang W, Xu L, Dang W, Qu C, Verhaar AP, Su J, Fuhler GM, Peppelenbosch MP, Pan Q. 6-Thioguanine inhibits rotavirus replication through suppression of Rac1 GDP/GTP cycling. *Antiviral Res* 2018; **156**: 92-101 [PMID: 29920300 DOI: 10.1016/j.antiviral.2018.06.011]
88 **Kawamoto A**, Nagata S, Anzai S, Takahashi J, Kawai M, Hama M, Nogawa D, Yamamoto K, Kuno R, Suzuki K, Shimizu H, Hiraguri Y, Yui S, Oshima S, Tsuchiya K, Nakamura T, Ohtsuka K, Kitagawa M, Okamoto R, Watanabe M. Ubiquitin D is Upregulated by Synergy of Notch Signalling and TNF-α in the Inflamed Intestinal Epithelia of IBD Patients. *J Crohns Colitis* 2019; **13**: 495-509 [PMID: 30395194 DOI: 10.1093/ecco-jcc/jjy180]
89 **Xu P**, Elizalde M, Masclee A, Pierik M, Jonkers D. Corticosteroid enhances epithelial barrier function in intestinal organoids derived from patients with Crohn's disease. *J Mol Med (Berl)* 2021; **99**: 805-815 [PMID: 33575854 DOI: 10.1007/s00109-021-02045-7]
90 **Weber CR**, Raleigh DR, Su L, Shen L, Sullivan EA, Wang Y, Turner JR. Epithelial myosin light chain kinase activation induces mucosal interleukin-13 expression to alter tight junction ion selectivity. *J Biol Chem* 2010; **285**: 12037-12046 [PMID: 20177070 DOI: 10.1074/jbc.M109.064808]
91 **Zeissig S**, Bürgel N, Günzel D, Richter J, Mankertz J, Wahnschaffe U, Kroesen AJ, Zeitz M, Fromm M, Schulzke JD. Changes in expression and distribution of claudin 2, 5 and 8 lead to discontinuous tight junctions and barrier dysfunction in active Crohn's disease. *Gut* 2007; **56**: 61-72 [DOI: 10.1136/gut.2006.094375]
92 **Lei H**, Crawford MS, McCole DF. JAK-STAT Pathway Regulation of Intestinal Permeability: Pathogenic Roles and Therapeutic Opportunities in Inflammatory Bowel Disease. *Pharmaceuticals (Basel)* 2021; **14** [PMID: 34577540 DOI: 10.3390/ph14090840]
93 **Lloyd K**, Papoutsopoulou S, Smith E, Stegmaier P, Bergey F, Morris L, Kittner M, England H, Spiller D, White MHR, Duckworth CA, Campbell BJ, Poroikov V, Martins Dos Santos VAP, Kel A, Muller W, Pritchard DM, Probert C, Burkitt MD; SysmedIBD Consortium. Using systems medicine to identify a therapeutic agent with potential for repurposing in inflammatory bowel disease. *Dis Model Mech* 2020; **13** [PMID: 32958515 DOI: 10.1242/dmm.044040]
94 **Bayrer JR**, Wang H, Nattiv R, Suzawa M, Escusa HS, Fletterick RJ, Klein OD, Moore DD, Ingraham HA. LRH-1 mitigates intestinal inflammatory disease by maintaining epithelial homeostasis and cell survival. *Nat Commun* 2018; **9**: 4055 [PMID: 30305617 DOI: 10.1038/s41467-018-06137-w]
95 **Sablin EP**, Blind RD, Uthayaruban R, Chiu HJ, Deacon AM, Das D, Ingraham HA, Fletterick RJ. Structure of Liver Receptor Homolog-1 (NR5A2) with PIP3 hormone bound in the ligand binding pocket. *J Struct Biol* 2015; **192**: 342-348 [PMID: 26416531 DOI: 10.1016/j.jsb.2015.09.012]
96 **Sablin EP**, Krylova IN, Fletterick RJ, Ingraham HA. Structural basis for ligand-independent activation of the orphan nuclear receptor LRH-1. *Mol Cell* 2003; **11**: 1575-1585 [PMID: 12820970 DOI: 10.1016/s1097-2765(03)00236-3]
97 **Deuring JJ**, Li M, Cao W, Chen S, Wang W, de Haar C, van der Woude CJ, Peppelenbosch M. Pregnane X receptor activation constrains mucosal NF-κB activity in active inflammatory bowel disease. *PLoS One* 2019; **14**: e0221924 [PMID: 31581194 DOI: 10.1371/journal.pone.0221924]
98 **Glal D**, Sudhakar JN, Lu HH, Liu MC, Chiang HY, Liu YC, Cheng CF, Shui JW. ATF3 Sustains IL-22-Induced STAT3 Phosphorylation to Maintain Mucosal Immunity Through Inhibiting Phosphatases. *Front Immunol* 2018; **9**: 2522 [PMID: 30455690 DOI: 10.3389/fimmu.2018.02522]
99 **Zhang YG**, Zhu X, Lu R, Messer JS, Xia Y, Chang EB, Sun J. Intestinal epithelial HMGB1 inhibits bacterial infection *via* STAT3 regulation of autophagy. *Autophagy* 2019; **15**: 1935-1953 [PMID: 30894054 DOI: 10.1080/15548627.2019.1596485]
100 **van der Giessen J**, van der Woude CJ, Peppelenbosch MP, Fuhler GM. A Direct Effect of Sex Hormones on Epithelial Barrier Function in Inflammatory Bowel Disease Models. *Cells* 2019; **8** [PMID: 30893871 DOI: 10.3390/cells8030261]
101 **Lie MRKL**, van der Giessen J, Fuhler GM, de Lima A, Peppelenbosch MP, van der Ent C, van der Woude CJ. Low dose Naltrexone for induction of remission in inflammatory bowel disease patients. *J Transl Med* 2018; **16**: 55 [PMID: 29523156 DOI: 10.1186/s12967-018-1427-5]
102 **Li Y**, Zhang T, Guo C, Geng M, Gai S, Qi W, Li Z, Song Y, Luo X, Wang N. Bacillus subtilis RZ001 improves intestinal integrity and alleviates colitis by inhibiting the Notch signalling pathway and activating ATOH-1. *Pathog Dis* 2020; **78** [PMID: 32166323 DOI: 10.1093/femspd/ftaa016]
103 **Wlodarska M**, Luo C, Kolde R, d'Hennezel E, Annand JW, Heim CE, Krastel P, Schmitt EK, Omar AS, Creasey EA, Garner AL, Mohammadi S, O'Connell DJ, Abubucker S, Arthur TD, Franzosa EA, Huttenhower C, Murphy LO, Haiser HJ, Vlamakis H, Porter JA, Xavier RJ. Indoleacrylic Acid Produced by Commensal Peptostreptococcus Species Suppresses Inflammation. *Cell Host Microbe* 2017; **22**: 25-37.e6 [PMID: 28704649 DOI: 10.1016/j.chom.2017.06.007]
104 **Means AL**, Freeman TJ, Zhu J, Woodbury LG, Marincola-Smith P, Wu C, Meyer AR, Weaver CJ, Padmanabhan C, An H, Zi J, Wessinger BC, Chaturvedi R, Brown TD, Deane NG, Coffey RJ, Wilson KT, Smith JJ, Sawyers CL, Goldenring JR, Novitskiy SV, Washington MK, Shi C, Beauchamp RD. Epithelial Smad4 Deletion Up-Regulates Inflammation and Promotes Inflammation-Associated Cancer. *Cell Mol Gastroenterol Hepatol* 2018; **6**: 257-276 [PMID: 30109253 DOI: 10.1016/j.jcmgh.2018.05.006]
105 **Li C**, Zhou Y, Rychahou P, Weiss HL, Lee EY, Perry CL, Barrett TA, Wang Q, Evers BM. SIRT2 Contributes to the

Regulation of Intestinal Cell Proliferation and Differentiation. *Cell Mol Gastroenterol Hepatol* 2020; **10**: 43-57 [PMID: 31954883 DOI: 10.1016/j.jcmgh.2020.01.004]

106 **Kim Y**, West GA, Ray G, Kessler SP, Petrey AC, Fiocchi C, McDonald C, Longworth MS, Nagy LE, de la Motte CA. Layilin is critical for mediating hyaluronan 35kDa-induced intestinal epithelial tight junction protein ZO-1 in vitro and in vivo. *Matrix Biol* 2018; **66**: 93-109 [PMID: 28978412 DOI: 10.1016/j.matbio.2017.09.003]

107 **Davoudi Z**, Peroutka-Bigus N, Bellaire B, Wannemuehler M, Barrett TA, Narasimhan B, Wang Q. Intestinal organoids containing poly(lactic-co-glycolic acid) nanoparticles for the treatment of inflammatory bowel diseases. *J Biomed Mater Res A* 2018; **106**: 876-886 [PMID: 29226615 DOI: 10.1002/jbm.a.36305]

108 **Steinway SN**, Saleh J, Koo BK, Delacour D, Kim DH. Human Microphysiological Models of Intestinal Tissue and Gut Microbiome. *Front Bioeng Biotechnol* 2020; **8**: 725 [PMID: 32850690 DOI: 10.3389/fbioe.2020.00725]

World Journal of Gastroenterology

Submit a Manuscript: https://www.f6publishing.com

World J Gastroenterol 2022 June 28; 28(24): 2654-2666

DOI: 10.3748/wjg.v28.i24.2654

ISSN 1007-9327 (print) ISSN 2219-2840 (online)

MINIREVIEWS

Drug-induced autoimmune hepatitis: A minireview

Chin Kimg Tan, Danielle Ho, Lai Mun Wang, Rahul Kumar

Specialty type: Gastroenterology and hepatology

Provenance and peer review: Invited article; Externally peer reviewed.

Peer-review model: Single blind

Peer-review report's scientific quality classification

Grade A (Excellent): 0
Grade B (Very good): B, B
Grade C (Good): 0
Grade D (Fair): 0
Grade E (Poor): 0

P-Reviewer: Komori A, Japan; Malnick SDH, Israel

Received: August 5, 2021
Peer-review started: August 5, 2021
First decision: September 4, 2021
Revised: September 15, 2021
Accepted: May 14, 2022
Article in press: May 14, 2022
Published online: June 28, 2022

Chin Kimg Tan, Danielle Ho, Rahul Kumar, Gastroenterology and Hepatology, Changi General Hospital, Singapore 529889, Singapore

Chin Kimg Tan, Rahul Kumar, Medicine Academic Clinical Programme, SingHealth Duke-NUS Academic Medical Centre, Singapore 529889, Singapore

Lai Mun Wang, Section of Pathology, Department of Laboratory Medicine, Changi General Hospital, Singapore 529889, Singapore

Lai Mun Wang, Pathology Academic Clinical Programme, SingHealth Duke-NUS Academic Medical Centre, Singapore 529889, Singapore

Corresponding author: Rahul Kumar, FRCP, Assistant Professor, Gastroenterology and Hepatology, Changi General Hospital, 2 Simei Street 3, Singapore 529889, Singapore. rahul.kumar@singhealth.com.sg

Abstract

Drug-induced autoimmune hepatitis (DIAIH) is a specific phenotype of drug-induced liver injury that may lead to the devastating outcome of acute liver failure requiring liver transplantation. Drugs implicated in DIAIH include antimicrobials such as nitrofurantoin and minocycline, non-steroidal anti-inflammatory drugs, statins as well as anti-tumor necrosis agents. The clinical features of drug-induced liver injury are indistinguishable from idiopathic autoimmune hepatitis (AIH) as both may have positive AIH-related autoantibodies, elevated immunoglobulin G, as well as similar histopathological findings. In patients who show no clinical improvement, or there is progressive liver injury despite cessation of the suspected drug, a liver biopsy should be considered, whereby the presence of advance fibrosis on histology favors the diagnosis of idiopathic AIH. Empirical treatment with corticosteroids may be required in patients with non-resolving liver injury. A typical clinical scenario supportive of DIAIH includes a history of drug exposure with spontaneous resolution of liver injury after drug withdrawal and the absence of relapse after rapid steroid taper. In this article we report two cases of DIAIH secondary to Sorafenib and Atorvastatin along with a review of currently available literature. Early identification and treatment often lead to a favorable outcome in DIAIH.

Key Words: Drug-induced liver injury; Drug-induced autoimmune hepatitis; Autoimmune hepatitis; Review

Core Tip: Drug-induced autoimmune hepatitis is uncommon in clinical practice but may have devastating consequences. It is important to distinguish drug-induced autoimmune hepatitis from idiopathic autoimmune hepatitis as the former may not require prolong course of immunosuppressant. This minireview highlights the key differences between these two closely-linked entities.

Citation: Tan CK, Ho D, Wang LM, Kumar R. Drug-induced autoimmune hepatitis: A minireview. *World J Gastroenterol* 2022; 28(24): 2654-2666
URL: https://www.wjgnet.com/1007-9327/full/v28/i24/2654.htm
DOI: https://dx.doi.org/10.3748/wjg.v28.i24.2654

INTRODUCTION

Idiosyncratic drug-induced liver injury (DILI) is rare and affects 14-19 per 100000 persons yearly[1,2]. Despite its relatively low incidence, it is a leading cause of acute liver failure in the United States[3], Europe[4,5], and Japan[6]. In patients with DILI, liver-related death and liver transplantation occur in 3.6%-10% of cases[7].

Drug-induced autoimmune hepatitis (DIAIH) is a specific phenotype of idiosyncratic DILI with features indistinguishable from idiopathic autoimmune hepatitis (AIH), as it shares serological markers and/or histological features with idiopathic AIH[8]. Various terms have been used synonymously with DIAIH, including immune-mediated DILI[9] and drug-induced AIH-like injury[10].

Due to its rare occurrence, it is difficult to estimate the frequency of DIAIH. In addition, studies use varying definitions of DIAIH and drug causality assessments, as well as having diverse patient populations with different follow-up periods (Tables 1 and 2). It is estimated that DIAIH accounts for 2%-18% of AIH cases[10-14], and 2.9%-8.8% of all DILI are due to DIAIH[15,16]. The increasing incidence of AIH has been in part attributed to prevalent use of anti-tumor necrosis factor agents[14].

DRUGS ASSOCIATED WITH DIAIH

Multiple drugs that have been associated with DIAIH are classified into those with definite association (*e.g.*, Minocycline, Nitrofurantoin, Infliximab), probable association (*e.g.*, Diclofenac, Atorvastatin, Rosuvastatin, Etanercept), and possible association, depending on the cases reported and associations as summarized in the most recent American Association Society of Liver Disease AIH Practice Guidance [10].

DIAIH is classically associated with minocycline, nitrofurantoin, methyldopa, dihydralazine, and tienilic acid[17]. DILI with autoimmune phenotype defined as DILI with presence of AIH antibodies (antibodies to nuclear antigen, smooth muscle, and soluble liver antigen) occur in 83%, 74%, 60%, and 43% of nitrofurantoin, minocycline, methyldopa, and hydralazine related DILI cases, respectively[15]. Immuno-allergic phenotype characterized by any combination of rash, fever, facial edema, lymphadenopathy, and eosinophilia is common in DILI associated with these four drugs as well, ranging from 11%-27%[15]. Another important cause of DIAIH include statins, where DIAIH or DILI with immune features occurs in about 8.5%-27.2% of all statin related DILI[18,19].

In recent years, there has been a change in the predominant culprit drugs causing DIAIH to anti-tumor necrosis factor[14], statins, and non-steroidal anti-inflammatory drugs[16,20,21] with notable contribution from complementary alternative medicines in studies from Asia[22].

PATHOGENESIS OF DIAIH

Reactive metabolites generated from hepatic metabolism of drugs bind to cellular proteins such as components of CYP450, which is then recognized as neoantigens by heightened immunological response leading to AIH[11,23,24] as a result of misdirected immune response against self[25].

In this minireview, we highlight two recent cases of DIAIH induced by Sorafenib and Atorvastatin seen at our center. We also aim to review the current literature on DIAIH and discuss distinguishing features between DIAIH and AIH.

Table 1 Studies comparing drug-induced autoimmune hepatitis and drug-induced liver injury

Ref.	a: Study population; b: Study period; c: Follow-up period	a: Definition of DIAIH; b: Causality tool assessment	No. of DIAIH cases, % of all DILI	No. of DILI cases	Key findings for DIAIH (in addition to Table 3)
Stephens *et al*[37], 2021, Spain	a: Prospective multicentre DILI database, *n* = 869; b: 1994-2018; c: Median 96-117 d in HC injury	a: Simplified AIH criteria; b: RUCAM (definite, highly probable, probable and possible)	26, 2.9%	843	Culprit drugs: Statins (31%); antimicrobials (23%)
De Boer *et al*[15], 2015, United States	a: National prospective DILI database (*n* = 1322), subgroup of DILI secondary to Nitrofurantoin, hydralazine, Minocycline and methyldopa (*n* = 88); b: 2004-2014; c: 6 mo, 12 mo or 24 mo until normalization of LFT	a: Autoimmune (AI) DILI–AI score based on seropositivity for AIH antibodies and raised IgG); b: RUCAM (definite, highly probable and probable)	47, 3.6%	Two groups: (a) 18 non-AI DILI due to 4 drugs; (b) 67 (reference cohort, DILI due to Augmentin, Isoniazid, Diclofenac)	Similar HLA-DRB1*03:01 (15%) and HLADRB1*04:01 (9%) percentage in patients with DILI compared to population controls from National Marrow Donor Program (12% and 9%, respectively)
Hisamochi *et al*[22], 2016, Japan	a: All DILI who underwent liver biopsy, *n* = 62; b: 1988-2010; c: Median 2290 d	a: Revised IAIHG criteria; b: RUCAM and JDD-W scale	23, NA	39	Culprit drugs: CAM (69.6%); NSAIDs (8.7%). IgG reduction in 87%. 50% (8/16) relapsed (4 not treated with steroids, 2 previously received steroids and 2 on tapering dose of steroid dosage). Median time to relapse 283 d (range, 47-1090 d). Rise in IgG with relapse
Licata *et al*[16], 2014, Italy	a: Single centre hospitalized patients with DILI, *n* =136 (44 with liver biopsy); b: 2000-2011; c: Mean 26 mo (12-84 mo), at least 1 yr after stopping immunosuppressants	a: Simplified AIH score ≥ 6; b: RUCAM (definite, highly probable, probable and possible)	12, 8.8%	124	Culprit drugs: NSAIDs (50%) - (Nimesulide/ketoprofen); Antimicrobials (25%) (Augmentin/Ceftriaxone); CAM (17%). 38.2% of all DILI patients had positive AIH antibodies but only 42.9% with positive antibodies have DIAIH. All DIAIH were treated with corticosteroids and all achieved remission at 15 mo. 58.3% (7/12) had addition of Azathioprine. One patient had a flare while on tapering prednisolone. In 41% (5/12), immunosuppressant was stopped after 2 yr, with no relapse

DIAIH: Drug-induced autoimmune hepatitis; DILI: Drug-induced liver injury; RUCAM: The Roussel Uclaf Causality Assessment Model; NSAIDs: Non-steroidal anti-inflammatory drugs; AIH: Autoimmune hepatitis; IAIHG: International AIH Group; IgG: Immunoglobulin G; CAM: Complementary alternative medicines.

CASE DISCUSSION

Patient A

A 61-year-old man and teetotaler presented with a 1-week history of jaundice and malaise. He was on Atorvastatin 40 mg daily for 4 years for hyperlipidemia. He had a normal liver function test (LFT) prior to admission. He was started on Sorafenib 6 wk prior to presentation with jaundice for recurrent sarcoma of the left thigh. Clinical examination was unremarkable apart from scleral icterus. The LFT showed severe hepatocellular (HC) injury [bilirubin 4.56 mg/dL, alkaline phosphatase (ALP) 190 U/L, alanine transaminase (ALT) 1004 U/L, aspartate transaminase (AST) 790 U/L, international normalized ratio (INR) of 1.53]. Viral hepatitis screen, AIH-specific antibodies, and abdominal imaging were unremarkable. Of note, serum immunoglobulin G (IgG) was elevated (18.6 g/L). The liver biopsy showed features supportive of DILI and AIH (Figure 1). The Simplified AIH score was 6. The Roussel Uclaf Causality Assessment Model (RUCAM) score was 9 for Sorafenib and 6 for Atorvastatin. Diagnosis of Sorafenib-induced AIH was made. His LFT improved spontaneously with normalization of LFT 8 wk after stopping Sorafenib (Figure 2A).

Patient B

A 65-year-old man who was on Atorvastatin 40 mg daily presented with an incidental finding of acute HC pattern of liver injury 18 mo after initiation of Atorvastatin (albumin 39 g/L, globulin 39 g/L, bilirubin 0.64 mg/dL, ALP 107 IU/L, ALT 696 U/L, AST 381 U/L). Viral hepatitis screening, AIH-specific antibodies, and abdominal imaging were unremarkable. His serum IgG was normal (14.28 g/L). Atorvastatin was stopped, and an improvement in LFT was noted within the 1 wk (albumin ALT 474 U/L, AST 195 U/L). The RUCAM score for Atorvastatin was 4. As such, he was given the diagnosis of possible Atorvastatin-induced DILI. However, despite this initial improvement in his LFT, there was subsequent deterioration 2 wk after stopping Atorvastatin (albumin 34 g/L, globulin 43 g/L, ALP 137

Table 2 Studies comparing drug-induced autoimmune hepatitis and autoimmune hepatitis

Ref.	a: Study population; b: Study period; c: Follow-up period	a: Definition of DIAIH/AIH; b: Causality tool assessment	No. of DIAIH cases, % of all AIH	No. of AIH cases	Key findings for DIAIH (in addition to Table 4)
Valgeirsson *et al* [14], 2019, Iceland	a: Population based AIH study, *n* = 71; b: 2006-2018; c: Median 4.8 yr	a: Simplified AIH score, if not fulfilled, Revised IAIHG score is used; or received corticosteroids; b: RUCAM score (highly probable, probable and possible)	13, 18% (9/13 had liver biopsy)	58	Culprit drugs: Biologics (77%) - 80% were due to infliximab; Nitrofurantoin (15%)
Martínez-Casas *et al*[34], 2018, Columbia	a: Single centre retrospective review of AIH cases, *n* = 190; b: 2010-2016; c: Mean 47.4 mo	a: Simplified AIH score; b: RUCAM	12, 6.3%	178	Culprit drugs: Nitrofurantoin (67%); NSAIDs (17%)
Wang *et al*[20], 2017, China	a: Single centre retrospective review of AIH and DILI patients; b: 2010-2014; c: NA	a: DILI with positive antibody; simplified AIH score; b: NA (DILI due to drugs/CAM within 6 mo of hospitalization)	18 (12.4% of all DILI with positive antibody)	52	Culprit drugs: CAM, NSAIDs and antibiotics (no breakdown)
Yeong *et al*[32], 2016, United Kingdom	a: Single centre retrospective AIH cases, *n* = 82; b: 2005-2013; c: Median 86.3 mo (14.6% < 18 mo)	a: Revised IAIHG criteria; b: RUCAM (highly probable, probable)	11, 13.4%	71	Culprit drugs: Nitrofurantoin (36.4%); Statins (36.4%); CAM (18%)
Weber *et al*[21], 2019, Germany	a: Single centre cohort of 288 acute liver injury patients who received corticosteroid for DILI/AIH, *n* = 44; b: 2013-2018; c: Median 19 mo in DILI; 23 mo in AIH	a: Simplified AIH score and revised IAIHG criteria; b: RUCAM	22	22	Culprit drugs: NSAIDs (27.3%); Statins (9%); Direct oral anticoagulants (9%)
Björnsson *et al* [13], 2010, United States	a: Single centre retrospective review of all AIH cases, *n* = 261; b: 1997-2007	a: Simplified AIH score	24, 9.2% (24/261)	237	Culprit drugs: Minocycline (45.8%); Nitrofurantoin (45.8%)

DIAIH: Drug-induced autoimmune hepatitis; DILI: Drug-induced liver injury; RUCAM: The Roussel Uclaf Causality Assessment Model; NSAIDs: Non-steroidal anti-inflammatory drugs; AIH: Autoimmune hepatitis; IAIHG: International AIH Group; CAM: Complementary alternative medicines.

U/L, ALT 1404 U/L, AST 676 U/L, INR 1.09). A liver biopsy was performed 3 wk after stopping Atorvastatin in view of worsening acute liver injury. This showed marked HC injury with histological features suggestive of AIH (Figure 3). Following the liver biopsy, there was again spontaneous improvement (ALT 699 U/L), but this did not persist. Two months after cessation of Atorvastatin, he had severe HC injury with jaundice (bilirubin 11.87 mg/dL, ALP 96 U/L, ALT 1095 U/L, AST 938 U/L, INR 1.33) and elevated IgG (28.35 g/L). Liver biopsy was repeated, and this again demonstrated features of AIH. He was then started on prednisolone with rapid improvement of LFT (Figure 2B). The final diagnosis was Atorvastatin-induced AIH.

WHEN TO SUSPECT DIAIH IN PATIENTS WHO PRESENTS WITH DILI

The cases described above highlight two possible presentations of DIAIH. The first patient (patient A) had DILI and histological features compatible with AIH on liver biopsy. Although Sorafenib has not been reported to be associated with DIAIH, the temporal sequence of this case presentation and subsequent spontaneous resolution after cessation of Sorafenib is in keeping with DIAIH.

DIAIH shares many similar characteristics with DILI without features of AIH. More than half of DIAIH present with acute liver injury associated with jaundice in 70%-75% of cases[16], which is similar to DILI. On top of that, rash may be present in 4.5% of DIAIH and 7.9% of DILI[26].

The following pointers are useful in identification of DIAIH in patients who present with DILI. The main differences between these two conditions are also summarized in Table 3: (1) DIAIH and AIH should always be considered as differentials in a patient with a hepatocellular pattern of DILI. DIAIH is rarely associated with a cholestatic/mixed picture, and it is only seen in 8% of cases[16]; (2) A detailed medication history with a focus on recent drug exposures including complementary alternative medicines is essential[10]; (3) The latency period of drug exposure in DIAIH is usually prolonged compared to other types of DILI, some with a latency period exceeding 1 year, *e.g.*, nitrofurantoin and minocycline[15]; (4) Seropositivity for AIH antibodies, *e.g.*, antinuclear antibody (ANA), anti-smooth muscle antibody, anti-liver kidney antibody, and elevated serum IgG suggest possible DIAIH. However, not all patients with DIAIH have detectable autoantibodies or elevated IgG. Similarly, a proportion of patients with DILI may have detectable AIH antibodies[15,16]; (5) In the presence of detectable AIH antibodies and elevated IgG, AIH scoring (either pre-treatment score for Revised International AIH Group criteria[27] or simplified AIH score[28]) is useful to assess for possible or

Table 3 Comparison between drug-induced autoimmune hepatitis and drug-induced liver injury

Clinical features	DIAIH	DILI
Demographics		
Female, %	62%[37]	48% (P = 0.162)[37]
Age (yr), mean ± SD	57± 17[37]; 59 ± 17[22]	54 ± 18 (P = 0.550)[37]; 47 (P = 0.002)[22]
Clinical presentation		
Jaundice, %	69%[37]; 68%[15]; 66%[16]	69% (P = 0.953)[37]; 56% (P = 0.4)[15]; 40%-47.6% (P = 0.2)[16]
Rash, %	4.5%[37]; 19%[15]	7.9% (P = 1.000)[37]; 22% (P = 0.7)[15]
Hepatocellular injury, %	92%[37]	57% (P = 0.002)[37]
Latency period (d), median (range)	65 (27-274)[37]; 277 (8-7032)[15]; 4 (1-9)[16]	27 (8-64) (P = 0.004)[37]; 100 (13-1572) (P = 0.03)[15]; 7-10 (5-50) (P = 0.7)[16]
Latency period (d), mean ± SD	143 ± 188[22]	32 ± 120 (P = 0.000)[22]
Culprit drug due to CAM, %	70%[22]	25% (P = 0.000)[22]
Biochemical results		
ALT × ULN, mean ± SD	28 ± 19[37]	19 ± 22 (P = 0.0002)[37]
AST × ULN, mean ± SD	24 ± 17[37]	15 ± 21 (P = 0.0001)[37]
Autoimmune antibodies and serology		
Detectable ANA, %	88%[37]; 72%[15]; 52%[22]	12 (P < 0.001)[37]; 22[15]; 15 (P = 0.003)[22]
Detectable ASMA, %	44%[37]; 60%[15]	8.9% (P < 0.001)[37]; 13%[15]
Detectable AMA, %	4%[37]	1.9% (P = 0.397)[37]
Detectable anti-LKM-1, %	0%[37]	1.1% (P = 1.000)[37]
Elevated IgG, %	39%[15]; (25% > 1.1 × ULN)[15]	9%[15]
Serum IgG (g/L), mean ± SD	19.5 ± 10.7[37]; 1.07 × ULN ± 0.51[22]	11.9 ± 4.6 (P < 0.001)[37]; 0.69 × ULN ± 0.28 (P = 0.000)[22]
Histopathology		
Liver biopsy[16]		
Severe portal inflammation, %	100%	56.2%-62.5%
Prominent portal plasma cells, %	58.3%	6.3%-12.5%
Rosette formation, %	66.7%	6.3%-12.5%
Severe focal necrosis, %	66%	6.3%-25%
Treatment and response to treatment		
Corticosteroid therapy, %	43%[15]	61% (P = 0.3)[15]
Immunosuppressive therapy, (corticosteroid/Azathioprine), %	58%[37]; 60.8%[22]	9.9% (P < 0.001)[37]; 10.3% (P = 0.000)[22]
Outcomes		
Mild/mod/severe DILI, %	35%/45%/7.7%[37]	31%/59%/6.2% (P = 0.784)[1][37]
Outcomes (liver transplant/death), %	3.8%/0%[37]; 6%/4%[15]	2.1%/1.5% (P = 0.784)[1][37]; 0/0 (P = 0.6 for liver transplant, P = 1.0 for death)[15]
Chronicity rate, %	17%[15]	21% (P = 0.70)[15]

[1]Combined comparisons of severity of drug-induced liver injury, mortality, and liver transplantation.

DIAIH: Drug-induced autoimmune hepatitis; DILI: Drug-induced liver injury; ALT: Alanine transaminase; AST: Aspartate transaminase; ULN: Upper limit of normal; CAM: Complementary alternative medicines; Anti-LKM: Anti-liver kidney antibody; SD: Standard deviation; IAIHG: International AIH Group.

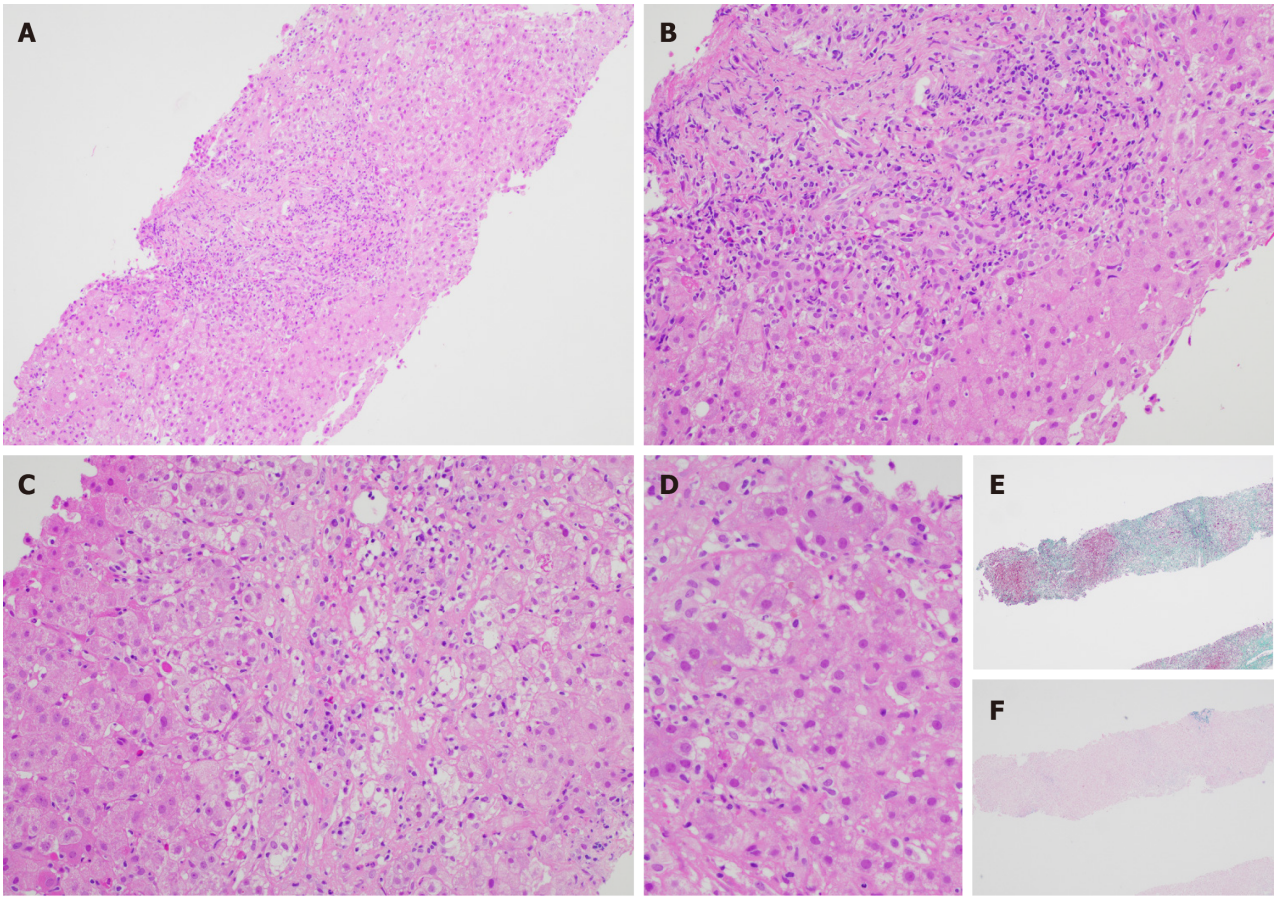

DOI: 10.3748/wjg.v28.i24.2654

Figure 1 Liver biopsy specimen for patient A. A: Low power view [hematoxylin & eosin (H&E) 100 ×] displays conspicuous portal and lobular inflammation with lobular disarray. Mild steatosis is also noted; B: Higher magnification of the portal tract (H&E 200 ×), zone 1, shows moderate chronic inflammation, lymphoplasmacytic predominantly, and rare eosinophils, with interface damage; C: At similar magnification (H&E 200 ×), the lobule including the perivenular region, *e.g.*, zones 2 and 3, exhibits lobulitis characterized by aggregates of plasma cells, swollen hepatocytes with rosetting, Councilman bodies, and hepatocyte drop-out; D: High power view (H&E 400 ×) demonstrates rosetting of hepatocytes with droplets of orange-brown bile pigment; E and F: Histochemical stains Masson trichrome (E, 40 ×) showing collapse with mild early young fibrosis and Victoria blue (F, 40 ×) revealing paucity of elastic fibers, thus in keeping with subacute injury. Overall, the appearances are supportive of subacute drug-induced liver injury in association with autoimmune hepatitis histological pattern.

probable AIH; (6) Liver-specific causality assessment tools may be used to ascertain the strength of association between drug exposure and clinical manifestation, *e.g.*, RUCAM[29]; and (7) Liver biopsy is the cornerstone for the diagnosis of DIAIH and should be considered in the following scenarios: (a) Non resolving or worsening liver injury despite stopping possible culprit drugs; (b) Seropositivity of AIH antibodies, raised IgG, or possible AIH based on AIH scoring systems.

Known culprit drugs of DIAIH such as nitrofurantoin may be overlooked as these agents are associated with longer latency period and have a lower ALT at presentation. A higher fibrosis stage or cirrhosis may be observed as a higher proportion of these patients are unknowingly continued on Nitrofurantoin prior to the diagnosis[30]. This underscores the importance of understanding the common culprits of DIAIH, where a significant proportion of DILI presents with DIAIH[15]. LiverTox® is an up-to-date online resource that provides information on hepatotoxicity caused by medications and supplements[31].

With the increasing use of targeted tumor therapies such as kinase inhibitor and immunotherapy, there are some case reports of DIAIH associated with these medications. To our knowledge, this is the first case report of Sorafenib-induced AIH. Imatinib, another type of kinase inhibitor, has also been reported to be associated with DIAIH[14,32].

Several studies have attempted to compare the differences between DIAIH and DILI (Table 1)[15,16,22], with key features of DIAIH including significantly longer duration of drug exposure and latency; higher ALT and AST; higher proportion of patients with positive ANA and SMA, and higher level of serum IgG, as summarized in Table 3.

Liver biopsy is key in differentiating DIAIH from DILI without features of AIH[10,33]. In patients with DIAIH, the histopathological features are similar to that of idiopathic AIH with significantly higher proportion of patients showing severe portal inflammation, prominent portal-plasma cells, rosettes, and severe focal necrosis as compared to other types of DILI[16].

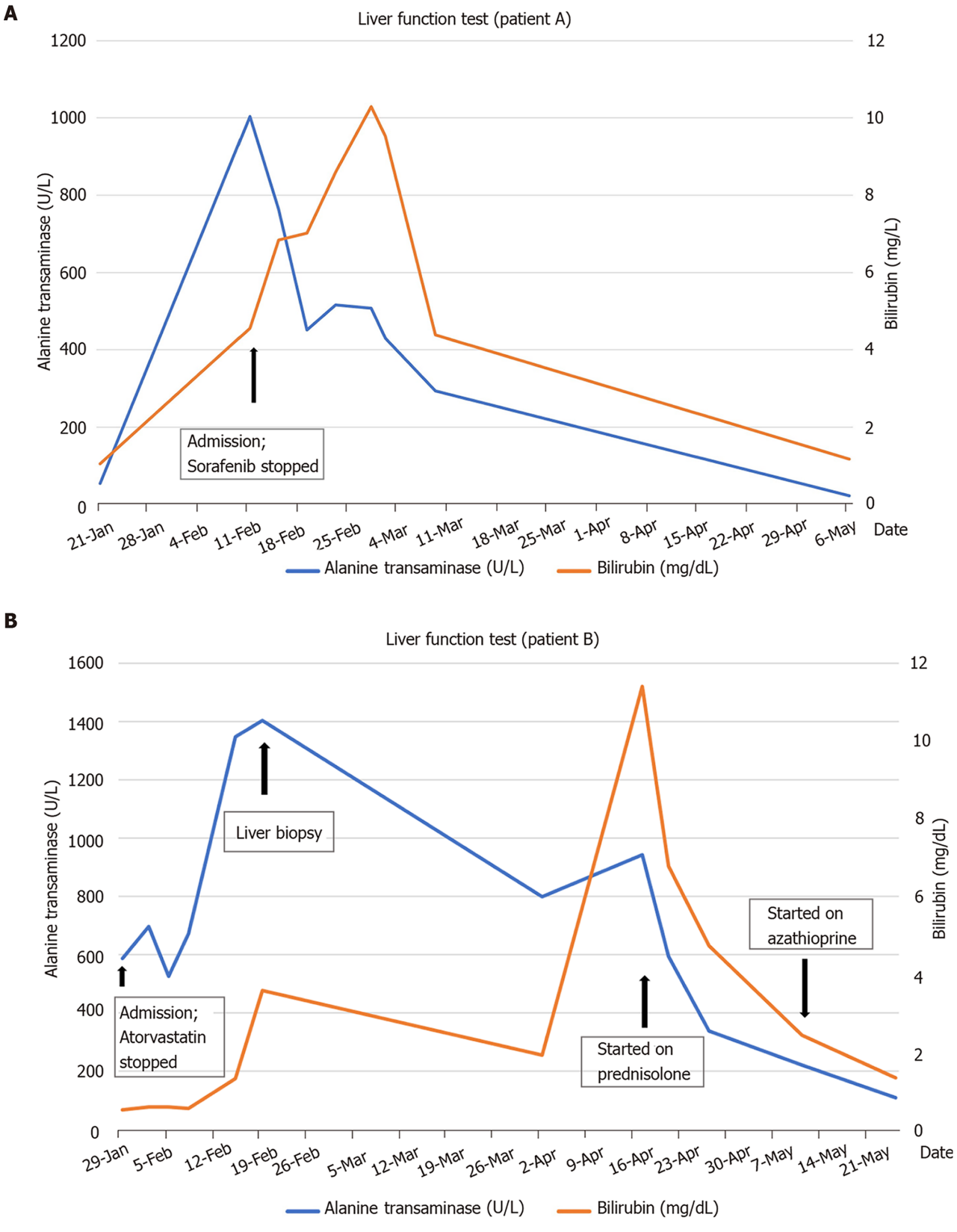

DOI: 10.3748/wjg.v28.i24.2654

Figure 2 Bilirubin and alanine transaminase trend for patients A and B. A: Patient A; B: Patient B.

Though there is no significant difference in the severity and outcomes of DIAIH compared to other types of DILI, it is crucial to identify DIAIH in patients who present with DILI, as DIAIH may require treatment with immunosuppressants if liver injury does not improve with cessation of possible culprit drugs[10,31,33]. A significantly higher proportion of patients (50% to 80%) with DIAIH are treated with corticosteroids/immunosuppressants as compared to non-DIAIH DILI, and DIAIH will need longer

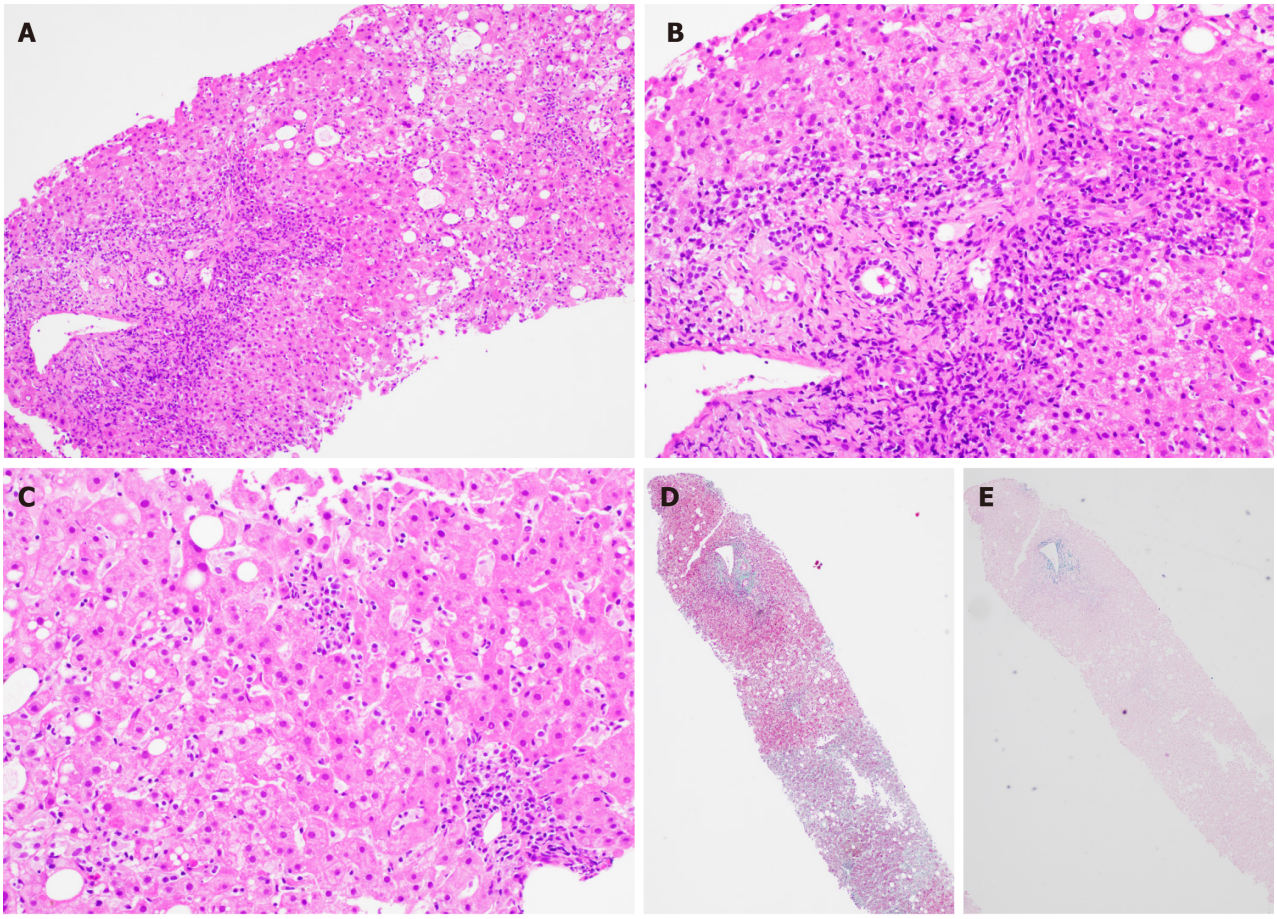

DOI: 10.3748/wjg.v28.i24.2654

Figure 3 Liver biopsy findings for patient B. A: Low power view [hematoxylin & eosin (H&E) 100 ×] shows portal and lobular inflammation with lobular disarray and mild steatosis; B: Higher magnification of the portal tract (H&E 200 ×) demonstrates moderate plasma cell-rich chronic inflammation with continuous interface damage; C: Lobulitis with aggregates of plasma cells and rosetting of hepatocytes is present in the lobule (H&E 200 ×); D and E: Masson trichrome (D, 40 ×) and Victoria blue (E, 40 ×) display mild early young fibrosis and paucity of elastic fibers, respectively. The absence of old mature type fibrosis suggested not a chronic injury. The autoimmune hepatitis histological pattern observed was therefore interpreted to be drug related, atorvastatin-induced.

term follow up even when LFT normalizes as late relapses may occur in up to 50% of cases where immunosuppressants are stopped[22]. Majority of relapses occur within a year, but some may present late up to 3 years after the initial diagnosis, and risk factors for late disease recurrence are not clear.

DIFFERENTIATING DIAIH AND IDIOPATHIC AIH

The second case highlights the difficulty in differentiating DIAIH from idiopathic AIH. Both conditions have overlapping clinical presentations with HC pattern of liver injury and may have detectable ANA, SMA, and raised IgG in some cases[10,11]. A number of studies compared the difference between DIAIH and AIH (Table 2), with the key differences summarized in Table 4. Some useful features to distinguish between these two entities:

Clinical presentation

Majority (60%-83%) of DIAIH present with an acute presentation, whereas it is seen in less than 20%-35% of cases with idiopathic AIH[10,34]. Most studies of the two conditions do not demonstrate a significant difference in LFT levels[14,21,30,34], but ALT[13,30,34], AST[14,34], and bilirubin[14,34] tend to be higher in patients with DIAIH. Only one study[20] showed a significantly higher level of bilirubin, AST, and ALT in patients with DIAIH. There was no significant difference in the proportion of patients with detectable ANA (77-94%)[20,21] and elevated IgG (36%-59%)[14], although one study showed AIH had higher level of serum IgG compared to DIAIH; it was not, however, statistically significant[14]. Immuno-allergic presentation with skin rash, fever, lymphadenopathy, and eosinophilia favor DIAIH, as it may occur in up to 30% of DIAIH[10,11].

Table 4 Comparison between drug-induced autoimmune hepatitis and autoimmune hepatitis

Clinical features	DIAIH	AIH
Demographics		
Female, %	82%[32]; 91%[34]	80% (P = 0.635)[32]; 92% (P = 0.95)[34]
Clinical presentation		
Acute presentation	> 60%[14]; 55%[32]; 83%[34]	< 20%[14]; 47% (P = 0.618)[32]; 35% (P < 0.001)[34]
Hypersensitivity reaction (fever, rash, eosinophilia)	Up to 30%[14]	Unusual[14]
Cirrhosis at presentation, %	0%[34]	34.8% (P = 0.07)[34]
Temporal relationship with drugs	Positive	Negative
Concurrent AI disease	Unusual[14]	Present in 14%-44%[14]
Biochemical results		
ALT (U/L), mean ± SD	548 ± 335[20]	227 ± 121 (P = 0.021)[20]
AST (U/L), mean ± SD	460 ± 321[20]	202 ± 57 (P = 0.018)[20]
Serology		
IgG, mean ± SD (g/L)	13.4 g/L[14]; 21.4 ± 7.5 [34]	18.6 g/L (P value non-significant)[14]; 24.3 ± 11.2 (P = 0.422)[34]
Pre-treatment score		
RUCAM score, median (range)	6 (3-10)[21]	3.5 (0-7) (P < 0.01)[21]
Revised IAIHG score, median (range)	9.5 (4-14)[21]	13 (9-18)[21]
Simplified AIH score, median (range)	4 (2-6)[21]	5 (1-7) (P = 0.385)[21]
Histopathology		
F3-F4, %	33.3%[34]	54.4% (P = 0.15)[34]
Typical histology (portal inflammation, interface hepatitis, plasma cells infiltrates)	18.2%[20]	54%[20]
Treatment and response to treatment		
Time to biochemical remission, mean (mo)	2[34]	16.8 (P <0.001)[34]
Treatment with Azathioprine or Mycophenolic acid in addition to corticosteroids, %	57%[13]; 15%[14]; 28% [20]; 20%[21]	86% (P = 0.024)[13]; 83% (P < 0.001)[14]; 90% (P = 0.023)[20]; 85% (P < 0.01)[21]
Biochemical remission, %	95%[21]	77.3% (P = 0.08)[21]
Treatment discontinuation, %	69%[14]; 100%[20]; 85% [21]; 25%[34]	26% (P < 0.02)[14]; 25% (P = 0.013)[20]; 5% (P < 0.1)[21]; 3% (P < 0.001) [34]
Relapse rate, %	0%[14]; 15%[21]; 60% [32]; 0%[34]	43% (P = 0.022)[14]; 70% (P < 0.01)[21]; 83% (P = 0.538)[32]; 18% (P = 0.10) [34]
Time to relapse (wk), median (range)	131 (37-216)[34]	14 (1-155) (P = 0.033)[34]
Outcomes		
Liver transplant/death, %	0%/0%[32,34]	2.8%/7% (P = 0.748 for liver transplant; p = 0.65 for death)[32]; 5.6%/2.8% (P = 0.40 for liver transplant; P = 0.55 for death)[34]

DIAIH: Drug-induced autoimmune hepatitis; DILI: Drug-induced liver injury; ALT: Alanine transaminase; AST: Aspartate transaminase; RUCAM: The Roussel Uclaf Causality Assessment Model; SD: Standard deviation.

AIH scoring and causality assessment

In a cohort of 44 patients with DIAIH and AIH, the simplified AIH score was not useful in differentiating the two entities[21]. Of note, patients with AIH had significantly higher pre-treatment AIH score compared to patients with DIAIH. The sensitivity and the specificity for pre-treatment AIH score (using a cut off of ≥ 12 – probable AIH) was shown to be 59% and 82%, respectively. As for RUCAM, using a cut off of ≥ 6 (probable), the specificity reaches 91%, albeit with a low sensitivity at 32%. When these are used in combination, there is still a potential for misdiagnosis in up to 11% of patients.

Histopathology

Both DIAIH and AIH share similar histological findings (portal and periportal infiltrates of lymphocytes, lobular hepatitis, plasma cells, and eosinophils) with no clear differentiating features, except presence of advance fibrosis or cirrhosis favoring idiopathic AIH[11,34]. However, a significantly higher proportion of patients with AIH showed typical features of AIH (54%) as compared to DIAIH (18.2%)[20], specifically in terms of portal inflammation with interface hepatitis and plasma cell infiltrates. The same study also found that DIAIH tended to have more eosinophilic infiltrates, which was not noted in other studies[21].

Treatment and response to treatment

The cornerstone in the management of DIAIH is to stop the culprit drug. Spontaneous improvement of LFT may then occur, as was observed in patient A. The most consistent and significant differentiating feature between DIAIH and AIH in published case series thus far lies in the response to treatment (Table 4). In cases where liver injury does not resolve despite cessation of the culprit drug or where the degree of DILI is severe, corticosteroids are usually started as per the initial management of AIH. Most studies on DIAIH exclusively include patients who were treated with immunosuppressants[14,20,21,30]. Both DIAIH and AIH showed excellent response to corticosteroids, with remission rate exceeding 90% in most cases[21,30-34].

It should be borne in mind that there is discrepancy in literature regarding the mean time to achieve immunosuppression induced remission in DIAIH and AIH. While one study demonstrated similar 3 mo mean time to remission[21] in both conditions, another showed a significant difference, where DIAIH took a significantly shorter time than AIH to achieve remission[34] (2 mo *vs* 16.8 mo). This may be attributed to the heterogeneity of the study population. Resolution of DIAIH usually occurs after 1 mo (rarely up to 3 mo) of immunosuppression. Unlike in AIH, DIAIH rarely requires long term immunosuppression and has very low relapse rates after cessation of immunosuppressants over a long follow-up of up to 4 years[10,11,13-15,20,21,34] (Table 2). In cases where DIAIH relapses, the time to relapse is significantly longer compared to AIH[30], which implies that patients with DIAIH will require a longer period of follow-up after resolution of liver injury as compared to the usual DILI. Interestingly, despite similar time to remission in the two groups, Weber *et al*[21] showed that an early rapid response to corticosteroid treatment differentiates DIAIH from AIH with good sensitivity and specificity at 77%, respectively. The early rapid response was defined by 9% drop of ALT per day in the first week of corticosteroid therapy.

The use of steroids appears to be a promising means of differentiating DIAIH or AIH in the early course of disease with better sensitivity than RUCAM and AIH score[21]. This also has the potential benefit of avoiding long term immunosuppressive therapy in DIAIH. Also, in 30%-35% of DIAIH cases that were initially seropositive for ANA and SMA, the antibodies became undetectable at 6 mo following the initial DILI, which was independent of treatment with corticosteroids[15].

Major hepatology society guidelines recommend a similar approach in terms of corticosteroids initiation in non-resolving DIAIH and AIH[10,11]. However, there is no consensus regarding treatment duration and methods to confirm remission before discontinuation of immunosuppressants. Thus, the decision and timing to stop treatment should be assessed on case-by-case basis[10]. In fact, one study has shown success in tapering off immunosuppression within 3-17 mo without evidence of relapse[20].

Risk alleles and monocyte-derived hepatocyte like cells

Risk alleles for idiopathic AIH such as HLA DRB1 DRB1*03:01 or DRB1*04:01 are uncommon in DIAIH and, if this is detected, may favor a diagnosis of AIH[10]. The MetaHeps® test, which uses monocyte-derived hepatocyte-like cells, has been used to differentiate DIAIH from AIH with high sensitivity and specificity[21]. However, this test is not readily available, thereby limiting its utility in clinical practice. The lymphocyte toxicity assay described by Neuman *et al*[35] can sometimes be helpful in differentiating drug hypersensitivity syndromes from idiopathic AIH as well.

Outcomes

The long-term outcome of DIAIH is excellent with a survival rate between 90%-100% without liver transplantation[10]. This is in contrast with idiopathic AIH, where there is a high risk of relapse upon treatment withdrawal and risk of progression to cirrhosis, resulting in the need for liver transplantation [10,11,34]. It is also noteworthy that DIAIH can lead to chronic DILI with abnormal LFT lasting more than 6 mo in 17%-22% of cases[15,36].

CONCLUSION

In summary, it is important to differentiate between DIAIH and AIH in patients who present with DILI, as the management and outcome differ. Early recognition of DIAIH is key as the mainstay of management is cessation of culprit drug and in some cases, initiation of corticosteroids with the aim to

avoid long-term immunosuppression.

ACKNOWLEDGEMENTS

We acknowledge all our colleagues in the Department of Gastroenterology and Hepatology and Pathology at Changi General Hospital who help manage the 2 patients described in the manuscript. We would also like to thank the 2 patients described here who readily consented to be described in this manuscript.

FOOTNOTES

Author contributions: Kumar R and Tan CK conceptualized the study; Tan CK, Ho D, and Kumar R wrote the initial manuscript; Wand LM provided critical input and histo-pathological slides for the manuscript; all authors were involved in the critical revision.

Conflict-of-interest statement: All authors have no relevant conflict of interest to report.

Country/Territory of origin: Singapore

ORCID number: Chin Kimg Tan 0000-0002-3918-4340; Danielle Ho 0000-0003-0652-406x; Lai Mun Wang 0000-0001-7113-4215; Rahul Kumar 0000-0002-5092-4821.

S-Editor: Yan JP
L-Editor: Filipodia
P-Editor: Yan JP

REFERENCES

1 **Björnsson ES**, Bergmann OM, Björnsson HK, Kvaran RB, Olafsson S. Incidence, presentation, and outcomes in patients with drug-induced liver injury in the general population of Iceland. *Gastroenterology* 2013; **144**: 1419-1425, 1425.e1 [PMID: 23419359 DOI: 10.1053/j.gastro.2013.02.006]
2 **Shen T**, Liu Y, Shang J, Xie Q, Li J, Yan M, Xu J, Niu J, Liu J, Watkins PB, Aithal GP, Andrade RJ, Dou X, Yao L, Lv F, Wang Q, Li Y, Zhou X, Zhang Y, Zong P, Wan B, Zou Z, Yang D, Nie Y, Li D, Wang Y, Han X, Zhuang H, Mao Y, Chen C. Incidence and Etiology of Drug-Induced Liver Injury in Mainland China. *Gastroenterology* 2019; **156**: 2230-2241.e11 [PMID: 30742832 DOI: 10.1053/j.gastro.2019.02.002]
3 **Ostapowicz G**, Fontana RJ, Schiødt FV, Larson A, Davern TJ, Han SH, McCashland TM, Shakil AO, Hay JE, Hynan L, Crippin JS, Blei AT, Samuel G, Reisch J, Lee WM; U. S. Acute Liver Failure Study Group. Results of a prospective study of acute liver failure at 17 tertiary care centers in the United States. *Ann Intern Med* 2002; **137**: 947-954 [PMID: 12484709 DOI: 10.7326/0003-4819-137-12-200212170-00007]
4 **Wei G**, Bergquist A, Broomé U, Lindgren S, Wallerstedt S, Almer S, Sangfelt P, Danielsson A, Sandberg-Gertzén H, Lööf L, Prytz H, Björnsson E. Acute liver failure in Sweden: etiology and outcome. *J Intern Med* 2007; **262**: 393-401 [PMID: 17697161 DOI: 10.1111/j.1365-2796.2007.01818.x]
5 **Björnsson E**, Jerlstad P, Bergqvist A, Olsson R. Fulminant drug-induced hepatic failure leading to death or liver transplantation in Sweden. *Scand J Gastroenterol* 2005; **40**: 1095-1101 [PMID: 16165719 DOI: 10.1080/00365520510023846]
6 **Ohmori S**, Shiraki K, Inoue H, Okano H, Yamanaka T, Deguchi M, Sakai T, Takase K, Nakano T, Tameda Y. Clinical characteristics and prognostic indicators of drug-induced fulminant hepatic failure. *Hepatogastroenterology* 2003; **50**: 1531-1534 [PMID: 14571779]
7 **Chalasani N**, Bonkovsky HL, Fontana R, Lee W, Stolz A, Talwalkar J, Reddy KR, Watkins PB, Navarro V, Barnhart H, Gu J, Serrano J; United States Drug Induced Liver Injury Network. Features and Outcomes of 899 Patients With Drug-Induced Liver Injury: The DILIN Prospective Study. *Gastroenterology* 2015; **148**: 1340-52.e7 [PMID: 25754159 DOI: 10.1053/j.gastro.2015.03.006]
8 **Aithal GP**, Watkins PB, Andrade RJ, Larrey D, Molokhia M, Takikawa H, Hunt CM, Wilke RA, Avigan M, Kaplowitz N, Bjornsson E, Daly AK. Case definition and phenotype standardization in drug-induced liver injury. *Clin Pharmacol Ther* 2011; **89**: 806-815 [PMID: 21544079 DOI: 10.1038/clpt.2011.58]
9 **Weiler-Normann C**, Schramm C. Drug induced liver injury and its relationship to autoimmune hepatitis. *J Hepatol* 2011; **55**: 747-749 [PMID: 21396413 DOI: 10.1016/j.jhep.2011.02.024]

10 **Mack CL**, Adams D, Assis DN, Kerkar N, Manns MP, Mayo MJ, Vierling JM, Alsawas M, Murad MH, Czaja AJ. Diagnosis and Management of Autoimmune Hepatitis in Adults and Children: 2019 Practice Guidance and Guidelines From the American Association for the Study of Liver Diseases. *Hepatology* 2020; **72**: 671-722 [PMID: 31863477 DOI: 10.1002/hep.31065]

11 **European Association for the Study of the Liver**. EASL Clinical Practice Guidelines: Autoimmune hepatitis. *J Hepatol* 2015; **63**: 971-1004 [PMID: 26341719 DOI: 10.1016/j.jhep.2015.06.030]

12 **Gordon V**, Adhikary R, Appleby V, Das D, Day J, Delahooke T, Dixon S, Elphick D, Hardie C, Hoeroldt B, Hooper P, Hutchinson J, Jones R, Khan F, Aithal GP, McGonigle J, Nelson A, Nkhoma A, Pelitari S, Prince M, Prosser A, Sathanarayana V, Savva S, Shah N, Saksena S, Thayalasekaran S, Vani D, Yeoman A, Gleeson D; UK Multi-Centre AIH Audit Group. Diagnosis, presentation and initial severity of Autoimmune Hepatitis (AIH) in patients attending 28 hospitals in the UK. *Liver Int* 2018; **38**: 1686-1695 [PMID: 29455458 DOI: 10.1111/liv.13724]

13 **Björnsson E**, Talwalkar J, Treeprasertsuk S, Kamath PS, Takahashi N, Sanderson S, Neuhauser M, Lindor K. Drug-induced autoimmune hepatitis: clinical characteristics and prognosis. *Hepatology* 2010; **51**: 2040-2048 [PMID: 20512992 DOI: 10.1002/hep.23588]

14 **Valgeirsson KB**, Hreinsson JP, Björnsson ES. Increased incidence of autoimmune hepatitis is associated with wider use of biological drugs. *Liver Int* 2019; **39**: 2341-2349 [PMID: 31436903 DOI: 10.1111/liv.14224]

15 **de Boer YS**, Kosinski AS, Urban TJ, Zhao Z, Long N, Chalasani N, Kleiner DE, Hoofnagle JH; Drug-Induced Liver Injury Network. Features of Autoimmune Hepatitis in Patients With Drug-induced Liver Injury. *Clin Gastroenterol Hepatol* 2017; **15**: 103-112.e2 [PMID: 27311619 DOI: 10.1016/j.cgh.2016.05.043]

16 **Licata A**, Maida M, Cabibi D, Butera G, Macaluso FS, Alessi N, Caruso C, Craxì A, Almasio PL. Clinical features and outcomes of patients with drug-induced autoimmune hepatitis: a retrospective cohort study. *Dig Liver Dis* 2014; **46**: 1116-1120 [PMID: 25224696 DOI: 10.1016/j.dld.2014.08.040]

17 **Czaja AJ**. Drug-induced autoimmune-like hepatitis. *Dig Dis Sci* 2011; **56**: 958-976 [PMID: 21327704 DOI: 10.1007/s10620-011-1611-4]

18 **Russo MW**, Scobey M, Bonkovsky HL. Drug-induced liver injury associated with statins. *Semin Liver Dis* 2009; **29**: 412-422 [PMID: 19826975 DOI: 10.1055/s-0029-1240010]

19 **Perdices EV**, Medina-Cáliz I, Hernando S, Ortega A, Martín-Ocaña F, Navarro JM, Peláez G, Castiella A, Hallal H, Romero-Gómez M, González-Jiménez A, Robles-Díaz M, Lucena MI, Andrade RJ. Hepatotoxicity associated with statin use: analysis of the cases included in the Spanish Hepatotoxicity Registry. *Rev Esp Enferm Dig* 2014; **106**: 246-254 [PMID: 25075655]

20 **Wang H**, Fu J, Liu G, Wang L, Yan A, Wang G. Drug induced autoimmune hepatitis (DIAIH): Pathological and clinical study. *Biomed Res* 2017; **28**: 6028-6034

21 **Weber S**, Benesic A, Rotter I, Gerbes AL. Early ALT response to corticosteroid treatment distinguishes idiosyncratic drug-induced liver injury from autoimmune hepatitis. *Liver Int* 2019; **39**: 1906-1917 [PMID: 31319011 DOI: 10.1111/liv.14195]

22 **Hisamochi A**, Kage M, Ide T, Arinaga-Hino T, Amano K, Kuwahara R, Ogata K, Miyajima I, Kumashiro R, Sata M, Torimura T. An analysis of drug-induced liver injury, which showed histological findings similar to autoimmune hepatitis. *J Gastroenterol* 2016; **51**: 597-607 [PMID: 26519284 DOI: 10.1007/s00535-015-1131-7]

23 **Beaune P**, Dansette PM, Mansuy D, Kiffel L, Finck M, Amar C, Leroux JP, Homberg JC. Human anti-endoplasmic reticulum autoantibodies appearing in a drug-induced hepatitis are directed against a human liver cytochrome P-450 that hydroxylates the drug. *Proc Natl Acad Sci U S A* 1987; **84**: 551-555 [PMID: 3540968 DOI: 10.1073/pnas.84.2.551]

24 **Bourdi M**, Larrey D, Nataf J, Bernuau J, Pessayre D, Iwasaki M, Guengerich FP, Beaune PH. Anti-liver endoplasmic reticulum autoantibodies are directed against human cytochrome P-450IA2. A specific marker of dihydralazine-induced hepatitis. *J Clin Invest* 1990; **85**: 1967-1973 [PMID: 2347920 DOI: 10.1172/JCI114660]

25 **Czaja AJ**. Autoimmune hepatitis. Part A: pathogenesis. *Expert Rev Gastroenterol Hepatol* 2007; **1**: 113-128 [PMID: 19072440 DOI: 10.1586/17474124.1.1.113]

26 **Liu ZX**, Kaplowitz N. Immune-mediated drug-induced liver disease. *Clin Liver Dis* 2002; **6**: 755-774 [PMID: 12362579 DOI: 10.1016/s1089-3261(02)00025-9]

27 **Alvarez F**, Berg PA, Bianchi FB, Bianchi L, Burroughs AK, Cancado EL, Chapman RW, Cooksley WG, Czaja AJ, Desmet VJ, Donaldson PT, Eddleston AL, Fainboim L, Heathcote J, Homberg JC, Hoofnagle JH, Kakumu S, Krawitt EL, Mackay IR, MacSween RN, Maddrey WC, Manns MP, McFarlane IG, Meyer zum Büschenfelde KH, Zeniya M. International Autoimmune Hepatitis Group Report: review of criteria for diagnosis of autoimmune hepatitis. *J Hepatol* 1999; **31**: 929-938 [PMID: 10580593 DOI: 10.1016/s0168-8278(99)80297-9]

28 **Czaja AJ**. Performance parameters of the diagnostic scoring systems for autoimmune hepatitis. *Hepatology* 2008; **48**: 1540-1548 [PMID: 18924244 DOI: 10.1002/hep.22513]

29 **Danan G**, Benichou C. Causality assessment of adverse reactions to drugs--I. A novel method based on the conclusions of international consensus meetings: application to drug-induced liver injuries. *J Clin Epidemiol* 1993; **46**: 1323-1330 [PMID: 8229110 DOI: 10.1016/0895-4356(93)90101-6]

30 **Yeong TT**, Lim KH, Goubet S, Parnell N, Verma S. Natural history and outcomes in drug-induced autoimmune hepatitis. *Hepatol Res* 2016; **46**: E79-E88 [PMID: 25943838 DOI: 10.1111/hepr.12532]

31 LiverTox: Clinical and Research Information on Drug-Induced Liver Injury [Internet]. Bethesda (MD): National Institute of Diabetes and Digestive and Kidney Diseases; 2012– [PMID: 31643176]

32 **Aliberti S**, Grignani G, Allione P, Fizzotti M, Galatola G, Pisacane A, Aglietta M. An acute hepatitis resembling autoimmune hepatitis occurring during imatinib therapy in a gastrointestinal stromal tumor patient. *Am J Clin Oncol* 2009; **32**: 640-641 [PMID: 19955903 DOI: 10.1097/COC.0b013e31802b4ef7]

33 **Chalasani NP**, Maddur H, Russo MW, Wong RJ, Reddy KR; Practice Parameters Committee of the American College of Gastroenterology. ACG Clinical Guideline: Diagnosis and Management of Idiosyncratic Drug-Induced Liver Injury. *Am J Gastroenterol* 2021; **116**: 878-898 [PMID: 33929376 DOI: 10.14309/ajg.0000000000001259]

34 **Martínez-Casas OY**, Díaz-Ramírez GS, Marín-Zuluaga JI, Muñoz-Maya O, Santos O, Donado-Gómez JH, Restrepo-Gutiérrez JC. Differential characteristics in drug-induced autoimmune hepatitis. *JGH Open* 2018; **2**: 97-104 [PMID:

30483571 DOI: 10.1002/jgh3.12054]

35 **Neuman MG**, Malkiewicz IM, Shear NH. A novel lymphocyte toxicity assay to assess drug hypersensitivity syndromes. *Clin Biochem* 2000; **33**: 517-524 [PMID: 11124336 DOI: 10.1016/s0009-9120(00)00146-6]

36 **Castiella A**, Zapata E, Lucena MI, Andrade RJ. Drug-induced autoimmune liver disease: A diagnostic dilemma of an increasingly reported disease. *World J Hepatol* 2014; **6**: 160-168 [PMID: 24799984 DOI: 10.4254/wjh.v6.i4.160]

37 **Stephens C**, Robles-Diaz M, Medina-Caliz I, Garcia-Cortes M, Ortega-Alonso A, Sanabria-Cabrera J, Gonzalez-Jimenez A, Alvarez-Alvarez I, Slim M, Jimenez-Perez M, Gonzalez-Grande R, Fernández MC, Casado M, Soriano G, Román E, Hallal H, Romero-Gomez M, Castiella A, Conde I, Prieto M, Moreno-Planas JM, Giraldez A, Moreno-Sanfiel JM, Kaplowitz N, Lucena MI, Andrade RJ; Participating clinical centres. Comprehensive analysis and insights gained from long-term experience of the Spanish DILI Registry. *J Hepatol* 2021; **75**: 86-97 [PMID: 33539847 DOI: 10.1016/j.jhep.2021.01.029]

World Journal of Gastroenterology

Submit a Manuscript: https://www.f6publishing.com

World J Gastroenterol 2022 June 28; 28(24): 2667-2679

DOI: 10.3748/wjg.v28.i24.2667

ISSN 1007-9327 (print) ISSN 2219-2840 (online)

MINIREVIEWS

Rebuilding trust in proton pump inhibitor therapy

Alla Turshudzhyan, Sonia Samuel, Angela Tawfik, Micheal Tadros

Specialty type: Gastroenterology and hepatology

Provenance and peer review: Invited article; Externally peer reviewed.

Peer-review model: Single blind

Peer-review report's scientific quality classification

Grade A (Excellent): 0
Grade B (Very good): B, B
Grade C (Good): 0
Grade D (Fair): 0
Grade E (Poor): 0

P-Reviewer: Chen LW, Taiwan; Sano W, Japan

Received: January 10, 2022
Peer-review started: January 10, 2022
First decision: March 8, 2022
Revised: March 15, 2022
Accepted: May 8, 2022
Article in press: May 8, 2022
Published online: June 28, 2022

Alla Turshudzhyan, Department of Medicine, University of Connecticut, Farmington, CT 06030, United States

Sonia Samuel, Department of Medicine, Albany Medical College, Albany, NY 12208, United States

Angela Tawfik, Guilderland High School, Guilderland Center, Albany, NY 12085, United States

Micheal Tadros, Department of Gastroenterology and Hepatology, Albany Medical College, Albany, NY 12208, United States

Corresponding author: Micheal Tadros, FACG, MD, Associate Professor, Department of Gastroenterology and Hepatology, Albany Medical College, 49 New Scotland Ave, Albany, NY 12208, United States. tadrosm1@amc.edu

Abstract

Introduction of proton pump inhibitor (PPI) therapy into clinical practice has revolutionized treatment approach to acid-related diseases. With its clinical success came a widespread use of PPI therapy. Subsequently, several studies found that PPIs were oftentimes overprescribed in primary care and emergency setting, likely attributed to seemingly low side-effect profile and physicians having low threshold to initiate therapy. However, now there is a growing concern over PPI side-effect profile among both patients and providers. We would like to bring more awareness to the currently available guidelines on PPI use, discuss clinical indications for PPIs and the evidence behind the reported side-effects. We hope that increased awareness of proper PPI use will make the initiation or continuation of therapy a well informed and an evidence-based decision between patient and physician. We also hope that discussing evidence behind the reported side-effect profile will help clarify the growing concerns over PPI therapy.

Key Words: Proton pump inhibitor; Side-effects; Gastro-esophageal reflux disease; Therapy

Core Tip: Proton pump inhibitor (PPI) therapy is a cornerstone therapy for acid-related diseases. Its clinical success can be attributed to anti-secretory properties superior to any prior agents and seemingly low side-effects profile. As more patients were started and continued PPI therapy long-term, some studies began reporting side-effects associated with this therapy. Concerns over risks associated with PPI use grew over the last couple of years among both patients and providers. We hope to bring awareness to the current guidelines and the evidence behind the reported side-effects as better understanding of this evidence can improve medical practice. Both patients and providers should have all the evidence at hand when discussing initiation or continuation of PPI therapy.

Citation: Turshudzhyan A, Samuel S, Tawfik A, Tadros M. Rebuilding trust in proton pump inhibitor therapy. *World J Gastroenterol* 2022; 28(24): 2667-2679
URL: https://www.wjgnet.com/1007-9327/full/v28/i24/2667.htm
DOI: https://dx.doi.org/10.3748/wjg.v28.i24.2667

INTRODUCTION

Proton pump inhibitors (PPIs) were first introduced more than two decades ago but have quickly become a cornerstone therapy for the acid-related diseases. They were regarded for their superior antisecretory properties and seemingly low side-effect profile, which ultimately contributed to low threshold for therapy initiation[1]. They became first-line treatment for esophagitis, gastro-esophageal reflux disease (GERD), peptic ulcer disease (PUD), Zollinger-Ellison syndrome (ZES), and *Helicobacter pylori* (*H. pylori*) infection[2]. Many patients started on PPI therapy continued it long-term without a clear expectation of the therapy duration. Rising number of patients on chronic PPI therapy led to growing concerns over medication side-effect profile. Especially as some reports claimed that improper long-term PPI use has risen significantly in the last decade with some data suggesting that only half of patients on PPI therapy had an appropriate indication[3,4]. Improper PPI use is multifactorial and comes from a pattern of preventable chain of events (Figure 1). This discussion is important because PPIs affect patients' quality of life, and need to be taken judiciously and according to the evidence-based guidelines.

BACKGROUND

PPIs work by suppressing gastric acid secretion by directly inhibiting gastric acid pump (H+/K+ adenosine triphosphatase (ATPase)) of the parietal cells[5]. PPIs are prodrugs that are only activated once exposed to the acidic environment of the parietal cells[6]. Once active, their half-life ranges from 0.6-1.9 h, depending on the type of PPIs used (Table 1)[7-9]. After PPIs are no longer metabolically active, they are metabolized by the hepatic P450 enzymes, primarily by CYP2C19 with minor contribution from CYP3A4 (Table 1)[6,10]. Once metabolized, they are excreted renally, with lansoprazole and dexlasoprazole also being excreted by the gut (Table 1)[11].

Not all patients metabolize PPIs at the same rate, causing variation in bioavailability. The hepatic P450 system is partially responsible for this variation. Patients of Asian ethnicity and older patients tend to have slower P450 systems and, as a result, have increased bioavailability of PPIs[6].

Currently available PPIs include esomeprazole, lansoprazole, omeprazole, dexlansoprazole, pantoprazole, and rabeprazole[12]. None of the PPIs has shown superiority in their antisecretory properties and are used interchangeably in clinical practice[13]. While there are no studies to support superiority, omeprazole is among the 10 most prescribed medications in the United States[6]. From the variety of PPIs available, esomeprazole and lansoprazole have the highest bioavailability: 89% and 80%-90%, respectively (Table 1)[11]. The lowest bioavailability is seen with rabeprazole at 52%[11]. Majority of PPIs must be taken 30 min prior to the first meal of the day. Esomeprazole requires 60 min prior to food intake administration[14]. Pharmacokinetics of dexlansoprazole, pantoprazole, and rabeprazole are unaffected by the food ingestion and can be taken at any time (Table 1)[14].

CLINICAL INDICATIONS

PPIs are used as a first line therapy for GERD, acid-related erosive esophagitis, peptic stricture, Barrett esophagus, and high risk of ulcer bleeding while on nonsteroidal anti-inflammatory drugs (NSAID) therapy[15]. It is also considered for treatment of eosinophilic esophagitis (EoE), non-erosive reflux disease (NERD), *H. pylori* infection (in combination with antibiotics), hypersecretory syndromes (*e.g.*

Table 1 Type of proton pump inhibitor available

PPI	Omeprazole	Esomeprazole	Lansoprazole	Dexlansoprazole	Pantoprazole	Rabeprazole
Half-life (T1/2) (hrs)[7-9]	0.6-1.0[7]	1.1[8]	0.9-1.6[7]	1-2[9]	0.9-1.9[7]	1[7]
Hepatic metabolism[10]	Major: CYP2C19; minor: CYP3A4	Major: CYP2C19; minor: CYP3A4	Major: CYP2C19; minor: CYP3A4	Major: CYP2C19; minor: CYP3A4	Minor: CYP3A4 CYP2C19	Non-enzymatic reduction minor: CYP2C19 and CYP3A4
Elimination[11]	Renal	Renal	Renal/fecal	Renal/fecal	Renal	Renal
Oral bioavailability (%)[11]	40-50	89	80-90	50-60	77	52
Food effect[14]	30 min before breakfast	60 min before breakfast	30 min before breakfast	Pharmacokinetics unaffected by meals	Pharmacokinetics unaffected by meals (exception oral suspension: 30 min prior to meal)	Pharmacokinetics unaffected by meals (exception capsule sprinkle: 30 min prior to meal)

PPI: Proton pump inhibitor.

DOI: 10.3748/wjg.v28.i24.2667

Figure 1 Improper proton pump inhibitor use is multifactorial and comes from a pattern of preventable chain of events. PPI: Proton pump inhibitor.

ZES), prolonged mechanical ventilation, and functional dyspepsia[16]. While PPIs are considered for gastroprotection for patients on NSAID therapy, steroids are not an indication to start PPIs when used in ambulatory setting[17,18]. Some reports did suggest that there is an increased risk of PUD in patients taking steroids, but it was only statistically significant in hospitalized patients on brief courses of steroids[18]. As a result, these patients may be considered for a brief PPI therapy while inpatient. PPIs can also be used in conjunction with pancreatic enzyme replacement for refractory steatorrhea[17,19].

CURRENT GUIDELINES ON PPI USE

The current guidelines for PPIs are created for clinicians to prescribe PPIs appropriately and effectively to the patients who would benefit from the therapy. We are going to discuss guidelines proposed by multiple societies including the American College of Gastroenterology (ACG), American Gastroenterological Association (AGA), Society of American Gastrointestinal and Endoscopic Surgeons (SAGES), the Canadian Association of Gastroenterology (CAG), and the European guidelines (Table 2). All these guidelines are of moderate to high quality of evidence and are recommended strongly unless indicated

Table 2 Guidelines on proton pump inhibitor use

ACG/ACG/CAG/SAGES/European guidelines	Recommendation
GERD[19,20,22]	Trial an 8-wk duration of once daily PPI in patients with heartburn and regurgitation without reflux symptoms
	Once daily dosing-administer PPIs 30 min to 1 h before a meal; twice daily dosing-administer PPIs 30 min to 1 h before breakfast and dinner
	For patients experiencing refractory GERD, optimize PPI therapy with patient compliance, dosage and timing to achieve symptom control before further exploration
	Prescribe continuous daily PPIs over H2RAs for erosive esophagitis maintenance healing
	Continue lifelong PPIs in patients with LA Grade C or D erosive esophagitis
	If patients with normal esophageal mucosa or LA Grade A esophagitis have normal ambulatory reflux monitoring results after 2-4 wk discontinuation of PPI therapy, it is strongly recommended to stop PPI use (low level of evidence)
Dyspepsia[23]	Patients < 60 years old, tested *H. pylori* negative or symptoms persist after eradication therapy, should start empiric PPI therapy
	Functional dyspepsia patients, tested *H. pylori* negative or symptomatic after infection treatment, should be on PPIs
H. pylori infection[24]	If active or history of PUD, and tested *H. pylori* positive, start eradication treatment (10-14 d) with PPIs and antibiotics
	Dyspepsia patients found to be *H. pylori* positive on gastric biopsy, treat with eradication therapy consisting of PPIs and antibiotics for 10-14 d
	GERD patients who are found *H. pylori* positive should be offered eradication therapy for 10-14 d course
	Use levofloxacin triple regimen consisting of PPI, amoxicillin and levofloxacin as salvage therapy if first line eradication therapy fails
Barrett's esophagus[25,26]	Recommend once daily dosing PPIs primarily indicated for symptomatic relief
	Twice daily dosing can be considered in patients with esophagitis or poor symptomatic relief
EoE [28,29]	Recommend PPI therapy for clinical and histological remission of EoE
NSAIDs[31,32]	PPIs are indicated for patients at risk of GI bleeds for gastroprotection (age > 65 years, high dose NSAID use, previous history of ulcers, concomitant therapy with corticosteroids, anticoagulants and antithrombotics)
	Prescribe continuous or intermittent high dose PPI the following 3 d after GI ulcer bleed was stopped endoscopically

ACG: American College of Gastroenterology; AGA: American Gastroenterological Association; SAGES: Society of American Gastrointestinal and Endoscopic Surgeons; CAG: Canadian Association of Gastroenterology; PPI: Proton pump inhibitor; *H. pylori*: *Helicobacter pylori*; H2RA: Histamine 2 receptor antagonist; GERD: Gastro-esophageal reflux disease; PUD: Peptic ulcer disease; LA: Los Angeles; EoE: Eosinophilic esophagitis; NSAID: Nonsteroidal anti-inflammatory drug; GI: Gastrointestinal.

otherwise.

GERD treatment guidelines

An 8-wk duration of once daily PPIs is strongly recommended in patients with GERD to assess for adequate response. However, if GERD appears to be refractory, optimal PPI therapy should be confirmed first before further investigation. While there is no standardized definition of long-term PPI use, based on the ACG 2021 GERD guidelines, 8-wk therapy is the therapy duration following which patients get stratified into those who responded to therapy and those who are refractory to therapy[20]. Optimal therapy includes ensuring the patient is compliant with PPI therapy and takes medications appropriately with correct timing and dosage. Multiple studies show that a significant number of patients who optimize therapy improve symptoms[20]. In patients with known erosive esophagitis, medical therapy with daily PPIs is recommended but is given at half of the healing dose for maintenance to prevent recurrence[21]. PPIs should be prescribed over histamine 2 receptor antagonists (H2RAs) for erosive esophagitis due to their superiority in faster healing rates and better heartburn symptom control. It was found that almost all patients with Los Angeles (LA) grade C erosive esophagitis who stopped PPI therapy relapsed within 6 mo. However, recurrence of erosive esophagitis may occur as soon as 1 wk to 2 wk after PPI discontinuation. It is therefore recommended patients who have a more severe esophagitis (LA grade C or D) should be on a lifelong PPI therapy[20]. It is

important to note that PPI therapy may be ineffective in patients with large hiatal hernias. Transabdominal or transthoracic large hiatal hernia repairs should be strongly considered in patients who experience symptoms of severe gastroesophageal reflux, gastric outlet obstruction and/or strangulation. Fundoplication as a treatment option for reflux produced mixed outcomes and therefore no strong recommendation can be made[22].

In patients with an unclear GERD diagnosis, ambulatory reflux monitoring may be helpful in guiding PPI therapy in patients with refractory reflux symptoms and without severe esophagitis[23]. This diagnostic approach helps support or negate a GERD diagnosis. Patients with incomplete symptom relief after an 8-wk course of PPI therapy can discontinue PPIs for 2-4 wk. If normal results in reflux monitoring are seen after PPI cessation in patients with normal EGD findings or LA Grade A esophagitis, then other causes of symptoms should be investigated, and PPI therapy can be stopped. Although this approach is strongly recommended, more studies are necessary for high evidence support [20].

Dyspepsia treatment guidelines

Several randomized control trials (RCTs) found a statistically significant effect in use of once daily PPI dosing for symptomatic relief of dyspepsia symptoms. It is therefore strongly recommended that patients under 60 years of age who tested *H. pylori* negative or continue to experience symptoms after *H. pylori* treatment should be prescribed empiric PPI therapy. Functional dyspepsia patients are also recommended a two-to-eight-week duration of PPI course for symptomatic improvement with some RCTs suggesting a number needed to treat of 10. However, if patients do not respond after 8 wk of therapy, PPIs should be discontinued as there was no utility found in increasing the dose. Other drug therapies can therefore be considered in symptomatic management[24].

H. pylori treatment guidelines

Patients with current or history of peptic ulcer without known *H. pylori* eradication should be tested with a urea breath test, fecal antigen test or gastric mucosal biopsy. If *H. pylori* positive, treatment options should be offered. Eradication treatments include first line bismuth quadruple therapy (PPI, bismuth, tetracycline and nitroimidazole) or clarithromycin triple therapy (PPI, clarithromycin, and amoxicillin or metronidazole) for 10-14 d. If gastric biopsies are done in patients with dyspepsia and are found to be *H. pylori* positive, multiple studies demonstrated that eradication treatment improves symptoms. If patients with GERD do not experience symptoms of dyspepsia or have a history of PUD, it is unnecessary to test for *H. pylori*. However, if found to be positive, treatment options should be offered. If first line therapy for eradication treatment fails, it is recommended to use the levofloxacin triple regimen as a salvage treatment. The regimen consists of PPI, amoxicillin, and levofloxacin. A treatment duration of 14 d can be effective but supported by low quality of evidence so further studies are warranted[25].

Barrett's esophagus treatment guidelines

Patients with Barrett's esophagus are typically prescribed PPIs due to GERD symptoms and to reduce the risk of neoplastic changes. Several studies demonstrated that maintenance PPI therapy reduced risk of neoplastic changes compared to H2RA therapy or no anti-acid reflux medications. According to the AGA and ACG guidelines, once-daily PPI therapy is recommended for patients with Barrett's esophagus[26,27]. Twice daily dosing can be considered in BE patients with inadequate symptomatic control or in patients with esophagitis[26].

EoE

Previous guidelines suggested PPI use as a trial therapy to differentiate EoE from GERD[28]. However, the PPI trial should no longer be used as GERD and EoE share many similarities and are not mutually exclusive entities[29]. The 2017 United European Gastroenterology (UEG) guidelines suggested PPIs as recommended treatment for EoE which is proven to demonstrate symptomatic improvement and histological remission. Early observational studies and case reports demonstrated this phenomenon and many RCTs followed which supported the use of PPI therapy in EoE. A recent systematic review with meta-analysis showed clinical improvement and histological remission with PPI therapy[30]. Duration and dosage for treatment is however still under investigation; twice daily administration and long-term PPI therapy is recommended but has low evidence[30].

NSAID use

PPI therapy is necessary to prevent NSAID-related ulcer complications including upper gastrointestinal (GI) bleeds. Many studies reported decreased prevalence of upper GI ulcers and bleeds while on NSAID therapy if PPIs are co-administered[31]. PPI therapy is indicated in NSAID users at risk for GI bleeds which includes those on high dose NSAIDs, age greater than 65 years, prior history of ulcers, and/or concurrent use of antiplatelets, anticoagulants or corticosteroids[31,32]. Long term daily PPI therapy is not supported by high quality evidence and is a conditional recommendation. For patients who have a bleeding GI ulcer that was managed endoscopically with hemostatic therapy, high dose PPI therapy

should be given continuously or intermittently for the following 3 d for further gastroprotection[33].

RISKS ASSOCIATED WITH PPI USE

PPIs have been associated with electrolyte disturbances, increased fracture risk, gastrointestinal and lung infections, kidney disease, dementia, cardiovascular events, and gastric mucosal changes associated with potential increased risk of neoplasia. We are going to discuss the PPI-associated side-effects and the supporting data behind them (Table 3).

Electrolyte abnormalities

PPIs are thought to cause reduction in vitamins and minerals due to reduced intestinal absorption caused by decreased gastric acid secretion. While there is data on B12 and iron malabsorption associated with PPI use, some studies argue against this association. One large case control study confirmed that PPIs were associated with increased risk of iron deficiency anemia and vitamin B12 deficiency[34,35]. In contrast, a small observational study evaluated patients with ZES on chronic PPI therapy and did not find any association with iron malabsorption[36]. Another cross-sectional study found no association between long term PPI use and vitamin B12 deficiency[35].

Hypomagnesemia is another electrolyte derangement that has been attributed to PPI therapy. The first case report that linked hypomagnesemia with PPI use was in 2006, which prompted further research on this topic[37]. A 2014 meta-analysis of 9 observational studies found an association between PPI use and hypomagnesemia, but there was notable heterogeneity among the studies reported[38]. After review of 38 cases in Adverse Event Reporting System and 23 case reports, the United States Food and Drug Administration (FDA) recommends obtaining magnesium levels prior to PPI therapy initiation[39].

Hypocalcemia/fracture risk

PPIs are associated with hypocalcemia and potentially increased risk of bone fractures. Calcium salts, such as calcium carbonate, need highly acidic environment for absorption. PPIs block acid production and, as a result, prevent absorption of calcium carbonate[40]. Calcium malabsorption increases risk of osteoporosis and subsequent bone fractures. A large case control study from the United Kingdom reported that patients on chronic PPI therapy were more likely to fracture their hip with incidence rate of 4.0/1000 person years compared to non-users of 1.8/1000 person years. It is important to note that patients in the study had multiple comorbidities that could have served as confounding factors[40]. In contrast, a large-scale case control study performed among the Danish population found no dose-dependent relationship between PPI use and the risk of bone fracture[41]. In a 2018 meta-analysis, 12 of the included studies failed to show an association between PPI use and fracture incidence or decrease in bone mineral density[42]. Another meta-analysis of 18 observational studies demonstrated a modest hip, spine, and any-site fracture risk[43].

Kidney disease

In the recent studies, PPIs were noted to have an association with acute kidney injury (AKI) and subsequent development of chronic kidney disease (CKD). One of the proposed mechanisms is that PPIs lead to a cell mediated immune response causing acute intestinal nephritis (AIN). A meta-analysis of 9 observational studies supported an association relationship between PPI use with AKI and CKD[44]. Furthermore, Lazarus *et al*[45] found that PPIs were associated with a 20%-50% higher incidence rate of CKD. It was unclear from the study, however, if comorbidities served as confounding factors. Interestingly, an observational study of a veterans database consisting of mainly elderly males reported an association between PPI use and development of CKD with duration-dependent risk of end stage renal disease (ESRD)[46]. In contrast, a recent large observational study evaluating CKD patients did not confirm an association of PPI use and ESRD[47]. Although there is no clear guideline yet available, clinicians can choose to routinely monitor creatinine levels and/or obtain urinalysis testing in high-risk patients on PPI therapy to assess for kidney disease progression[48].

Dementia

PPIs are thought to increase production of β-amyloid plaques and increase affinity of tau proteins towards brain tissue. Both processes are key in pathogenesis of Alzheimer's Disease (AD)[40]. A systematic review established a 1.4-fold increased risk of dementia with PPI use. However, one of the studies demonstrated a negative correlation[49]. Additionally, a 2019 meta-analysis of 6 cohort studies found no significant association between PPI use and AD[50].

Gastrointestinal infections

PPIs are thought to alter intestinal microbiota and, as a result, may predispose patients to gastrointestinal infections[51,52]. A systemic review and a meta-analysis of 56 studies found that PPI therapy

Table 3 Proton pump inhibitor associated side effects

PPI associated adverse risks	Proposed mechanism	Evidence type	Conditional recommendations to reduce risk
Electrolyte abnormalities: Hypomagnesemia, vitamin B12, iron	Decreased acid secretion decreases intestinal absorption of minerals/vitamins	Observational studies, conflicting evidence[33,34,36,37]	Unless other risk factors present, no recommendation to increase intake of vitamins/minerals or have routine screening of levels[19]
Fracture risk/hypocalcemia	Decreased acid secretion decreases calcium carbonate absorption	Observational studies, conflicting evidence[39,40-42]	Without other risk factors for bone disease, no recommendations to increase calcium/vitamin D intake or have routine bone mineral density exam[19]
AIN/CKD/ESRD	Initiate cell mediated immune response in kidneys	Observational studies, conflicting evidence[43-46]	Without other risk factors, there is no recommendation to routinely screen for kidney function in patients on PPIs[19]
Dementia	Increase β-amyloid plaque production and increase affinity of tau proteins	Observational studies, conflicting evidence[48,49]	No recommendations on dementia prevention in patients on PPI
Gastrointestinal infections: *C. diff*, SIBO, SBP	Alter gut microbiota due to decreased acidic environment	Observational studies, conflicting evidence[34,51-55]	For patients who develop *C.diff* infection while on PPI, can consider switching to H2 blockers [55]
Community acquired Pneumonia	Increase bacterial colonization in stomach from hypochlorhydria leading to lung micro-aspiration events Alter respiratory flora	Observational studies, RCTs, conflicting evidence[57-59]	No strong recommendation can be made
Gastrointestinal malignancies	Hypergastrinemia resultant from decreased acid production increases ECL cell hyperplasia	Observational studies, RCTs, conflicting evidence[60-62,64,65]	Given conflicting data, no recommendation on prevention can be made
Adverse Cardiovascular effects- arrythmias, decreased clopidogrel bioavailability, increased digoxin toxicity	Hypomagnesemia- torsade de pointes CYP450 inhibitor- decreases drug bioavailability Interaction with ATP-dependent P-glycoprotein impair endothelial function and platelet induction	Observational studies, RCTs, conflicting evidence[59,66]	For patients with significant esophagitis (grade C or D) or with poorly controlled GERD, PPI treatment outweighs the debatable cardiovascular risks[19]

GERD: Gastro-esophageal reflux disease; PPI: Proton pump inhibitor; AIN: Acute intestinal nephritis; CKD: Chronic kidney disease; ESRD: End stage renal disease; *C. diff*: *Clostridium difficile*; SIBO: Small intestinal bacterial overgrowth; SBP: Spontaneous bacterial peritonitis; ECL: Enterochromaffin-like; RCTs: Randomized control trials.

increases the risk of *clostridium difficile (C. difficile)* infection[53]. While a nationwide cohort study in Denmark found that the risk of community acquired *C. difficile* doubles in patients on PPI, but several other studies failed to replicate these results[52,53].

A meta-analysis of 19 observational studies reported a moderate risk of small intestinal bacterial overgrowth (SIBO) for patients on long-term PPI[52]. In contrast, a retrospective case control study found no significant association between the two[54].

Another type of gastrointestinal infection that PPIs have been associated with is spontaneous bacterial peritonitis (SBP). A meta-analysis from 8 observation studies revealed a threefold higher risk of developing SBP while on PPIs in cirrhotic patients[35]. Another meta-analysis of 16 observational studies confirmed this association but only in the case control studies of the meta-analysis[55]. In contrast, one retrospective cohort study established that PPI therapy did not increase the risk of recurrent SBP in cirrhotic patient population[56].

Pneumonia risk

PPIs are thought to increase bacterial colonization in the stomach from hypochlorhydria and lead to lung micro-aspiration events or potentially alter respiratory flora leading to pulmonary infections[57,58]. A systemic review of 33 studies and a meta-analysis of 26 studies including 4 selected RCTs found a 1.5-fold increased risk of community acquired pneumonia (CAP) for patients on PPI therapy and a 1.6-fold increased hospitalization risk[58]. In contrast, another meta-analysis of RCTs found no association between PPI use and respiratory infections[59]. PPIs have been reported as possible contributors to the ventilator associated pneumonia, but the quality of evidence is low[60].

GI malignancies

There is growing number of studies reporting association of chronic PPI therapy with gastric cancer[61-63]. The decreased acid production and subsequent hypergastrinemia may cause hyperplasia of enterochromaffin-like (ECL) cells[35,64]. A meta-analysis of 7 observational studies and 1 RCT showed an increased risk of fundic gastric polyps while on PPI therapy, but the clinical significance of this finding remains undetermined[65]. It is important to note that another meta-analysis of 6 RCTs revealed that while there was ECL cell hyperplasia noted with chronic PPI use, the hyperplasia had no stigmata of dysplasia or neoplasia[66].

Adverse cardiovascular events

While PPIs do not have a direct association with cardiovascular complications, they have cardiovascular side-effects primarily thought their effects on magnesium (hypomagnesemia), drug-drug interactions, impairment of endothelial function and induction of platelets[67]. PPIs, particularly omeprazole, were thought to decrease clopidogrel efficacy from interference of its metabolism leading to increased cardiovascular events. Therefore, the FDA recommends against omeprazole and clopidogrel co-administration[67]. The COGENT study found no difference in cardiovascular events among patients on clopidogrel and omeprazole compared to patients on clopidogrel alone. Although the study was terminated early due to loss of funding[60].

The data on PPI side effect profile remains controversial. It is important to note that the evidence provided by ACG in their 2021 guidelines presented 95% confidence intervals for reported adverse events such as cardiovascular events, kidney disease, gastrointestinal complications, dementia, bone fractures, Vitamin 12 deficiency, gastric cancer, hypomagnesemia, and all-cause mortality-all of which crossed 1, making these hazard ratio and odds ratio statistically insignificant.

DRUG-DRUG INTERACTIONS

PPIs can decrease drug solubility either due to alteration in gastric pH or inhibition of the CYP450 system leading to decreased metabolism of certain drugs. The bioavailability of ketoconazole and atazanavir, for example, may be decreased by 50% or more with PPI co-administration. The metabolism of clopidogrel, simvastatin, phenytoin and many other drugs depends on the CYP450 system and coadministration of PPIs can decrease its clearance[68]. Also, PPI interaction with the ATP-dependent P-glycoprotein can inhibit digoxin efflux and increase its toxicity[69]. Another important consideration is in patients with hepatitis C who are placed on direct-acting antivirals (DAAs). There is a significant risk of failure of hepatitis C therapy in patients on concurrent PPI therapy likely because of decreased DAA bioavailability in the setting of altered gastric acidity[70]. It is important to be mindful of PPI administration especially in cases of polypharmacy in the elderly to ensure adequate efficacy of the prescribed medications.

STRATEGIES TO MINIMIZE SIDE-EFFECT PROFILE

As perception of PPI therapy is starting to change with more studies reporting consequences of long-term PPI use, strategies to minimize harm from its use become an important discussion. It is equally as important to understand the evidence behind the reported side effects and educate patients on their risks and benefits.

Strategy 1: Evidence-based initiation of therapy

The decision of starting PPI therapy should be evidence-based. There are several guidelines on disease processes that require PPI therapy, and it is important to have a good understanding of level of evidence and recommendation behind them. The 2021 ACG guidelines on GERD management have a strong recommendation supported by moderate quality evidence to start patients with heartburn and regurgitation symptoms on empiric PPI therapy for 8 wk[20]. Sometimes, further evaluation may be needed after the first empiric trial. These guidelines also have a strong recommendation supported by moderate evidence for patients who have high suspicion of GERD, but diagnosis is not definitive, to undergo reflux monitoring with BRAVO performed off PPI therapy to either confirm or rule out GERD [20]. This study may help differentiate dyspepsia from GERD. The 2017 ACG guidelines on dyspepsia and *H. pylori* had a strong recommendation supported by high quality evidence to start empiric PPI therapy on patients who were confirmed to have *H. pylori* infection, have dyspepsia but are *H. pylori* negative, have symptoms of dyspepsia persist despite *H. pylori* eradication, have functional dyspepsia [24,25]. The 2016 ACG guidelines on Barrett's esophagus provided a strong recommendation supported by moderate evidence that once-daily PPI therapy should be implemented in patients at high risk for developing Barrett's esophagus-male gender with more than 5 years of frequent (weekly or more) heartburn or regurgitation and two or more risk factors such as age greater than 50, Caucasian race,

central obesity, current or history of smoking, confirmed family history of Barrett's esophagus or esophageal adenocarcinoma[26]. While there are no official guidelines supporting this, PPIs have been successfully implemented in EoE treatment with 69.2% of patient achieving histologic remission compared to 41.7% of patients on empiric elimination diet alone[71].

Strategy 2: Need for ongoing treatment revisited at follow up

Another important strategy is to minimize risks by evaluating whether patient needs to stay on PPI therapy. Ongoing risks and benefit discussion with the patient along with weaning trials play a key role. As of 2021, ACG has a conditional recommendation supported by low evidence to have discontinuation trials of PPI therapy for patients with reflux symptoms who responded to 8-wk empiric PPI treatment attempted or for patients who have endoscopic or histologic evidence of esophageal or gastric mucosal healing[20,72]. It is important to note that weaning trials should not be attempted in patients with significant erosive esophagitis, BE, or history of esophageal adenocarcinoma[15,26].

In 2017, American Gastroenterological Association (AGA) came up with best practice advice[15]. They supported weaning off trials for patients with uncomplicated GERD. For patients who are unable to wean off therapy, BRAVO study or high-resolution manometry (HRM) are indicated to distinguish GERD from a functional syndrome[15]. HRM can be further used as a diagnostic evaluation in patients with refractory reflux symptoms prior to anti-reflux surgery[73]. HRM helps differentiate reflux from hiatal hernia and esophageal dysmotility[73]. The AGA recommended that if patients had an episode of bleeding from NSAID therapy should be started on long-term PPI therapy, especially is they must continue NSAID therapy.

Strategy 3: Dosing adjustment tailored to patient

As discussed previously, PPI metabolism relies on hepatic P450 system. Some patients are fast metabolizers, others may be slow, so it is not always easy to predict a particular patient's ability to metabolize PPIs. We know that patients of Asian descent and older patients tend to have slower P450 system and may have a higher concentration of PPIs available from the same dose[6]. This is something that is important to consider when selecting a starting dose or trying to decrease the dose later in treatment. The 2021 ACG guidelines provided conditional recommendation supported by low quality evidence that patients who require maintenance therapy with PPIs should be given the lower dose that controls their symptoms and maintains healing of tissues[20]. This was echoed in 2017 AGA guidelines as well suggesting that the lowest effective PPI dose should be used[15]. Same degree recommendation and evidence was put forward for as needed PPI therapy for patients with NERD[20]. pH testing (such as BRAVO) along with pH impedance can help facilitate titration to the minimum possible PPI dose to achieve optimal anti-secretory effects[74]. pH testing can also help tailor PPI therapy dosage and duration in Barrett's esophagus patient population[75].

Strategy 4: Looking for alternative options

While some conditions, such as erosive esophagitis, BE, prior history of esophageal adenocarcinoma, gastric ulcers, EoE require long-term acid-suppression with PPI therapy, many other conditions may be considered for an alternative therapy with H2 blockers, life-style modifications, or both[76]. One of the most common indication for PPI therapy is GERD and dyspepsia. Both conditions can be trialed with H2 blockers in attempts to come off PPI therapy. There are novel medications being developed such as potassium-competitive acid blockers (P-CABs), which bind to potassium inions thus blocking the hydrogen-potassium ATPase enzyme[77]. Similar to PPIs, P-CABs have a dose depended effects on gastric acid production[77]. Weight loss in overweight and obese patients had moderate evidence and strong recommendations for patients struggling with GERD suggested by ACG in 2021[20]. The rest of the life-style modifications, such as avoiding meals within 2-3 h of bedtime, tobacco products, trigger foods, and elevation of the head of the bed for nocturnal symptoms-all had only conditional recommendation supported by low quality evidence[20].

Surgical options need to be discussed with patients unwilling to commit to long-term PPI. Anti-reflux Surgery (LARS) is an alternative treatment to long-term pharmacologic therapy, especially in patients with large hiatal hernias or Barrett's esophagus but was noted to have higher risks of symptom recurrence, especially in obese patients[78,79]. As a result, some studies reported that the utilization of anti-reflux surgery is greater when used in conjunction with weight loss in patients with BMI over 35 [80]. Despite initial success with LARS, studies reported that as many as 48% patients who have undergone LARS resumed PPI therapy at 5-year mark[81]. Additionally, LARS requires pre-surgery work up, which includes HRM.

PATIENT'S PERCEPTION OF PPI THERAPY

Patients understanding of therapy and how it works directly contribute to patient satisfaction and treatment success. Shared decision-making regarding duration of treatment and side-effect profile is key. Patient's participation and understanding of therapy are especially important because PPI

treatment comes with limitations of short-half life and meal dependent administration.

In the setting of new concerns regarding PPI's side-effects and growing media coverage of this topic, patients are increasingly more worried about staying on PPIs long-term. Therefore, increasing awareness among primary care providers on the proper use of PPIs is crucial. Additionally, managing patient's expectations and educating on the evidence behind the reported side effects becomes important. Prior to the therapy initiation, anticipated duration of treatment should be discussed with the patient. Risks and benefit discussion needs to take place. Whether the PPI therapy is prescribed by the primary care or gastroenterology physician, the decision to start the therapy should be evidence-based and rely on most recent guidelines supported by high quality evidence. Additionally, prescribing physicians should have an ongoing discussion with their patients and re-evaluation of their need to stay on PPI therapy. Working together with the patient, setting realistic expectations from the beginning, following evidence-based guidelines, and continuing to re-evaluate of need for therapy could increase patient satisfaction with medical care, provide reassurance, and help more people to safely benefit from PPI therapy.

CONCLUSION

Since their first introduction to the medical practice, PPIs have come a long way and we now know much more about their pharmacodynamics and side-effect profile. The side-effect data remains controversial with most recent ACG guidelines arguing against significant risks associated with this therapy. While data provided by ACG is reassuring, PPI therapy should still be utilized according to evidence-based practice. We now know more about which patients are more likely to benefit from this therapy and why some patients should only be on it short term. As our understanding of this therapy deepens, our practice should change to help more patients to safely benefit from PPIs. Following evidence-based guidelines and working together with a patient managing expectations and educating on risks may be the key to successful come back of PPI therapy.

FOOTNOTES

Author contributions: Turshudzhyan A, Samuel S, and Tawfik A wrote the manuscript; Tadros M revised the manuscript.

Conflict-of-interest statement: There are no conflicts of interest to report.

Country/Territory of origin: United States

ORCID number: Alla Turshudzhyan 0000-0001-6867-7569; Sonia Samuel 0000-0003-3359-0222; Angela Tawfik 0000-0002-0001-8126; Micheal Tadros 0000-0003-3118-3893.

S-Editor: Chen YL
L-Editor: A
P-Editor: Chen YL

REFERENCES

1 **Chiba T**, Malfertheiner P, Satoh H. Proton Pump Inhibitors: A Balanced View. *Front Gastrointest Res* 2013; **32**: 1-17 [DOI: 10.1159/000350624]
2 **Lassen AT**. Acid-related disorders and use of antisecretory medication. *Dan Med Bull* 2007; **54**: 18-30 [PMID: 17349216]
3 **Walker MJ**, Crews NR, El-Halabi M, Fayad NF. Educational Intervention Improves Proton Pump Inhibitor Stewardship in Outpatient Gastroenterology Clinics. *Gastroenterology Res* 2019; **12**: 305-311 [PMID: 31803310 DOI: 10.14740/gr1238]
4 **Batuwitage BT**, Kingham JG, Morgan NE, Bartlett RL. Inappropriate prescribing of proton pump inhibitors in primary care. *Postgrad Med J* 2007; **83**: 66-68 [PMID: 17267683 DOI: 10.1136/pgmj.2006.051151]
5 **Robinson M**, Horn J. Clinical pharmacology of proton pump inhibitors: what the practising physician needs to know. *Drugs* 2003; **63**: 2739-2754 [PMID: 14664653 DOI: 10.2165/00003495-200363240-00004]
6 **Ahmed A**, Clarke JO. Proton Pump Inhibitors (PPI). Aug 1, 2021. [cited 10 January 2022]. Available from: https://www.ncbi.nlm.nih.gov/books/NBK557385/

7 **Stedman CA**, Barclay ML. Review article: comparison of the pharmacokinetics, acid suppression and efficacy of proton pump inhibitors. *Aliment Pharmacol Ther* 2000; **14**: 963-978 [PMID: 10930890 DOI: 10.1046/j.1365-2036.2000.00788.x]

8 **Scarpignato C**, Pelosini I. Review article: the opportunities and benefits of extended acid suppression. *Aliment Pharmacol Ther* 2006; **23** Suppl 2: 23-34 [PMID: 16700900 DOI: 10.1111/j.1365-2036.2006.02945.x]

9 **Wittbrodt ET**, Baum C, Peura DA. Delayed release dexlansoprazole in the treatment of GERD and erosive esophagitis. *Clin Exp Gastroenterol* 2009; **2**: 117-128 [PMID: 21694835 DOI: 10.2147/ceg.s5765]

10 **Ishizaki T**, Horai Y. Review article: cytochrome P450 and the metabolism of proton pump inhibitors--emphasis on rabeprazole. *Aliment Pharm Ther* 1999; **13**: 27-36 [DOI: 10.1046/j.1365-2036.1999.00022.x]

11 **Chubineh S**, Birk J. Proton pump inhibitors: the good, the bad, and the unwanted. *South Med J* 2012; **105**: 613-618 [PMID: 23128806 DOI: 10.1097/SMJ.0b013e31826efbea]

12 **Sachs G**, Shin JM, Howden CW. Review article: the clinical pharmacology of proton pump inhibitors. *Aliment Pharm Ther* 2006; **23** (2): 2-8 [DOI: 10.1111/j.1365-2036.2006.02943.x]

13 **Kaniecki T**, Abdi T, McMahan ZH. A practical approach to the evaluation and management of gastrointestinal symptoms in patients with systemic sclerosis. *Best Pract Res Clin Rheumatol* 2021; **35**: 101666 [PMID: 33676855 DOI: 10.1016/j.berh.2021.101666]

14 **Wiesner A**, Zwolińska-Wcisło M, Paśko P. Effect of Food and Dosing Regimen on Safety and Efficacy of Proton Pump Inhibitors Therapy-A Literature Review. *Int J Environ Res Public Health* 2021; **18** [PMID: 33805341 DOI: 10.3390/ijerph18073527]

15 **Freedberg DE**, Kim LS, Yang YX. The Risks and Benefits of Long-term Use of Proton Pump Inhibitors: Expert Review and Best Practice Advice From the American Gastroenterological Association. *Gastroenterology* 2017; **152**: 706-715 [PMID: 28257716 DOI: 10.1053/j.gastro.2017.01.031]

16 **Savarino V**, Dulbecco P, de Bortoli N, Ottonello A, Savarino E. The appropriate use of proton pump inhibitors (PPIs): Need for a reappraisal. *Eur J Intern Med* 2017; **37**: 19-24 [PMID: 27784575 DOI: 10.1016/j.ejim.2016.10.007]

17 **Scarpignato C**, Gatta L, Zullo A, Blandizzi C; SIF-AIGO-FIMMG Group; Italian Society of Pharmacology, the Italian Association of Hospital Gastroenterologists, and the Italian Federation of General Practitioners. Effective and safe proton pump inhibitor therapy in acid-related diseases - A position paper addressing benefits and potential harms of acid suppression. *BMC Med* 2016; **14**: 179 [PMID: 27825371 DOI: 10.1186/s12916-016-0718-z]

18 **Narum S**, Westergren T, Klemp M. Corticosteroids and risk of gastrointestinal bleeding: a systematic review and meta-analysis. *BMJ Open* 2014; **4**: e004587 [PMID: 24833682 DOI: 10.1136/bmjopen-2013-004587]

19 **He Q**, Xia B, Meng W, Fan D, Kuo ZC, Huang J, Qin X, Zou H, He Y, Zhang C, Fang S, Pan Y, Yang M, Yuan J. No Associations Between Regular Use of Proton Pump Inhibitors and Risk of All-Cause and Cause-Specific Mortality: A Population-Based Cohort of 0.44 Million Participants. *Am J Gastroenterol* 2021; **116**: 2286-2291 [PMID: 34313608 DOI: 10.14309/ajg.0000000000001377]

20 **Katz PO**, Dunbar KB, Schnoll-Sussman FH, Greer KB, Yadlapati R, Spechler SJ. ACG Clinical Guideline for the Diagnosis and Management of Gastroesophageal Reflux Disease. *Am J Gastroenterol* 2022; **117**: 27-56 [PMID: 34807007 DOI: 10.14309/ajg.0000000000001538]

21 **Kahrilas PJ**, Shaheen NJ, Vaezi MF; American Gastroenterological Association Institute; Clinical Practice and Quality Management Committee. American Gastroenterological Association Institute technical review on the management of gastroesophageal reflux disease. *Gastroenterology* 2008; **135**: 1392-1413, 1413.e1 [PMID: 18801365 DOI: 10.1053/j.gastro.2008.08.044]

22 **Kohn GP**, Price RR, DeMeester SR, Zehetner J, Muensterer OJ, Awad Z, Mittal SK, Richardson WS, Stefanidis D, Fanelli RD; SAGES Guidelines Committee. Guidelines for the management of hiatal hernia. *Surg Endosc* 2013; **27**: 4409-4428 [PMID: 24018762 DOI: 10.1007/s00464-013-3173-3]

23 **Yadlapati R**, Masihi M, Gyawali CP, Carlson DA, Kahrilas PJ, Nix BD, Jain A, Triggs JR, Vaezi MF, Kia L, Kaizer A, Pandolfino JE. Ambulatory Reflux Monitoring Guides Proton Pump Inhibitor Discontinuation in Patients With Gastroesophageal Reflux Symptoms: A Clinical Trial. *Gastroenterology* 2021; **160**: 174-182.e1 [PMID: 32949568 DOI: 10.1053/j.gastro.2020.09.013]

24 **Moayyedi P**, Lacy BE, Andrews CN, Enns RA, Howden CW, Vakil N. ACG and CAG Clinical Guideline: Management of Dyspepsia. *Am J Gastroenterol* 2017; **112**: 988-1013 [PMID: 28631728 DOI: 10.1038/ajg.2017.154]

25 **Chey WD**, Leontiadis GI, Howden CW, Moss SF. ACG Clinical Guideline: Treatment of Helicobacter pylori Infection. *Am J Gastroenterol* 2017; **112**: 212-239 [PMID: 28071659 DOI: 10.1038/ajg.2016.563]

26 **Shaheen NJ**, Falk GW, Iyer PG, Gerson LB; American College of Gastroenterology. ACG Clinical Guideline: Diagnosis and Management of Barrett's Esophagus. *Am J Gastroenterol* 2016; **111**: 30-50; quiz 51 [PMID: 26526079 DOI: 10.1038/ajg.2015.322]

27 **American Gastroenterological Association**. American Gastroenterological Association medical position statement on the management of Barrett's esophagus. *Gastroenterology* 2011; **140**: 1084-1091 [DOI: 10.1053/j.gastro.2011.01.030]

28 **Dellon ES**, Gonsalves N, Hirano I, Furuta GT, Liacouras CA, Katzka DA; American College of Gastroenterology. ACG clinical guideline: Evidenced based approach to the diagnosis and management of esophageal eosinophilia and eosinophilic esophagitis (EoE). *Am J Gastroenterol* 2013; **108**: 679-92; quiz 693 [PMID: 23567357 DOI: 10.1038/ajg.2013.71]

29 **Dellon ES**, Liacouras CA, Molina-Infante J, Furuta GT, Spergel JM, Zevit N, Spechler SJ, Attwood SE, Straumann A, Aceves SS, Alexander JA, Atkins D, Arva NC, Blanchard C, Bonis PA, Book WM, Capocelli KE, Chehade M, Cheng E, Collins MH, Davis CM, Dias JA, Di Lorenzo C, Dohil R, Dupont C, Falk GW, Ferreira CT, Fox A, Gonsalves NP, Gupta SK, Katzka DA, Kinoshita Y, Menard-Katcher C, Kodroff E, Metz DC, Miehlke S, Muir AB, Mukkada VA, Murch S, Nurko S, Ohtsuka Y, Orel R, Papadopoulou A, Peterson KA, Philpott H, Putnam PE, Richter JE, Rosen R, Rothenberg ME, Schoepfer A, Scott MM, Shah N, Sheikh J, Souza RF, Strobel MJ, Talley NJ, Vaezi MF, Vandenplas Y, Vieira MC, Walker MM, Wechsler JB, Wershil BK, Wen T, Yang GY, Hirano I, Bredenoord AJ. Updated International Consensus Diagnostic Criteria for Eosinophilic Esophagitis: Proceedings of the AGREE Conference. *Gastroenterology* 2018; **155**: 1022-1033.e10 [PMID: 30009819 DOI: 10.1053/j.gastro.2018.07.009]

30 **Lucendo AJ**, Molina-Infante J, Arias Á, von Arnim U, Bredenoord AJ, Bussmann C, Amil Dias J, Bove M, González-

Cervera J, Larsson H, Miehlke S, Papadopoulou A, Rodríguez-Sánchez J, Ravelli A, Ronkainen J, Santander C, Schoepfer AM, Storr MA, Terreehorst I, Straumann A, Attwood SE. Guidelines on eosinophilic esophagitis: evidence-based statements and recommendations for diagnosis and management in children and adults. *United European Gastroenterol J* 2017; **5**: 335-358 [PMID: 28507746 DOI: 10.1177/2050640616689525]

31 **Lanza FL**, Chan FK, Quigley EM; Practice Parameters Committee of the American College of Gastroenterology. Guidelines for prevention of NSAID-related ulcer complications. *Am J Gastroenterol* 2009; **104**: 728-738 [PMID: 19240698 DOI: 10.1038/ajg.2009.115]

32 **Laine L**, Nagar A. Long-Term PPI Use: Balancing Potential Harms and Documented Benefits. *Am J Gastroenterol* 2016; **111**: 913-915 [PMID: 27113114 DOI: 10.1038/ajg.2016.156]

33 **Laine L**, Barkun AN, Saltzman JR, Martel M, Leontiadis GI. ACG Clinical Guideline: Upper Gastrointestinal and Ulcer Bleeding. *Am J Gastroenterol* 2021; **116**: 899-917 [PMID: 33929377 DOI: 10.14309/ajg.0000000000001245]

34 **Tran-Duy A**, Connell NJ, Vanmolkot FH, Souverein PC, de Wit NJ, Stehouwer CDA, Hoes AW, de Vries F, de Boer A. Use of proton pump inhibitors and risk of iron deficiency: a population-based case-control study. *J Intern Med* 2019; **285**: 205-214 [PMID: 30141278 DOI: 10.1111/joim.12826]

35 **Eusebi LH**, Rabitti S, Artesiani ML, Gelli D, Montagnani M, Zagari RM, Bazzoli F. Proton pump inhibitors: Risks of long-term use. *J Gastroenterol Hepatol* 2017; **32**: 1295-1302 [PMID: 28092694 DOI: 10.1111/jgh.13737]

36 **Stewart CA**, Termanini B, Sutliff VE, Serrano J, Yu F, Gibril F, Jensen RT. Iron absorption in patients with Zollinger-Ellison syndrome treated with long-term gastric acid antisecretory therapy. *Aliment Pharmacol Ther* 1998; **12**: 83-98 [PMID: 9692706 DOI: 10.1046/j.1365-2036.1998.00274.x]

37 **William JH**, Danziger J. Magnesium Deficiency and Proton-Pump Inhibitor Use: A Clinical Review. *J Clin Pharmacol* 2016; **56**: 660-668 [PMID: 26582556 DOI: 10.1002/jcph.672]

38 **Park CH**, Kim EH, Roh YH, Kim HY, Lee SK. The association between the use of proton pump inhibitors and the risk of hypomagnesemia: a systematic review and meta-analysis. *PLoS One* 2014; **9**: e112558 [PMID: 25394217 DOI: 10.1371/journal.pone.0112558]

39 **U. S. Food and Drug Administration**. FDA drug safety communication: low magnesium levels can be associated with long-term use of proton pump inhibitor drugs (PPIs). [cited December 20, 2021]. Available from: http://www.fda.gov/Drugs/DrugSafety/ucm245011.htm

40 **Yang YX**, Lewis JD, Epstein S, Metz DC. Long-term proton pump inhibitor therapy and risk of hip fracture. *JAMA* 2006; **296**: 2947-2953 [PMID: 17190895 DOI: 10.1001/jama.296.24.2947]

41 **Ito T**, Jensen RT. Association of long-term proton pump inhibitor therapy with bone fractures and effects on absorption of calcium, vitamin B12, iron, and magnesium. *Curr Gastroenterol Rep* 2010; **12**: 448-457 [PMID: 20882439 DOI: 10.1007/s11894-010-0141-0]

42 **Nassar Y**, Richter S. Proton-pump Inhibitor Use and Fracture Risk: An Updated Systematic Review and Meta-analysis. *J Bone Metab* 2018; **25**: 141-151 [PMID: 30237993 DOI: 10.11005/jbm.2018.25.3.141]

43 **Zhou B**, Huang Y, Li H, Sun W, Liu J. Proton-pump inhibitors and risk of fractures: an update meta-analysis. *Osteoporos Int* 2016; **27**: 339-347 [PMID: 26462494 DOI: 10.1007/s00198-015-3365-x]

44 **Nochaiwong S**, Ruengorn C, Awiphan R, Koyratkoson K, Chaisai C, Noppakun K, Chongruksut W, Thavorn K. The association between proton pump inhibitor use and the risk of adverse kidney outcomes: a systematic review and meta-analysis. *Nephrol Dial Transplant* 2018; **33**: 331-342 [PMID: 28339835 DOI: 10.1093/ndt/gfw470]

45 **Lazarus B**, Chen Y, Wilson FP, Sang Y, Chang AR, Coresh J, Grams ME. Proton Pump Inhibitor Use and the Risk of Chronic Kidney Disease. *JAMA Intern Med* 2016; **176**: 238-246 [PMID: 26752337 DOI: 10.1001/jamainternmed.2015.7193]

46 **Xie Y**, Bowe B, Li T, Xian H, Balasubramanian S, Al-Aly Z. Proton Pump Inhibitors and Risk of Incident CKD and Progression to ESRD. *J Am Soc Nephrol* 2016; **27**: 3153-3163 [PMID: 27080976 DOI: 10.1681/ASN.2015121377]

47 **Cholin L**, Ashour T, Mehdi A, Taliercio JJ, Daou R, Arrigain S, Schold JD, Thomas G, Nally J, Nakhoul NL, Nakhoul GN. Proton-pump inhibitor vs. H2-receptor blocker use and overall risk of CKD progression. *BMC Nephrol* 2021; **22**: 264 [PMID: 34266395 DOI: 10.1186/s12882-021-02449-0]

48 **Moledina DG**, Perazella MA. Proton Pump Inhibitors and CKD. *J Am Soc Nephrol* 2016; **27**: 2926-2928 [PMID: 27080978 DOI: 10.1681/ASN.2016020192]

49 **Ortiz-Guerrero G**, Amador-Muñoz D, Calderón-Ospina CA, López-Fuentes D, Nava Mesa MO. Proton Pump Inhibitors and Dementia: Physiopathological Mechanisms and Clinical Consequences. *Neural Plast* 2018; **2018**: 5257285 [PMID: 29755512 DOI: 10.1155/2018/5257285]

50 **Li M**, Luo Z, Yu S, Tang Z. Proton pump inhibitor use and risk of dementia: Systematic review and meta-analysis. *Medicine (Baltimore)* 2019; **98**: e14422 [PMID: 30762748 DOI: 10.1097/MD.0000000000014422]

51 **Inghammar M**, Svanström H, Voldstedlund M, Melbye M, Hviid A, Mølbak K, Pasternak B. Proton-Pump Inhibitor Use and the Risk of Community-Associated Clostridium difficile Infection. *Clin Infect Dis* 2021; **72**: e1084-e1089 [PMID: 33629099 DOI: 10.1093/cid/ciaa1857]

52 **Su T**, Lai S, Lee A, He X, Chen S. Meta-analysis: proton pump inhibitors moderately increase the risk of small intestinal bacterial overgrowth. *J Gastroenterol* 2018; **53**: 27-36 [PMID: 28770351 DOI: 10.1007/s00535-017-1371-9]

53 **Trifan A**, Stanciu C, Girleanu I, Stoica OC, Singeap AM, Maxim R, Chiriac SA, Ciobica A, Boiculese L. Proton pump inhibitors therapy and risk of Clostridium difficile infection: Systematic review and meta-analysis. *World J Gastroenterol* 2017; **23**: 6500-6515 [PMID: 29085200 DOI: 10.3748/wjg.v23.i35.6500]

54 **Ratuapli SK**, Ellington TG, O'Neill MT, Umar SB, Harris LA, Foxx-Orenstein AE, Burdick GE, Dibaise JK, Lacy BE, Crowell MD. Proton pump inhibitor therapy use does not predispose to small intestinal bacterial overgrowth. *Am J Gastroenterol* 2012; **107**: 730-735 [PMID: 22334250 DOI: 10.1038/ajg.2012.4]

55 **Yu T**, Tang Y, Jiang L, Zheng Y, Xiong W, Lin L. Proton pump inhibitor therapy and its association with spontaneous bacterial peritonitis incidence and mortality: A meta-analysis. *Dig Liver Dis* 2016; **48**: 353-359 [PMID: 26795544 DOI: 10.1016/j.dld.2015.12.009]

56 **Kim JH**, Lim KS, Min YW, Lee H, Min BH, Rhee PL, Kim JJ, Koh KC, Paik SW. Proton pump inhibitors do not increase

the risk for recurrent spontaneous bacterial peritonitis in patients with cirrhosis. *J Gastroenterol Hepatol* 2017; **32**: 1064-1070 [PMID: 28449345 DOI: 10.1111/jgh.13637]

57 **Thomson AB**, Sauve MD, Kassam N, Kamitakahara H. Safety of the long-term use of proton pump inhibitors. *World J Gastroenterol* 2010; **16**: 2323-2330 [PMID: 20480516 DOI: 10.3748/wjg.v16.i19.2323]

58 **Lambert AA**, Lam JO, Paik JJ, Ugarte-Gil C, Drummond MB, Crowell TA. Risk of community-acquired pneumonia with outpatient proton-pump inhibitor therapy: a systematic review and meta-analysis. *PLoS One* 2015; **10**: e0128004 [PMID: 26042842 DOI: 10.1371/journal.pone.0128004]

59 **Sultan N**, Nazareno J, Gregor J. Association between proton pump inhibitors and respiratory infections: a systematic review and meta-analysis of clinical trials. *Can J Gastroenterol* 2008; **22**: 761-766 [PMID: 18818790 DOI: 10.1155/2008/821385]

60 **Jaynes M**, Kumar AB. The risks of long-term use of proton pump inhibitors: a critical review. *Ther Adv Drug Saf* 2019; **10**: 2042098618809927 [PMID: 31019676 DOI: 10.1177/2042098618809927]

61 **Ahn JS**, Eom CS, Jeon CY, Park SM. Acid suppressive drugs and gastric cancer: a meta-analysis of observational studies. *World J Gastroenterol* 2013; **19**: 2560-2568 [PMID: 23674860 DOI: 10.3748/wjg.v19.i16.2560]

62 **Cheung KS**, Leung WK. Long-term use of proton-pump inhibitors and risk of gastric cancer: a review of the current evidence. *Therap Adv Gastroenterol* 2019; **12**: 1756284819834511 [PMID: 30886648 DOI: 10.1177/1756284819834511]

63 **Abrahami D**, McDonald EG, Schnitzer ME, Barkun AN, Suissa S, Azoulay L. Proton pump inhibitors and risk of gastric cancer: population-based cohort study. *Gut* 2022; **71**: 16-24 [PMID: 34226290 DOI: 10.1136/gutjnl-2021-325097]

64 **Yibirin M**, De Oliveira D, Valera R, Plitt AE, Lutgen S. Adverse Effects Associated with Proton Pump Inhibitor Use. *Cureus* 2021; **13**: e12759 [PMID: 33614352 DOI: 10.7759/cureus.12759]

65 **Tran-Duy A**, Spaetgens B, Hoes AW, de Wit NJ, Stehouwer CD. Use of Proton Pump Inhibitors and Risks of Fundic Gland Polyps and Gastric Cancer: Systematic Review and Meta-analysis. *Clin Gastroenterol Hepatol* 2016; **14**: 1706-1719.e5 [PMID: 27211501 DOI: 10.1016/j.cgh.2016.05.018]

66 **Song H**, Zhu J, Lu D. Long-term proton pump inhibitor (PPI) use and the development of gastric pre-malignant lesions. *Cochrane Database Syst Rev* 2014; CD010623 [PMID: 25464111 DOI: 10.1002/14651858.CD010623.pub2]

67 **Ariel H**, Cooke JP. Cardiovascular Risk of Proton Pump Inhibitors. *Methodist Debakey Cardiovasc J* 2019; **15**: 214-219 [PMID: 31687101 DOI: 10.14797/mdcj-15-3-214]

68 **Ogawa R**, Echizen H. Drug-drug interaction profiles of proton pump inhibitors. *Clin Pharmacokinet* 2010; **49**: 509-533 [PMID: 20608754 DOI: 10.2165/11531320-000000000-00000]

69 **Blume H**, Donath F, Warnke A, Schug BS. Pharmacokinetic drug interaction profiles of proton pump inhibitors. *Drug Saf* 2006; **29**: 769-784 [PMID: 16944963 DOI: 10.2165/00002018-200629090-00002]

70 **Wijarnpreecha K**, Chesdachai S, Thongprayoon C, Jaruvongvanich V, Ungprasert P, Cheungpasitporn W. Efficacy and Safety of Direct-acting Antivirals in Hepatitis C Virus-infected Patients Taking Proton Pump Inhibitors. *J Clin Transl Hepatol* 2017; **5**: 327-334 [PMID: 29226099 DOI: 10.14218/JCTH.2017.00017]

71 **Laserna-Mendieta EJ**, Casabona S, Savarino E, Perelló A, Pérez-Martínez I, Guagnozzi D, Barrio J, Guardiola A, Asensio T, de la Riva S, Ruiz-Ponce M, Rodríguez-Oballe JA, Santander C, Arias Á, Lucendo AJ; EUREOS EoE CONNECT research group. Efficacy of Therapy for Eosinophilic Esophagitis in Real-World Practice. *Clin Gastroenterol Hepatol* 2020; **18**: 2903-2911.e4 [PMID: 31988045 DOI: 10.1016/j.cgh.2020.01.024]

72 **Pandolfino J**. Discontinuation of proton pump inhibitor therapy and the role of esophageal testing. *Gastroenterol Hepatol (N Y)* 2013; **9**: 747-764 [PMID: 24764794]

73 **Keller J**. What Is the Impact of High-Resolution Manometry in the Functional Diagnostic Workup of Gastroesophageal Reflux Disease? *Visc Med* 2018; **34**: 101-108 [PMID: 29888238 DOI: 10.1159/000486883]

74 **Graham DY**. Optimal PPI Dosing for Improving GERD Symptoms: Is Timing Everything? *Dig Dis Sci* 2019; **64**: 4-6 [PMID: 30238199 DOI: 10.1007/s10620-018-5288-9]

75 **Neumann CS**, Cooper BT. Oesophageal pH monitoring in Barrett's oesophagus. *Gut* 2003; **52**: 153; author reply 153-153; author reply 154 [PMID: 12477781 DOI: 10.1136/gut.52.1.153-a]

76 **Sollano JD**, Romano RP, Ibanez-Guzaman L, Lontok MADC, de Ocampo SQ, Policarpio AA, de Guzman Jr RN, Dulanpang CD, Galang AJG, Olympia EG, Chua MAL, Moscoso BA, Tan JA, Pangilinan JAN, Vitug AO, Naval MC, Encarnacion DA, Sy PP, Ong EG, Cabahug OT, Daez MLO, Ismael AE, Bocobo JC. Clinical Practice Guidelines on the Diagnosis and Treatment of Gastroesophageal Reflux Disease (GERD). *hilippine J of Intern Med* 2015; **53** (3): 1-17

77 **Rawla P**, Sunkara T, Ofosu A, Gaduputi V. Potassium-competitive acid blockers - are they the next generation of proton pump inhibitors? *World J Gastrointest Pharmacol Ther* 2018; **9**: 63-68 [PMID: 30595950 DOI: 10.4292/wjgpt.v9.i7.63]

78 **Abdelrahman T**, Latif A, Chan DS, Jones H, Farag M, Lewis WG, Havard T, Escofet X. Outcomes after laparoscopic anti-reflux surgery related to obesity: A systematic review and meta-analysis. *Int J Surg* 2018; **51**: 76-82 [PMID: 29367036 DOI: 10.1016/j.ijsu.2018.01.013]

79 **Simonka Z**, Paszt A, Abrahám S, Pieler J, Tajti J, Tiszlavicz L, Németh I, Izbéki F, Rosztóczy A, Wittmann T, Rárosi F, Lázár G. The effects of laparoscopic Nissen fundoplication on Barrett's esophagus: long-term results. *Scand J Gastroenterol* 2012; **47**: 13-21 [PMID: 22150083 DOI: 10.3109/00365521.2011.639081]

80 **Kaplan LM**. Treatment of gastroesophageal reflux disease in obese patients. *Gastroenterol Hepatol (N Y)* 2008; **4**: 841-843 [PMID: 21904472]

81 **Robertson AG**, Patel RN, Couper GW, de Beaux AC, Paterson-Brown S, Lamb PJ. Long-term outcomes following laparoscopic anterior and Nissen fundoplication. *ANZ J Surg* 2017; **87**: 300-304 [PMID: 26478259 DOI: 10.1111/ans.13358]

World Journal of Gastroenterology

Submit a Manuscript: https://www.f6publishing.com

World J Gastroenterol 2022 June 28; 28(24): 2680-2688

DOI: 10.3748/wjg.v28.i24.2680

ISSN 1007-9327 (print) ISSN 2219-2840 (online)

MINIREVIEWS

Pancreatic involvement in celiac disease

Daniel Vasile Balaban, Iulia Enache, Marina Ciochina, Alina Popp, Mariana Jinga

Specialty type: Gastroenterology and hepatology

Provenance and peer review: Invited article; Externally peer reviewed.

Peer-review model: Single blind

Peer-review report's scientific quality classification

Grade A (Excellent): 0
Grade B (Very good): B, B
Grade C (Good): 0
Grade D (Fair): D
Grade E (Poor): 0

P-Reviewer: Ashkar M, United States; Ghazanfar A, United Kingdom; Lee Y, South Korea
A-Editor: Yao QG, China

Received: January 15, 2022
Peer-review started: January 15, 2022
First decision: April 12, 2022
Revised: April 17, 2022
Accepted: May 27, 2022
Article in press: May 27, 2022
Published online: June 28, 2022

Daniel Vasile Balaban, Iulia Enache, Marina Ciochina, Mariana Jinga, Department of Internal Medicine and Gastroenterology, Carol Davila University of Medicine and Pharmacy, Bucharest 020021, Romania

Daniel Vasile Balaban, Iulia Enache, Marina Ciochina, Mariana Jinga, Dr. Carol Davila Central Military Emergency University Hospital, Bucharest 020021, Romania

Alina Popp, Department of Pediatrics, Carol Davila University of Medicine and Pharmacy, Bucharest 020021, Romania

Alina Popp, National Institute for Mother and Child Health, Bucharest 020021, Romania

Corresponding author: Daniel Vasile Balaban, MD, PhD, Senior Lecturer, Department of Internal Medicine and Gastroenterology, Carol Davila University of Medicine and Pharmacy, 134 Calea Plevnei, Bucharest 020021, Romania. vbalaban@yahoo.com

Abstract

Celiac disease (CD) is well recognized as a systemic, chronic autoimmune disease mainly characterized by gluten-sensitive enteropathy in genetically predisposed individuals but with various extraintestinal features. One of the affected organs in CD is the pancreas, consisting of both endocrine and exocrine alterations. Over the last decades there has been increasing interest in the pancreatic changes in CD, and this has been reflected by a great number of publications looking at this extraintestinal involvement during the course of CD. While pancreatic endocrine changes in CD, focusing on type 1 diabetes mellitus, are well documented in the literature, the relationship with the exocrine pancreas has been less studied. This review summarizes currently available evidence with regard to pancreatic exocrine alterations in CD, focusing on risk of pancreatitis in CD patients, association with autoimmune pancreatitis, prevalence and outcomes of pancreatic exocrine insufficiency in newly diagnosed and gluten-free diet treated CD patients, and the link with cystic fibrosis. In addition, we discuss mechanisms behind the associated pancreatic exocrine impairment in CD and highlight the recommendations for clinical practice.

Key Words: Pancreas; Celiac disease; Autoimmune; Pancreatitis; Cystic fibrosis; Exocrine insufficiency

Core Tip: Celiac disease (CD) is currently regarded as a systemic, chronic, immune-mediated disease triggered by gluten ingestion in genetically susceptible individuals. In the last decade there has been an increasing number of publications on extraintestinal involvement during the course of CD, some of which have assessed the pancreatic changes associated with this disease. This review summarizes currently available data with respect to exocrine pancreatic changes in CD, focusing on practices for clinicians.

Citation: Balaban DV, Enache I, Ciochina M, Popp A, Jinga M. Pancreatic involvement in celiac disease. *World J Gastroenterol* 2022; 28(24): 2680-2688
URL: https://www.wjgnet.com/1007-9327/full/v28/i24/2680.htm
DOI: https://dx.doi.org/10.3748/wjg.v28.i24.2680

INTRODUCTION

Celiac disease (CD) is an immune-mediated enteropathy that occurs in genetically predisposed individuals upon ingestion of gluten. Initially considered a small bowel disease, now it is widely recognized as a systemic illness, which accounts for its many protean manifestations. The systemic character along with its various clinical presentations make CD a sometimes difficult to recognize clinical chameleon. The wide spectrum of presenting features, sometimes subclinical, hinders case-finding strategies and delays diagnosis, as CD is often not considered among the differential diagnoses [1,2]. Moreover, there is also the further drawback of poor awareness among different medical specialties[3].

Among the extraintestinal features of CD[4-6], pancreatic involvement has rarely been reported compared to other organ-specific manifestations such as cutaneous, hematologic, liver-related, rheumatologic, cardiovascular, or neurological impairments[7-13]. Moreover, while some of these systemic features have been incorporated into case-finding and screening strategies such as anemia, osteoporosis or chronic liver disease[14], pancreatic-associated involvement in CD is scarcely reported in currently available guidelines[15-17]. The association between the pancreas and CD covered in guidelines is limited to the need to consider pancreatic exocrine insufficiency (PEI) as an alternative diagnosis in non-responsive CD and the fact that upper gastrointestinal surgery including pancreas-related indications may unmask subclinical CD[15,16]. This has also been highlighted by previous reports on the impact of CD on exocrine and endocrine pancreas, which also set the need for further research focused on this association[18]. Contrasting the well-documented pancreatic endocrine changes in CD, referring to type 1 diabetes mellitus in particular, the relationship with the exocrine pancreas has been less covered in the literature.

On the other hand, the wide spectrum of pancreatic diseases does not include CD as a risk factor or associated condition, except counting CD as a potential cause of PEI[19]. Pancreatic involvement can occur in patients with CD, either caused by the small-bowel disease or co-existing with it. The main mechanisms for this association are believed to be the impaired cholecystokinin (CCK) and secretin release, but also the chronic duodenal inflammation that can lead to secondary modifications of papillary mucosal area[20].

Our aim was to summarize currently available evidence with regard to exocrine pancreatic involvement in CD, looking at CD as a risk factor or associated condition with pathologies of the exocrine pancreas, and testing indications regarding the bidirectional association of the two diseases.

SEARCH STRATEGY

For this purpose, we searched PubMed in January 2022 for all publications on the association between pancreas and CD, using the medical subject headings (MeSH) terms–"pancreas" (ID: D010179) and "celiac disease" (ID: D002446), with the following search syntax (("pancreas" [Mesh]) OR (pancreas [Title/Abstract])) AND (("celiac disease" [Mesh]) OR (celiac disease [Title/Abstract])). We performed additional searches with pancreas-related terms, "Pancreas, exocrine" (ID: D046790), "pancreatitis" (ID: D010195), "pancreatitis, chronic" (ID: D050500), "autoimmune pancreatitis" (ID: D000081012) and "celiac disease" (ID: D002446). The extended search yielded a total of 889 results, of which 145 were duplicates. Search results were imported into Reference Citation Analysis (Baishideng Publishing Group, Inc.), which was used for article processing and selection. We filtered the search for reviews, editorials, comments and opinion articles (n = 140). We excluded papers referring to the association of CD with diabetes or alterations of the endocrine pancreas (n = 66). The remaining titles and consecutive abstracts were screened for pertinence to the topic. We selected relevant articles on exocrine pancreatic involvement in CD for full-text analysis and summarized findings according to significant associations. References and citing articles of selected papers were also analyzed for potentially relevant articles that

might have been missed in the initial search. The process of article selection is detailed in Figure 1.

CD AND RISK OF PANCREATITIS

CD patients are at risk both for acute pancreatitis (AP) and chronic pancreatitis (CP)[21-23]. While some have described worse outcomes and increased medical burden among CD individuals[21], others have found lower morbidity and mortality among this patient group[24] (Table 1).

Several pathogenic mechanisms have been theorized to account for the elevated pancreatitis risk in CD–malnutrition, papillary stenosis, and immune phenomena[25] (Figure 2). Severe malnutrition affects pancreatic secretion and can cause pancreatic atrophy[26]. Also, chronic inflammation of the duodenal mucosa in CD patients can also involve the papillary area and lead to papillary stenosis and consequent pancreatic disease[20]. Finally, autoimmune pancreatitis (AIP) or other autoimmune phenomena such as islet-specific autoantibodies in CD-associated type 1 diabetes mellitus can contribute to the link between pancreatitis and CD[27,28].

With regard to CP, results are also discordant using similar diagnostic criteria; while some authors have reported CP features to be common in CD patients undergoing endoscopic ultrasound (EUS) assessment[29], others did not reveal significant structural alterations in the pancreatic parenchyma of CD individuals[30]. In their study using EUS criteria and elastography, Rana *et al*[30] concluded that PEI is functional and reversible after gluten-free diet (GFD). Supporting this finding, the pathognomonic pancreatic calcifications have been rarely reported in CD[31-35]. However, a biopsy-based study published as abstract has shown CD prevalence as high as 7.4% in established CP, recommending screening in this group[36].

Concerning CD screening in pancreatic diseases, there have been reports of asymptomatic hyperenzymemia, macrolipasemia, or macroamylasemia[37-42] in CD patients, but prevalence studies are missing. According to these reports, decrease or even resolution of macroamylasemia/macrolipasemia or elevated pancreatic enzyme levels can be seen on GFD. Of note, the occurrence of hyperenzymemia in CD can be a confounder for the reported elevated risk of AP associated with CD, by overdiagnosing AP in this scenario.

On the other hand, idiopathic recurrent pancreatitis and sphincter of Oddi dysfunction might be considered a testing indication for CD, given the mechanism of chronic papillitis[20,43]. Non-response to treatment in CP might warrant testing for CD, as suggested in some case reports[31].

EXOCRINE PANCREATIC INSUFFICIENCY AND CD

CD is a well-recognized less common etiology of PEI[19,44,45]. This is well reported in currently available guidelines[46]. EPI has been reported with variable frequency in CD patients, depending on the test used to diagnose it. Early studies were based on direct pancreatic function testing (pancreatic enzyme or bicarbonate secretions measurements) and found that PEI is common in classical CD, but non-severe[47]. Fecal elastase (FE) is recommended for detecting PEI in newly diagnosed CD[48]. Impairment of pancreatic exocrine function can be seen both in newly diagnosed CD, in up to 80% of cases[19], and in treated CD, where it should be considered a cause of treatment failure in patients unresponsive to GFD[49,50]. In this latter group comprising GFD-treated CD patients with continuing diarrhea, EPI has been reported in 12%-18% of cases[51,52]. While CD patients improve with pancreatic enzyme replacement therapy (PERT), probably paralleling the restoring of mucosal architecture on GFD, some authors have reported that PERT could be discontinued in some patients who experience improvement in symptoms[53]. However, in CD patients with PEI, who report good adherence to GFD but experience continued malabsorption with adequate dosing PERT, additional pathogenic mechanisms such as enteric infections (*e.g.*, *Giardia*), small intestinal bacterial overgrowth, or complications such as refractory CD and enteropathy associated T-cell lymphoma should be sought[54]. Moreover, gastroparesis in the setting of type 1 diabetes mellitus associated with CD could contribute to incomplete response to PERT. PEI should be readily recognized in slowly recovering children with CD on GFD, as it might accelerate weight increase with adequate enzyme supplementation[55].

Correlation of certain genetic polymorphisms with PEI has also been studied, but without conclusive associations in a small cohort of CD patients[56].

A concern with using FE is represented by the lower diagnostic accuracy compared to direct pancreatic function testing, variability among different tests and analytical processing of samples, taking into account the potential dilution due to diarrhea[57-59].

Despite the increased risk of pancreatitis in CD discussed above, changes in pancreatic enzyme secretion in these patients seen to be mainly functional, as reported by Rana *et al*[30], who found no correlation with structural parenchymal alterations, assessed by EUS. Another study, based on magnetic resonance imaging assessment, did not reveal morphological changes in CD patients with PEI[60]. This impaired function of the exocrine pancreas is also supported by the inverse correlation between mucosal damage and pancreatic enzyme levels, with reversal of PEI on GFD[19,61]. However, protein

Table 1 Summary of studies looking at acute pancreatitis and chronic pancreatitis prevalence among individuals with celiac disease

Ref.	CD, *n*	Pancreatitis prevalence	OR of AP	Outcome
Alkhayyat *et al* [21], 2021	133400	AP 1.06%; CP 0.52%	OR for AP = 2.66; OR for CP = 2.18	Worse outcomes compared to non-CD
Osagiede *et al* [24], 2020	337201	AP 2.2%	OR = 1.92	Lower morbidity and mortality, attributed to less severe forms of AP or lower baseline comorbidities
Sadr-Azodi *et al* [22], 2012	28908	Pancreatitis 1.4%	HR for gallstone-related AP = 1.59; HR for non-gallstone-related AP = 1.86; HR for CP = 3.33	Increased risk of severe AP (gallstone-related: HR = 3.18; non-gallstone related: HR = 2.00)
Ludvigsson *et al* [23], 2007	14239	Pancreatitis any type 0.66%	HR for pancreatitis of any type = 3.3; HR for CP = 19.8	Patient population was represented by hospital inpatients, leaving out those managed as outpatients

AP: Acute pancreatitis; CD: Celiac disease; CP: Chronic pancreatitis; HR: Hazard ratio; OR: Odds ratio.

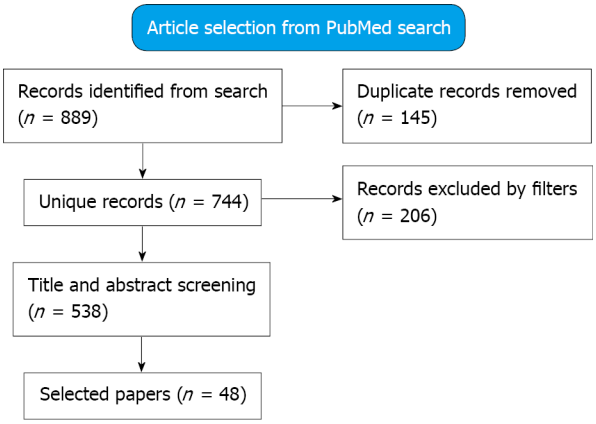

DOI: 10.3748/wjg.v28.i24.2680

Figure 1 Flow diagram of the article selection process.

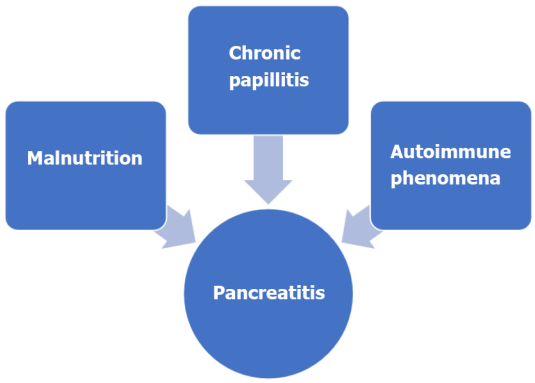

DOI: 10.3748/wjg.v28.i24.2680

Figure 2 Mechanism behind the increased pancreatitis risk in celiac disease patients.

malnutrition, also present in CD patients, has been shown to be associated with acinar cell atrophy and fibrosis[18].

The main mechanism of PEI in CD patients is disruption of mucosal release of enteric hormones, mainly CCK and secretin, which represent a potent stimulus for pancreatic function. While exocrine pancreatic function is intrinsically normal, impaired CCK and secretin release from the atrophic mucosa leads to decreased secretion of enzymes into the duodenal lumen. The functional PEI that occurs in CD is reversible upon exogenous administration of CCK-pancreozymin[62]. Others have suggested that PEI can develop independent of this reduced entero-hormone release[63]. Another theorized mechanism is deficiency of amino acids, which leads to reduced protein synthesis for pancreatic enzymes. This mechanism is also backed up by the fact that correction of deficiencies alleviates PEI in CD patients[64].

Table 2 Mechanisms of pancreatic exocrine insufficiency in celiac disease

No.	
1	Impaired secretion of cholecystokinin and secretin from the diseased small bowel mucosa
2	Reduced amino acid uptake in the small bowel, which subsequently leads to reduction in precursors for synthesis of pancreatic enzymes
3	Morphologic alterations in pancreatic parenchyma secondary to protein malnutrition

Another hypothesis, but probably of less significance, is that of structural changes in the pancreatic parenchyma (acinar atrophy, fibrosis) seen in advanced malnutrition[65]. Mechanisms behind EPI in CD are summarized in Table 2[18,47,50,66].

CYSTIC FIBROSIS AND CD

Another underrecognized, pancreas-related association for CD is cystic fibrosis (CF), an autosomal recessive disease characterized by mutations in the CF transmembrane conductance regulator gene, which encodes a chloride and bicarbonate channel expressed in epithelial cells in multiple organs[67]. While the pancreatic dysfunction in CF is well known, altered immune regulation has been described in these patients, which predisposes them to developing autoimmune phenomena. The systematic review and meta-analysis by Imrei *et al*[68] showed pooled prevalence of 1.8%-2.3% of biopsy-proven CD among CF patients, which is more than twice that of the general population[69]. Based on this observation, the authors recommend routine screening for CD in CF patients. This recommendation is supported by another group[70], who suggested performing CD screening in CF with persistent gastrointestinal symptoms or malabsorption (including improper weight and/or height gain in pediatric patients), despite adequate enzyme replacement therapy.

AIP AND CD

AIP is a chronic fibroinflammatory disease of the pancreas, with a relapsing steroid-responsive pattern. Given the common immune dysregulation background of both AIP and CD, researchers have looked whether there is an association of the two. While some isolated reports have shown a potential link between AIP and CD[71,72], a study looking at CD frequency in a cohort of AIP patients did not show an increased CD prevalence among this group (1.4%) and concluded that serologic screening for CD is not supported[73]. However, a murine model of AIP has provided insight that gliadin sensitization and challenge can induce pancreatitis and extrapancreatic inflammation in HLA-DQ8 transgenic mice[74]. On the other hand, immunoglobulin G4-positive cells, which have been searched for in duodenal/ampullary biopsies as an alternative to pancreatic biopsy for diagnosing AIP, have also been reported in 7 of 18 CD patients in the study by Cebe *et al*[75]. Given the scarce data on AIP and CD, further research is warranted to conclude if there is a link between the two beyond the plausible biologic mechanism. A recognized association is that of type 2 AIP and ulcerative colitis, and considering the also established connection between CD and inflammatory bowel diseases[76], linking the three diseases might provide some insight on the relationship between AIP and CD.

CONCLUSION

Pancreatic involvement, both endocrine and exocrine, is frequent in CD and should be searched for in the appropriate clinical setting. Conversely, certain pancreatic-related diseases should prompt looking for CD–CF with ongoing digestive symptoms, non-responsive CP, idiopathic recurrent pancreatitis. Concomitant pancreatic disease in a CD patient may contribute to aggravated malnutrition and should be readily recognized in order to improve nutritional status and prognosis. Also, there is increasing data that impaired pancreatic function in CD can improve on a GFD.

FOOTNOTES

Author contributions: Balaban DV proposed the research idea; Balaban DV, Enache I, and Ciochina M performed the literature search and article selection, and drafted the initial version of the manuscript; Popp A and Jinga M critically reviewed the manuscript and supervised the project; All authors contributed to drawing the figures and tables, and have read and approved the final version of the manuscript.

Conflict-of-interest statement: All the authors report no relevant conflicts of interest for this article.

Country/Territory of origin: Romania

ORCID number: Daniel Vasile Balaban 0000-0003-3436-8041; Iulia Enache 0000-0001-6905-5008; Marina Ciochina 0000-0002-1573-6358; Alina Popp 0000-0002-7809-5762; Mariana Jinga 0000-0001-5826-0815.

Corresponding Author's Membership in Professional Societies: European Society for Gastrointestinal Endoscopy, No. 45910264; Association for Pancreatic Pathology Romania; European Society for the Study of Coeliac Disease (ESsCD); Romanian Society of Gastroenterology and Hepatology; Romanian Society of Digestive Endoscopy; European Pancreatic Club; World Endoscopy Organization

S-Editor: Fan JR
L-Editor: Filipodia
P-Editor: Fan JR

REFERENCES

1 **Makharia GK**, Singh P, Catassi C, Sanders DS, Leffler D, Ali RAR, Bai JC. The global burden of coeliac disease: opportunities and challenges. *Nat Rev Gastroenterol Hepatol* 2022 [PMID: 34980921 DOI: 10.1038/s41575-021-00552-z]
2 **Pinto-Sanchez MI**, Silvester JA, Lebwohl B, Leffler DA, Anderson RP, Therrien A, Kelly CP, Verdu EF. Society for the Study of Celiac Disease position statement on gaps and opportunities in coeliac disease. *Nat Rev Gastroenterol Hepatol* 2021; **18**: 875-884 [PMID: 34526700 DOI: 10.1038/s41575-021-00511-8]
3 **Jinga M**, Popp A, Balaban DV, Dima A, Jurcut C. Physicians' attitude and perception regarding celiac disease: A questionnaire-based study. *Turk J Gastroenterol* 2018; **29**: 419-426 [PMID: 30249556 DOI: 10.5152/tjg.2018.17236]
4 **Therrien A**, Kelly CP, Silvester JA. Celiac Disease: Extraintestinal Manifestations and Associated Conditions. *J Clin Gastroenterol* 2020; **54**: 8-21 [PMID: 31513026 DOI: 10.1097/MCG.0000000000001267]
5 **Leffler DA**, Green PH, Fasano A. Extraintestinal manifestations of coeliac disease. *Nat Rev Gastroenterol Hepatol* 2015; **12**: 561-571 [PMID: 26260366 DOI: 10.1038/nrgastro.2015.131]
6 **Durazzo M**, Ferro A, Brascugli I, Mattivi S, Fagoonee S, Pellicano R. Extra-Intestinal Manifestations of Celiac Disease: What Should We Know in 2022? *J Clin Med* 2022; **11** [PMID: 35011999 DOI: 10.3390/jcm11010258]
7 **Balaban DV**, Mihai A, Dima A, Popp A, Jinga M, Jurcut C. Celiac disease and Sjögren's syndrome: A case report and review of literature. *World J Clin Cases* 2020; **8**: 4151-4161 [PMID: 33024773 DOI: 10.12998/wjcc.v8.i18.4151]
8 **Dima A**, Jurcut C, Jinga M. Rheumatologic manifestations in celiac disease: what should we remember? *Rom J Intern Med* 2019; **57**: 3-5 [PMID: 30375355 DOI: 10.2478/rjim-2018-0024]
9 **Ciaccio EJ**, Lewis SK, Biviano AB, Iyer V, Garan H, Green PH. Cardiovascular involvement in celiac disease. *World J Cardiol* 2017; **9**: 652-666 [PMID: 28932354 DOI: 10.4330/wjc.v9.i8.652]
10 **Haggård L**, Glimberg I, Lebwohl B, Sharma R, Verna EC, Green PHR, Ludvigsson JF. High prevalence of celiac disease in autoimmune hepatitis: Systematic review and meta-analysis. *Liver Int* 2021; **41**: 2693-2702 [PMID: 34219350 DOI: 10.1111/liv.15000]
11 **Mearns ES**, Taylor A, Thomas Craig KJ, Puglielli S, Leffler DA, Sanders DS, Lebwohl B, Hadjivassiliou M. Neurological Manifestations of Neuropathy and Ataxia in Celiac Disease: A Systematic Review. *Nutrients* 2019; **11** [PMID: 30759885 DOI: 10.3390/nu11020380]
12 **Rodrigo L**, Beteta-Gorriti V, Alvarez N, Gómez de Castro C, de Dios A, Palacios L, Santos-Juanes J. Cutaneous and Mucosal Manifestations Associated with Celiac Disease. *Nutrients* 2018; **10** [PMID: 29933630 DOI: 10.3390/nu10070800]
13 **Laurikka P**, Nurminen S, Kivelä L, Kurppa K. Extraintestinal Manifestations of Celiac Disease: Early Detection for Better Long-Term Outcomes. *Nutrients* 2018; **10** [PMID: 30081502 DOI: 10.3390/nu10081015]
14 **Elwenspoek MMC**, Jackson J, O'Donnell R, Sinobas A, Dawson S, Everitt H, Gillett P, Hay AD, Lane DL, Mallett S, Robins G, Watson JC, Jones HE, Whiting P. The accuracy of diagnostic indicators for coeliac disease: A systematic review and meta-analysis. *PLoS One* 2021; **16**: e0258501 [PMID: 34695139 DOI: 10.1371/journal.pone.0258501]
15 **Al-Toma A**, Volta U, Auricchio R, Castillejo G, Sanders DS, Cellier C, Mulder CJ, Lundin KEA. European Society for the Study of Coeliac Disease (ESsCD) guideline for coeliac disease and other gluten-related disorders. *United European Gastroenterol J* 2019; **7**: 583-613 [PMID: 31210940 DOI: 10.1177/2050640619844125]
16 **Rubio-Tapia A**, Hill ID, Kelly CP, Calderwood AH, Murray JA; American College of Gastroenterology. ACG clinical guidelines: diagnosis and management of celiac disease. *Am J Gastroenterol* 2013; **108**: 656-76; quiz 677 [PMID: 23609613 DOI: 10.1038/ajg.2013.79]
17 **Ludvigsson JF**, Bai JC, Biagi F, Card TR, Ciacci C, Ciclitira PJ, Green PH, Hadjivassiliou M, Holdoway A, van Heel DA, Kaukinen K, Leffler DA, Leonard JN, Lundin KE, McGough N, Davidson M, Murray JA, Swift GL, Walker MM, Zingone F, Sanders DS; BSG Coeliac Disease Guidelines Development Group; British Society of Gastroenterology. Diagnosis and

management of adult coeliac disease: guidelines from the British Society of Gastroenterology. *Gut* 2014; **63**: 1210-1228 [PMID: 24917550 DOI: 10.1136/gutjnl-2013-306578]

18 **Freeman HJ**. Pancreatic endocrine and exocrine changes in celiac disease. *World J Gastroenterol* 2007; **13**: 6344-6346 [PMID: 18081222 DOI: 10.3748/wjg.v13.i47.6344]

19 **Singh VK**, Haupt ME, Geller DE, Hall JA, Quintana Diez PM. Less common etiologies of exocrine pancreatic insufficiency. *World J Gastroenterol* 2017; **23**: 7059-7076 [PMID: 29093615 DOI: 10.3748/wjg.v23.i39.7059]

20 **Patel RS**, Johlin FC Jr, Murray JA. Celiac disease and recurrent pancreatitis. *Gastrointest Endosc* 1999; **50**: 823-827 [PMID: 10570344 DOI: 10.1016/s0016-5107(99)70166-5]

21 **Alkhayyat M**, Saleh MA, Abureesh M, Khoudari G, Qapaja T, Mansoor E, Simons-Linares CR, Vargo J, Stevens T, Rubio-Tapia A, Chahal P. The Risk of Acute and Chronic Pancreatitis in Celiac Disease. *Dig Dis Sci* 2021; **66**: 2691-2699 [PMID: 32809104 DOI: 10.1007/s10620-020-06546-2]

22 **Sadr-Azodi O**, Sanders DS, Murray JA, Ludvigsson JF. Patients with celiac disease have an increased risk for pancreatitis. *Clin Gastroenterol Hepatol* 2012; **10**: 1136-1142.e3 [PMID: 22801059 DOI: 10.1016/j.cgh.2012.06.023]

23 **Ludvigsson JF**, Montgomery SM, Ekbom A. Risk of pancreatitis in 14,000 individuals with celiac disease. *Clin Gastroenterol Hepatol* 2007; **5**: 1347-1353 [PMID: 17702659 DOI: 10.1016/j.cgh.2007.06.002]

24 **Osagiede O**, Lukens FJ, Wijarnpreecha K, Corral JE, Raimondo M, Kröner PT. Acute Pancreatitis in Celiac Disease: Has the Inpatient Prevalence Changed and Is It Associated With Worse Outcomes? *Pancreas* 2020; **49**: 1202-1206 [PMID: 32898005 DOI: 10.1097/MPA.0000000000001657]

25 **Basha J**, Appasani S, Vaiphei K, Singh K, Kochhar R. Celiac disease presenting as recurrent pancreatitis and pseudocyst. *JOP* 2012; **13**: 533-535 [PMID: 22964961 DOI: 10.6092/1590-8577/1091]

26 **Brooks SE**, Golden MH. The exocrine pancreas in kwashiorkor and marasmus. Light and electron microscopy. *West Indian Med J* 1992; **41**: 56-60 [PMID: 1523833]

27 **Leeds JS**, Sanders DS. Risk of pancreatitis in patients with celiac disease: is autoimmune pancreatitis a biologically plausible mechanism? *Clin Gastroenterol Hepatol* 2008; **6**: 951; author reply 951 [PMID: 18674737 DOI: 10.1016/j.cgh.2007.12.025]

28 **Sasamori H**, Fukui T, Hayashi T, Yamamoto T, Ohara M, Yamamoto S, Kobayashi T, Hirano T. Analysis of pancreatic volume in acute-onset, slowly-progressive and fulminant type 1 diabetes in a Japanese population. *J Diabetes Investig* 2018; **9**: 1091-1099 [PMID: 29427469 DOI: 10.1111/jdi.12816]

29 **Kumar S**, Gress F, Green PH, Lebwohl B. Chronic Pancreatitis is a Common Finding in Celiac Patients Who Undergo Endoscopic Ultrasound. *J Clin Gastroenterol* 2019; **53**: e128-e129 [PMID: 27749638 DOI: 10.1097/MCG.0000000000000726]

30 **Rana SS**, Dambalkar A, Chhabra P, Sharma R, Nada R, Sharma V, Rana S, Bhasin DK. Is pancreatic exocrine insufficiency in celiac disease related to structural alterations in pancreatic parenchyma? *Ann Gastroenterol* 2016; **29**: 363-366 [PMID: 27366039 DOI: 10.20524/aog.2016.0042]

31 **Rana SS**, Bhasin DK, Sinha SK, Singh K. Coexistence of chronic calcific pancreatitis and celiac disease. *Indian J Gastroenterol* 2007; **26**: 150; author reply 150 [PMID: 17704598]

32 **Pitchumoni CS**, Thomas E, Balthazar E, Sherling B. Chronic calcific pancreatitis in association with celiac disease. *Am J Gastroenterol* 1977; **68**: 358-361 [PMID: 605891]

33 **Fitzgerald O**, Fitzgerald P, Fennelly J, Mcmullin JP, Boland SJ. A clinical study of chronic pancreatitis. *Gut* 1963; **4**: 193-216 [PMID: 14058261 DOI: 10.1136/gut.4.3.193]

34 **Nanda R**, Anand BS. Celiac disease and tropical calcific pancreatitis. *Am J Gastroenterol* 1993; **88**: 1790-1792 [PMID: 8213729]

35 **Arya S**, Rana SS, Sinha SK, Nagi B, Bhasin DK. Celiac disease and chronic calcific pancreatitis with pancreas divisum. *Gastrointest Endosc* 2006; **63**: 1080-1081 [PMID: 16733138 DOI: 10.1016/j.gie.2006.01.001]

36 **Nett A**, Wamsterker E, DiMagno M. Should Patients With Established Chronic Pancreatitis Undergo Testing for Celiac Disease? Abstracts of Papers Submitted to the 47th Meeting of the American Pancreatic Association, October 26–29, 2016, Boston, Massachusetts. Pancreas 2016: 1494–551

37 **Rabsztyn A**, Green PH, Berti I, Fasano A, Perman JA, Horvath K. Macroamylasemia in patients with celiac disease. *Am J Gastroenterol* 2001; **96**: 1096-1100 [PMID: 11316153 DOI: 10.1111/j.1572-0241.2001.03746.x]

38 **Bonetti G**, Serricchio G, Giudici A, Bettonagli M, Vadacca GB, Bruno R, Coslovich E, Moratti R. Hyperamylasemia due to macroamylasemia in adult gluten enteropathy. *Scand J Clin Lab Invest* 1997; **57**: 271-273 [PMID: 9238763 DOI: 10.3109/00365519709060036]

39 **Bermejo JF**, Carbone J, Rodriguez JJ, Macias R, Rodriguez M, Gil J, Marin MA, Torres F, Fernandez-Cruz E. Macroamylasaemia, IgA hypergammaglobulinaemia and autoimmunity in a patient with Down syndrome and coeliac disease. *Scand J Gastroenterol* 2003; **38**: 445-447 [PMID: 12739720 DOI: 10.1080/00365520310000933]

40 **Barera G**, Bazzigaluppi E, Viscardi M, Renzetti F, Bianchi C, Chiumello G, Bosi E. Macroamylasemia attributable to gluten-related amylase autoantibodies: a case report. *Pediatrics* 2001; **107**: E93 [PMID: 11389291 DOI: 10.1542/peds.107.6.e93]

41 **La Villa G**, Pantaleo P, Tarquini R, Cirami L, Perfetto F, Mancuso F, Laffi G. Multiple immune disorders in unrecognized celiac disease: a case report. *World J Gastroenterol* 2003; **9**: 1377-1380 [PMID: 12800261 DOI: 10.3748/wjg.v9.i6.1377]

42 **Liu Z**, Wang J, Qian J, Tang F. Hyperamylasemia, reactive plasmacytosis, and immune abnormalities in a patient with celiac disease. *Dig Dis Sci* 2007; **52**: 1444-1447 [PMID: 17443408 DOI: 10.1007/s10620-006-9268-0]

43 **Rodrigo L**, Alvarez N, Riestra S, de Francisco R, González Bernardo O, García Isidro L, López Vázquez A, López Larrea C. [Relapsing acute pancreatitis associated with gluten enteropathy. Clinical, laboratory, and evolutive characteristics in thirty-four patients]. *Rev Esp Enferm Dig* 2008; **100**: 746-751 [PMID: 19222332 DOI: 10.4321/s1130-01082008001200002]

44 **Kunovský L**, Dítě P, Jabandžiev P, Eid M, Poredská K, Vaculová J, Sochorová D, Janeček P, Tesaříková P, Blaho M, Trna J, Hlavsa J, Kala Z. Causes of Exocrine Pancreatic Insufficiency Other Than Chronic Pancreatitis. *J Clin Med* 2021; **10** [PMID: 34945075 DOI: 10.3390/jcm10245779]

45 **Leeds JS**, Hopper AD, Hurlstone DP, Edwards SJ, McAlindon ME, Lobo AJ, Donnelly MT, Morley S, Sanders DS. Is exocrine pancreatic insufficiency in adult coeliac disease a cause of persisting symptoms? *Aliment Pharmacol Ther* 2007; **25**: 265-271 [PMID: 17269988 DOI: 10.1111/j.1365-2036.2006.03206.x]

46 **Gheorghe C**, Seicean A, Saftoiu A, Tantau M, Dumitru E, Jinga M, Negreanu L, Mateescu B, Gheorghe L, Ciocirlan M, Cijevschi C, Constantinescu G, Dima S, Diculescu M; Romanian Association for Pancreatic Pathology. Romanian guidelines on the diagnosis and treatment of exocrine pancreatic insufficiency. *J Gastrointestin Liver Dis* 2015; **24**: 117-123 [PMID: 25822444 DOI: 10.15403/jgld.2014.1121.app]

47 **DiMagno M**. Exocrine Pancreatic Insufficiency and Pancreatitis Associated with Celiac Disease [Internet]. [cited 10 January 2022]. Available from: https://pancreapedia.org/sites/default/files/Exocrine-Pancreatic-Insufficiency-Pancreatitis-Celiac-Disease_0.pdf

48 **Pezzilli R**. Exocrine pancreas involvement in celiac disease: a review. *Recent Pat Inflamm Allergy Drug Discov* 2014; **8**: 167-172 [PMID: 25417707 DOI: 10.2174/1872213x08666141122210738]

49 **Weizman Z**, Hamilton JR, Kopelman HR, Cleghorn G, Durie PR. Treatment failure in celiac disease due to coexistent exocrine pancreatic insufficiency. *Pediatrics* 1987; **80**: 924-926 [PMID: 3684405]

50 **Regan PT**, DiMagno EP. Exocrine pancreatic insufficiency in celiac sprue: a cause of treatment failure. *Gastroenterology* 1980; **78**: 484-487 [PMID: 7351287]

51 **Fine KD**, Meyer RL, Lee EL. The prevalence and causes of chronic diarrhea in patients with celiac sprue treated with a gluten-free diet. *Gastroenterology* 1997; **112**: 1830-1838 [PMID: 9178673 DOI: 10.1053/gast.1997.v112.pm9178673]

52 **Abdulkarim AS**, Burgart LJ, See J, Murray JA. Etiology of nonresponsive celiac disease: results of a systematic approach. *Am J Gastroenterol* 2002; **97**: 2016-2021 [PMID: 12190170 DOI: 10.1111/j.1572-0241.2002.05917.x]

53 **Evans KE**, Leeds JS, Morley S, Sanders DS. Pancreatic insufficiency in adult celiac disease: do patients require long-term enzyme supplementation? *Dig Dis Sci* 2010; **55**: 2999-3004 [PMID: 20458623 DOI: 10.1007/s10620-010-1261-y]

54 **Struyvenberg MR**, Martin CR, Freedman SD. Practical guide to exocrine pancreatic insufficiency - Breaking the myths. *BMC Med* 2017; **15**: 29 [PMID: 28183317 DOI: 10.1186/s12916-017-0783-y]

55 **Carroccio A**, Iacono G, Lerro P, Cavataio F, Malorgio E, Soresi M, Baldassarre M, Notarbartolo A, Ansaldi N, Montalto G. Role of pancreatic impairment in growth recovery during gluten-free diet in childhood celiac disease. *Gastroenterology* 1997; **112**: 1839-1844 [PMID: 9178674 DOI: 10.1053/gast.1997.v112.pm9178674]

56 **Licul V**, Cizmarević NS, Ristić S, Mikolasević I, Mijandrusić BS. CTLA-4 +49 and TNF-alpha-308 gene polymorphisms in celiac patients with exocrine pancreatic insufficiency. *Coll Antropol* 2013; **37**: 1191-1194 [PMID: 24611333]

57 **Brydon WG**, Kingstone K, Ghosh S. Limitations of faecal elastase-1 and chymotrypsin as tests of exocrine pancreatic disease in adults. *Ann Clin Biochem* 2004; **41**: 78-81 [PMID: 14713391 DOI: 10.1258/000456304322664753]

58 **Kampanis P**, Ford L, Berg J. Development and validation of an improved test for the measurement of human faecal elastase-1. *Ann Clin Biochem* 2009; **46**: 33-37 [PMID: 19008259 DOI: 10.1258/acb.2008.008123]

59 **Vanga RR**, Tansel A, Sidiq S, El-Serag HB, Othman MO. Diagnostic Performance of Measurement of Fecal Elastase-1 in Detection of Exocrine Pancreatic Insufficiency: Systematic Review and Meta-analysis. *Clin Gastroenterol Hepatol* 2018; **16**: 1220-1228.e4 [PMID: 29374614 DOI: 10.1016/j.cgh.2018.01.027]

60 **Vujasinovic M**, Tepes B, Volfand J, Rudolf S. Exocrine pancreatic insufficiency, MRI of the pancreas and serum nutritional markers in patients with coeliac disease. *Postgrad Med J* 2015; **91**: 497-500 [PMID: 26253920 DOI: 10.1136/postgradmedj-2015-133262]

61 **Nousia-Arvanitakis S**, Karagiozoglou-Lamboudes T, Aggouridaki C, Malaka-Lambrellis E, Galli-Tsinopoulou A, Xefteri M. Influence of jejunal morphology changes on exocrine pancreatic function in celiac disease. *J Pediatr Gastroenterol Nutr* 1999; **29**: 81-85 [PMID: 10400109 DOI: 10.1097/00005176-199907000-00019]

62 **DiMagno EP**, Go WL, Summerskill WH. Impaired cholecystokinin-pancreozymin secretion, intraluminal dilution, and maldigestion of fat in sprue. *Gastroenterology* 1972; **63**: 25-32 [PMID: 5055745]

63 **Carroccio A**, Iacono G, Montalto G, Cavataio F, Di Marco C, Balsamo V, Notarbartolo A. Exocrine pancreatic function in children with coeliac disease before and after a gluten free diet. *Gut* 1991; **32**: 796-799 [PMID: 1855688 DOI: 10.1136/gut.32.7.796]

64 **Tandon BN**, Banks PA, George PK, Sama SK, Ramachandran K, Gandhi PC. Recovery of exocrine pancreatic function in adult protein-calorie malnutrition. *Gastroenterology* 1970; **58**: 358-362 [PMID: 5437989]

65 **Tandon BN**, George PK, Sama SK, Ramachandran K, Gandhi PC. Exocrine pancreatic function in protein--calorie malnutrition disease of adults. *Am J Clin Nutr* 1969; **22**: 1476-1482 [PMID: 5350763 DOI: 10.1093/ajcn/22.11.1476]

66 **Buchan AM**, Grant S, Brown JC, Freeman HJ. A quantitative study of enteric endocrine cells in celiac sprue. *J Pediatr Gastroenterol Nutr* 1984; **3**: 665-671 [PMID: 6150077 DOI: 10.1097/00005176-198411000-00004]

67 **Shteinberg M**, Haq IJ, Polineni D, Davies JC. Cystic fibrosis. *Lancet* 2021; **397**: 2195-2211 [PMID: 34090606 DOI: 10.1016/S0140-6736(20)32542-3]

68 **Imrei M**, Németh D, Szakács Z, Hegyi P, Kiss S, Alizadeh H, Dembrovszky F, Pázmány P, Bajor J, Párniczky A. Increased Prevalence of Celiac Disease in Patients with Cystic Fibrosis: A Systematic Review and Meta-Analysis. *J Pers Med* 2021; **11** [PMID: 34575636 DOI: 10.3390/jpm11090859]

69 **Singh P**, Arora A, Strand TA, Leffler DA, Catassi C, Green PH, Kelly CP, Ahuja V, Makharia GK. Global Prevalence of Celiac Disease: Systematic Review and Meta-analysis. *Clin Gastroenterol Hepatol* 2018; **16**: 823-836.e2 [PMID: 29551598 DOI: 10.1016/j.cgh.2017.06.037]

70 **Emiralioglu N**, Ademhan Tural D, Hizarcioglu Gulsen H, Ergen YM, Ozsezen B, Sunman B, Saltık Temizel İ, Yalcin E, Dogru D, Ozcelik U, Kiper N. Does cystic fibrosis make susceptible to celiac disease? *Eur J Pediatr* 2021; **180**: 2807-2813 [PMID: 33765186 DOI: 10.1007/s00431-021-04011-4]

71 **Patel BJ**, Cantor M, Retrosi G, Gheorghe R, Wrogemann J, Mujawar Q. Autoimmune Pancreatitis Masquerading as Celiac Disease. *Pancreas* 2019; **48**: e53-e54 [PMID: 31206470 DOI: 10.1097/MPA.0000000000001326]

72 **Masoodi I**, Wani H, Alsayari K, Sulaiman T, Hassan NS, Nazmi Alqutub A, Al Omair A, H Al-Lehibi A. Celiac disease and autoimmune pancreatitis: an uncommon association. A case report. *Eur J Gastroenterol Hepatol* 2011; **23**: 1270-1272

[PMID: 21946127 DOI: 10.1097/MEG.0b013e32834c7bad]

73 **De Marchi G**, Zanoni G, Conti Bellocchi MC, Betti E, Brentegani M, Capelli P, Zuliani V, Frulloni L, Klersy C, Ciccocioppo R. There Is No Association between Coeliac Disease and Autoimmune Pancreatitis. *Nutrients* 2018; **10** [PMID: 30149525 DOI: 10.3390/nu10091157]

74 **Moon SH**, Kim J, Kim MY, Park do H, Song TJ, Kim SA, Lee SS, Seo DW, Lee SK, Kim MH. Sensitization to and Challenge with Gliadin Induce Pancreatitis and Extrapancreatic Inflammation in HLA-DQ8 Mice: An Animal Model of Type 1 Autoimmune Pancreatitis. *Gut Liver* 2016; **10**: 842-850 [PMID: 27114422 DOI: 10.5009/gnl15484]

75 **Cebe KM**, Swanson PE, Upton MP, Westerhoff M. Increased IgG4+ cells in duodenal biopsies are not specific for autoimmune pancreatitis. *Am J Clin Pathol* 2013; **139**: 323-329 [PMID: 23429368 DOI: 10.1309/AJCPT00NHQHXAHDS]

76 **Pinto-Sanchez MI**, Seiler CL, Santesso N, Alaedini A, Semrad C, Lee AR, Bercik P, Lebwohl B, Leffler DA, Kelly CP, Moayyedi P, Green PH, Verdu EF. Association Between Inflammatory Bowel Diseases and Celiac Disease: A Systematic Review and Meta-Analysis. *Gastroenterology* 2020; **159**: 884-903.e31 [PMID: 32416141 DOI: 10.1053/j.gastro.2020.05.016]

World Journal of Gastroenterology

Submit a Manuscript: https://www.f6publishing.com

World J Gastroenterol 2022 June 28; 28(24): 2689-2704

DOI: 10.3748/wjg.v28.i24.2689

ISSN 1007-9327 (print) ISSN 2219-2840 (online)

ORIGINAL ARTICLE

Basic Study

Downregulation of *TNFR2* decreases survival gene expression, promotes apoptosis and affects the cell cycle of gastric cancer cells

Ana Flávia Teixeira Rossi, Fernanda da Silva Manoel-Caetano, Joice Matos Biselli, Ágata Silva Cabral, Marilia de Freitas Calmon Saiki, Marcelo Lima Ribeiro, Ana Elizabete Silva

Specialty type: Gastroenterology and hepatology

Provenance and peer review: Invited article; Externally peer reviewed.

Peer-review model: Single blind

Peer-review report's scientific quality classification

Grade A (Excellent): A, A
Grade B (Very good): 0
Grade C (Good): 0
Grade D (Fair): 0
Grade E (Poor): 0

P-Reviewer: Keikha M, Iran; Tilahun M, Ethiopia

Received: January 15, 2022
Peer-review started: January 15, 2022
First decision: February 7, 2022
Revised: February 21, 2022
Accepted: May 7, 2022
Article in press: May 7, 2022
Published online: June 28, 2022

Ana Flávia Teixeira Rossi, Fernanda da Silva Manoel-Caetano, Joice Matos Biselli, Ágata Silva Cabral, Marilia de Freitas Calmon Saiki, Ana Elizabete Silva, Department of Biological Sciences, Sao Paulo State University (UNESP), São José do Rio Preto 15054-000, São Paulo, Brazil

Marcelo Lima Ribeiro, Clinical Pharmacology and Gastroenterology Unit, São Francisco University (USF), Bragança Paulista 12916-900, São Paulo, Brazil

Corresponding author: Ana Elizabete Silva, PhD, Adjunct Associate Professor, Department of Biological Sciences, Sao Paulo State University (UNESP), Rua Cristóvão Colombo 2265, São José do Rio Preto 15054-000, São Paulo, Brazil. ae.silva@unesp.br

Abstract

BACKGROUND

Chronic inflammation due to *Helicobacter pylori* (*H. pylori*) infection promotes gastric carcinogenesis. Tumour necrosis factor-α (TNF-α), a key mediator of inflammation, induces cell survival or apoptosis by binding to two receptors (TNFR1 and TNFR2). TNFR1 can induce both survival and apoptosis, while TNFR2 results only in cell survival. The dysregulation of these processes may contribute to carcinogenesis.

AIM

To evaluate the effects of TNFR1 and TNFR2 downregulation in AGS cells treated with *H. pylori* extract on the TNF-α pathway.

METHODS

AGS cell lines containing TNFR1 and TNFR2 receptors downregulated by specific shRNAs and nonsilenced AGS cells were treated with *H. pylori* extract for 6 h. Subsequently, quantitative polymerase chain reaction with TaqMan® assays was used for the relative quantification of the mRNAs (*TNFA, TNFR1, TNFR2, TRADD, TRAF2, CFLIP, NFKB1, NFKB2, CASP8, CASP3*) and miRNAs (miR-19a, miR-34a, miR-103a, miR-130a, miR-181c) related to the TNF-α signalling pathway. Flow cytometry was employed for cell cycle analysis and apoptosis assays.

RESULTS

In nonsilenced AGS cells, *H. pylori* extract treatment increased the expression of genes involved in cell survival and inhibited both apoptosis (*NFKB1, NFKB2* and *CFLIP*) and the *TNFR1* receptor. TNFR1 downregulation significantly decreased

the expression of the *TRADD* and *CFLIP* genes, although no change was observed in the cellular process or miRNA expression. In contrast, TNFR2 downregulation decreased the expression of the *TRADD* and *TRAF2* genes, which are both important downstream mediators of the TNFR1-mediated pathway, as well as that of the *NFKB1* and *CFLIP* genes, while upregulating the expression of miR-19a and miR-34a. Consequently, a reduction in the number of cells in the G0/G1 phase and an increase in the number of cells in the S phase were observed, as well as the promotion of early apoptosis.

CONCLUSION

Our findings mainly highlight the important role of TNFR2 in the TNF-α pathway in gastric cancer, indicating that silencing it can reduce the expression of survival and anti-apoptotic genes.

Key Words: Gastric cancer; *Helicobacter pylori*; Tumour necrosis factor-α signalling pathway; *TNFR1*; *TNFR2*; miRNAs

Core Tip: This study demonstrated for the first time the effect of TNFR1 and TNFR2 downregulation on an AGS cell line treated with *Helicobacter pylori* extract. Although TNFR1 downregulation did not promote significant changes in the expression of mRNA and miRNAs of the tumour necrosis factor-α (TNF-α) signalling pathway, TNFR2 downregulation promoted important changes in the signalling mediators evaluated. We observed a reduction in the expression of cell survival and anti-apoptotic genes and an increase in the expression of miR-19a and miR-34a, which affected cell cycle kinetics and contributed to early apoptosis. Thus, our findings highlight the important role of TNFR2 in the TNF-α signalling pathway in gastric carcinogenesis.

Citation: Rossi AFT, da Silva Manoel-Caetano F, Biselli JM, Cabral ÁS, Saiki MFC, Ribeiro ML, Silva AE. Downregulation of *TNFR2* decreases survival gene expression, promotes apoptosis and affects the cell cycle of gastric cancer cells. *World J Gastroenterol* 2022; 28(24): 2689-2704

URL: https://www.wjgnet.com/1007-9327/full/v28/i24/2689.htm

DOI: https://dx.doi.org/10.3748/wjg.v28.i24.2689

INTRODUCTION

Gastric cancer (GC) has high rates of incidence and mortality worldwide, especially in Eastern Asia, Eastern Europe and Latin America[1]. In Brazil, it is the fourth most common cancer in men and the sixth most common in women[2]. *Helicobacter pylori* (*H. pylori*) is the main risk factor for the development of gastric neoplasms, since it is responsible for chronic inflammation in the gastric mucosa and for the GC progression cascade[3]. Consequently, it can trigger the host's immune response, which leads to changes in the expression of genes related to inflammation, cell kinetic regulation and miRNAs [4-6]. After infection by this bacterium, tumour necrosis factor-α (TNF-α) stands out among the mediators of inflammation and is considered to be a key mediator linking inflammation and cancer[7,8].

TNF-α is a pleiotropic proinflammatory cytokine that is important in the signalling and regulation of multiple cellular responses and processes, such as the production of other inflammatory cytokines, and cell communication, survival, proliferation and apoptosis[9]. These different functions are accomplished due to the ability of TNF-α to bind to TNFR1 (TNFRSF1A) or TNFR2 (TNFRSF1B) receptors, thus resulting in different cellular processes. Both receptors are transmembrane proteins, and although they are largely similar in terms of extracellular structure, their intracellular domains are different, and thus dictate the cellular fate for either survival or death. Though only TNFR1 has a death domain, the TNF-α signalling pathway triggered by this receptor is able to induce both cell survival and apoptosis, while TNFR2 results only in cell survival[10,11]. The signalling cascade after TNF-α/TNFR1 binding that results in cell survival starts with the recruitment of TRADD and is mediated by activation of nuclear factor-kappaB (NF-κB) and transcription of pro-survival and anti-apoptotic genes, such as cellular inhibitor of apoptosis proteins (cIAP), TRAF2 and cFLIP, and of inflammatory cytokines. However, this signal complex is transient; TNF-α rapidly dissociates from TNFR1 and binds to the Fas-associated death domain protein to form another signal complex, which coordinates downstream signalling of the caspase cascade and apoptosis. Conversely, as TNFR2 does not have a death domain, it induces long-lasting NF-kB activation by recruiting existing cytoplasmic TRAF-2/cIAP-1/cIAP-2 complexes that can inhibit pro-apoptotic factors and maintain cell survival and proliferation[9-12].

Regulation of signal transduction triggered by TNF-α requires a constant balance between the opposing functions of cell survival and cell death to maintain homeostasis. Thus, an imbalance in these processes due to changes in the expression of receptors, downstream genes, ligands and pro-/anti-apoptotic mediators may support the tumorigenic process[13]. A recent study by our research group showed dysregulation in the TNF-α signalling pathway in GC samples with an upregulation of cell survival-related genes and of TNFR2 expression, thus suggesting a prominent protumor role by TNA-α /TNFR2 binding in gastric neoplasm[14]. Furthermore, we showed through a miRNA:mRNA interaction network that this signalling pathway can be regulated by miRNAs. In addition, *H. pylori* infection was also associated with an increased expression of *TNF-α* mRNA and protein, and dysregulated miRNA expression in chronic gastritis patients. The expression pattern of these genes/miRNAs was normalized after treatment to eradicate bacteria, indicating that this pathogen influences the host's inflammatory response in part by its action on miRNAs[6].

In accordance with our previous results, we thought it was important to evaluate the effect of silencing TNFR1 and TNFR2 receptors in an AGS gastric cell line after treatment with an *H. pylori* extract on *TNF-α* mRNA expression and on downstream genes related to its signalling pathway (*TRADD, TRAF2, CFLIP, NFKB1, NFKB2, CASP8* and *CASP3)*. In addition, we also investigated the same miRNAs previously studied (miR-19a, miR-34a, miR-103a, miR-130a and miR-181c)[14], as well as the cell cycle and apoptosis. Overall, our results highlight the main role of the TNFR2 in TNF-α signalling in an AGS cell line, while treatment with *H. pylori* extract induces prosurvival gene expression mainly through TNFR1.

MATERIALS AND METHODS

Cell culture

AGS GC cells from the Cell Bank of Rio de Janeiro, Brazil (BCRJ code 0311) were incubated at 37 °C and 5% CO_2 in HAM-F10 medium (Cultilab, SP, Brazil) supplemented with 10% foetal bovine serum and 1× antibiotic/antimycotic (Gibco, Invitrogen Life Technologies, Carlsbad, CA, United States). The culture medium was replaced every two to three days. The HGC-27 GC cell line, provided by Dr Marcelo Lima Ribeiro (São Francisco University-USF, SP, Brazil), was also used in early experiments as an alternative line for follow-up experiments, and 293T cells of human embryonic kidney were provided by Dr Luisa Lina Villa (University of São Paulo–USP, SP, Brazil) for transfection experiments. The cells were maintained under the same conditions as the AGS cell line except for the culture medium, which was Dulbecco's modified Eagle medium (Gibco, Invitrogen Life Technologies, Carlsbad, CA, United States). Stable shRNA-expressing cell lines with reduced expression of TNFR1 (called shTNFR1) and TNFR2 (called shTNFR2) were kept in a similar culture medium to the nonsilenced AGS cells, and further supplemented with 0.5 μg/mL puromycin or 200 μg/mL G418, respectively.

Treatment with H. pylori extract

The previously described *H. pylori* Tox+ strain (cagA+/vacA s1m1) was grown in a selective medium (pylori-Gelose; BioMérieux, Marcy-l'Étoile, France) at 37 °C under microaerophilic conditions[15]. This strain is not resistant to any antibiotic used to treat *H. pylori*. *H. pylori* extract was prepared according to the protocol described by Li *et al*[16]. In brief, the *H. pylori* Tox+ strain was harvested and suspended in distilled water at a concentration of 2 × 10^8 CFU/mL. Next, the suspension was incubated at room temperature for 40 min and centrifuged at 20000 *g* for 20 min. The supernatant was filtered using a 0.2 mm filter and stored at -20 °C until use. The extract was tested several times (4, 6 and 24 h) using differing *H. pylori* extract volumes (50, 100, 150 and 200 μL) to verify the best experimental conditions. Then, 2 × 10^5 nonsilenced AGS cells and AGS cells with downregulation of TNFR1 (shTNFR1) and TNFR2 (shTNFR2) were seeded in 12-well plates. After 48 h, the medium was replaced with 500 μL of HAM-F10 containing 30% v/v *H. pylori* extract or the same proportion of water (control). Cells were incubated with *H. pylori* extract for 6 h in an incubator at 37 °C. For all experiments, three temporally independent events were performed.

Cell viability assay

MTT ([3-(4,5-dimethylthiazol-2-yl)-2,5-diphenyltetrazolium bromide]) assays (Sigma–Aldrich, St. Louis, MO, United States) were employed to evaluate the viability of silenced and nonsilenced AGS cells after different treatment conditions with *H. pylori* extract (times and *H. pylori* extract volumes). In summary, the culture medium was removed, and 300 μL of fresh medium containing 1 mg/mL MTT reagent was added to each well. After 30 min of incubation at 37 °C, the medium with MTT reagent was replaced by the same volume of dimethyl sulfoxide (DMSO) (Sigma–Aldrich, St. Louis, MO, United States). The absorbance at 540 nm was measured using a FLUOstar Omega spectrophotometer (BMG Labtech, Ortenberg, Germany).

Transfection with shRNA

MISSION® Lentiviral Transduction Particles (Cat. SHCLNV, Sigma–Aldrich, St. Louis, MO, United States) were used to integrate shRNA into the genome of AGS cells to knockdown TNFR1 and TNFR2 expression. Verified viral vectors were purchased from Sigma–Aldrich, and the standard manufacturer's protocol was followed to generate the cell line. Stably transfected clones were selected by growing the cells in the presence of puromycin or G418, which acted as selection pressure (for TNFR1: 1 μg/mL puromycin and for TNFR2: 400 μg/mL G418). Different plasmids containing shRNAs were used to generate clones, of which the one showing the best knockdown efficiency was used for all experiments. The sequence of the shRNA in the construct was CTTGAAGGAACTACTACTAAG for *TNFR1* and GCCGGCTCAGAGAATACTATG for *TNFR2*. TNFR1 and TNFR2 levels were assessed by quantitative polymerase chain reaction (PCR) and Western blotting to verify the knockdown. Similar transfections were carried out with an empty vector (Sigma–Aldrich, St. Louis, MO, United States), which served as the transfection control.

Western blot analysis

Protein extraction was performed by lysis of nonsilenced AGS cells and AGS cells containing a shRNA or an empty vector with CelLytic™ MT Cell Lysis Reagent (Sigma–Aldrich, St. Louis, MO, United States). The lysis reaction was centrifuged at 12000 *g* for 10 min after a 15 min incubation. The protein concentration was determined using a Pierce™ BCA Protein Assay kit (Thermo Scientific, Massachusetts, United States) according to the manufacturer's protocol. Thirty micrograms of protein was separated on an 8%-12% sodium dodecyl sulphate-polyacrylamide gel by electrophoresis (120 min) and then transferred to PVDF or nitrocellulose membranes (MilliPore Corporation, Burlington, Massachusetts, EUA) using an Electrotransfer TE70XP system (Hoefer) for 80 min. Membranes were blocked with 5% nonfat dry milk for 60 min and were then incubated overnight at 4 °C with the following primary antibodies: Anti-TNFR1 (dilution 1:500) (Cell Signalling, Massachusetts, United States), anti-TNFR2 (dilution 1:5000) (Abcam Cambridge, United Kingdom) and anti-GAPDH (dilution 1:30000) (Abcam, Cambridge, United Kingdom). After being washed, the membranes were incubated at room temperature under stirring with horseradish peroxidase-conjugated goat anti-rabbit (dilution 1:2000) secondary antibodies (Abcam, Cambridge, United Kingdom). Bands were revealed by enhanced chemiluminescence, visualized in a ChemiDoc™ Imaging System (BioRad, Hercules, California, United States) and quantified using Image Lab 6.0 Software (BioRad, Hercules, California, United States).

Quantification of mRNA and miRNA expression by RT–qPCR

After 6 h of incubation, the medium containing *H. pylori* extract or water was removed, and total RNA was extracted from AGS cells with a miRNeasy Micro Kit (Qiagen, Valencia, CA, United States) according to the manufacturer's protocol. Complementary DNA (cDNA) for mRNA and miRNA was synthesized using a High-Capacity cDNA Archive Kit (Applied Biosystems, Foster City, CA, United States) and a TaqMan® MicroRNA Reverse Transcription Kit (Applied Biosystems, Foster City, CA, United States), respectively. Quantitative PCR (qPCR) was performed with TaqMan® assays (Applied Biosystems, California, United States) for the genes *TNFA* (Hs01113624_g1), *TNFR1* (*TNFRSF1A*) (Hs01042313_m1), *TNFR2* (*TNFRSF1B*) (Hs00961749_m1), *TRADD* (Hs00182558_m1), *TRAF2* (Hs00184192_m1), *CFLIP* (*CFLAR*) (Hs00153439_m1), *NFKB1* (Hs 00765730_m1), *NFKB2* (Hs01028901_g1), *CASP8* (Hs01116281_m1) and *CASP3* (Hs00234387_m1) and for the target miRNAs hsa-miR-19a-3p (MIMAT0000073; ID 000395), hsa-miR-34a-3p (MIMAT0004557; ID 002316), hsa-miR-103a-3p (MIMAT0000101; ID 000439), hsa-miR-130a-3p (MIMAT0000425; ID 000454) and hsa-miR-181c-5p (MIMAT0000258; ID 000482) (Applied Biosystems, California, United States), as described in our previous study[14]. *ACTB* (Catalogue#: 4352935E) and *GAPDH* (Catalogue#: 4352934E) genes were used for normalization of mRNA quantification, while endogenous RNU6B (ID 001093) and RNU48 (ID 001006) levels were used for miRNAs. All reactions were performed in triplicate. Relative quantification (RQ) of mRNA and miRNA expression was calculated by the $2^{(-\Delta\Delta Ct)}$ method[17], and nonsilenced AGS without *H. pylori* extract treatment was used as a calibrator (AGS-C). RQ values are expressed as the mean ± SD of gene and miRNA expression for all experimental groups in relation to nonsilenced and untreated AGS, with RQ = 1.

Cell cycle analysis

The cell distribution at different phases of the cell cycle was estimated by measuring the cellular DNA content using flow cytometry. After incubation with *H. pylori* extract or water, nonsilenced AGS, shTNFR1 and shTNFR2 cell lines were harvested with trypsin and fixed in 70% ethanol at 4 °C for at least 24 h. Subsequently, the cells were washed, centrifuged and incubated with 200 μL of Guava® Cell Cycle Reagent (Merck Millipore, Burlington, Massachusetts, United States) for 30 min in the dark. Cell cycle distribution was measured by a Guava® EasyCyte Flow Cytometer and analysed with Guava® InCyte software (Merck Millipore, Burlington, Massachusetts, United States).

Apoptosis analysis

Apoptotic cell death was also measured by flow cytometry using a fluorescein isothiocyanate (FITC)

Annexin V Apoptosis Detection Kit (BD Pharmingen™; BD Biosciences, Franklin Lakes, NJ, United States) according to the modified manufacturer's protocol. After treatment, adherent cells were harvested with Accutase® (Sigma–Aldrich, St. Louis, MO, United States) since this solution avoids membrane damage[18]. After this step, the cells were washed with cold phosphate-buffered saline, centrifuged, resuspended in 1× binding buffer and stained with 5 μL of Annexin V-FITC and 5 μL of propidium iodide (PI, 50 μg/mL) for 15 min at room temperature in the dark. The labelling of cells was evaluated using a flow cytometer and was analysed with Guava® InCyte software. From the scatter diagram and quadrant plotting, the results are presented as follows: Living cells (FITC-/PI-) located in the lower left quadrant, early apoptotic cells (FITC+/PI-) in the lower right quadrant and late apoptotic cells (FITC+/PI+) in the upper right quadrant.

Statistical analysis

Statistical analysis of the data was performed in GraphPad Prism Software version 6.01 using two-way ANOVA with Bonferroni post hoc test. The results are expressed as the mean ± SD from three experiments conducted independently. A $P < 0.05$ was considered statistically significant.

RESULTS

The AGS cell line treated with H. pylori extract expresses TNFA, TNFR1, and TNFR2 receptors

Initially, both AGS and HGC-27 cell lines were cultured to evaluate the mRNA expression levels of *TNFA, TNFR1* and *TNFR2* receptors by qPCR. The analyses showed that both cell lines expressed *TNFA* and *TNFR1,* but *TNFR2* was expressed at lower levels in HGC-27 cells than it was in AGS cells (Supplementary Figure 1). The AGS cell line was chosen for additional experiments since it was not reasonable to use HGC-27 in the TNFR2 silencing experiments.

To standardize treatment conditions, several volumes of *H. pylori* extract (50, 100, 150 and 200 μL) were tested at different incubation times (4, 6 and 24 h) in the AGS cell line to establish the best conditions for inducing *TNFA* expression without reducing cell viability. The best results were obtained with an *H. pylori* extract concentration of 30% v/v (150 μL) at 6 h of incubation (Supplementary Figures 2 and 3). Under these conditions, there was an increase in *TNFA* expression (RQ = 3.59) without an impact on cell viability (98.9%).

The effect of TNFR1 and TNFR2 downregulation and treatment with H. pylori extract on TNF-α signalling downstream gene expression

The effect of TNFR1 and TNFR2 downregulation on GC cells was evaluated after transfection of the AGS cell line with two specific shRNAs targeting the genes, *TNFR1* (called shTNFR1) and *TNFR2* (called shTNFR2), followed by antibiotic selection. RT–qPCR and Western blotting were used to evaluate the efficiency of silencing. Stable lines with the shRNAs exhibited a 59% reduction in TNFR1 and a 63% reduction in TNFR2 protein expression (Figure 1).

Initially, we evaluated the effect of treatment with *H. pylori* extract on the expression of genes of the TNF-α signalling pathway in nonsilenced AGS cells. After *H. pylori* extract treatment (AGS-*H. pylori* extract), nonsilenced AGS cells showed significantly upregulated mRNA expression of *TNFR1* and of anti-apoptotic and cell proliferation genes, such as *CFLIP, NFKB1* and *NFKB2* (Supplementary Figure 4A), compared to the control (AGS-C). In addition, *H. pylori* extract treatment increased the mRNA expression of *NFKB1* and *NFKB2* in a TNFR1-downregulated cell line (shTNFR1-*H. pylori* extract), whereas the expression of *TNFR2* and *TRADD* was reduced (Supplementary Figure 4B). On the other hand, the expression of the evaluated genes was not significantly changed by *H. pylori* extract treatment in the shTNFR2 cell line (Supplementary Figure 4C).

With regard to the influence of *TNFR1* and *TNFR2* downregulation on the expression of TNF-α signalling genes (Figure 2), a significantly downregulated mRNA expression of *TNFR1* (RQ = 0.83 and 1.03, respectively), *TRADD* (RQ = 0.60 and 0.41, respectively) and *CFLIP* (RQ = 1.25 and 1.36, respectively) was observed in shTNFR1-*H. pylori* extract and shTNFR2-*H. pylori* extract cells compared to that in AGS-*H. pylori* extract cells (RQ = 1.73, 0.98 and 2.09, respectively) (Figure 2B, D and F). Furthermore, *TNFR2* (RQ = 0.27, $P < 0.05$), *TRAF2* (RQ = 0.68, $P < 0.05$) and *NFKB1* (RQ = 1.67, $P < 0.05$) were reduced in shTNFR2-*H. pylori* extract cells compared to AGS-*H. pylori* extract cells (RQ = 0.86, 1.29 and 2.39, respectively) (Figure 2C, E and I). When we compared the nonsilenced and silenced AGS cell lines without *H. pylori* extract treatment (control-C), *TNFR2* mRNA expression was increased in shTNFR1-C (RQ = 1.49) compared to AGS-C (RQ = 1.00) and reduced in shTNFR2-C (RQ = 0.50) compared to shTNFR1-C and AGS-C. Likewise, *TRADD* mRNA expression was downregulated in shTNFR2-C (RQ = 0.35) compared to the other control groups (AGS-C and shTNFR1-C). There was no significant change in *TNFA, CASP3, CASP8* and *NFKB2* mRNA expression.

In general, the downregulation of TNFR1 and TNFR2 significantly influenced the mRNA expression of *TRADD* ($P < 0.001$) and *TRAF2* ($P < 0.01$), whereas the expression of *TNFR1, TNFR2* and *CFLIP* was also affected by treatment with *H. pylori* extract ($P < 0.01$ for all). In contrast, only the *H. pylori* extract

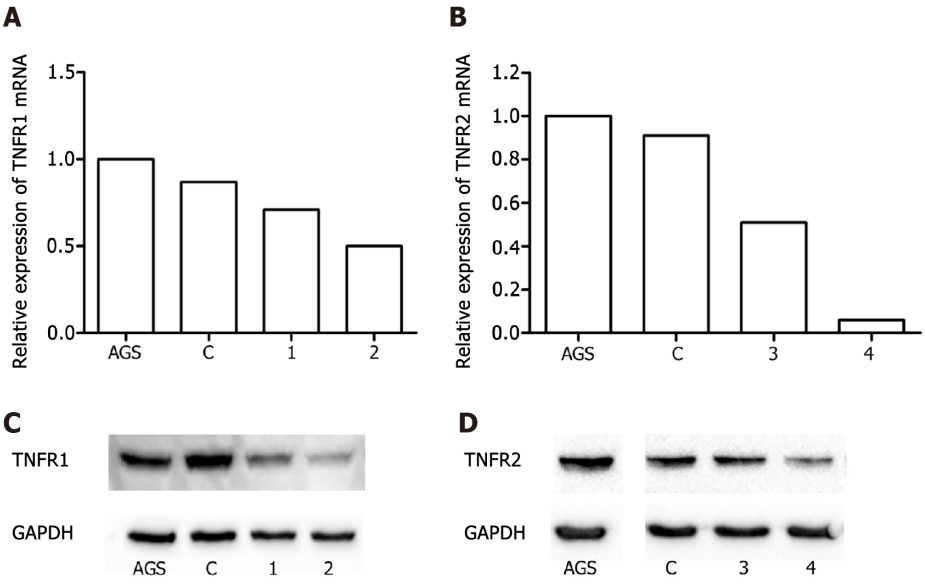

DOI: 10.3748/wjg.v28.i24.2689

Figure 1 The efficiency of *TNFR1* and *TNFR2* expression silencing in AGS cells. A and B: Expression levels of *TNFR1* and *TNFR2* mRNA evaluated by real-time reverse transcription-quantitative polymerase chain reaction; C and D: Protein expression of *TNFR1* and *TNFR2* evaluated by Western blotting. Downregulation of *TNFR1* (A-C) and *TNFR2* (B-D) was confirmed by the reduction in the expression of receptors *TNFR1* and *TNFR2* following treatment with shRNAs 2 and 4, respectively. AGS: Nonsilenced cell line; C: Control transfected with empty vector; 1 and 2: Different shRNA clones for *TNFR1*; 3 and 4: Different shRNA clones for *TNFR2*.

treatment contributed to the differences observed in *NFKB1* and *NFKB2* mRNA expression ($P < 0.001$ for both).

TNFR2 downregulation upregulates miR-19a and miR-34a expression

The expression of miRNAs miR-19a, miR-34a, miR-103a, miR-130a and miR-181c was evaluated in the AGS, shTNFR1 and shTNFR2 cell lines with and without *H. pylori* extract treatment (Figure 3 and Supplementary Figure 5). No significant change in the expression of these miRNAs was found in AGS and shTNFR1 cells regardless of *H. pylori* extract treatment. However, TNFR2 receptor downregulation resulted in a significant increase in the expression of miR-19a and miR-34a in shTNFR2-C cells (RQ = 3.70 and 2.64, respectively) compared with that of the AGS-C ($P < 0.01$ and $P < 0.001$, respectively) and shTNFR1-C cells ($P < 0.05$ and $P < 0.001$, respectively) cells and in shTNFR2-*H. pylori* extract cells (RQ = 3.89 and 1.69, respectively) compared to AGS-*H. pylori* extract ($P < 0.01$ and $P < 0.05$, respectively) and shTNFR1-*H. pylori* extract cells ($P < 0.01$ and $P < 0.01$, respectively) (Figure 3A and B).

TNFR2 downregulation promotes a reduction in G0/G1 phases and an increase in S phase

The effect of TNFR1 and TNFR2 downregulation after *H. pylori* extract treatment on cell cycle progression was evaluated by flow cytometry. Overall, *H. pylori* extract treatment did not affect the cellular distribution in the G0/G1, S and G2/M phases in nonsilenced AGS, shTNFR1 and shTNFR2 cells (Supplementary Figure 6). However, TNFR2 downregulation significantly reduced the number of cells in G0/G1 phase regardless of *H. pylori* extract treatment and led to an increase in the number of cells in S and G2/M phases in shTNFR2-C cells compared to that of the AGS-C cells (Figure 4).

Downregulation of TNFR2 promotes early apoptosis

In addition, we also investigated the effect of partial TNFR1 and TNFR2 inhibition and *H. pylori* extract treatment on apoptosis, which was evaluated through Annexin-V and PI double staining by flow cytometry. Treatment with *H. pylori* extract did not induce changes in the rates of early and late apoptosis in the nonsilenced AGS and both silenced AGS cell lines compared to the respective untreated cell lines (Supplementary Figure 7). However, after *H. pylori* extract treatment, the percentage of early apoptotic cells was significantly higher in shTNFR2 cells (1.27%) than in AGS (0.56%) and shTNFR1 cells (0.52%), whereas the percentage of late apoptotic cells was significantly reduced after *H. pylori* extract treatment (Figure 5). Together with the cell cycle results, these data indicate a relationship between decreased cell quantity in the G0/G1 phase and increased early apoptosis as a result of TNFR2 downregulation.

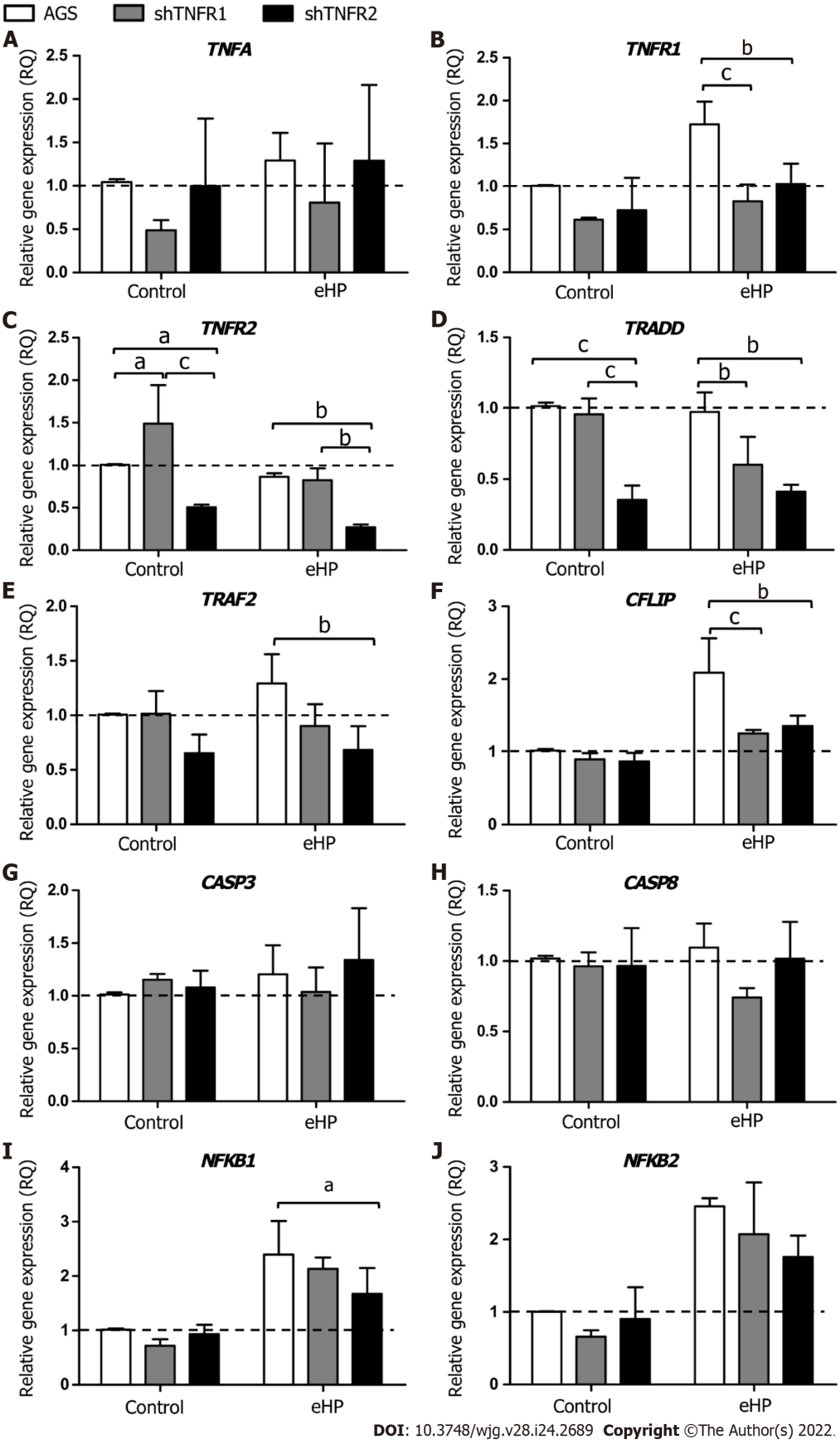

DOI: 10.3748/wjg.v28.i24.2689

Figure 2 Relative expression of tumour necrosis factor-α signalling pathway genes. Expression levels of *TNFA*, *TNFR1*, *TNFR2*, *TRADD*, *TRAF2*, *CFLIP*, *CASP8*, *CASP3*, *NFKB1* and *NFKB2* mRNA in nonsilenced AGS, AGS with TNFR1 downregulation (shTNFR1), and AGS with TNFR2 downregulation (shTNFR2) either not treated (control) or treated with a *Helicobacter pylori* extract. A: *TNFA*; B: *TNFR1*; C: *TNFR2*; D: *TRADD*; E: *TRAF2*; F: *CFLIP*; G: *CASP8*; H: *CASP3*; I: *NFKB1*; J: *NFKB2*. Bars represent the mean ± SD from three independent trials. The dotted line indicates relative quantification: RQ = 1.0. Statistically

significant difference: $^{a}P < 0.05$; $^{b}P < 0.01$; $^{c}P < 0.001$. eHP: *Helicobacter pylori* extract.

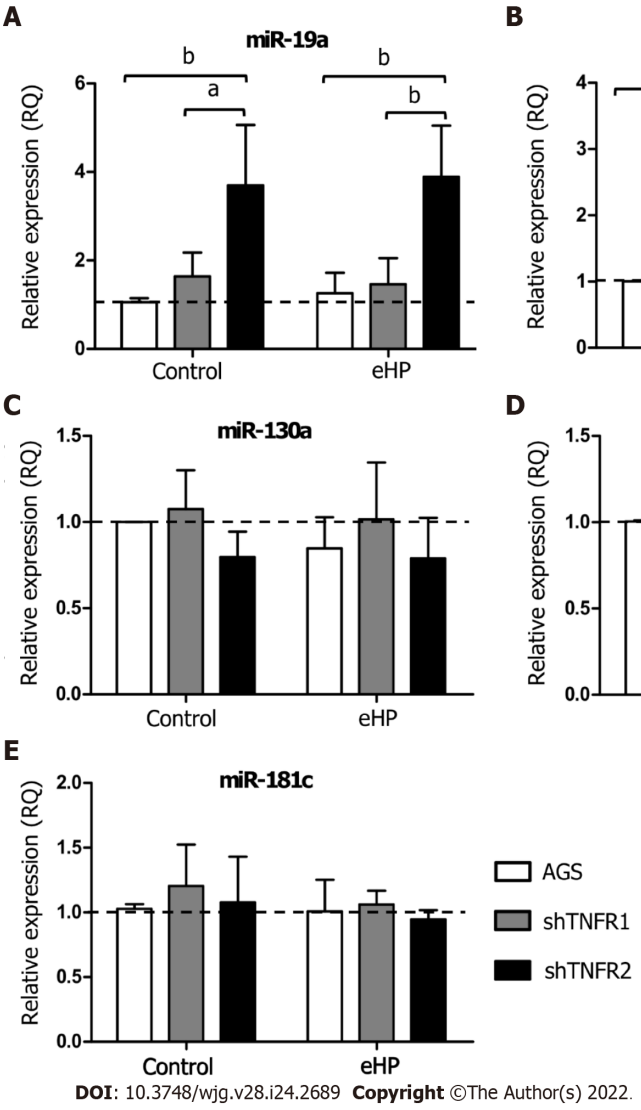

DOI: 10.3748/wjg.v28.i24.2689

Figure 3 Relative expression of miRNAs related to the tumour necrosis factor-α pathway. Expression levels of miR-19a, miR-34a, miR-103a, miR-130a and miR-181c in nonsilenced AGS, AGS with TNFR1 downregulation (shTNFR1), and AGS with TNFR2 downregulation (shTNFR2) either not treated (control) or treated with the *Helicobacter pylori* extract. A: miR-19a; B: miR-34a; C: miR-103a; D: miR-130a; E: miR-181c. Bars represent the mean ± SD from three independent trials. The dotted line indicates relative quantification: RQ = 1.0. Statistically significant difference: $^{a}P < 0.05$; $^{b}P < 0.01$; $^{c}P < 0.001$. eHP: *Helicobacter pylori* extract.

DISCUSSION

TNFR1 and TNFR2 differ in their intracellular domains and cellular expression; thus, the role of each receptor in the TNF-α-triggered signalling pathway varies according to the pathological condition, activating different cellular processes, such as cell survival and apoptosis[10]. This is the first study to investigate the effect of TNFR1 and TNFR2 downregulation on AGS cells treated with *H. pylori* extract. Our results show that *H. pylori* extract treatment of nonsilenced AGS cells upregulated the mRNA expression of proliferation (*NFKB1* and *NFKB2*) and antiapoptotic genes (*CFLIP*) by activating TNFR1. TNFR1 downregulation did not promote extensive changes in the expression of genes or miRNAs involved in the TNF-α signalling pathway or in cellular processes. In contrast, TNFR2 downregulation significantly decreased *TRADD* and *TRAF2* mRNA expression, which may impair TNFR1-mediated TNF-α signalling, and increased miRNA expression, which promoted a block in the G_1/S transition and an increase in early apoptosis.

H. pylori infection can deregulate the expression of several genes and miRNAs, as previously shown by our research group[6]. Recently, increased mRNA levels of *TNFA* and other proinflammatory mediators, such as interleukin (IL)-1β and IL-8, have been reported in an AGS cell line after infection by

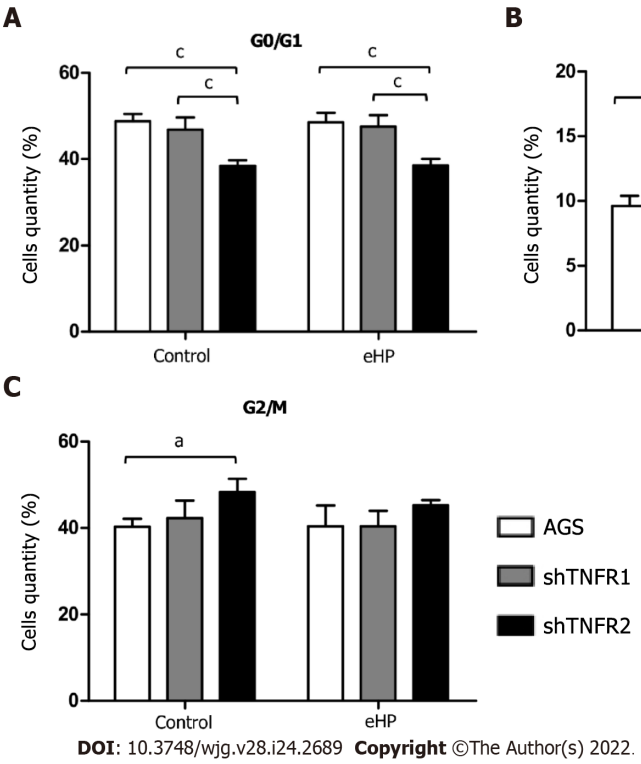

DOI: 10.3748/wjg.v28.i24.2689

Figure 4 Cell cycle distribution analysis. Number of cells in the G0/G1, S and G2/M phases of the cell cycle in nonsilenced AGS cells, cells with TNFR1 downregulated (shTNFR1), and cells with TNFR2 downregulated (shTNFR2) without additional treatment (control) and those treated with the *Helicobacter pylori* extract. A: G0/G1; B: S; C: G2/M. Bars represent the mean ± SD from three independent trials. Statistically significant difference: $^{a}P < 0.05$; $^{b}P < 0.01$; $^{c}P < 0.001$. eHP: *Helicobacter pylori* extract.

H. pylori[19]. Our results show high *TNFR1* mRNA expression after *H. pylori* extract treatment in nonsilenced AGS cells, suggesting that *H. pylori* infection promotes activation of the TNFR1-mediated TNF-α signalling pathway in AGS cells, directing signal transduction to the cell survival pathway due to the increased expression of *NFKB1, NFKB2* and *CFLIP* (Figure 6A). In agreement with this finding, previous studies showed that *H. pylori* activates NF-κB in a manner dependent on the bacterial cell number[20] due to significant IκB-α degradation[21], resulting in the induction of anti-apoptotic gene transcription, such as *CFLIP* transcription[22]. Therefore, our results indicate that *H. pylori* extract also induces cell survival and inflammation due to TNFR1-mediated TNF-α signalling, which leads to NF-κB activation and the consequent production of antiapoptotic mediators, such as cFLIP.

TNFR1 downregulation resulted in a significant increase in *TNFR2* mRNA expression in nontreated AGS cells, while a decrease in the expression of T*RADD* and *CFLIP* mRNA was observed in cells treated with *H. pylori* extract, although no change was observed in apoptosis and cell cycle assays (Figure 6B). In oesophageal carcinoma cells treated with TNFR1-siRNA, Changhui *et al*[23] demonstrated an increase in cell proliferation and a reduction in apoptosis rate after 24 h of transfection, and the cell proliferation level was time-dependent[19]. The present study, when evaluated together with the results of *H. pylori* extract, suggests that the assays of cellular processes after 6 h of treatment may have been insufficient in shTNFR1 and nonsilenced AGS cells. Wan *et al*[24] showed that AGS cell coculture with *H. pylori* inhibited apoptosis and increased viability through upregulation of TRAF1, which was triggered by NF-κB activation. However, the peak of TRAF1 expression occurred after 12 h of infection, and its effect on cell viability started only after 24 h. Therefore, the role of TNFR1 downregulation in GC cell lines still needs to be further investigated.

Conversely, the downregulation of TNFR2 expression significantly decreased the expression of two important mediators of the TNFR1-mediated signalling pathway, TRAF2 and TRADD, in addition to *NFKB*1, *CFLIP* and *TNFR1* expression. Moreover, there was an increase in early apoptosis, with concomitant G1/S transition phase arrest (Figure 6C). These results agree with those previously reported by our group in GC patient samples, in which we found upregulation of *TNF/TNFR2* and cellular survival genes such as *TRAF2*, *CFLIP*, and *NFKB2* and downregulation of *TNFR1* and *CASP3* [14], thus emphasizing the important role of TNFR2 in gastric carcinogenesis and TNFR2 silencing as a promising strategy for anticancer therapy[25].

TRADD is an essential adaptor protein that functions in TNFR1-mediated apoptotic signalling under physiological conditions[26]. However, the dependence of this mediator seems to be cell-type specific [27], as TRADD knockout mice were resistant to TNFR1-induced toxicity in a hepatitis model[28]. However, this pathway was not completely impaired in macrophages deprived of TRADD[27].

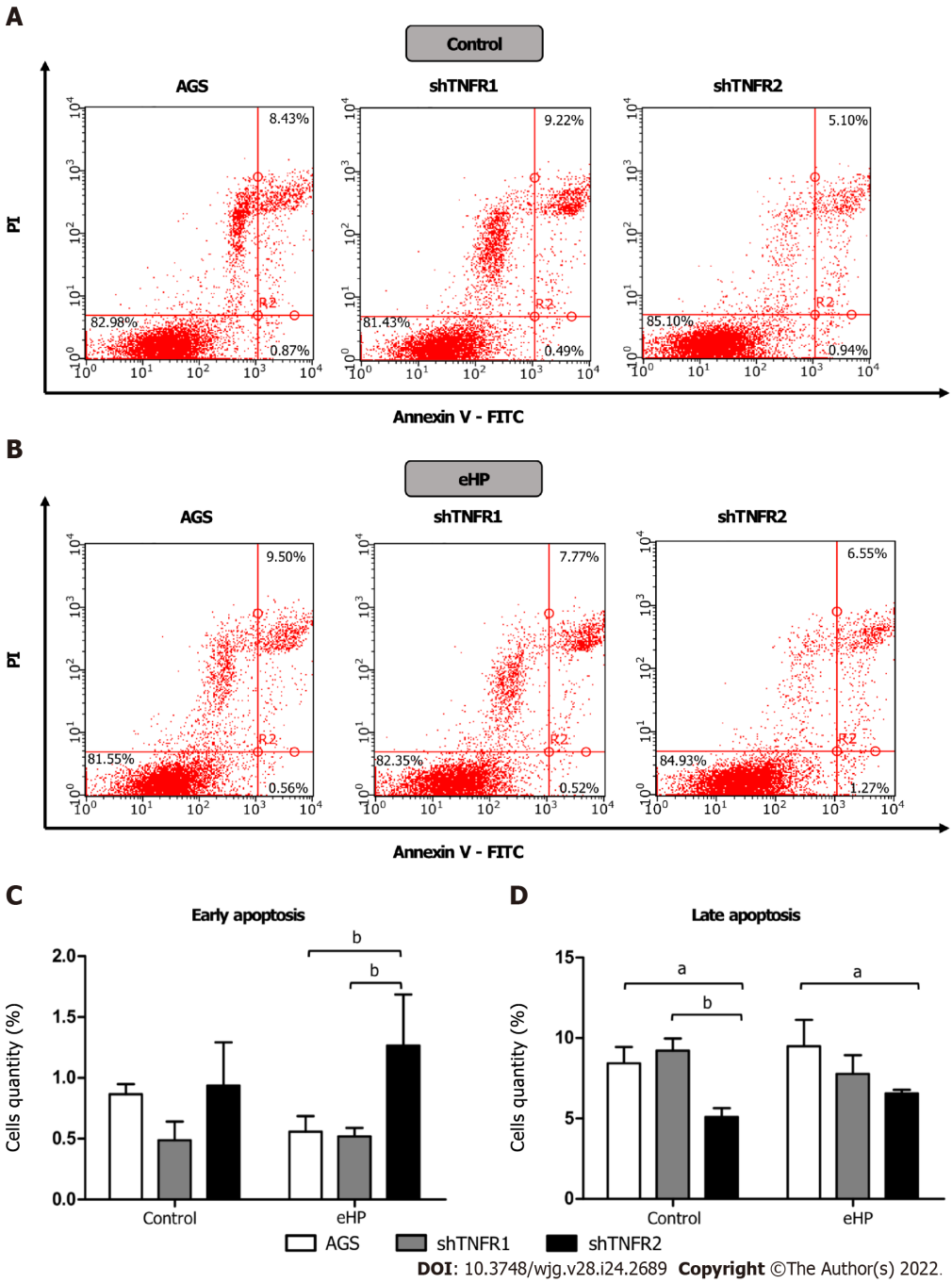

DOI: 10.3748/wjg.v28.i24.2689

Figure 5 Apoptosis distribution analysis in nonsilenced AGS cells, cells with TNFR1 downregulated (shTNFR1), and cells with TNFR2 downregulated (shTNFR2). A: Cells without additional treatment (control); B: Cells treated with the *Helicobacter pylori* extract; A and B: Representative images of the cell distribution and percentage in the different quadrants indicating viable cells (Annexin V-/PI-) in the lower left, early apoptotic cells (Annexin V+/PI-) in the lower right and late apoptotic cells (Annexin V+/PI+) in the upper right; C and D: Histogram bars represent the mean ± SD from three independent trials for early (C) and late (D) apoptosis. Statistically significant difference: $^{a}P < 0.05$; $^{b}P < 0.01$. eHP: *Helicobacter pylori* extract.

Therefore, apoptosis can occur even with reduced expression of TRADD, as observed in the present study after TNFR2 downregulation. In turn, TRADD inhibition reduces NF-κB activation[12], impairing the transcription of anti-apoptotic genes, such as *TRAF2* and *CFLIP*, as observed in this study.

As mentioned, shTNFR2 cells also exhibited reduced expression of TRAF2. This protein has an essential role in signal transduction and is triggered by both TNFR1 and TNFR2, suggesting the existence of crosstalk between them[29], which influences the signalling outcome after TNF binding [30]. TRAF2 recruits cIAP1 and cIAP2 after interaction with these receptors, thereby triggering nuclear translocation of NF-κB[30]. Therefore, TRAF2 is a negative regulator of TNF-induced apoptosis[30], and the use of this protein after TNFR2 activation results in TNFR1-induced apoptosis to the detriment of proliferation[25]. Therefore, a decrease in TRAF2 expression favours TNFR1-mediated apoptosis, contributing to the increase in the percentage of early apoptotic cells after TNFR2 downregulation.

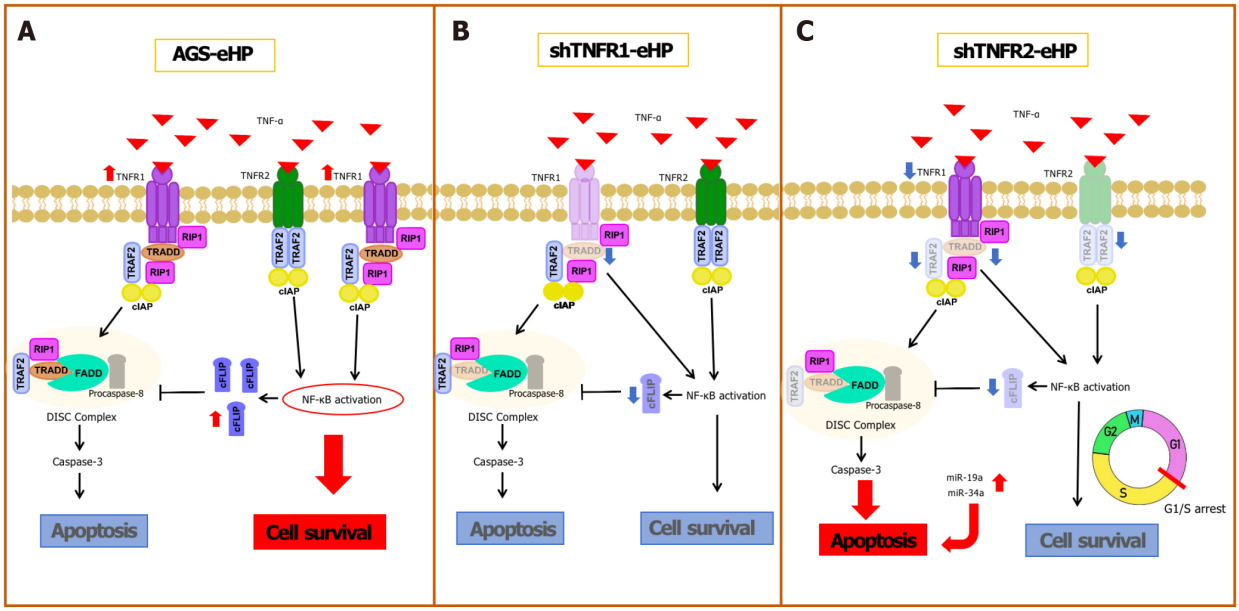

DOI: 10.3748/wjg.v28.i24.2689

Figure 6 Schematic comparison of the tumour necrosis factor-α signalling pathway and cell fate in nonsilenced AGS, shTNFR1 and shTNFR2 cells with downregulation after treatment with *Helicobacter pylori* extract. After the tumour necrosis factor (TNF)-α/TNFR1 interaction, TRADD, RIP1, TRAF2 and cellular inhibitor of apoptosis proteins are recruited, which results in nuclear factor-kappaB (NF-κB) activation and transcription of prosurvival and antiapoptotic genes, such as CFLIP, that inhibit the activity of the death-inducing signalling complex, which is formed after dissociation between TRADD and TNFR1. As with TNFR1, TNFR2 stimulation leads to NF-κB activation and cell survival; A: Treatment with *Helicobacter pylori* (*H. pylori*) extract resulted in increased expression of TNFR1, NFKB1, NFKB2 and CFLIP mRNAs in nonsilenced AGS cells. Therefore, the cell survival pathway is activated due to NF-kB activation (red ellipse) through the TNFR1-TNF signalling pathway with consequent production of the antiapoptotic CFLIP; B: In shTNFR1-*H. pylori* extract cells, TNFR1 downregulation resulted in decreased expression of TRADD and CFLIP mRNAs; however, it did not change cell fate; C: In shTNFR2-*H. pylori* extract cells, TNFR2 downregulation decreased the expression of TRAF2 and TRADD, decreased NFKB1, CFLIP and TNFR1 expression, and upregulated miR-19a and miR-34a. This led to an increase in apoptosis, impairing cell survival due to arrest in the G1/S transition phase.

Moreover, we found that TNFR2 downregulation also promoted a decrease in the ratio of cells in the G0/G1 phase and an increase the ratio of cells in the S and G2/M phases, suggesting that TNFR2 inhibition may delay cell cycle progression and arrest cells at the G1/S transition[31]. These changes in the cell cycle could also be related to the DNA damage response[32], leading cells to early apoptosis, as seen in our results. Recent studies have shown increased expression of genes related to the response to DNA damage and repair, such as *APE1, H2AX* and *PARP-1,* in GC samples, thus possibly influencing the survival of tumour cells[33,34]. Yang *et al*[35] demonstrated that TNFR2 enhances DNA damage repair by regulating PARP expression in breast cancer cells. Furthermore, they showed that TNFR2 silencing led to an increase in pH2AX, which is a DNA damage marker.

Based on the function of each receptor and the existence of crosstalk between them, it is possible that the simultaneous inhibition of both TNFR1 and TNFR2 may have a greater antitumor effect on GC than the downregulation of TNFR2 alone. Furthermore, TNF-α and its receptors, in addition to being expressed by tumour cells, are also expressed by cells present in the tumour microenvironment as immune cells[36]. Oshima *et al*[8] demonstrated that the stimulation of TNFR1-mediated TNF-α signalling in cells in the tumour microenvironment promoted gastric tumorigenesis through the induction of tumour-promoting factors (*Noxo1* and *Gna14*) in tumour epithelial cells, highlighting the importance of the tumour microenvironment[37] and the need for *in vivo* studies.

Furthermore, considering the important role of miRNAs in the development of cancer, as they act as regulators of signalling pathways and are consequently involved in various cellular processes, we also evaluated the expression of miRNAs miR-19a, miR-34a, miR-103a, miR-130a and miR-181c. These miRNAs were chosen from data analysis publishedin public databases[38-42] and due to their interaction with TNF-α pathway genes, as observed in our recent study[14]. Regardless of *H. pylori* extract treatment, shTNFR1 and nonsilenced AGS cells did not dysregulate miRNA expression. However, TNFR2 downregulation caused an upregulation of miR-19a and miR-34a (Figure 3A and B).

MiR-34a is dysregulated in different types of cancer and is linked to the proliferation, differentiation, migration, invasion, treatment, and prognosis of cancer[43]. Although most studies suggest a tumour-suppressor role for miR-34a[44-46], we recently observed overexpression of this miRNA in GC samples [14], thus also indicating its oncogenic action. In contrast, in both AGS and BGC-823 cell lines, an upregulation of this miRNA inhibited proliferative and migratory abilities in sevoflurane-induced GC cells, whereas *in vivo* knockdown of miR-34a stimulated tumour growth, indicating its action as a tumour suppressor in the AGS cell line[47]. In addition, stable transfection of pre-mir-34a in KatoII cells

increased the percentage of apoptotic cells and reduced the proliferation rate, suggesting that its high expression promotes apoptosis[48]. In the present study, upregulation of this miRNA in shTNFR2 cells suggests that miR-34a expression can be modulated by TNFR2-mediated TNF-α signalling and is able to exert an anti-proliferative and pro-apoptotic effect. Similarly, miR-19a was overexpressed in the shTNFR2 cell line, indicating that miR-19a and TNFR2 are related to each other in GC. miR-19a has a known oncogenic function in various kinds of cancer[49], with *TNFA, TNFR1* and *TNFR2* being its validated targets[38,39,50]. However, miR19a may play a tumour-suppressive role, as reported in prostate cancer, by suppressing invasion and migration in bone metastasis[51], and in rectal cancer cells, by inducing apoptosis[52]. For both miRNAs, functional studies are needed to assess what targets the miRNAs are related to with respect to TNF-α signalling in GC.

The other miRNAs evaluated (miR-103a, miR-130a and miR-181c) were not dysregulated in the AGS cell line. Although different studies have shown the involvement of these miRNAs in gastric neoplasms [53-55], their pro- or antitumor roles are still controversial. This is due to the influence of several factors in the regulation of gene expression, such as the stage of tumour development and the presence or absence of infectious agents[6].

CONCLUSION

In conclusion, based on our results, shRNA-mediated downregulation of TNFR2 in AGS cells was able to reduce the expression of pro-survival and anti-apoptotic genes, in addition to affecting miRNA expression, the cell cycle, and promoter apoptosis. The blocking of TNFR2 expression may cause antitumor effects, suggesting possible targets for future studies into therapeutic strategies for treating GC. Furthermore, the *H. pylori* extract increased the expression of prosurvival genes, mainly through TNFR1-mediated TNF-α signalling, thus emphasizing the role of bacterial infection in promoting GC progression.

ARTICLE HIGHLIGHTS

Research background

The tumour necrosis factor-α (TNF-α) signalling pathway triggered by TNFR1 and TNFR2 controls several biological processes, influencing cell fate. Thus, the deregulation of this pathway to cause an imbalance between the processes of cell survival and death may contribute to the tumorigenic process. This variety of functions is exercised by the ability of TNF-α to bind to TNFR1 or TNFR2, which results in different cellular processes. Both receptors are transmembrane proteins and are largely similar in extracellular structure, but their intracellular domains are different, and dictate the cellular fate for either survival or death. Since only TNFR1 has a death domain, the TNF-α signalling pathway triggered by TNFR1 is able to induce both cell survival and apoptosis, whereas TNFR2 results only in cell survival. The TNF-α signalling pathway also modulates the immune response and inflammation, so deregulation of this pathway has been implicated in inflammatory diseases and cancer. Therefore, studies are needed to better understand the relationships of this signalling network *via* TNFR1 and TNFR2 and its protumorigenic or antitumorigenic effects.

Research motivation

We proposed the present study based on our previous studies, which showed deregulation in the expression of genes and miRNAs of the TNF-α signalling pathway and its receptors TNFR1 and TNFR2 in fresh tissues of chronic gastritis and gastric cancer (GC) patients. Therefore, we decided to evaluate the effect of silencing TNFR1 and TNFR2 on GC cell lines.

Research objectives

According to the role of TNFR1 and TNFR2 in cellular responses triggered by TNF-α, and considering that studies addressing the role of these receptors in gastric neoplasm are limited and inconclusive, we proposed to couple the silencing of TNFR1 and TNFR2 receptors in an AGS gastric cell line and the treatment with *Helicobacter pylori* (*H. pylori*) extract to determine the effects on *TNF-α* mRNA expression and on downstream genes related to its signalling pathway. Moreover, we also investigated previously studied miRNAs that target genes in the TNF-α pathway to jointly determine their influence on the cell cycle and apoptosis.

Research methods

Stable AGS GC cells containing TNFR1 and TNFR2 receptors downregulated by specific shRNAs and nonsilenced cell lines were treated with 30% v/v *H. pylori* extract [*H. pylori* Tox+ strain (cagA+/vacA s1m1)] for 6 h. After silencing, TNFR1 and TNFR2 levels were assessed by quantitative polymerase

chain reaction (qPCR) and Western blotting to confirm the knockdown effect. Subsequently, mRNA and miRNAs were quantified by qPCR using TaqMan gene and miRNA expression assays. The MTT assay was employed to evaluate the viability of silenced and nonsilenced AGS cells after different treatment conditions with *H. pylori* extract, and flow cytometry was used for cell cycle analysis and apoptosis.

Research results

Our results showed that *H. pylori* extract treatment increased the expression of genes involved in cell survival (*NFKB1* and *NFKB2*) and inhibited apoptosis (*CFLIP*) and *TNFR1* in nonsilenced AGS cells. TNFR1 downregulation significantly decreased the expression of the *TRADD* and *CFLIP* genes; however, no change in the cell cycle, apoptosis or miRNA levels was observed. In turn, TNFR2 downregulation decreased the expression of the *TRADD* and *TRAF2 genes*, which are both important downstream mediators of the TNFR1-mediated pathway, as well as the *NFKB1* and *CFLIP* genes, while upregulating the expression of miR-19a and miR-34a. Consequently, there was a decrease in the ratio of cells in the G0/G1 phase and an increase in cells in the S phase, as well as the promotion of early apoptosis.

Research conclusions

Our findings highlight that treatment with *H. pylori* extract increased the expression of pro-survival genes, mainly through TNFR1-mediated TNF-α signalling, emphasizing the role of bacterial infection in promoting GC progression. In the AGS cell line, TNFR1 and TNFR2 downregulation decreased the expression of prosurvival and antiapoptotic genes and affected miRNA expression and cellular processes, such as the cell cycle and apoptosis, emphasizing that shRNA-mediated downregulation of these receptors can have an antitumor effect.

Research perspectives

According to our results, we can mainly highlight the important role of TNFR2 in the TNF-α pathway in GC, indicating that silencing TNFR2 can reduce the expression of survival and anti-apoptotic genes. Thus, blocking this receptor may result in antitumor effects, suggesting possible targets for future *in vivo* studies into therapeutic strategies for treating GC.

ACKNOWLEDGEMENTS

We thank Dr Sonia Maria Oliani, Department of Biological Sciences, UNESP, for making the flow cytometer available, Janesly Prates for training on the flow cytometer, Dr Fernando Ferrari, Department of Computer Science and Statistics, UNESP, for the statistical support, André Brandão do Amaral for contribution to Figure 6, and Marilanda Ferreira Bellini for recording the audio core tip.

FOOTNOTES

Author contributions: Rossi AFT analysed and interpreted the results; Rossi AFT, Manoel-Caetano FS and Biselli JM performed the experiments; Rossi AFT and Silva AE outlined the study, and drafted and revised the manuscript; Cabral AS performed the Western blot assays; Saiki MFC provided technical support for the shRNA transfection experiments; Ribeiro ML provided the HGC-27 cell line and produced the *H. pylori* extract; all authors approved the final version of the manuscript.

Supported by São Paulo Research Foundation (FAPESP), No. 2015/21464-0 and No. 2015/23392-7; and National Counsel of Technological and Scientific Development (CNPq), No. 310120/2015-2.

Institutional review board statement: Not applicable. This study was performed with cell line only.

Conflict-of-interest statement: The authors declare that they have no conflict of interest.

Data sharing statement: This study was performed with cell line only. The datasets generated during the current study are available from the corresponding author on reasonable request.

Country/Territory of origin: Brazil

ORCID number: Ana Flávia Teixeira Rossi 0000-0002-3476-2885; Fernanda da Silva Manoel-Caetano 0000-0001-6717-5874; Joice Matos Biselli 0000-0001-5105-9537; Ágata Silva Cabral 0000-0002-7215-9331; Marilia de Freitas Calmon Saiki 0000-0001-5203-0103; Marcelo Lima Ribeiro 0000-0003-4529-7832; Ana Elizabete Silva 0000-0003-1491-8878.

S-Editor: Fan JR
L-Editor: A
P-Editor: Chen YX

REFERENCES

1 **International Agency for Research on Cancer**. Cancer Today fact Sheets, 2018. [cited 11 January 2022]. Available from http://gco.iarc.fr/today/data/factsheets/cancers/7-Stomach-fact-sheet.pdf
2 **Ministério da Saúde**, Instituto Nacional de Câncer José Alencar Gomes da Silva. Estimativa 2020-Incidência de câncer no Brasil. 2019. [cited 11 January 2022]. Available from: https://www.inca.gov.br/sites/ufu.sti.inca.local/files//media/document//estimativa-2020-incidencia-de-cancer-no-brasil.pdf
3 **Yousefi B**, Mohammadlou M, Abdollahi M, Salek Farrokhi A, Karbalaei M, Keikha M, Kokhaei P, Valizadeh S, Rezaiemanesh A, Arabkari V, Eslami M. Epigenetic changes in gastric cancer induction by Helicobacter pylori. *J Cell Physiol* 2019; **234**: 21770-21784 [PMID: 31169314 DOI: 10.1002/jcp.28925]
4 **Cadamuro AC**, Rossi AF, Maniezzo NM, Silva AE. Helicobacter pylori infection: host immune response, implications on gene expression and microRNAs. *World J Gastroenterol* 2014; **20**: 1424-1437 [PMID: 24587619 DOI: 10.3748/wjg.v20.i6.1424]
5 **Chen R**, Yang M, Huang W, Wang B. Cascades between miRNAs, lncRNAs and the NF-κB signaling pathway in gastric cancer (Review). *Exp Ther Med* 2021; **22**: 769 [PMID: 34055068 DOI: 10.3892/etm.2021.10201]
6 **Rossi AF**, Cadamuro AC, Biselli-Périco JM, Leite KR, Severino FE, Reis PP, Cordeiro JA, Silva AE. Interaction between inflammatory mediators and miRNAs in Helicobacter pylori infection. *Cell Microbiol* 2016; **18**: 1444-1458 [PMID: 26945693 DOI: 10.1111/cmi.12587]
7 **Mahdavi Sharif P**, Jabbari P, Razi S, Keshavarz-Fathi M, Rezaei N. Importance of TNF-alpha and its alterations in the development of cancers. *Cytokine* 2020; **130**: 155066 [PMID: 32208336 DOI: 10.1016/j.cyto.2020.155066]
8 **Oshima H**, Ishikawa T, Yoshida GJ, Naoi K, Maeda Y, Naka K, Ju X, Yamada Y, Minamoto T, Mukaida N, Saya H, Oshima M. TNF-α/TNFR1 signaling promotes gastric tumorigenesis through induction of Noxo1 and Gna14 in tumor cells. *Oncogene* 2014; **33**: 3820-3829 [PMID: 23975421 DOI: 10.1038/onc.2013.356]
9 **Yang S**, Wang J, Brand DD, Zheng SG. Role of TNF-TNF Receptor 2 Signal in Regulatory T Cells and Its Therapeutic Implications. *Front Immunol* 2018; **9**: 784 [PMID: 29725328 DOI: 10.3389/fimmu.2018.00784]
10 **Gough P**, Myles IA. Tumor Necrosis Factor Receptors: Pleiotropic Signaling Complexes and Their Differential Effects. *Front Immunol* 2020; **11**: 585880 [PMID: 33324405 DOI: 10.3389/fimmu.2020.585880]
11 **Josephs SF**, Ichim TE, Prince SM, Kesari S, Marincola FM, Escobedo AR, Jafri A. Unleashing endogenous TNF-alpha as a cancer immunotherapeutic. *J Transl Med* 2018; **16**: 242 [PMID: 30170620 DOI: 10.1186/s12967-018-1611-7]
12 **Li Z**, Yuan W, Lin Z. Functional roles in cell signaling of adaptor protein TRADD from a structural perspective. *Comput Struct Biotechnol J* 2020; **18**: 2867-2876 [PMID: 33163147 DOI: 10.1016/j.csbj.2020.10.008]
13 **Brenner D**, Blaser H, Mak TW. Regulation of tumour necrosis factor signalling: live or let die. *Nat Rev Immunol* 2015; **15**: 362-374 [PMID: 26008591 DOI: 10.1038/nri3834]
14 **Rossi AFT**, Contiero JC, Manoel-Caetano FDS, Severino FE, Silva AE. Up-regulation of tumor necrosis factor-α pathway survival genes and of the receptor TNFR2 in gastric cancer. *World J Gastrointest Oncol* 2019; **11**: 281-294 [PMID: 31040894 DOI: 10.4251/wjgo.v11.i4.281]
15 **Santos JC**, Gambeloni RZ, Roque AT, Oeck S, Ribeiro ML. Epigenetic Mechanisms of ATM Activation after Helicobacter pylori Infection. *Am J Pathol* 2018; **188**: 329-335 [PMID: 29128564 DOI: 10.1016/j.ajpath.2017.10.005]
16 **Li HQ**, Xu C, Li HS, Xiao ZP, Shi L, Zhu HL. Metronidazole-flavonoid derivatives as anti-Helicobacter pylori agents with potent inhibitory activity against HPE-induced interleukin-8 production by AGS cells. *ChemMedChem* 2007; **2**: 1361-1369 [PMID: 17628869 DOI: 10.1002/cmdc.200700097]
17 **Livak KJ**, Schmittgen TD. Analysis of relative gene expression data using real-time quantitative PCR and the 2(-Delta Delta C(T)) Method. *Methods* 2001; **25**: 402-408 [PMID: 11846609 DOI: 10.1006/meth.2001.1262]
18 **Riedl S**, Rinner B, Asslaber M, Schaider H, Walzer S, Novak A, Lohner K, Zweytick D. In search of a novel target - phosphatidylserine exposed by non-apoptotic tumor cells and metastases of malignancies with poor treatment efficacy. *Biochim Biophys Acta* 2011; **1808**: 2638-2645 [PMID: 21810406 DOI: 10.1016/j.bbamem.2011.07.026]
19 **Yeon MJ**, Lee MH, Kim DH, Yang JY, Woo HJ, Kwon HJ, Moon C, Kim SH, Kim JB. Anti-inflammatory effects of Kaempferol on Helicobacter pylori-induced inflammation. *Biosci Biotechnol Biochem* 2019; **83**: 166-173 [PMID: 30286691 DOI: 10.1080/09168451.2018.1528140]
20 **Maeda S**, Yoshida H, Ogura K, Mitsuno Y, Hirata Y, Yamaji Y, Akanuma M, Shiratori Y, Omata M. H. pylori activates NF-kappaB through a signaling pathway involving IkappaB kinases, NF-kappaB-inducing kinase, TRAF2, and TRAF6 in gastric cancer cells. *Gastroenterology* 2000; **119**: 97-108 [PMID: 10889159 DOI: 10.1053/gast.2000.8540]
21 **Ham B**, Fernandez MC, D'Costa Z, Brodt P. The diverse roles of the TNF axis in cancer progression and metastasis. *Trends Cancer Res* 2016; **11**: 1-27 [PMID: 27928197]
22 **Micheau O**, Lens S, Gaide O, Alevizopoulos K, Tschopp J. NF-kappaB signals induce the expression of c-FLIP. *Mol Cell Biol* 2001; **21**: 5299-5305 [PMID: 11463813 DOI: 10.1128/MCB.21.16.5299-5305.2001]
23 **Changhui M**, Tianzhong M, Zhongjing S, Ling C, Ning W, Ningxia Z, Xiancai C, Haibin C. Silencing of tumor necrosis

factor receptor 1 by siRNA in EC109 cells affects cell proliferation and apoptosis. *J Biomed Biotechnol* 2009; **2009**: 760540 [PMID: 19826638 DOI: 10.1155/2009/760540]

24 **Wan XK**, Yuan SL, Wang YC, Tao HX, Jiang W, Guan ZY, Cao C, Liu CJ. *Helicobacter pylori* inhibits the cleavage of TRAF1 *via* a CagA-dependent mechanism. *World J Gastroenterol* 2016; **22**: 10566-10574 [PMID: 28082808 DOI: 10.3748/wjg.v22.i48.10566]

25 **Moatti A**, Cohen JL. The TNF-α/TNFR2 Pathway: Targeting a Brake to Release the Anti-tumor Immune Response. *Front Cell Dev Biol* 2021; **9**: 725473 [PMID: 34712661 DOI: 10.3389/fcell.2021.725473]

26 **Pobezinskaya YL**, Liu Z. The role of TRADD in death receptor signaling. *Cell Cycle* 2012; **11**: 871-876 [PMID: 22333735 DOI: 10.4161/cc.11.5.19300]

27 **Pobezinskaya YL**, Kim YS, Choksi S, Morgan MJ, Li T, Liu C, Liu Z. The function of TRADD in signaling through tumor necrosis factor receptor 1 and TRIF-dependent Toll-like receptors. *Nat Immunol* 2008; **9**: 1047-1054 [PMID: 18641653 DOI: 10.1038/ni.1639]

28 **Ermolaeva MA**, Michallet MC, Papadopoulou N, Utermöhlen O, Kranidioti K, Kollias G, Tschopp J, Pasparakis M. Function of TRADD in tumor necrosis factor receptor 1 signaling and in TRIF-dependent inflammatory responses. *Nat Immunol* 2008; **9**: 1037-1046 [PMID: 18641654 DOI: 10.1038/ni.1638]

29 **Naudé PJ**, den Boer JA, Luiten PG, Eisel UL. Tumor necrosis factor receptor cross-talk. *FEBS J* 2011; **278**: 888-898 [PMID: 21232019 DOI: 10.1111/j.1742-4658.2011.08017.x]

30 **Borghi A**, Verstrepen L, Beyaert R. TRAF2 multitasking in TNF receptor-induced signaling to NF-κB, MAP kinases and cell death. *Biochem Pharmacol* 2016; **116**: 1-10 [PMID: 26993379 DOI: 10.1016/j.bcp.2016.03.009]

31 **Qiao F**, Gong P, Song Y, Shen X, Su X, Li Y, Wu H, Zhao Z, Fan H. Downregulated PITX1 Modulated by MiR-19a-3p Promotes Cell Malignancy and Predicts a Poor Prognosis of Gastric Cancer by Affecting Transcriptionally Activated PDCD5. *Cell Physiol Biochem* 2018; **46**: 2215-2231 [PMID: 29734189 DOI: 10.1159/000489590]

32 **DiPaola RS**. To arrest or not to G(2)-M Cell-cycle arrest : commentary re: A. K. Tyagi *et al*, Silibinin strongly synergizes human prostate carcinoma DU145 cells to doxorubicin-induced growth inhibition, G(2)-M arrest, and apoptosis. Clin. cancer res., 8: 3512-3519, 2002. *Clin Cancer Res* 2002; **8**: 3311-3314 [PMID: 12429616]

33 **Afzal H**, Yousaf S, Rahman F, Ahmed MW, Akram Z, Akhtar Kayani M, Mahjabeen I. PARP1: A potential biomarker for gastric cancer. *Pathol Res Pract* 2019; **215**: 152472 [PMID: 31174925 DOI: 10.1016/j.prp.2019.152472]

34 **Manoel-Caetano FS**, Rossi AFT, Calvet de Morais G, Severino FE, Silva AE. Upregulation of the *APE1* and *H2AX* genes and miRNAs involved in DNA damage response and repair in gastric cancer. *Genes Dis* 2019; **6**: 176-184 [PMID: 31194025 DOI: 10.1016/j.gendis.2019.03.007]

35 **Yang F**, Zhao N, Wu N. TNFR2 promotes Adriamycin resistance in breast cancer cells by repairing DNA damage. *Mol Med Rep* 2017; **16**: 2962-2968 [PMID: 28677724 DOI: 10.3892/mmr.2017.6898]

36 **Wu Y**, Zhou BP. TNF-alpha/NF-kappaB/Snail pathway in cancer cell migration and invasion. *Br J Cancer* 2010; **102**: 639-644 [PMID: 20087353 DOI: 10.1038/sj.bjc.6605530]

37 **Bubnovskaya L**, Osinsky D. Tumor microenvironment and metabolic factors: contribution to gastric cancer. *Exp Oncol* 2020; **42**: 2-10 [PMID: 32231198 DOI: 10.32471/exp-oncology.2312-8852.vol-42-no-1.14056]

38 **Vlachos IS**, Paraskevopoulou MD, Karagkouni D, Georgakilas G, Vergoulis T, Kanellos I, Anastasopoulos IL, Maniou S, Karathanou K, Kalfakakou D, Fevgas A, Dalamagas T, Hatzigeorgiou AG. DIANA-TarBase v7.0: indexing more than half a million experimentally supported miRNA:mRNA interactions. *Nucleic Acids Res* 2015; **43**: D153-D159 [PMID: 25416803 DOI: 10.1093/nar/gku1215]

39 **Dweep H**, Gretz N. miRWalk2.0: a comprehensive atlas of microRNA-target interactions. *Nat Methods* 2015; **12**: 697 [PMID: 26226356 DOI: 10.1038/nmeth.3485]

40 **Liu W**, Wang X. Prediction of functional microRNA targets by integrative modeling of microRNA binding and target expression data. *Genome Biol* 2019; **20**: 18 [PMID: 30670076 DOI: 10.1186/s13059-019-1629-z]

41 **Agarwal V**, Bell GW, Nam JW, Bartel DP. Predicting effective microRNA target sites in mammalian mRNAs. *Elife* 2015; **4** [PMID: 26267216 DOI: 10.7554/eLife.05005]

42 **Miranda KC**, Huynh T, Tay Y, Ang YS, Tam WL, Thomson AM, Lim B, Rigoutsos I. A pattern-based method for the identification of MicroRNA binding sites and their corresponding heteroduplexes. *Cell* 2006; **126**: 1203-1217 [PMID: 16990141 DOI: 10.1016/j.cell.2006.07.031]

43 **Kong J**, Wang W. A Systemic Review on the Regulatory Roles of miR-34a in Gastrointestinal Cancer. *Onco Targets Ther* 2020; **13**: 2855-2872 [PMID: 32308419 DOI: 10.2147/OTT.S234549]

44 **Deng X**, Zheng H, Li D, Xue Y, Wang Q, Yan S, Zhu Y, Deng M. MicroRNA-34a regulates proliferation and apoptosis of gastric cancer cells by targeting silent information regulator 1. *Exp Ther Med* 2018; **15**: 3705-3714 [PMID: 29581731 DOI: 10.3892/etm.2018.5920]

45 **Yu Y**, Wei SG, Weiss RM, Felder RB. TNF-α receptor 1 knockdown in the subfornical organ ameliorates sympathetic excitation and cardiac hemodynamics in heart failure rats. *Am J Physiol Heart Circ Physiol* 2017; **313**: H744-H756 [PMID: 28710070 DOI: 10.1152/ajpheart.00280.2017]

46 **Wang B**, Li D, Kovalchuk I, Apel IJ, Chinnaiyan AM, Wóycicki RK, Cantor CR, Kovalchuk O. miR-34a directly targets $tRNA_i^{Met}$ precursors and affects cellular proliferation, cell cycle, and apoptosis. *Proc Natl Acad Sci U S A* 2018; **115**: 7392-7397 [PMID: 29941603 DOI: 10.1073/pnas.1703029115]

47 **Chen H**, Zhu XM, Luo ZL, Hu YJ, Cai XC, Gu QH. Sevoflurane induction alleviates the progression of gastric cancer by upregulating the miR-34a/TGIF2 axis. *Eur Rev Med Pharmacol Sci* 2020; **24**: 11883-11890 [PMID: 33275259 DOI: 10.26355/eurrev_202011_23846]

48 **Jafari N**, Abediankenari S, Hossein-Nataj H. miR-34a mimic or pre-mir-34a, which is the better option for cancer therapy? *Cancer Cell Int* 2021; **21**: 178 [PMID: 33740991 DOI: 10.1186/s12935-021-01872-5]

49 **Cheng J**, Yang A, Cheng S, Feng L, Wu X, Lu X, Zu M, Cui J, Yu H, Zou L. Circulating miR-19a-3p and miR-483-5p as Novel Diagnostic Biomarkers for the Early Diagnosis of Gastric Cancer. *Med Sci Monit* 2020; **26**: e923444 [PMID: 32487978 DOI: 10.12659/MSM.923444]

50 **Liu M**, Wang Z, Yang S, Zhang W, He S, Hu C, Zhu H, Quan L, Bai J, Xu N. TNF-α is a novel target of miR-19a. *Int J Oncol* 2011; **38**: 1013-1022 [PMID: 21271217 DOI: 10.3892/ijo.2011.924]

51 **Wa Q**, Li L, Lin H, Peng X, Ren D, Huang Y, He P, Huang S. Downregulation of miR19a3p promotes invasion, migration and bone metastasis *via* activating TGFβ signaling in prostate cancer. *Oncol Rep* 2018; **39**: 81-90 [PMID: 29138858 DOI: 10.3892/or.2017.6096]

52 **Su YF**, Zang YF, Wang YH, Ding YL. MiR-19-3p Induces Tumor Cell Apoptosis *via* Targeting FAS in Rectal Cancer Cells. *Technol Cancer Res Treat* 2020; **19**: 1533033820917978 [PMID: 32266860 DOI: 10.1177/1533033820917978]

53 **Cui M**, Yue L, Fu Y, Yu W, Hou X, Zhang X. Association of microRNA-181c expression with the progression and prognosis of human gastric carcinoma. *Hepatogastroenterology* 2013; **60**: 961-964 [PMID: 23425811 DOI: 10.5754/hge121333]

54 **Hu X**, Miao J, Zhang M, Wang X, Wang Z, Han J, Tong D, Huang C. miRNA-103a-3p Promotes Human Gastric Cancer Cell Proliferation by Targeting and Suppressing ATF7 *in vitro*. *Mol Cells* 2018; **41**: 390-400 [PMID: 29754469 DOI: 10.14348/molcells.2018.2078]

55 **Wang S**, Han H, Hu Y, Yang W, Lv Y, Wang L, Zhang L, Ji J. MicroRNA-130a-3p suppresses cell migration and invasion by inhibition of TBL1XR1-mediated EMT in human gastric carcinoma. *Mol Carcinog* 2018; **57**: 383-392 [PMID: 29091326 DOI: 10.1002/mc.22762]

World Journal of Gastroenterology

Submit a Manuscript: https://www.f6publishing.com

World J Gastroenterol 2022 June 28; 28(24): 2705-2732

DOI: 10.3748/wjg.v28.i24.2705

ISSN 1007-9327 (print) ISSN 2219-2840 (online)

ORIGINAL ARTICLE

Clinical and Translational Research

Novel multiplex stool-based assay for the detection of early-stage colon cancer in a Chinese population

Hui-Hong Jiang, Si-Wei Xing, Xuan Tang, Ying Chen, Kang Lin, Lu-Wei He, Mou-Bin Lin, Er-Jiang Tang

Specialty type: Gastroenterology and hepatology

Provenance and peer review: Unsolicited article; Externally peer reviewed.

Peer-review model: Single blind

Peer-review report's scientific quality classification

Grade A (Excellent): 0
Grade B (Very good): B, B
Grade C (Good): 0
Grade D (Fair): 0
Grade E (Poor): 0

P-Reviewer: Jiménez Pérez M, Spain; Sharara AI, Lebanon

Received: December 4, 2021
Peer-review started: December 4, 2021
First decision: January 8, 2022
Revised: January 14, 2022
Accepted: May 13, 2022
Article in press: May 13, 2022
Published online: June 28, 2022

Hui-Hong Jiang, Xuan Tang, Kang Lin, Mou-Bin Lin, Department of General Surgery, Yangpu Hospital, Tongji University, Shanghai 200090, China

Hui-Hong Jiang, Ying Chen, Lu-Wei He, Mou-Bin Lin, Er-Jiang Tang, Institute of Gastrointestinal Surgery and Translational Medicine, Tongji University School of Medicine, Shanghai 200090, China

Si-Wei Xing, Department of Urology, Ruijin Hospital, Shanghai Jiaotong University School of Medicine, Shanghai 200025, China

Si-Wei Xing, Ying Chen, Kang Lin, Lu-Wei He, Mou-Bin Lin, Er-Jiang Tang, Center for Clinical Research and Translational Medicine, Yangpu Hospital, Tongji University, Shanghai 200090, China

Corresponding author: Er-Jiang Tang, MSc, Statistician, Center for Clinical Research and Translational Medicine, Yangpu Hospital, Tongji University, No. 450 Tengyue Road, Shanghai 200090, China. tangerjiang1988051@163.com

Abstract

BACKGROUND

Stool DNA (sDNA) methylation analysis is a promising, noninvasive approach for colorectal cancer screening; however, reliable biomarkers for detecting early-stage colon cancer (ECC) are lacking, particularly in the Chinese population.

AIM

To identify a novel stool-based assay that can improve the effectiveness of ECC screening.

METHODS

A blinded case-control study was performed using archived stool samples from 125 ECC patients, and 125 control subjects with normal colonoscopy. The cohort was randomly divided into training and test sets at a 1.5:1 ratio. Targeted bisulfite sequencing (TBSeq) was conducted on five pairs of preoperative and postoperative sDNA samples from ECC patients to identify DNA methylation biomarkers, which were validated using pyrosequencing. By logistic regression analysis, a multiplex stool-based assay was developed in the training set, and the detection performance was further assessed in the test set and combined set. The χ^2 test was used to investigate the association of detection sensitivity with clinico-

pathological features.

RESULTS

Following TBSeq, three hypermethylated cytosine-guanine sites were selected as biomarkers, including paired box 8, Ras-association domain family 1 and secreted frizzled-related protein 2, which differed between the groups and were involved in important cancer pathways. An sDNA panel containing the three biomarkers was constructed with a logistic model. Receiver operating characteristic (ROC) analysis revealed that this panel was superior to the fecal immunochemical test (FIT) or serum carcinoembryonic antigen for the detection of ECC. We further found that the combination of the sDNA panel with FIT could improve the screening effectiveness. In the combined set, the sensitivity, specificity and area under the ROC curve for this multiplex assay were 80.0%, 93.6% and 0.918, respectively, and the performance remained excellent in the subgroup analysis by tumor stage. In addition, the detection sensitivity did not differ with tumor site, tumor stage, histological differentiation, age or sex, but was significantly higher in T4 than in T1-3 stage tumors (P = 0.041).

CONCLUSION

We identified a novel multiplex stool-based assay combining sDNA methylation biomarkers and FIT, which could detect ECC with high sensitivity and specificity throughout the colon, showing a promising application perspective.

Key Words: Colon cancer; Early screening; Stool biomarker; DNA methylation; Fecal immunochemical test

Core Tip: Stool DNA (sDNA) methylation analysis has a promising application in the early diagnosis of colorectal cancer. However, reliable biomarkers for detecting early-stage colon cancer (ECC) are lacking. In this study, by targeted bisulfite sequencing, we identified a novel multiplex stool-based assay combining three sDNA methylation biomarkers and fecal immunochemical test. Further validation in larger samples by pyrosequencing showed that it enabled the diagnosis of ECC with high sensitivity and specificity throughout the colon. To our knowledge, this is the first study to focus on ECC screening in China.

Citation: Jiang HH, Xing SW, Tang X, Chen Y, Lin K, He LW, Lin MB, Tang EJ. Novel multiplex stool-based assay for the detection of early-stage colon cancer in a Chinese population. *World J Gastroenterol* 2022; 28(24): 2705-2732

URL: https://www.wjgnet.com/1007-9327/full/v28/i24/2705.htm

DOI: https://dx.doi.org/10.3748/wjg.v28.i24.2705

INTRODUCTION

Colorectal cancer (CRC) has emerged as a major public health issue in China, with 521400 new cases and 248000 deaths occurring in 2018[1]. The incidence of colon cancer has increased significantly in the past decades, with a trend in younger patients, and most cases are in advanced stages at initial diagnosis[2]. Early screening is the key to improving survival and reducing morbidity[3]. Compared with the high positive rate of rectal palpation in rectal cancer, colonoscopy is currently the main tool and gold standard for detecting colon cancer, but is invasive, costly and poorly tolerated[4]. The fecal immunochemical test (FIT), computed tomography (CT) colonography and blood tumor markers, such as serum carcinoembryonic antigen (CEA), provide relatively noninvasive and painless methods, but their sensitivity for detecting early-stage colon cancer (ECC) is limited[5,6]. Thus, the identification of novel biomarkers that are highly specific, sensitive, and noninvasive is urgently needed for the screening of ECC.

CRC development is characterized by the progressive accumulation of genetic and epigenetic alterations that transform colonic epithelial cells into adenocarcinoma cells[7,8]. These cells are continuously shed into the colonic lumen and mixed with stool[9]. Moreover, the molecular changes caused by CRC tumorigenesis are reportedly present in the stool earlier than in the blood[10]. Hence, detecting aberrant DNA methylation in stool DNA (sDNA) has been proposed as a promising noninvasive alternative for CRC screening. To date, a number of sDNA methylation biomarkers have been reported for the detection of different stages of CRC, including secreted frizzled-related protein 2

(SFRP2), N-myc downstream-regulated gene 4 (NDRG4), ventralis intermedius, COL4A2 and GATA4 [11]. Further studies revealed that the combination of multiple biomarkers contributed to a higher diagnostic accuracy than a single biomarker[12]. For instance, a multitarget sDNA test Cologuard, combining NDRG4 and BMP3 methylation, Kirsten rat sarcoma mutations, β-actin and a hemoglobin assay, has been approved for average-risk CRC screening by the US Food and Drug Administration and is now available clinically[13]. However, the reported sensitivity and specificity of the same sDNA methylation biomarker varied greatly among studies, due to the different study populations (mainly the ethnic, geographic and dietary differences), inclusion criteria and levels of examination[14,15]. Moreover, few studies have focused on the sDNA screening test for ECC, especially in the Chinese population.

In this study, using targeted bisulfite sequencing (TBSeq), we identified a novel panel of sDNA methylation biomarkers for ECC detection, which was validated in a training and test design with pyrosequencing (PSQ). We further investigated the detection performance of the sDNA panel combining conventional screening methods, and assessed the effects of clinical covariates on test performance. To our knowledge, this is the first work to focus on ECC screening in China.

MATERIALS AND METHODS

Study design and study population

Between November 2018 and June 2020, a single-center, case-control study was performed at Yangpu Hospital Affiliated to Tongji University, using archived stool samples from 125 patients with sporadic ECC and 125 individuals with normal colonoscopy results. The diagnosis of stage I and II colon cancer was histologically confirmed after surgery. All subjects were of Han race living in Shanghai, and the inclusion of patients and controls was carried out to achieve a good match in terms of age and sex. Those who had a history of digestive cancer, inflammatory bowel disease or familial adenomatous polyposis, or an unconfirmed diagnosis were excluded. In addition, clinical information including tumor site, histological differentiation, tumor stage and preoperative serum CEA level was abstracted from medical records. These participants were randomly divided into training and test sets with a sample size ratio of 1.5:1. All subjects provided written informed consent, and this study was approved by the Ethical Committee and Institutional Review Board of our hospital (LL-2018-SCI-003). This study was registered at the Chinese Clinical Trial Registry (ChiCTR1800019552). The study design consisted of three stages: Biomarker selection, biomarker validation and model evaluation, as shown in Figure 1.

Sample collection and processing

All participants were required to undergo screening colonoscopy and provide a fresh stool sample before bowel purgation. In addition, 20 randomly selected ECC patients (6 stage I and 14 stage II cases) were asked to provide stool samples at six months after radical surgery with no tumor recurrence. One part of the stool sample was used for FIT (FASURE; NewScen Coast, China), and the result was evaluated at the manufacturer's recommended positivity cut-off of 200 ng hemoglobin/mL buffer. The other part (minimum 50 g) was immediately extracted or stored at -80 °C for further use, sDNA was extracted with a QIAamp DNA Fast Stool Mini Kit (Qiagen, Germany), and the quality and concentration were determined by spectrophotometry (NanoDrop 2000; Thermo-Fisher Scientific, United States). Among the 20 pairs of preoperative and postoperative sDNA samples, five pairs (2 stage I and 3 stage II cases) were randomly selected for biomarker identification using TBSeq and named cancer sample group (CSG) and healthy sample group (HSG), respectively.

TBSeq

We used CATCH-Seq target enrichment technology (Novogene, China) to perform bisulfite sequencing, to evaluate 23441 [cytosine-guanine (CpG) islands] (CGIs) (about 83% of the 28226 CGIs in the human genome) and the promoter regions of 19369 RefSeq genes (within 2 kb before the transcription start site) [16,17]. Briefly, according to the manufacturer's protocol, genomic DNA (1 μg) was fragmented into 200-300 bp fragments using a Covaris S220 (Covarias, United States). The DNA fragments were then sheared, end-repaired and dephosphorylated. The blunt fragments were subsequently A-tailed and ligated to sequencing adaptors that were synthesized with 5′-methylcytosine instead of 5′-cytosine and index sequences. Following the liquid hybridization capture procedure, the target enriched library was bisulfite-converted (EZ DNA Methylation Kit; Zymo Research, United States) and then amplified by polymerase chain reaction (PCR). After quantification and quality control, sequencing was performed on an Illumina Hiseq 2500 platform (Illumina, United States).

Analysis of sequencing data

Preprocessing included quality control using FastQC, adapter trimming using cutadapt, and read alignment and methylation calling using Bismark with Bowtie2 (hg19/GRCh37). The coverage depth of each base and CpG site was calculated, and the results were filtered by criteria of at least 5X coverage.

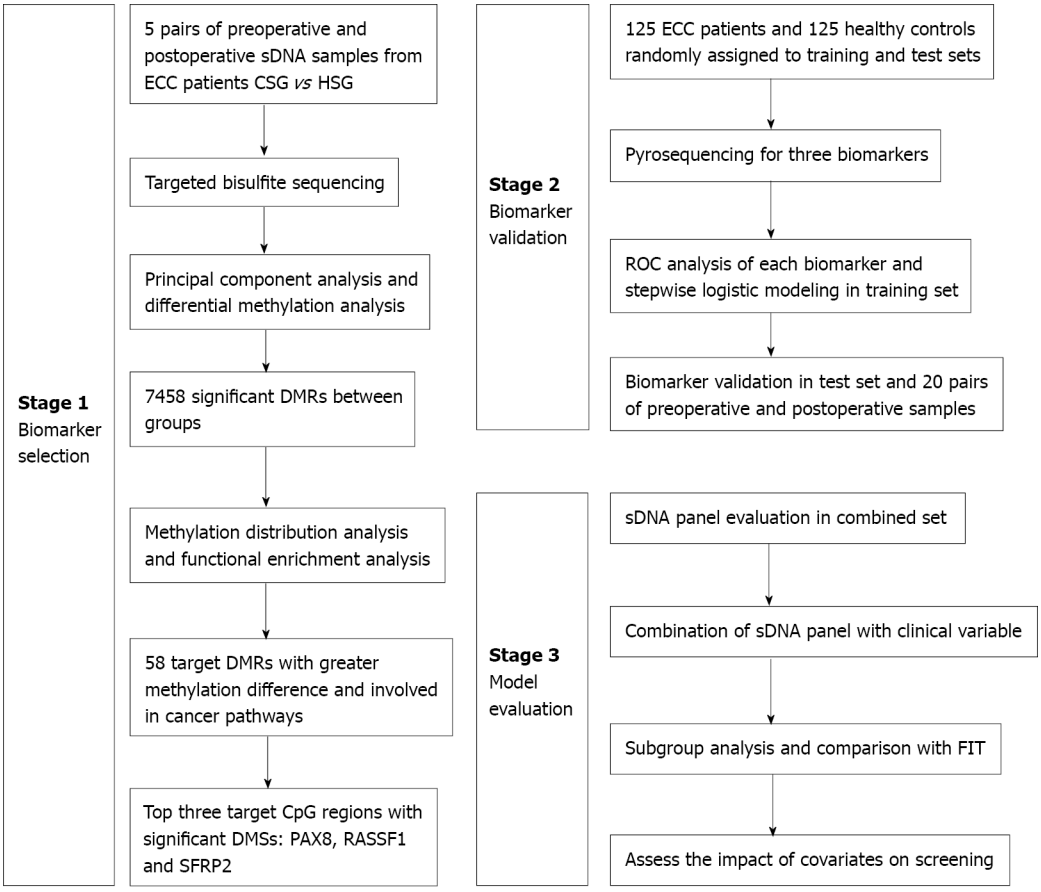

DOI: 10.3748/wjg.v28.i24.2705

Figure 1 Flow diagram of the study design. Candidate methylation biomarkers were selected by targeted bisulfite sequencing and then validated using pyrosequencing. At last, a diagnostic model was constructed and evaluated. CSG: Cancer sample group; HSG: Healthy sample group; DMRs: Differentially methylated regions; DMSs: Differentially methylated sites; ROC: Receiver operating characteristic; sDNA: Stool DNA; FIT: Fecal immunochemical test; PAX8: Paired box 8; RASSF1: Ras-association domain family 1; SFRP2: Secreted frizzled-related protein 2; CpG: Cytosine-guanine; ECC: Early-stage colon cancer.

The CpG sites that were located on the Y chromosome and overlapped with single nucleotide polymorphisms (SNPs) registered in the SNP database (http://www.ncbi.nlm.nih.gov/projects/SNP/) were excluded from the analysis. For the methylated sites, the methylation level was calculated using the formula: ML = mC/(mC + umC), where ML represents the methylation level, and mC and umC represent the number of methylated and unmethylated C-sites, respectively. Methylation levels of the specified functional regions including CGI, CGI shore (0-2 kb from CGI), CGI shelf (2-4 kb from CGI), promoter, 5′ untranslated regions (UTR), 3′UTR and exon, were summarized to show the distribution [18]. Methylation density was defined as the percentage of methylated CpG sites among all CpG sites within the given region.

In-house scripts were used to identify a differentially methylated site (DMS) by Fisher's exact test with false discovery rate correction. Statistical significance for DMS between the two groups was determined if the adjusted P value < 0.05 and the difference in methylation level > 0.25. A differentially methylated region (DMR) was identified by swDMR software (http://122.228.158.106/swDMR/) using the sliding-window approach, in which the window was set to 1000 bp and the step length was 100 bp. The DMR should contain at least two CpG sites (all sites are hypermethylated or hypomethylated), and the distance between the adjacent CpG sites was < 100 bp. In addition, the DMRs with an adjusted P value < 0.05 and a difference in methylation level > 0.1 were considered candidate DMRs.

Biomarker selection

By comparing the methylation status between the CSG and HSG, 7458 DMRs were obtained based on the above standards. To strengthen the robustness of the candidate biomarker, the DMRs located far from CGIs and promoter regions were filtered out. Moreover, to reduce the noise due to sample heterogeneity, it was essential to select biomarkers that had greater methylation difference between groups (P > 0.35) and that were significantly enriched in well-established cancer pathways (adjusted P < 0.05). In total, 58 target DMRs were selected, and each DMR contained at least two significant DMSs. According to the guanine-cytosine percent, primer lengths, amplicon lengths, predicted melting temperatures and the number of SNPs in the primers, the score representing the difficulty levels for all the candidate

Table 1 Primers for pyrosequencing of three DNA methylation biomarkers

Target gene	Primer	Sequence	Size (bp)	Target DMS
PAX8	Forward	5′-GGGGGTTAGGGGATTTTGATTATA-3′	166	chr2:114035984; 114035988; 114035995; 114035998; 114036006
	Reverse	Biotin-5′-ATCTCATACCCTTCTCCTAAATTTATAC-3′		
	Sequencing	5′-ATGGAGTTGTGAGGT-3′		
RASSF1	Forward	5′-TTTATTTATTGGGTGGGGTAGGA-3′	141	chr3:50378714; 50378718
	Reverse	Biotin-5′-CCTCAAAATCACCATCCAACCTCTAC-3′		
	Sequencing	5′-GGGAGATAGGTTAGTAGTTTTA-3′		
SFRP2	Forward	5′-GATTAGGGATAATTAGGTAAAAGGAGTT-3′	166	chr4:154711281; 154711305
	Reverse	Biotin-5′-ATTCATCCCCTACCTACCAAAAAACACC-3′		
	Sequencing	5′-AGTTAGAGATATTAGATTTTAGG-3′		

PAX8: Paired box 8; RASSF1: Ras-association domain family 1; SFRP2: Secreted frizzled-related protein 2; DMS: Differentially methylated site.

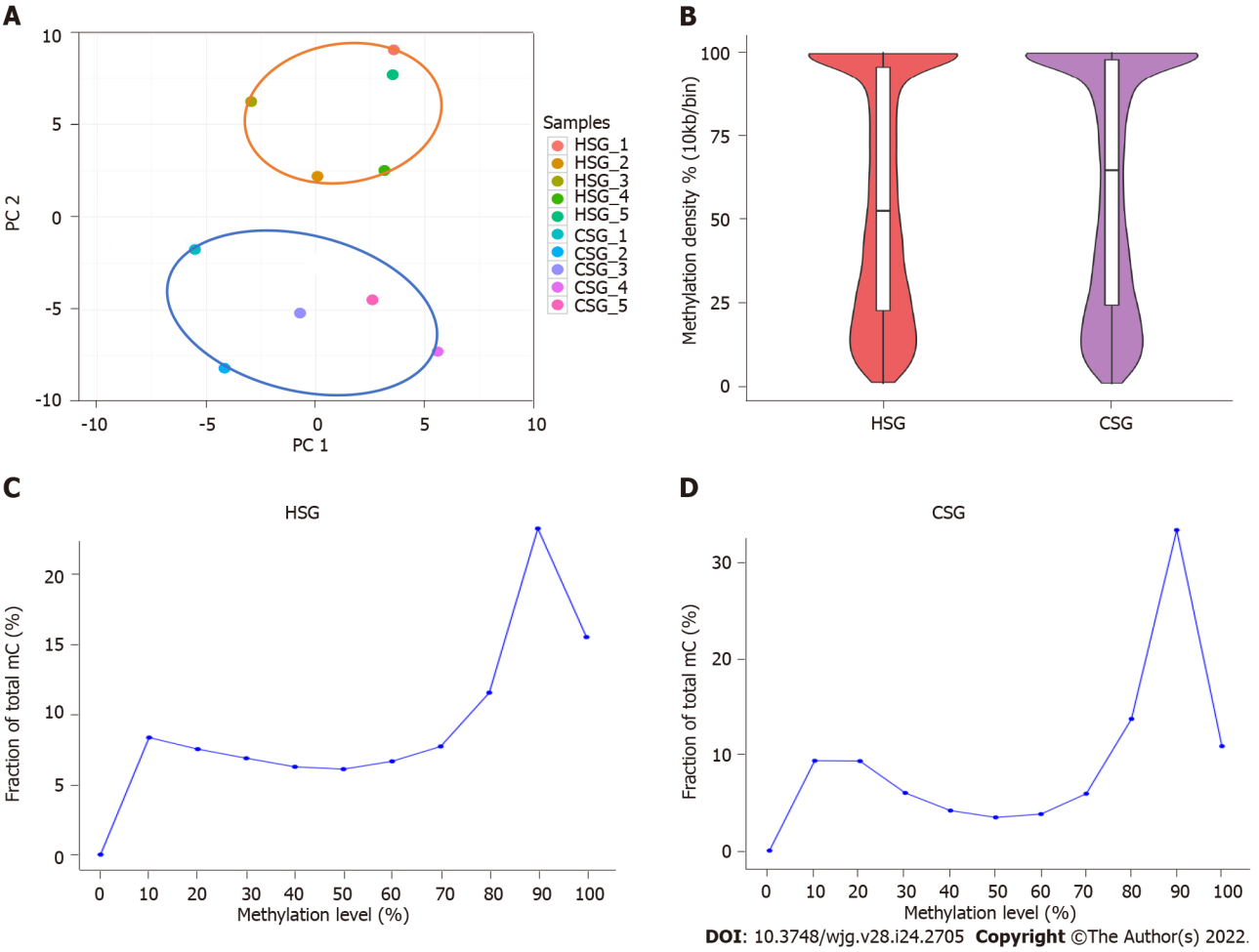

Figure 2 DNA methylation analysis by targeted bisulfite sequencing. A: Principal component analysis of the methylation profiles between cancer sample group (CSG) and healthy sample group (HSG); B: Comparison of methylation density between CSG and HSG; C: Comparison of methylation level distribution between CSG and HSG. CSG: Cancer sample group; HSG: Healthy sample group; PC: Principal component.

regions was obtained. Finally, we selected the top three target CpG regions with the best chance of being amplified and conducted in the PSQ assay, and removed the other candidate regions for further validation.

Table 2 Clinicopathological features of the early-stage colon cancer patients enrolled in this study, *n* (%)

Variable	Total (*n* = 125)	Training set (*n* = 75)	Test set (*n* = 50)
Age (yr)	69 (range, 48-94)	68 (range, 51-94)	70 (range, 48-88)
Sex			
Male	66 (52.8)	39 (52.0)	27 (54.0)
Female	59 (47.2)	36 (48.0)	23 (46.0)
Serum CEA (≥ 5 ng/mL)			
Positive	37 (29.6)	21 (28.0)	16 (32.0)
Negative	88 (70.4)	54 (72.0)	34 (68.0)
FIT (≥ 200 ng/mL)			
Positive	78 (62.4)	48 (64.0)	30 (60.0)
Negative	47 (37.6)	27 (36.0)	20 (40.0)
Tumor site			
Proximal	64 (51.2)	36 (48.0)	28 (56.0)
Distal	61 (48.8)	39 (52.0)	22 (44.0)
TNM stage			
I	47 (37.6)	30 (40.0)	17 (34.0)
II	78 (62.4)	45 (60.0)	33 (66.0)
T stage			
T1-3	71 (56.8)	44 (58.7)	27 (54.0)
T4	54 (43.2)	31 (41.3)	23 (46.0)
Histological differentiation			
Well/moderately	98 (78.4)	60 (80.0)	38 (76.0)
Poorly	27 (21.6)	15 (20.0)	12 (24.0)

CEA: Carcinoembryonic antigen; FIT: Fecal immunochemical test; TNM: Tumor-node-metastasis.

PSQ

To measure the methylation levels of the three target CpG regions in the 250 stool samples, PSQ was conducted (Oebiotech, China) without knowledge of either the clinical diagnosis or FIT result, sDNA extraction and bisulfite conversion were performed as previously described[19]. The PSQ primers were designed to amplify two to five CpG sites in target sequences using PyroMark Assay Design software (Qiagen, Germany). Primer sequences were listed in Table 1. For methylation-specific PCR (MSP), 50 ng of bisulfite modified DNA was amplified in a 25 μL reaction. The cycling conditions were recommended by the manufacturer and were as follows: A denaturing step of 15 min at 95 °C, then 45 cycles at 94 °C for 30 s, 56 °C for 30 s and 72 °C for 30 s, and a final elongation step of 10 min at 72 °C. PSQ was performed on a PSQ HS96A instrument according to the manufacturer's guidelines using PyroMark Gold Q96 Reagents (Qiagen, Germany). The methylation index of each gene in each sample was calculated as the mean percentage of mC for all examined CpGs in target regions. All experiments included a negative control without a template[19].

Diagnostic model building

Based on the PSQ results, a logistic regression model was developed to define a linear combination of variables that optimized the discrimination between ECC patients and healthy controls. The modeling strategy consisted of age, sex, FIT, preoperative CEA level and sDNA methylation biomarkers in a base model and adding quadratic and pairwise interactions of these variables using backward selection with $P < 0.05$ for retention. The formula was as follows: $Y = \beta0 + \beta1X1 + \beta2X2 + \ldots + \beta nXn$ where X represented the exploratory variable[20]. The linear discriminant score with the corresponding cut-off value was then applied to the study population. Receiver operating characteristic (ROC) analysis was applied to compare the accuracy of nested logistic models and to investigate the added value of each variable.

Table 3 Diagnostic sensitivity, specificity and area under the receiver operating characteristic curve for various indexes

Study population	Index	Sensitivity (%)	Specificity (%)	AUC (95%CI)
Training set	Serum CEA	28.0	100.0	0.640 (0.551-0.729)
(*n* = 150 subjects)	FIT	64.0	96.0	0.800 (0.726-0.874)
	PAX8_P4	76.0	77.3	0.810 (0.741-0.880)
	RASSF1_P1	50.7	93.3	0.782 (0.709-0.854)
	SFRP2_P1	50.7	86.7	0.697 (0.612-0.782)
	sDNA panel	82.7	77.3	0.866 (0.810-0.923)
	sDNA panel + FIT	86.7	86.7	0.924 (0.881-0.966)
Test set	Serum CEA	32.0	100.0	0.660 (0.552-0.768)
(*n* = 100 subjects)	FIT	60.0	98.0	0.790 (0.697-0.883)
	sDNA panel	76.0	84.0	0.864 (0.795-0.933)
	sDNA panel + FIT	82.0	96.0	0.909 (0.850-0.967)
Combined set	Serum CEA	29.6	100.0	0.648 (0.580-0.716)
(*n* = 250 subjects)	FIT	62.4	96.8	0.796 (0.738-0.854)
	sDNA panel	75.2	84.0	0.859 (0.815-0.904)
	sDNA panel + FIT	80.0	93.6	0.918 (0.884-0.952)
Subgroup for stage I	FIT	63.8	96.8	0.803 (0.716-0.891)
(*n* = 172 subjects)	sDNA panel + FIT	74.5	93.6	0.891 (0.832-0.950)
Subgroup for stage II	FIT	61.5	96.8	0.792 (0.721-0.863)
(*n* = 203 subjects)	sDNA panel + FIT	83.3	93.6	0.934 (0.899-0.970)

AUC: Area under the receiver operating characteristic curve; CI: Confidence interval; CEA: Carcinoembryonic antigen; FIT: Fecal immunochemical test; sDNA: Stool DNA.

Statistical analysis

All statistical analyses were conducted using Prism 8 for Windows (GraphPad, United States) and R software v3.5.2 (R Foundation for Statistical Computing, Austria). c^2 test or Fisher's exact test was used to compare categorical variables, and Student's *t*-test or Mann-Whitney *U* test was used to compare continuous variables. Principal component analysis (PCA) was performed to visualize the degree of similarity between samples according to their DNA methylation state[21]. A volcano plot and a Circos plot were used to present the differences in DMR methylation levels between groups[22]. To determine the functions and enriched pathways of these DMR-related genes, Gene Ontology (GO) and Kyoto Encyclopedia of Genes and Genomes (KEGG) pathway analyses were performed[23]. The sensitivity, specificity, and area under the ROC curve (AUC) with corresponding 95% confidence intervals (CIs) were calculated and compared. The χ^2 test was also used to assess the association of detection sensitivity with clinicopathological covariates. For all analyses, $P < 0.05$ was considered statistically significant.

RESULTS

Clinicopathological features of the study population

Overall, this study enrolled 125 ECC patients and 125 healthy controls, with a median age of 69 (range, 48-94) and 68 (range, 42-92) years, respectively; 47.2% of patients and 49.6% of controls were females. Age and sex were well-balanced between patients and controls. With the conventional 5 ng/mL cut-off, serum CEA positivity was observed in 29.6% of patients and 0% of controls, and the difference was statistically significant ($P < 0.001$). FIT also showed a significantly higher positivity rate in the patients than in the controls (62.4% *vs* 3.2%, $P < 0.001$). Of these ECCs, 64 (51.2%) tumors were located proximal to the splenic flexure and 61 (48.8%) were distal. According to the postoperative pathological examination, there were 47 (37.6%) stage I tumors and 78 (62.4%) stage II tumors; 98 (78.4%) cases were well or moderately differentiated, and 27 (21.6%) were poorly differentiated. In addition, study participants were randomly divided into training and test sets with a 1.5:1 split. The differences in all these features between the training and test sets were not significant (all $P > 0.05$), indicating similar

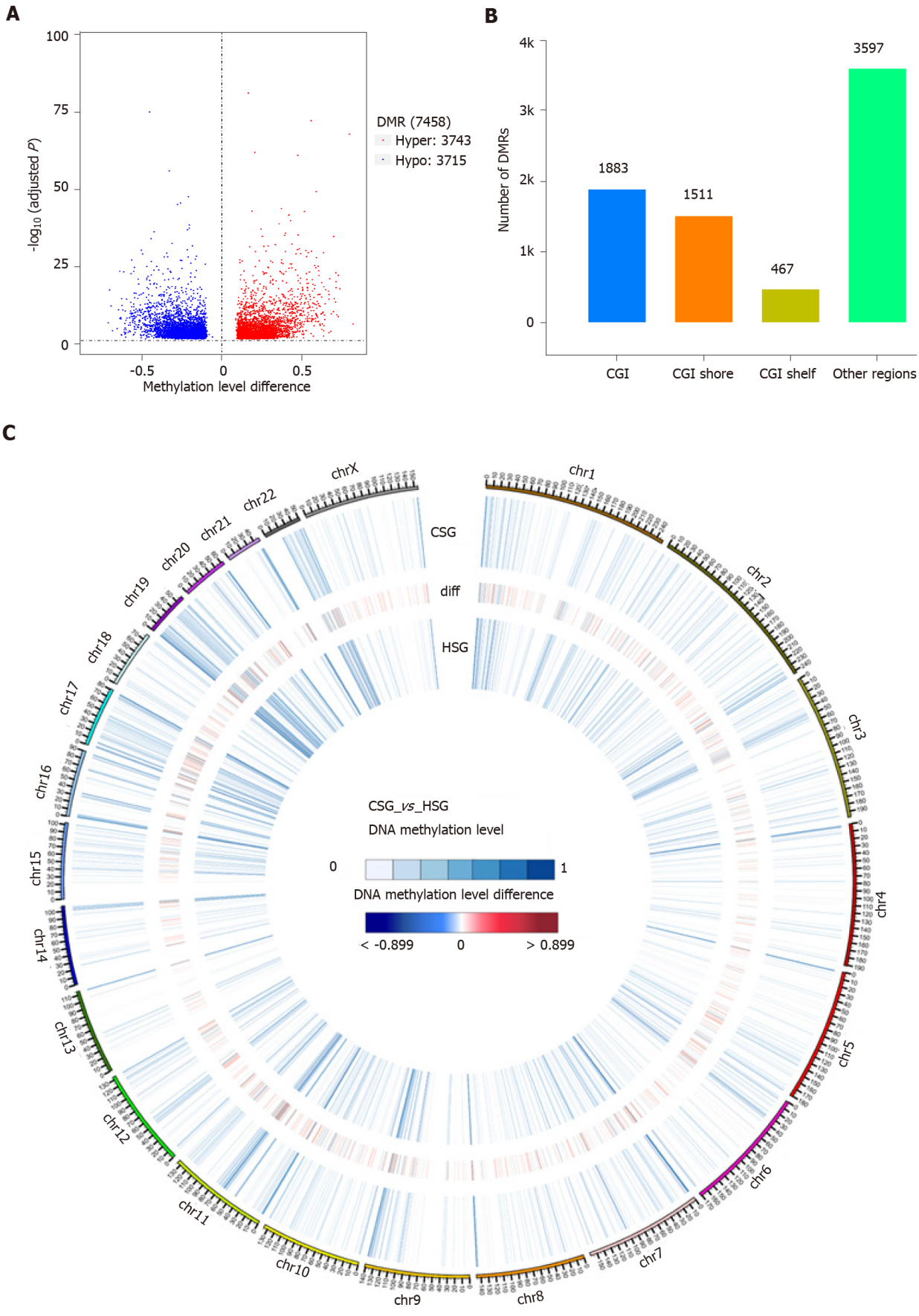
A
100
75
50
25
0
-log10 (adjusted P)
-0.5
0
0.5
Methylation level difference
DMR (7458)
Hyper: 3743
Hypo: 3715
B
4k
3k
2k
1k
0
Number of DMRs
1883
1511
467
3597
CGI
CGI shore
CGI shelf
Other regions
C
chrX
chr1
chr22
chr21
chr20
chr19
chr18
chr17
chr16
chr15
chr14
chr13
chr12
chr11
chr10
chr9
chr8
chr7
chr6
chr5
chr4
chr3
chr2
CSG
diff
HSG
CSG_vs_HSG
DNA methylation level
0
1
DNA methylation level difference
< -0.899
0
> 0.899

DOI: 10.3748/wjg.v28.i24.2705

Figure 3 Differentially methylated region analysis and biomarkers discovery. A: Volcano plot of differentially methylated regions (DMRs) in cancer sample group (CSG) *vs* healthy sample group (HSG); B: The distribution of the identified DMRs in the genome in relation to cytosine-guanine islands (CGIs); C:

Circos plot of 2531 candidate DMRs on each of the 22 autosomes and the X chromosome; D: Kyoto Encyclopedia of Genes and Genomes pathway analysis of 2062 DMR-related genes; E: Gene Ontology analysis of 2062 DMR-related genes; F: Venn diagram of the overlapping target DMRs among different signatures. [a]*P* < 0.05. DMRs: Differentially methylated regions; CGI: Cytosine-guanine islands.

composition and the comparability (Table 2).

DNA methylation analysis by TBSeq

A total of 11.69 G and 11.08 G raw bases were generated on average for the HSG and CSG, respectively. All samples showed a bisulfite conversion rate greater than 99%. After data filtering, approximately 2.8 million CpGs on the target sequencing region were obtained for each sample, and the depth of coverage ranged between 23.66 and 32.24 (Supplementary Table 1). A PCA was performed on the methylation profiles, and demonstrated that the groups had intragroup similarity, but also intergroup dissimilarity (Figure 2A). In addition, the mean methylation densities of the HSG and CSG were 52.8% and 65.4%, respectively (Figure 2B); compared with 50.4% of CpG sites in the HSG, 58.0% of CpG sites in the CSG had a methylation level above 80% (Figure 2C).

Candidate biomarkers discovery

As shown in Figure 3A, in total, 7458 DMRs were identified in the CSG compared with the HSG (adjusted $P < 0.05$ and methylation level difference > 0.1), including 3743 hypermethylated and 3715 hypomethylated DMRs. Among them, 1883 DMRs (25.3%) were located in the CGIs, and 1978 (26.5%) were located in the regions flanking CGIs (CGI shore and shelf) (Figure 3B). Moreover, of the 3861 CGI-related DMRs, 2531 overlapped with the promoter regions of the 20579 genes with known functions (Figure 3C). To determine changes in the methylation status of gene functions, GO and KEGG pathway analyses were conducted and revealed that these 2062 DMR-related genes were significantly enriched in cell migration, focal adhesion, Wnt, Ras, Rap1 and MAPK signaling pathways, *etc* (Figures 3D and 3E, adjusted $P < 0.05$). To mine the data for potential early screening biomarkers, 58 DMR-related genes that differed most in methylation level between the groups and that were involved in the important cancer pathways were selected (Figure 3F). With the PSQ criteria, the top three target CpG regions within the promoters of paired box 8 (PAX8), Ras-association domain family 1 (RASSF1) and SFRP2 were finally identified, and contained five, two and two significant DMSs, respectively (Table 1).

Biomarkers validation by PSQ

To assess the screening effectiveness of these three biomarkers, PSQ was successfully performed in all sDNA samples. Using the 150 subjects in the training set, ROC analyses showed that the AUCs for the five DMSs of PAX8 ranged from 0.784 to 0.826, the AUCs for the two DMSs of RASSF1 were 0.782 and 0.763, and the AUCs for the two DMSs of SFRP2 were 0.697 and 0.641, respectively (Supplementary Figures 1A, 1B and 1C). In addition, serum CEA positivity was detected in 14.0% of the 150 subjects, with a sensitivity of 28.0% and an AUC of 0.640; FIT positivity was detected in 34.0% of the 150 subjects, with a sensitivity of 64.0% and an AUC of 0.800 (Table 3). By stepwise logistic modeling, an sDNA methylation panel including three DMSs was constructed as follows: Y = -10.937 + 0.097 × PAX8_P4 + 0.054 × RASSF1_P1 + 0.058 × SFRP2_P1. These three DMSs showed significantly increased methylation in patients compared with controls (all $P < 0.05$; Figure 4A) as well as in the comparison between the 20 pairs of preoperative and postoperative patient samples (all $P < 0.05$; Supplementary Figures 1D, 1E and 1F). The sensitivity and AUC for this sDNA panel were 82.7% and 0.866 (95%CI: 0.810-0.923), respectively, which were superior to any single index above (Figure 4B, Table 3). Subsequently, this panel was validated in an independent test set, and the AUC reached 0.864 (95%CI: 0.795-0.933), also offering an advantage over FIT (Figure 4C).

Evaluation of the diagnostic model

The diagnostic performance of the sDNA panel was also confirmed in the combined set, achieving an AUC of 0.859 (0.815-0.904) (Figure 4D). In addition, among the 168 subjects with negative FIT and the 213 subjects with negative serum CEA, the AUCs for this panel reached 0.807 (95%CI: 0.734-0.880) and 0.864 (95%CI: 0.816-0.913), respectively (Supplementary Figure 2). We further investigated whether the combination of the sDNA panel with clinical variables could improve the effectiveness of ECC screening. The results showed that the inclusion of FIT was accompanied by a relative increase in sensitivity and AUC, as compared with the sDNA panel, serum CEA or FIT alone (Table 3, Figure 5). In contrast, the contribution of age, sex or preoperative CEA level to aggregate panel discrimination was minimal (data not shown). For example, in the combined set, the sensitivity, specificity and AUC for the sDNA panel combining FIT were up to 80.0%, 93.6% and 0.918 (95%CI: 0.884-0.952), respectively (Figure 4D, Table 3). In the subgroup analysis by tumor stage, this multiplex assay showed excellent performance for both stage I and II ECCs, with an AUC of 0.891 (95%CI: 0.832-0.950) and 0.934 (95%CI: 0.899-0.970), respectively (Figures 4E and 4F).

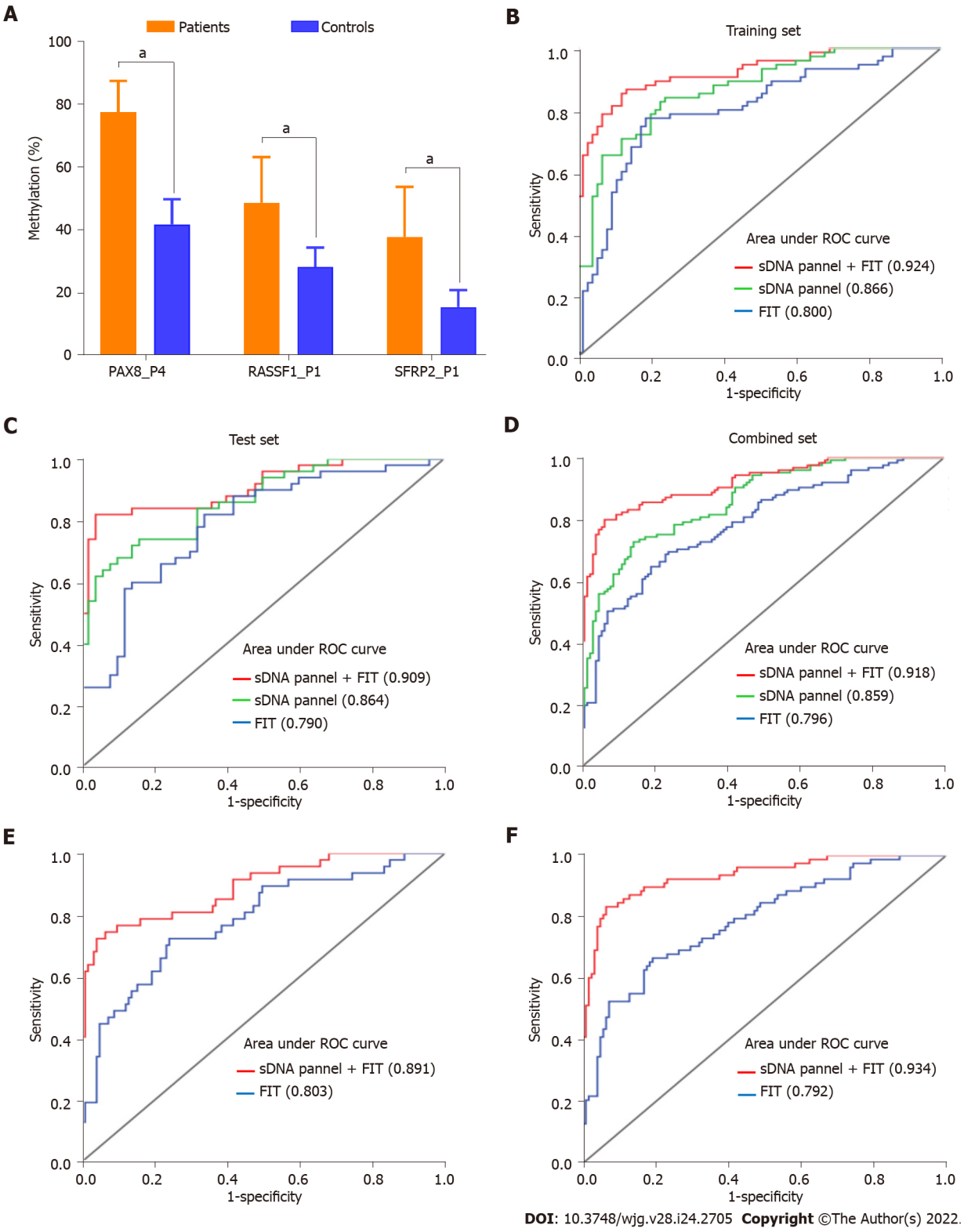

DOI: 10.3748/wjg.v28.i24.2705

Figure 4 The evaluation of diagnostic model based on pyrosequencing. A: Comparison of methylation percentage of the three target biomarkers between the patients and controls in training set; B: Receiver operating characteristic (ROC) curves comparing fecal immunochemical test (FIT), stool DNA (sDNA) panel and sDNA panel + FIT for the detection of early-stage colon cancer (ECC) in training set; C: ROC curves comparing FIT, sDNA panel and sDNA panel + FIT for the detection of ECC in test set; D: ROC curves comparing FIT, sDNA panel and sDNA panel + FIT for the detection of ECC in combined set; E: ROC curves comparing FIT and sDNA panel + FIT for the detection of stage I ECC in combined set; F: ROC curves comparing FIT and sDNA panel + FIT for the detection of stage II ECC in combined set. [a]*P* < 0.05. sDNA: Stool DNA; FIT: Fecal immunochemical test; ROC: Receiver operating characteristic; PAX8: Paired box 8; RASSF1: Ras-association domain family 1; SFRP2: Secreted frizzled-related protein 2.

Impact of covariates on screening

We also analyzed the impact of clinicopathologic covariates on assay screening. First, we found that the

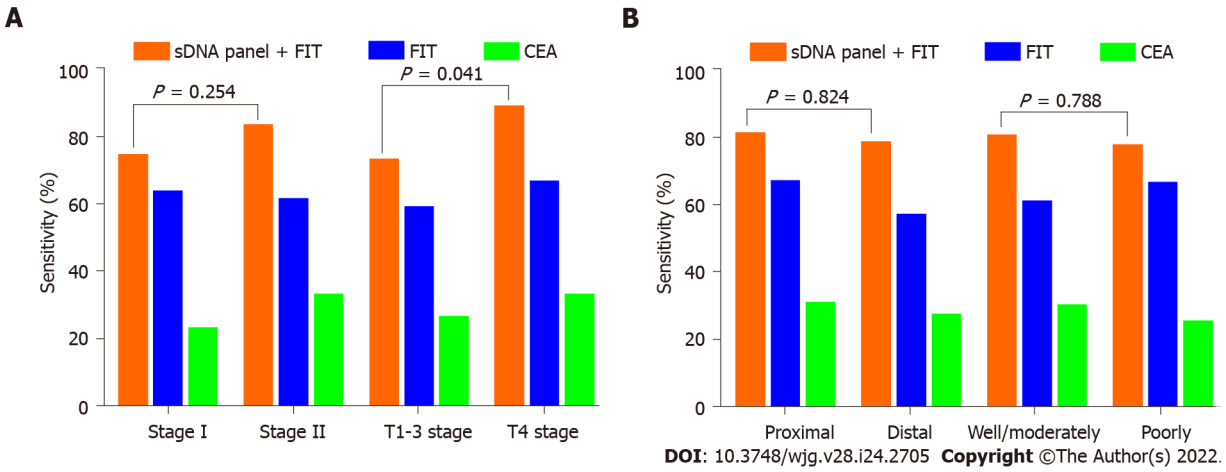

Figure 5 Impact of clinicopathologic covariates on screening. A: Sensitivities of fecal immunochemical test (FIT), serum carcinoembryonic antigen (CEA) and stool DNA (sDNA) panel + FIT for the detection of early-stage colon cancer (ECC), according to tumor-node-metastasis stage or T stage; B: Sensitivities of FIT, serum CEA and sDNA panel + FIT for the detection of ECC, according to tumor site or histological differentiation. sDNA: Stool DNA; FIT: Fecal immunochemical test; CEA: Carcinoembryonic antigen.

detection sensitivities of the sDNA panel combining FIT for stage I and II ECCs were 74.5% and 83.3%, respectively, with no statistical difference (P = 0.254; Figure 5A). However, the detection sensitivity of 88.9% for T4 stage tumors was significantly higher than the aggregate sensitivity of 73.2% for T1-3 stage tumors (P = 0.041; Figure 5A). Second, this multiplex assay detected 81.3% of proximal ECCs *vs* 78.7% of distal ECCs (P = 0.824; Figure 5B). Third, the detection rate for poorly differentiated tumors was comparable to that for well or moderately differentiated tumors (77.8% *vs* 80.6%, P = 0.788; Figure 5B). In addition, the sensitivity also did not vary significantly according to age or sex of the patients (data not shown).

DISCUSSION

CRC is the third most prevalent cancer in China, with an increasing proportion of colon cancer diagnoses over the decades[2]. Effective screening measures are highly needed to lessen this burden, especially for ECC due to its occult onset. Compared with conventional methods, the sDNA test provides a biologically rational approach based on tumor exfoliation and is noninvasive, requires no unpleasant cathartic preparation, no diet or medication restriction[24]. However, reliable biomarkers particularly for ECC detection are lacking. In the present study, we provided a novel multiplex stool-based assay that enabled the diagnosis of ECC with high sensitivity and specificity.

Aberrant DNA methylation is an early and frequent event in carcinogenesis and therefore has great potential for ECC screening[25]. To identify the candidate methylation biomarkers, we performed high throughput TBSeq with five pairs of preoperative and postoperative sDNA samples from ECC patients, where the paired design can help reduce the influence of background noise and improve the feature discriminability. Three of our candidate biomarkers were finally selected: RASSF1, SFRP2 and PAX8. The first two have been identified in various cancers including CRC[26,27], to be the commonly silenced tumor-suppressor genes by promoter hypermethylation[28]. PAX8 is a member of the paired box family of transcription factors[29], and its epigenetic silencing has also been observed in some tumor types, including colon cancer[30]. A recent study found that PAX8 hypermethylation accelerated gastrointestinal stromal tumor progression by downregulating Wnt4 expression[31]. Anglim *et al*[32] reported a panel of eight hypermethylated genes containing PAX8, which showed high sensitivity and specificity for the early detection of squamous cell lung cancer.

To date, there have been various methods for detecting abnormal DNA methylation[33,34]. MSP is a simple, rapid and inexpensive method, but is not capable of pattern recognition and identification of CpG sites outside the methylation-specific primers. Bisulfite sequencing was once considered the gold standard for DNA methylation determination. The disadvantage lies in its tedious and time-consuming procedure, and a minimum number of 10-20 clones are required to detect interindividual variabilities in DNA methylation. Methylation-sensitive high-resolution melting is a relatively new technique for methylation assessment based on post-PCR melting curve analysis. It gives a range of methylation estimates rather than a single value, being mainly suitable for large sample screening[35]. MethyLight is a sensitive, high-throughput methylation assay that was developed based on MSP, while the major disadvantage is the high cost of a TaqMan probe[36,37]. In our study, biomarker validation was performed using PSQ, which overcomes the defects of the above methods, combining the measurement

of multiple methylation biomarkers with high throughput in a single test[38]. Therefore, PSQ has been suggested as the new gold standard test for methylation detection. The results of PSQ confirmed that the three biomarkers by TBSeq were reliable and feasible.

By logistic regression analysis, a three-DMS panel was developed in this study and was proven more effective than a single biomarker for ECC screening. We further found that the combined detection of the sDNA panel and FIT was characterized by a relative increase in diagnostic performance, which was successfully validated in an independent test set, as well as in the combined dataset. Actually, many attempts at CRC early screening in the Chinese population have been made, but none have gained wide acceptance[12]. Liu *et al*[39] developed an sDNA methylation panel, including COL4A2 and TLX2, which showed a high sensitivity of 91% for advanced-stage CRC detection with 97% specificity, but the performance for early-stage CRC was significantly weakened, with a sensitivity of 52% and specificity of 86%. In the study by Zhang *et al*[40], an sDNA panel that examined SFRP2 and WIF-1 promoter methylation was identified, and the sensitivities for detecting stage I and II CRC were 55% and 80%, respectively. Recently, another novel multidimensional assay combining FIT, sDNA mutation, methylation and intestinal bacteria analysis was reported by Mo *et al*[41]. It displayed the highest sensitivity of 91.89% in stage III CRC, whereas the sensitivity for stage I-II CRC was relatively low (76.27%). Comparatively, the sensitivity, specificity and AUC of our multiplex stool-based assay for detecting ECC reached 80.0%, 93.6% and 0.918, respectively, showing a promising prospect for practical application.

The effect of covariates on test performance was also investigated. It has been suggested that the conventional screening modalities, including colonoscopy and FIT, seem less sensitive for proximal than distal colon neoplasms[42,43]. In this study, our stool multiplex assay showed comparable efficacy for the detection of both proximal and distal ECC, which was consistent with the previous finding by Imperiale *et al*[13]. Given this performance characteristic, the sDNA test has the potential to improve the screening efficiency for neoplasms throughout the colon, and would be a valuable complement to colonoscopy as an interval test. Furthermore, we found that the sensitivity of this stool multiplex assay for ECC did not vary significantly according to age, sex, histological differentiation or tumor stage, but was significantly higher at T4 stage. Further studies are needed to determine their association and causality. In addition, some studies revealed that the sDNA test sensitivity increased as the tumor size increased[13,41]. Unfortunately, this variable was not included in our study.

The major strength of our study was the training and test set design involving blinded assays in the laboratory, which provided objective data to assess the test performance. The limitations of this study should also be mentioned. First, these analyses were based on data obtained from a single institution in China, and the sample size was relatively small. Second, other factors not included in this study could not be examined for confounding effects. As a result, a large-scale, prospective multicenter study is warranted to further confirm the value of our assay.

CONCLUSION

In conclusion, we developed and validated a novel multiplex stool-based assay combining sDNA methylation biomarkers and FIT, which could detect ECC with high accuracy throughout the colon.

ARTICLE HIGHLIGHTS

Research background

Colorectal cancer (CRC) is one of the most prevalent malignancies in China with an increasing ratio of colon to rectal cancer over the decades. Early screening is the key to reducing this burden. The traditional screening methods, including colonoscopy, fecal immunochemical test (FIT) and serum carcinoembryonic antigen (CEA), have reached a bottleneck, especially for early-stage colon cancer (ECC) due to its occult onset. Thus, precision and effective non-invasive biomarkers are highly desirable.

Research motivation

Detection of aberrant methylated DNA in stool has been proven to be a promising noninvasive method for the early diagnosis of CRC. However, the reported screening efficacy of the same biomarker varied across different studies. Moreover, effective biomarkers for detecting ECC are scarce, especially in the Chinese population.

Research objectives

The objective of our study was to identify a novel assay based on stool DNA (sDNA) methylation biomarkers which could improve the effectiveness of ECC screening. We also investigated the influence of clinicopathologic covariates on test performance.

Research methods

We performed a blinded, single-center, case-control study using archived stool samples from 125 ECC patients and 125 individuals with normal colonoscopy (controls); the subjects were randomly assigned to a training or test set at a 1.5:1 ratio. Targeted bisulfite sequencing (TBSeq) was performed on five pairs of preoperative and postoperative sDNA samples from ECC patients to identify DNA methylation biomarkers. Pyrosequencing (PSQ) was used for validation of the candidate biomarkers in large samples. A stepwise logistic regression analysis was applied to the data of the training set to develop a multiplex stool-based assay. The detection performance was further evaluated in the test set and combined set. In addition, the association of detection sensitivity with clinicopathologic covariates were analyzed by χ^2 test.

Research results

Through TBSeq, the three top hypermethylated genes, paired box 8, Ras-association domain family 1 and secreted frizzled-related protein 2, that were involved in the important cancer pathways were selected as biomarkers. Based on the PSQ results, an sDNA panel containing the three biomarkers was developed by logistic regression modelling. Receiver operating characteristic (ROC) analysis showed that this panel offered an advantage over any single biomarker, FIT or serum CEA in the detection of ECC. Further analysis revealed that the inclusion of FIT could effectively improve the detection accuracy. In the combined set, the sensitivity, specificity and area under the ROC curve for the sDNA panel combining FIT reached 80.0%, 93.6% and 0.918, respectively. Moreover, this multiplex assay maintained excellent performance in the subgroup by tumor stage. Additionally, we found that the detection sensitivity of the multiplex assay was significantly higher in T4 than in T1-3 stage tumors (P = 0.041), but was not affected by tumor site, tumor stage, histological differentiation, age or sex.

Research conclusions

The present study identified a novel multiplex stool-based assay, including three sDNA methylation biomarkers and FIT, capable of detecting ECC with high sensitivity and specificity. Importantly, the detection rate by this assay was related to T stage but not tumor site, tumor stage, histological differentiation, *etc*.

Research perspectives

Our study provided a new and promising approach for improvement of ECC screening in the Chinese population. Further demonstrations on a large-scale, prospective multicenter study are needed to conclusively evaluate its value.

FOOTNOTES

Author contributions: Jiang HH, Xing SW and Lin K performed the experiments; Tang X, Chen Y, and Lin K participated to the collection of the clinical data and samples; Jiang HH, He LW, and Tang EJ analyzed and interpreted the data; Tang EJ, Lin MB and He LW conceived and managed the study; Jiang HH and Xing SW drafted the manuscript; and all authors have read and approve the final manuscript.

Supported by Shanghai Pujiang Program, No. 21PJD066; Shanghai Municipal Commission of Health and Family Planning, No. ZK2019A19; Shanghai Municipal Science and Technology Commission, No. 19411971500; and Shanghai Yangpu District Science and Technology Commission, No. YPM202101.

Institutional review board statement: This study was reviewed and approved by the Ethics Committee of Yangpu Hospital, Tongji University (LL-2018-SCI-003).

Clinical trial registration statement: This study was registered at the Chinese Clinical Trial Registry (ChiCTR1800019552).

Informed consent statement: All study participants or their legal guardian provided informed written consent about personal and medical data collection prior to study enrolment.

Conflict-of-interest statement: The authors have no conflicts of interest to declare.

Data sharing statement: No additional data are available.

Country/Territory of origin: China

ORCID number: Hui-Hong Jiang 0000-0002-7391-1767; Si-Wei Xing 0000-0002-7222-1043; Xuan Tang 0000-0002-5895-3467; Ying Chen 0000-0001-5084-7507; Kang Lin 0000-0002-3485-6574; Lu-Wei He 0000-0001-6564-848X; Mou-Bin Lin 0000-0002-0686-688X; Er-Jiang Tang 0000-0002-8042-5994.

S-Editor: Wang JJ
L-Editor: A
P-Editor: Wang JJ

REFERENCES

1 **Cao W**, Chen HD, Yu YW, Li N, Chen WQ. Changing profiles of cancer burden worldwide and in China: a secondary analysis of the global cancer statistics 2020. *Chin Med J (Engl)* 2021; **134**: 783-791 [PMID: 33734139 DOI: 10.1097/CM9.0000000000001474]
2 **Zhang L**, Cao F, Zhang G, Shi L, Chen S, Zhang Z, Zhi W, Ma T. Trends in and Predictions of Colorectal Cancer Incidence and Mortality in China From 1990 to 2025. *Front Oncol* 2019; **9**: 98 [PMID: 30847304 DOI: 10.3389/fonc.2019.00098]
3 **Levin TR**, Corley DA, Jensen CD, Schottinger JE, Quinn VP, Zauber AG, Lee JK, Zhao WK, Udaltsova N, Ghai NR, Lee AT, Quesenberry CP, Fireman BH, Doubeni CA. Effects of Organized Colorectal Cancer Screening on Cancer Incidence and Mortality in a Large Community-Based Population. *Gastroenterology* 2018; **155**: 1383-1391.e5 [PMID: 30031768 DOI: 10.1053/j.gastro.2018.07.017]
4 **Harrison NM**, Hjelkrem MC. Bowel cleansing before colonoscopy: Balancing efficacy, safety, cost and patient tolerance. *World J Gastrointest Endosc* 2016; **8**: 4-12 [PMID: 26788258 DOI: 10.4253/wjge.v8.i1.4]
5 **Lou S**, Shaukat A. Noninvasive strategies for colorectal cancer screening: opportunities and limitations. *Curr Opin Gastroenterol* 2021; **37**: 44-51 [PMID: 33074994 DOI: 10.1097/MOG.0000000000000688]
6 **Bailey JR**, Aggarwal A, Imperiale TF. Colorectal Cancer Screening: Stool DNA and Other Noninvasive Modalities. *Gut Liver* 2016; **10**: 204-211 [PMID: 26934885 DOI: 10.5009/gnl15420]
7 **Hong SN**. Genetic and epigenetic alterations of colorectal cancer. *Intest Res* 2018; **16**: 327-337 [PMID: 30090031 DOI: 10.5217/ir.2018.16.3.327]
8 **Ewing I**, Hurley JJ, Josephides E, Millar A. The molecular genetics of colorectal cancer. *Frontline Gastroenterol* 2014; **5**: 26-30 [PMID: 24416503 DOI: 10.1136/flgastro-2013-100329]
9 **Boynton KA**, Summerhayes IC, Ahlquist DA, Shuber AP. DNA integrity as a potential marker for stool-based detection of colorectal cancer. *Clin Chem* 2003; **49**: 1058-1065 [PMID: 12816901 DOI: 10.1373/49.7.1058]
10 **Ahlquist DA**. Molecular detection of colorectal neoplasia. *Gastroenterology* 2010; **138**: 2127-2139 [PMID: 20420950 DOI: 10.1053/j.gastro.2010.01.055]
11 **Tse JWT**, Jenkins LJ, Chionh F, Mariadason JM. Aberrant DNA Methylation in Colorectal Cancer: What Should We Target? *Trends Cancer* 2017; **3**: 698-712 [PMID: 28958388 DOI: 10.1016/j.trecan.2017.08.003]
12 **Raut JR**, Guan Z, Schrotz-King P, Brenner H. Fecal DNA methylation markers for detecting stages of colorectal cancer and its precursors: a systematic review. *Clin Epigenetics* 2020; **12**: 122 [PMID: 32778176 DOI: 10.1186/s13148-020-00904-7]
13 **Imperiale TF**, Ransohoff DF, Itzkowitz SH, Levin TR, Lavin P, Lidgard GP, Ahlquist DA, Berger BM. Multitarget stool DNA testing for colorectal-cancer screening. *N Engl J Med* 2014; **370**: 1287-1297 [PMID: 24645800 DOI: 10.1056/NEJMoa1311194]
14 **Jin H**, Wang J, Zhang C. The Value of Multi-targeted Fecal DNA Methylation Detection for Colorectal Cancer Screening in a Chinese Population. *J Cancer* 2021; **12**: 1644-1650 [PMID: 33613751 DOI: 10.7150/jca.47214]
15 **Kim MS**, Lee J, Sidransky D. DNA methylation markers in colorectal cancer. *Cancer Metastasis Rev* 2010; **29**: 181-206 [PMID: 20135198 DOI: 10.1007/s10555-010-9207-6]
16 **Lee EJ**, Luo J, Wilson JM, Shi H. Analyzing the cancer methylome through targeted bisulfite sequencing. *Cancer Lett* 2013; **340**: 171-178 [PMID: 23200671 DOI: 10.1016/j.canlet.2012.10.040]
17 **Morselli M**, Farrell C, Rubbi L, Fehling HL, Henkhaus R, Pellegrini M. Targeted bisulfite sequencing for biomarker discovery. *Methods* 2021; **187**: 13-27 [PMID: 32755621 DOI: 10.1016/j.ymeth.2020.07.006]
18 **Jones PA**. Functions of DNA methylation: islands, start sites, gene bodies and beyond. *Nat Rev Genet* 2012; **13**: 484-492 [PMID: 22641018 DOI: 10.1038/nrg3230]
19 **Delaney C**, Garg SK, Yung R. Analysis of DNA Methylation by Pyrosequencing. *Methods Mol Biol* 2015; **1343**: 249-264 [PMID: 26420722 DOI: 10.1007/978-1-4939-2963-4_19]
20 **LaValley MP**. Logistic regression. *Circulation* 2008; **117**: 2395-2399 [PMID: 18458181 DOI: 10.1161/CIRCULATIONAHA.106.682658]
21 **Jolliffe IT**, Cadima J. Principal component analysis: a review and recent developments. *Philos Trans A Math Phys Eng Sci* 2016; **374**: 20150202 [PMID: 26953178 DOI: 10.1098/rsta.2015.0202]
22 **Zhang H**, Meltzer P, Davis S. RCircos: an R package for Circos 2D track plots. *BMC Bioinformatics* 2013; **14**: 244 [PMID: 23937229 DOI: 10.1186/1471-2105-14-244]
23 **Yu G**, Wang LG, Han Y, He QY. clusterProfiler: an R package for comparing biological themes among gene clusters. *OMICS* 2012; **16**: 284-287 [PMID: 22455463 DOI: 10.1089/omi.2011.0118]
24 **Ahlquist DA**. Multi-target stool DNA test: a new high bar for noninvasive screening. *Dig Dis Sci* 2015; **60**: 623-633 [PMID: 25492503 DOI: 10.1007/s10620-014-3451-5]

25 **Verma M**, Kumar V. Epigenetic Biomarkers in Colorectal Cancer. *Mol Diagn Ther* 2017; **21**: 153-165 [PMID: 27878475 DOI: 10.1007/s40291-016-0244-x]

26 **Toyota M**, Yamamoto E. DNA methylation changes in cancer. *Prog Mol Biol Transl Sci* 2011; **101**: 447-457 [PMID: 21507361 DOI: 10.1016/B978-0-12-387685-0.00014-7]

27 **Strzelczyk JK**, Krakowczyk Ł, Owczarek AJ. Methylation status of SFRP1, SFRP2, RASSF1A, RARβ and DAPK1 genes in patients with oral squamous cell carcinoma. *Arch Oral Biol* 2019; **98**: 265-272 [PMID: 30576962 DOI: 10.1016/j.archoralbio.2018.12.001]

28 **Rasmussen SL**, Krarup HB, Sunesen KG, Pedersen IS, Madsen PH, Thorlacius-Ussing O. Hypermethylated DNA as a biomarker for colorectal cancer: a systematic review. *Colorectal Dis* 2016; **18**: 549-561 [PMID: 26998585 DOI: 10.1111/codi.13336]

29 **Laury AR**, Perets R, Piao H, Krane JF, Barletta JA, French C, Chirieac LR, Lis R, Loda M, Hornick JL, Drapkin R, Hirsch MS. A comprehensive analysis of PAX8 expression in human epithelial tumors. *Am J Surg Pathol* 2011; **35**: 816-826 [PMID: 21552115 DOI: 10.1097/PAS.0b013e318216c112]

30 **Ehrich M**, Turner J, Gibbs P, Lipton L, Giovanneti M, Cantor C, van den Boom D. Cytosine methylation profiling of cancer cell lines. *Proc Natl Acad Sci U S A* 2008; **105**: 4844-4849 [PMID: 18353987 DOI: 10.1073/pnas.0712251105]

31 **Miao Z**, Wu F, Wei H, Luo Z, Wu K, Zhang J. Enhancer of zeste homolog 2-mediated paired box 8 methylation promotes gastrointestinal stromal tumor progression through Wnt4 downregulation. *Cancer Gene Ther* 2021; **28**: 1162-1174 [PMID: 33479444 DOI: 10.1038/s41417-020-00266-5]

32 **Anglim PP**, Galler JS, Koss MN, Hagen JA, Turla S, Campan M, Weisenberger DJ, Laird PW, Siegmund KD, Laird-Offringa IA. Identification of a panel of sensitive and specific DNA methylation markers for squamous cell lung cancer. *Mol Cancer* 2008; **7**: 62 [PMID: 18616821 DOI: 10.1186/1476-4598-7-62]

33 **Hernández HG**, Tse MY, Pang SC, Arboleda H, Forero DA. Optimizing methodologies for PCR-based DNA methylation analysis. *Biotechniques* 2013; **55**: 181-197 [PMID: 24107250 DOI: 10.2144/000114087]

34 **Wani K**, Aldape KD. PCR Techniques in Characterizing DNA Methylation. *Methods Mol Biol* 2016; **1392**: 177-186 [PMID: 26843056 DOI: 10.1007/978-1-4939-3360-0_16]

35 **Akika R**, Awada Z, Mogharbil N, Zgheib NK. Region of interest methylation analysis: a comparison of MSP with MS-HRM and direct BSP. *Mol Biol Rep* 2017; **44**: 295-305 [PMID: 28676996 DOI: 10.1007/s11033-017-4110-7]

36 **Šestáková Š**, Šálek C, Remešová H. DNA Methylation Validation Methods: a Coherent Review with Practical Comparison. *Biol Proced Online* 2019; **21**: 19 [PMID: 31582911 DOI: 10.1186/s12575-019-0107-z]

37 **Umer M**, Herceg Z. Deciphering the epigenetic code: an overview of DNA methylation analysis methods. *Antioxid Redox Signal* 2013; **18**: 1972-1986 [PMID: 23121567 DOI: 10.1089/ars.2012.4923]

38 **Poulin M**, Zhou JY, Yan L, Shioda T. Pyrosequencing Methylation Analysis. *Methods Mol Biol* 2018; **1856**: 283-296 [PMID: 30178259 DOI: 10.1007/978-1-4939-8751-1_17]

39 **Liu X**, Wen J, Li C, Wang H, Wang J, Zou H. High-Yield Methylation Markers for Stool-Based Detection of Colorectal Cancer. *Dig Dis Sci* 2020; **65**: 1710-1719 [PMID: 31720923 DOI: 10.1007/s10620-019-05908-9]

40 **Zhang H**, Zhu YQ, Wu YQ, Zhang P, Qi J. Detection of promoter hypermethylation of Wnt antagonist genes in fecal samples for diagnosis of early colorectal cancer. *World J Gastroenterol* 2014; **20**: 6329-6335 [PMID: 24876755 DOI: 10.3748/wjg.v20.i20.6329]

41 **Mo S**, Wang H, Han L, Xiang W, Dai W, Zhao P, Pei F, Su Z, Ma C, Li Q, Wang Z, Cai S, Liu R, Cai G. Fecal Multidimensional Assay for Non-Invasive Detection of Colorectal Cancer: Fecal Immunochemical Test, Stool DNA Mutation, Methylation, and Intestinal Bacteria Analysis. *Front Oncol* 2021; **11**: 643136 [PMID: 33718241 DOI: 10.3389/fonc.2021.643136]

42 **Morikawa T**, Kato J, Yamaji Y, Wada R, Mitsushima T, Shiratori Y. A comparison of the immunochemical fecal occult blood test and total colonoscopy in the asymptomatic population. *Gastroenterology* 2005; **129**: 422-428 [PMID: 16083699 DOI: 10.1016/j.gastro.2005.05.056]

43 **Brenner H**, Chang-Claude J, Seiler CM, Rickert A, Hoffmeister M. Protection from colorectal cancer after colonoscopy: a population-based, case-control study. *Ann Intern Med* 2011; **154**: 22-30 [PMID: 21200035 DOI: 10.7326/0003-4819-154-1-201101040-00004]

World Journal of Gastroenterology

Submit a Manuscript: https://www.f6publishing.com

World J Gastroenterol 2022 June 28; 28(24): 2721-2732

DOI: 10.3748/wjg.v28.i24.2721

ISSN 1007-9327 (print) ISSN 2219-2840 (online)

ORIGINAL ARTICLE

Retrospective Cohort Study

Utility of a deep learning model and a clinical model for predicting bleeding after endoscopic submucosal dissection in patients with early gastric cancer

Ji Eun Na, Yeong Chan Lee, Tae Jun Kim, Hyuk Lee, Hong-Hee Won, Yang Won Min, Byung-Hoon Min, Jun Haeng Lee, Poong-Lyul Rhee, Jae J Kim

Specialty type: Gastroenterology and hepatology

Provenance and peer review: Unsolicited article; Externally peer reviewed.

Peer-review model: Single blind

Peer-review report's scientific quality classification

Grade A (Excellent): 0
Grade B (Very good): B, B
Grade C (Good): C
Grade D (Fair): 0
Grade E (Poor): 0

P-Reviewer: Pattarajierapan S, Thailand; Singh A, India; Sulbaran MN, Brazil

Received: October 30, 2021
Peer-review started: October 30, 2021
First decision: March 11, 2022
Revised: March 25, 2022
Accepted: May 8, 2022
Article in press: May 8, 2022
Published online: June 28, 2022

Ji Eun Na, Department of Internal Medicine, Inje University Haeundae Paik Hospital, Busan 48108, South Korea

Ji Eun Na, Tae Jun Kim, Hyuk Lee, Yang Won Min, Byung-Hoon Min, Jun Haeng Lee, Poong-Lyul Rhee, Jae J Kim, Department of Medicine, Samsung Medical Center, Sungkyunkwan University School of Medicine, Seoul 06351, South Korea

Yeong Chan Lee, Hong-Hee Won, Department of Digital Health, Samsung Advanced Institute for Health Science and Technology, Sungkyunkwan University, Seoul 06351, South Korea

Corresponding author: Hyuk Lee, MD, PhD, Doctor, Department of Medicine, Samsung Medical Center, Sungkyunkwan University School of Medicine, 81 Irwon-ro, Gangnam-gu, Seoul 06351, South Korea. leehyuk@skku.edu

Abstract

BACKGROUND

Bleeding is one of the major complications after endoscopic submucosal dissection (ESD) in early gastric cancer (EGC) patients. There are limited studies on estimating the bleeding risk after ESD using an artificial intelligence system.

AIM

To derivate and verify the performance of the deep learning model and the clinical model for predicting bleeding risk after ESD in EGC patients.

METHODS

Patients with EGC who underwent ESD between January 2010 and June 2020 at the Samsung Medical Center were enrolled, and post-ESD bleeding (PEB) was investigated retrospectively. We split the entire cohort into a development set (80%) and a validation set (20%). The deep learning and clinical model were built on the development set and tested in the validation set. The performance of the deep learning model and the clinical model were compared using the area under the curve and the stratification of bleeding risk after ESD.

RESULTS

A total of 5629 patients were included, and PEB occurred in 325 patients. The area

under the curve for predicting PEB was 0.71 (95% confidence interval: 0.63-0.78) in the deep learning model and 0.70 (95% confidence interval: 0.62-0.77) in the clinical model, without significant difference (P = 0.730). The patients expected to the low- (< 5%), intermediate- (≥ 5%, < 9%), and high-risk (≥ 9%) categories were observed with actual bleeding rate of 2.2%, 3.9%, and 11.6%, respectively, in the deep learning model; 4.0%, 8.8%, and 18.2%, respectively, in the clinical model.

CONCLUSION

A deep learning model can predict and stratify the bleeding risk after ESD in patients with EGC.

Key Words: Clinical model; Deep learning model; Post-endoscopic submucosal dissection bleeding; Stratification of bleeding risk

Core Tip: Bleeding is one of the major complications after endoscopic submucosal dissection (ESD) in early gastric cancer patients and requires hospital-based intervention. We established a deep learning model to stratify the bleeding risk after ESD and demonstrated its performance compared with a clinical model. The deep learning model showed acceptable area under the curve and could stratify the post-ESD bleeding risk as low-, intermediate-, and high-risk categories, which correlated with actual bleeding rate comparatively. A deep learning model would be valuable in assessing the bleeding risk after ESD in early gastric cancer patients.

Citation: Na JE, Lee YC, Kim TJ, Lee H, Won HH, Min YW, Min BH, Lee JH, Rhee PL, Kim JJ. Utility of a deep learning model and a clinical model for predicting bleeding after endoscopic submucosal dissection in patients with early gastric cancer. *World J Gastroenterol* 2022; 28(24): 2721-2732
URL: https://www.wjgnet.com/1007-9327/full/v28/i24/2721.htm
DOI: https://dx.doi.org/10.3748/wjg.v28.i24.2721

INTRODUCTION

In South Korea, gastric cancer has a high incidence and is the second most common malignancy and the fourth most common cause of cancer-related mortality[1]. After the advent of screening programs for gastric cancer in South Korea and Japan, up to 50%–70% of cases with gastric cancers have been diagnosed at an early stage[2-4]. With the increasing rate of diagnosis at early stages, endoscopic submucosal dissection (ESD) is being actively applied for the minimally invasive treatment of early gastric cancer (EGC) without suspicion of regional lymph node metastasis[5,6].

In accordance with the current trend of active use of ESD, it is necessary to pay attention to the post-ESD complications. Bleeding is one of the significant complications, with an incidence of 3.6%–6.9%[7, 8]. Because bleeding after ESD requires hospitalization and hemostatic interventions, there is a need to predict patients at a high risk of bleeding after ESD. Therefore, there have been reports on risk factors related to bleeding after ESD[9-12]. Recently, a predictive risk-scoring model for bleeding after ESD was proposed in Japan; this tool is expected to raise awareness regarding the potential bleeding sources and thus, help physicians manage patients with EGC who are treated with ESD[13].

Currently, artificial intelligence systems are being applied in various fields of gastroenterology[14]. The machine learning models showed good performance in the triage of necessity for intervention in patients with upper gastrointestinal bleeding and predicting recurrent ulcer bleeding[15,16]. Deep learning is advantageous over the machine learning model among artificial intelligence systems; its performance is optimized by automatic learning while experiencing various cases. It can integrate and interpret multiple factors simultaneously without external intervention. Hence, the automatically trained deep learning model can generalize well. There has been no study on the efficacy of deep learning for predicting post-ESD bleeding (PEB), and no study has compared these systems with a clinical model.

This study aimed to develop and compare the performance of the deep learning and clinical model for predicting PEB in EGC patients. We chose deep learning among the artificial intelligence systems as a sophisticated algorithm.

MATERIALS AND METHODS

Patients

Patients who underwent ESD for EGC between January 2010 and June 2020 at the Samsung Medical Center, Seoul, South Korea, were screened retrospectively. We excluded cases with: Failure to complete ESD (n = 1); prior gastrectomy (n = 2); additional gastrectomy within 28 d after ESD (n = 497); no residual tumor in the ESD specimen (n = 48); multiple procedures, such as EMR for other benign lesions and ESD for EGC (n = 46); and missing values for important variables (n = 7) (Figure 1). A total of 5629 patients were included in the analysis, and they were randomly categorized into the development set (80%) and the validation set (20%). The Institutional Review Board of the Samsung Medical Center, Korea, approved this study, and the requirement for obtaining informed consent was waived owing to the study's retrospective nature.

Outcome, data sources, study variables, and definitions

The main outcome included the development of a deep learning model and a clinical model that predict the bleeding after ESD in patients with EGC and the comparison of performance between the deep learning model and the clinical model.

The variables used to build the deep learning and clinical models were collected from the medical records retrospectively based on the date of ESD. These variables included: Age; sex; comorbidities such as hypertension, diabetes mellitus, liver cirrhosis, and chronic kidney disease (estimated glomerular filtration rate < 60 mL/min per 1.73 m^2); patient management with antithrombotic agents (ATs) [aspirin, P2Y12 receptor agonist (P2Y12RA), warfarin, direct-acting oral anticoagulants (DOAC), and cilostazol], non-steroidal anti-inflammatory drugs (NSAIDs), interruption of ATs, replacement of antiplatelet agents (APA), and heparin bridging; tumor characteristics (single or multiple lesions, location, pathologic size, type of differentiation); piecemeal resection; and laboratory data (albumin level and international normalized ratio).

Bleeding after ESD was defined as the presence of signs of bleeding (melena, hematemesis, or a decrease in the hemoglobin level by > 2 g/dL) along with endoscopic stigmata of recent bleeding, such as Forrest class Ia, Ib, IIa, and IIb, within 28 d after ESD. Interruption of ATs was defined as the discontinuation of these medications before the procedure, according to the recommended duration. Replacement of APA was described as when the procedure was performed with aspirin or cilostazol alone in patients who were receiving multiple APAs. Heparin bridging was defined as the administration of heparin during the period between the discontinuation and resumption of anticoagulants. A hemoglobin reduction of > 2 g/dL was evaluated by calculating the differences in the hemoglobin levels between the day before and after ESD.

Development of the deep learning and clinical models

We built a deep learning model and a clinical model based on the development set, which comprised 80% of the overall cohort. Subsequently, we validated the deep learning and clinical models in the validation set, which comprised 20% of the overall cohort. The categorical variables were converted using one-hot encoding, and the continuous variables were normalized, as preprocessing. We built the deep learning model as follows: First, we augmented the development set using the borderline synthetic minority over-sampling technique to overcome the imbalance of the dataset. Synthetic data were generated from 5%–100% of the majority class. Second, we constructed the deep learning model using automated machine learning, called Keras Tuner, to tune hyperparameters automatically. The initial architecture of the model was configured similarly to a transformer based on the attention mechanism [17]. Then, we set the number of neurons as a hyperparameter variable, ranging from 12 to 24, in four dense layers. The learning rate was also set to a range from 1e-2 − to 1e-4 −. The combination of hyperparameters was determined using Bayesian optimization. Finally, we evaluated the performance in the validation set using a model tuned with the 20% of synthetic data of the majority class. The optimal units of dense layers were selected to 24. The optimal number of attention head was chosen to 16. The architecture is depicted in Supplementary Figure 1. The optimal learning rate with Adam optimizer was 1e-3.

Multivariable logistic regression analysis was performed in the development set to build the clinical model. Then, the clinical model was constructed as a formula with the sum of the beta coefficient values of significant factors with a P value of < 0.05.

The calculated value from the deep learning and clinical models was multiplied by 1000 and converted as a score. The score that indicated the risk probability was divided by the decile in the development set. We selected cutoff to discriminate the risk categories as low-, intermediate-, and high-risk at a bleeding rate of < 5% and < 9% in the development set referred to in a previous report[13]. Decile 1st to 4th was allocated to low risk, 5th to 8th to intermediate risk, and 9th to 10th to high-risk category. Link to the deep learning and clinical models: https:// github.com/YeongChanLee/Predict-PEB.

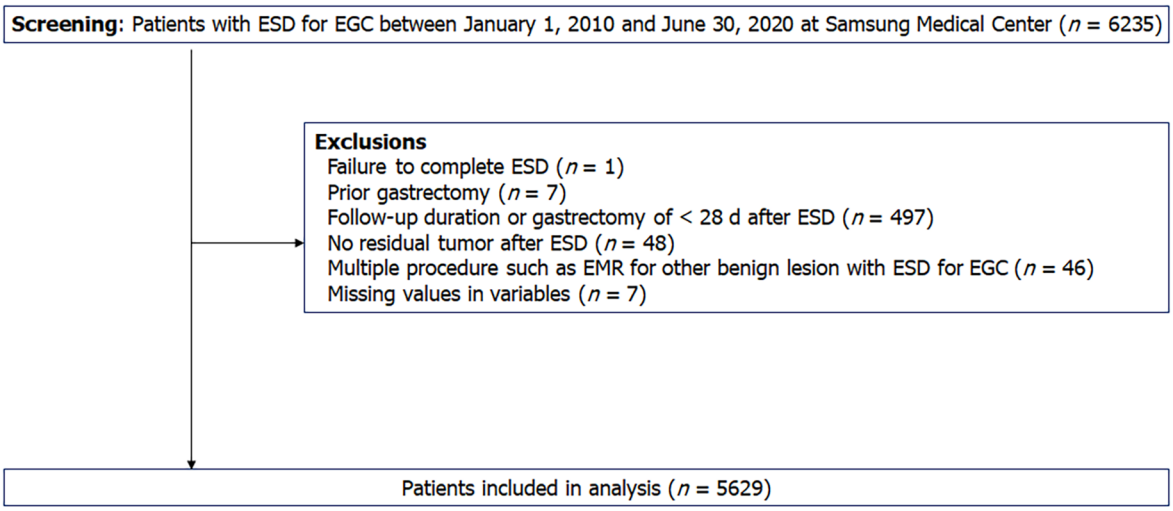

DOI: 10.3748/wjg.v28.i24.2721

Figure 1 Patient flowchart. EGC: Early gastric cancer; ESD: Endoscopic submucosal dissection.

Statistical analysis

Descriptive statistics for continuous and categorical variables are presented as means (standard deviation) and frequencies (%). The deep learning model and the clinical model for prediction of bleeding after ESD were evaluated using two methods. First, sensitivity, specificity, positive predictive value (PPV), negative predictive value (NPV), and receiver operating characteristic area (ROC) curve along with the area under the curve (AUC) were analyzed. The performance with AUC was compared using the bootstrap test. Second, the risk stratification of PEB based on the development set was applied to the validation set and compared with the actual bleeding rate in the validation set. For example, if the score of calculated cases belongs to the high-risk category, we verified that the real bleeding rate was in the predicted range of 9% or higher. The predictors for PEB were identified with multivariable logistic regression analysis in the entire cohort and development set. Model development for deep learning was performed using Tensor Flow 2.4.0, and Python 3.8.5. statistical analyses were performed using the R software (version 3.5.1, Vienna, Austria).

RESULTS

Baseline characteristics

Of the 5629 patients, 325 experienced post-ESD bleeding (PEB). The non-PEB and PEB groups were comparable in age, liver cirrhosis status, albumin level, international normalized ratio level, a proportion of aspirin or cilostazol use, undifferentiated tumor type, and piecemeal resection. The PEB group had a higher proportion of males and comorbidities (hypertension, diabetes mellitus, and chronic kidney disease) than the non-PEB group. P2Y12RA and anticoagulants (warfarin or DOAC) and the proportion of patients receiving replacement therapy or heparin bridging were higher in the PEB group than in the non-PEB group. The PEB group had a higher proportion of multiple tumors and middle location of tumors and larger size of tumors than the non-PEB group (Table 1). There was no difference in the baseline characteristics between the development and validation sets (Supplementary Table 1).

Predictors for bleeding after ESD

In the overall cohort, the independent predictors were identified as follows: Age [odds ratio (OR) = 0.98; 95% confidence interval (CI): 0.96–0.99; *P* value < 0.001], male (OR = 1.65; 95%CI: 1.19–2.28; *P* value = 0.003), hypertension (OR = 1.56; 95%CI: 1.19–2.03; p value = 0.001), chronic kidney disease (OR = 1.78; 95%CI: 1.18–2.70; *P* value = 0.006), P2Y12RA (OR = 2.40; 95%CI: 1.22–4.74; *P* value = 0.011), DOAC (OR = 4.31; 95%CI: 1.26–14.78; *P* value = 0.020), middle location (OR = 1.72; 95%CI: 1.07–2.74; *P* value = 0.024), and size (OR = 1.03; 95%CI: 1.02–1.04; *P* value < 0.001) (Supplementary Table 2).

In the development set, age (OR = 0.98; 95%CI: 0.96–0.99; *P* value = 0.001), male (OR = 1.54; 95%CI: 1.09–2.19; *P* value = 0.015), hypertension (OR = 1.35; 95%CI: 1.00–1.82; *P* value = 0.049), chronic kidney disease (OR = 1.78; 95%CI: 1.12–2.84; *P* value = 0.015), P2Y12RA (OR = 2.26; 95%CI: 1.05–4.88; *P* value = 0.037), middle location (OR = 1.97; 95%CI: 1.14–3.41; *P* value = 0.015), and size (OR = 1.04; 95%CI: 1.03–1.05; *P* value < 0.001) were identified as independent predictors. The clinical model was a formula described bottom of Table 2.

Table 1 Baseline characteristics of patients in entire cohort

Variable	Non-PEB, *n* = 5304	PEB, *n* = 325	*P* value[1]
Age[2]	64 ± 10	63 ± 11	0.065
Sex			0.001
Female	1245 (23.5)	49 (15.1)	
Male	4059 (76.5)	276 (84.9)	
Hypertension	1413 (26.6)	120 (36.9)	< 0.001
Diabetes mellitus	936 (17.6)	74 (22.8)	0.024
Liver cirrhosis	93 (1.8)	4 (1.2)	0.629
Chronic kidney disease	299 (5.6)	33 (10.2)	0.001
Aspirin	515 (9.7)	42 (12.9)	0.074
P2Y12RA	181 (3.4)	23 (7.1)	0.001
Warfarin	22 (0.4)	7 (2.2)	< 0.001
DOAC	31 (0.6)	6 (1.8)	0.017
Cilostazol	47 (0.9)	3 (0.9)	1.000
NSAIDs	28 (0.5)	3 (0.9)	0.583
Preprocedure management of AT			< 0.001
No indication	4605 (86.8)	264 (81.2)	
Interruption	676 (12.7)	53 (16.3)	
Replacement or heparin bridge	23 (0.4)	8 (2.5)	
Tumor			
Multiple	284 (5.4)	28 (8.6)	0.018
Location			< 0.001
Upper	433 (8.2)	22 (6.8)	
Middle	1728 (32.6)	157 (48.3)	
Lower	3143 (59.3)	146 (44.9)	
Size[2], mm	17 ± 10	21 ± 13	< 0.001
Undifferentiated type	125 (2.4)	7 (2.2)	0.963
Piecemeal resection	64 (1.2)	4 (1.2)	1.000
Laboratory data			
Albumin[2], g/dL	4.3 ± 0.3	4.4 ± 0.4	0.345
INR[2]	1.0 ± 0.1	1.0 ± 0.1	0.106

[1]*P* value calculated using Student's *t*-test for continuous variables or Pearson's chi-square test for categorical variables for overall data.
[2]mean ± SD presented for continuous variables.
Values are expressed as *n* (%) unless otherwise specified. AT: Antithrombotic; DOAC: Direct oral anticoagulant; INR: International normalized ratio; NSAIDs: Non-steroidal anti-inflammatory drugs; PEB: Post-endoscopic submucosal dissection bleeding; P2Y12RA: P2Y12 receptor antagonist.

Performance and comparison of deep learning model and clinical model

The deep learning model was found to have a sensitivity of 64.3%, specificity of 74.0%, PPV of 11.4%, NPV of 97.5%, and AUC of 0.71 (95%CI: 0.63–0.78). The clinical model had a sensitivity of 69.6%, specificity of 71.0%, PPV of 11.1%, NPV of 97.8%, and AUC of 0.70 (95%CI: 0.62–0.77) (Table 3 and Figure 2). There were no significant differences in the AUCs between the deep learning and clinical models (Table 3).

The score multiplied by 1000 to the derived value based on the deep learning and clinical models reflects the risk probability and was divided into deciles. The maximum cutoff was 35.9 in low risk, 57.5 in intermediate risk, and over the 57.5 was assigned to a high-risk category of the deep learning model based on development set (Table 4). In the clinical model, the maximum cutoff was 12.7 in low risk, 24.6

Table 2 Logistic regression analysis for predictors of bleeding after endoscopic submucosal dissection in development set

Variables		Multivariable			
		OR	95%CI	*P* value	ß regression coefficient
Age		0.98	0.96–0.99	0.001	-0.024
Sex	Female/male	1.54	1.09–2.19	0.015	0.435
Hypertension	No/yes	1.35	1.00–1.82	0.049	0.299
Diabetes mellitus	No/yes	1.27	0.92–1.75	0.145	0.238
Liver cirrhosis	No/yes	0.59	0.18–1.95	0.385	-0.532
Chronic kidney disease	No/yes	1.78	1.12–2.84	0.015	0.578
Aspirin	No/yes	1.51	0.62–3.69	0.363	0.414
P2Y12RA	No/yes	2.26	1.05–4.88	0.037	0.818
Warfarin	No/yes	1.51	0.28–8.07	0.629	0.413
DOAC	No/yes	3.24	0.76–13.82	0.113	1.174
Cilostazol	No/yes	1.35	0.35–5.18	0.662	0.300
NSAIDs	No/yes	2.65	0.77–9.14	0.124	0.973
Preprocedure management of AT	No indication	1			
	Interruption	0.63	0.24–1.67	0.353	-0.464
	Replacement orHeparin bridge	3.32	0.47–23.60	0.231	1.199
Multiple	No/yes	1.48	0.92–2.38	0.104	0.393
Location	Upper	1			
	Middle	1.97	1.14–3.41	0.015	0.680
	Lower	1.11	0.64–1.91	0.711	0.103
Size		1.04	1.03–1.05	< 0.001	0.036
Undifferentiated type	No/yes	0.56	0.20–1.57	0.271	-0.579
Piecemeal	No/yes	0.98	0.30–3.22	0.976	-0.019
Albumin, g/dL		1.33	0.89–2.00	0.168	0.286
INR		2.04	0.37–11.08	0.410	0.711

Clinical model = 1/[1 + exp(-1 × [-0.024 × Age in years + 0.435 × Sex (0: female, 1: male) + 0.299 × Hypertension (0: no, 1: yes) + 0.578 × Chronic kidney disease (0: no, yes: 1) + 0.818 × P2Y12RA (0: no, 1: yes) + 0.680 × Middle location (0: no, 1: yes) + 0.036 × Size in mm])]. AT: Antithrombotic; DOAC: Direct oral anticoagulant; ESD: Endoscopic submucosal dissection; INR: International normalized ratio; NSAIDs, Non-steroidal anti-inflammatory drugs; P2Y12RA: P2Y12 receptor antagonist; OR: Odds ratio; CI: Confidence interval.

in intermediate risk, and over 24.6 was considered a high-risk category based on development set (Table 4). In the validated set, the deep learning model showed an actual bleeding rate in low-, intermediate-, high-risk categories, respectively, of 2.2%, 3.9%, and 11.6%; the clinical model showed an actual bleeding rate of 4.0%, 8.8%, and 18.2%, respectively, in low-, intermediate-, high-risk categories (Table 4).

DISCUSSION

The deep learning and clinical models for predicting bleeding after ESD in patients with EGC showed good performance. We demonstrated that deep learning and clinical models could stratify the PEB risk, which correlated with actual bleeding rates. Hence, we suggest that the deep learning model can aid in the prediction of bleeding after ESD, in addition to the clinical model.

This study was the first to establish a deep learning model for predicting bleeding after ESD and demonstrate its performance compared to that of a clinical model. The strengths of this study were its large sample size and the relatively recent data from a single institution. In addition, we included all essential variables and sought the advantages of the deep learning model that can deal with extensive

Table 3 Utility of deep learning model and clinical model

	Deep learning model	Clinical model	*P* value
Sensitivity (%)	64.3 (45.8–84.1)	69.6 (54.2–80.8)	
Specificity (%)	74.0 (50.6–89.2)	71.0 (68.5–79.5)	
PPV (%)	11.4 (7.4–18.1)	11.1 (8.0–15.4)	
NPV (%)	97.5 (96.4–98.7)	97.8 (96.6–98.7)	
AUC (95%CI)	0.71 (0.63–0.78)	0.70 (0.62–0.77)	0.730

One thousand times for bootstrapping were conducted to measure 95% confidence intervals. *P* value for statistical significance between area under the curves was derived from Delong's test. AUC: Area under the curve; CI: Confidence interval; NPV: Negative predictive value; PPV: Positive predictive value.

Table 4 Decile of risk probability based on deep learning model and clinical model

Decile	Risk categories	Deep learning				Clinical model			
		Score[1]	Patients	Bleeding	Rate (%)	Score[1]	Patients	Bleeding	Rate (%)
Development set									
1	Low	25.7	451	11	2.4	8.4	451	12	2.6
2		29.1	451	15	3.3	12.2	451	15	3.3
3		32.5	451	6	1.3	12.4	451	12	2.6
4		35.9	450	17	3.8	12.7	450	20	4.4
5	Intermediate	40.2	450	27	6.0	14.8	450	34	7.6
6		45.3	450	29	6.4	16.6	450	15	3.3
7		50.8	450	36	8.0	23.3	450	24	5.3
8		57.5	450	24	5.3	24.6	450	32	7.1
9	High	67.2	450	41	9.1	31.0	450	54	12.0
10		197.0	450	63	14.0	122.0	450	51	11.3
Validation set									
	Low	35.9	411	9	2.2	12.7	956	38	4.0
	Intermediate	57.5	466	18	3.9	24.5	137	12	8.8
	High	147.0	249	29	11.6	155.0	33	6	18.2

[1]The score is calculated with probability multiplied by 1000 and presented as maximum cutoff in each decile.
Decile 1st to 4th: Low-risk category. Decile 5th to 8th: Intermediate-risk category. Decile 9th to 10th: High-risk category. The Cochran–Armitage test for trend was performed.

data and complex problems and improve its performance incrementally by automated learning. We included all types of ATs separately and clarified the distinction between patients without an indication for ATs, patients who received an interruption before the procedure, and patients who received replacement or heparin bridging.

Our study identified younger age, male sex, hypertension, chronic kidney disease, P2Y12RA use, DOAC use, middle tumor location, and tumor size as the predictors of PEB. Previous studies also reported that younger age was associated with PEB[18-20]. It is unclear why younger age was associated with PEB. Several reports proposed that atrophic change along with aging might relate to decreasing the vascularity on the mucosal and submucosal layers[18,20-23]. Although aging and changes in intestinal vasculature have not been clearly elucidated, a decrease in the volume of vasculature with aging was observed in animals[24]. Aspirin did not increase the PEB risk after discontinuation about 1 wk[25]. Although some reported that maintaining aspirin did not increase the PEB risk[25-28], a meta-analysis showed that aspirin was associated with increased bleeding risk, requiring clinical caution[29]. There is still controversial due to limited evidence for P2Y12R[9,13,20,30]. In comparison, an increased bleeding risk after ESD has been reported consistently in patients receiving dual antiplatelets. In addition, there

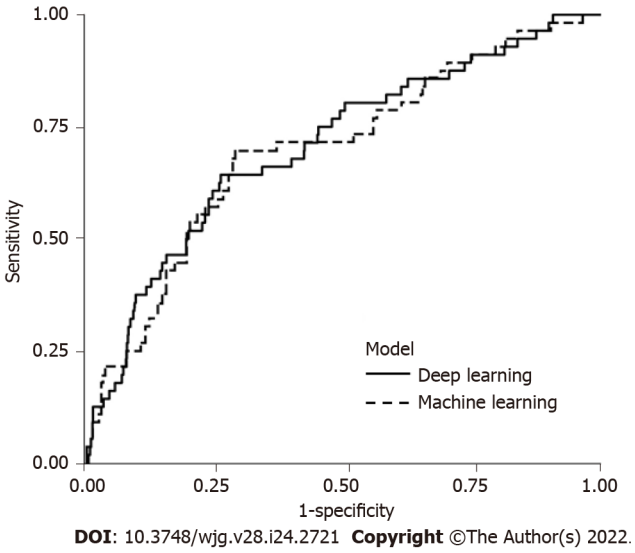

DOI: 10.3748/wjg.v28.i24.2721

Figure 2 Area under the curve for prediction of bleeding after endoscopic submucosal dissection in deep learning model and clinical model.

were reports that warfarin or DOAC are related to bleeding risk[13]; rather, some reported heparin bridging was associated with PEB risk[9,26]. The irony is that most of the patients who experience heparin bridging take warfarin or DOAC, but the results about each factor were inconsistent in previous retrospective studies. It is assumed that the duration of discontinuation and other individual factors might influence these results. In addition, it has been suggested that large size[8,19,20], CKD with hemodialysis[13,26,31], and long procedure time[20] were associated with bleeding after ESD. The upper location showed increased PEB risk[18,32]; in contrast, some others reported lower location related to increased PEB risk[18,32]; a recent meta-analysis did not prove significance according to the location[8].

Recently, a predictive risk-scoring model for PEB in Japan showed that CKD with hemodialysis, usage of aspirin, P2Y12RA, cilostazol, warfarin, DOAC, lower third tumor location, tumor size > 30 mm, and the presence of multiple tumors were the predictors of PEB, whereas interruption was a protective factor against PEB[13]. Another recent model proposed a simple algorithm including significant factors with continuous use of ATs, size ≥ 49 mm, and age < 62 years. We also found an association between P2Y12RA or DOAC usage and PEB; however, other ATs were not associated with PEB, and interruption and heparin bridging or replacement of APA were not identified as the protective factors. In our institution, ESD is classified as a high-risk procedure based on the national practice guidelines, and experts are consulted before ESD in patients receiving ATs. The expert assesses the thromboembolic risk depending on the underlying disease and recommends the possibility of interruption, duration of interruption, and the need for heparin bridging or replacement of APA[33-36]. Recently, a guideline published in South Korea also categorized ESD as an ultra-high-risk procedure and recommended interruption of ATs with heparin bridging or replacement of APA according to the thromboembolic risk [37].

The deep learning model in our study showed an AUC of 0.71, which was comparable to the AUC of 0.72 for a risk-scoring model in Japan[13] and the AUC of 0.70 for the clinical model in our study. In the validation set, predicted low-, intermediate-, and high-risk categories showed an actual bleeding rate of 2.2%, 3.9%, and 11.6%, respectively in the deep learning; 4.0%, 8.8%, and 18.2%, respectively, in the clinical model. Our study demonstrated that the deep learning and clinical models can stratify the bleeding risk after ESD. The predicted risk categories correlated with actual bleeding rate; even considering the actual bleeding rate was slightly lower than predicted range of ≥ 5% and < 9% (intermediate risk) in the deep learning and was close to upper range in the clinical model. Our findings support the clinical potential of the deep learning model for predicting PEB risk based on its comparable performance. Because bleeding after ESD requires intervention and hospitalization, physicians are concerned about the occurrence of PEB as a major complication. Based on the risk-prediction model, physicians could carefully assess the bleeding risk and perform preventive hemostasis during the procedure. Suppose additional management like the shielding method for preventing PEB in the selected high-risk group is attempted; in that case, it is anticipated that the deep learning model could support risk stratification.

Our study has several limitations. Due to its retrospective design, information such as the timing of the resumption of ATs, endoscopist's experience, defect size, and procedure duration was missing. Furthermore, our study was designed as a single-center study; hence, hospital-based validation in other hospitals was not performed, and further proof is warranted. However, the deep learning model might

be generalizable because it automatically identifies the risk or probability of bleeding without the external intervention of known relevant factors. Both the deep learning and clinical models showed a low PPV, which may be related to the low incidence of bleeding after ESD, even though bleeding is one of the major complications. In our cohort, the number of patients who received anticoagulants (warfarin or DOAC) was small; therefore, it is possible that the statistical significance of these variables was insufficient for establishing a clinical model in the development set. In this regard, despite the fact that our study focused on the development of a deep learning model and a clinical model, as well as the utility of the deep learning model, further accumulation of data and additional analysis will be required before the commencement of the clinical application of artificial intelligence systems.

CONCLUSION

In conclusion, we introduced a deep learning model to predict the risk of bleeding after ESD in patients with EGC. The model demonstrated its performance as comparable to the clinical model. The deep learning model could help physicians raise caution to the PEB and would be a desirable tool for supporting ESD application.

ARTICLE HIGHLIGHTS

Research background

With the increasing rate of diagnosis at early stages of gastric cancer, endoscopic submucosal dissection (ESD) is being actively applied as the minimally invasive treatment. Bleeding is one of the significant complications, with an incidence of 3.6%–6.9%. Because bleeding after ESD requires hospitalization and hemostatic interventions, there is a need to predict patients at a high risk of bleeding after ESD.

Research motivation

Currently, artificial intelligence systems are being applied in various fields of gastroenterology. Deep learning among artificial intelligence systems was automatically trained so that it could be generalized well. There has been no study on the efficacy of deep learning for predicting post-ESD bleeding (PEB), and no study has compared these systems with a clinical model.

Research objectives

This study aimed to develop and compare the performance of the deep learning and clinical model for predicting PEB in early gastric cancer (EGC) patients.

Research methods

Patients who underwent ESD for EGC between January 2010 and June 2020 at the Samsung Medical Center, Seoul, South Korea, were screened retrospectively. We built a deep learning model and a clinical model based on the development set, which comprised 80% of the overall cohort. Subsequently, we validated the deep learning and clinical models in the validation set, which comprised 20% of the overall cohort. The deep learning model and the clinical model for prediction of bleeding after ESD were evaluated using two methods. First, sensitivity, specificity, positive predictive value, negative predictive value, and receiver operating characteristic area curve along with the area under the curve (AUC) were analyzed. The performance with AUC was compared using the bootstrap test. Second, the risk stratification of PEB based on the development set was applied to the validation set and compared with the actual bleeding rate. The authors selected cutoff to discriminate the risk categories as low-, intermediate-, and high-risk at a bleeding rate of < 5% and < 9% in the development set referred to in a previous report.

Research results

Of the 5629 patients, 325 experienced PEB. The AUC for predicting PEB was 0.71 (95% confidence interval: 0.63-0.78) in the deep learning model and 0.70 (95% confidence interval: 0.62-0.77) in the clinical model, without significant difference (P = 0.730). In the validated set, the deep learning model showed an actual bleeding rate of 2.2%, 3.9%, and 11.6% in low-, intermediate-, high-risk categories, respectively; the clinical model showed an actual bleeding rate of 4.0%, 8.8%, and 18.2% in low-, intermediate-, high-risk categories, respectively.

Research conclusions

In conclusion, we introduced a deep learning model to predict the risk of bleeding after ESD in patients with EGC. The model demonstrated its performance as comparable to the clinical model.

Research perspectives

Based on the risk-prediction model, physicians could carefully assess the bleeding risk and perform preventive hemostasis during the procedure. Suppose additional management like the shielding method for preventing PEB in the selected high-risk group is attempted; in that case, it is anticipated that the deep learning model could support risk stratification.

FOOTNOTES

Author contributions: Na JE, Lee YC and Kim TJ contributed equally to this work as co-first authors of this paper; Na JE, Lee YC, Kim TJ, and Lee H contributed to the study concept and design, acquisition, analysis, or interpretation of data, and writing and drafting of the manuscript; Kim TJ, Lee H, Won HH, Min YW, Min BH, Lee JH, Rhee PL, and Kim JJ contributed to the critical revision of the manuscript for important intellectual content; Lee YC contributed to the statistical analysis; All authors approved the final submission.

Institutional review board statement: The Institutional review board of the Samsung Medical Center, Korea, approved this study, and the requirement for obtaining informed consent was waived owing to the study's retrospective nature.

Conflict-of-interest statement: The authors declare no conflict of interest.

Data sharing statement: Data available on request due to privacy. The data presented in this study are available on request from the corresponding author. The data are not publicly available due to privacy.

Country/Territory of origin: South Korea

ORCID number: Ji Eun Na 0000-0003-3092-9630; Yeong Chan Lee 0000-0002-2093-3161; Tae Jun Kim 0000-0001-8101-9034; Hyuk Lee 0000-0003-4271-7205; Hong-Hee Won 0000-0001-5719-0552; Yang Won Min 0000-0001-7471-1305; Byung-Hoon Min 0000-0001-8048-361X; Jun Haeng Lee 0000-0002-5272-1841; Poong-Lyul Rhee 0000-0003-0495-5296; Jae J. Kim 0000-0002-0226-1330.

S-Editor: Ma YJ
L-Editor: Filipodia
P-Editor: Ma YJ

REFERENCES

1 **Hong S**, Won YJ, Park YR, Jung KW, Kong HJ, Lee ES; Community of Population-Based Regional Cancer Registries. Cancer Statistics in Korea: Incidence, Mortality, Survival, and Prevalence in 2017. *Cancer Res Treat* 2020; **52**: 335-350 [PMID: 32178489 DOI: 10.4143/crt.2020.206]
2 **Kim YG**, Kong SH, Oh SY, Lee KG, Suh YS, Yang JY, Choi J, Kim SG, Kim JS, Kim WH, Lee HJ, Yang HK. Effects of screening on gastric cancer management: comparative analysis of the results in 2006 and in 2011. *J Gastric Cancer* 2014; **14**: 129-134 [PMID: 25061541 DOI: 10.5230/jgc.2014.14.2.129]
3 **Hamashima C**; Systematic Review Group and Guideline Development Group for Gastric Cancer Screening Guidelines. Update version of the Japanese Guidelines for Gastric Cancer Screening. *Jpn J Clin Oncol* 2018; **48**: 673-683 [PMID: 29889263 DOI: 10.1093/jjco/hyy077]
4 **Japanese Gastric Cancer Association Registration Committee**, Maruyama K, Kaminishi M, Hayashi K, Isobe Y, Honda I, Katai H, Arai K, Kodera Y, Nashimoto A. Gastric cancer treated in 1991 in Japan: data analysis of nationwide registry. *Gastric Cancer* 2006; **9**: 51-66 [PMID: 16767357 DOI: 10.1007/s10120-006-0370-y]
5 **Park CH**, Yang DH, Kim JW, Kim JH, Min YW, Lee SH, Bae JH, Chung H, Choi KD, Park JC, Lee H, Kwak MS, Kim B, Lee HJ, Lee HS, Choi M, Park DA, Lee JY, Byeon JS, Park CG, Cho JY, Lee ST, Chun HJ. Clinical Practice Guideline for Endoscopic Resection of Early Gastrointestinal Cancer. *Clin Endosc* 2020; **53**: 142-166 [PMID: 32252507 DOI: 10.5946/ce.2020.032]
6 **Hatta W**, Gotoda T, Koike T, Masamune A. History and future perspectives in Japanese guidelines for endoscopic resection of early gastric cancer. *Dig Endosc* 2020; **32**: 180-190 [PMID: 31529716 DOI: 10.1111/den.13531]
7 **Saito I**, Tsuji Y, Sakaguchi Y, Niimi K, Ono S, Kodashima S, Yamamichi N, Fujishiro M, Koike K. Complications related to gastric endoscopic submucosal dissection and their managements. *Clin Endosc* 2014; **47**: 398-403 [PMID: 25324997 DOI: 10.5946/ce.2014.47.5.398]
8 **Libânio D**, Costa MN, Pimentel-Nunes P, Dinis-Ribeiro M. Risk factors for bleeding after gastric endoscopic submucosal

dissection: a systematic review and meta-analysis. *Gastrointest Endosc* 2016; **84**: 572-586 [PMID: 27345132 DOI: 10.1016/j.gie.2016.06.033]

9 **Sato C**, Hirasawa K, Koh R, Ikeda R, Fukuchi T, Kobayashi R, Kaneko H, Makazu M, Maeda S. Postoperative bleeding in patients on antithrombotic therapy after gastric endoscopic submucosal dissection. *World J Gastroenterol* 2017; **23**: 5557-5566 [PMID: 28852315 DOI: 10.3748/wjg.v23.i30.5557]

10 **Yano T**, Tanabe S, Ishido K, Suzuki M, Kawanishi N, Yamane S, Watanabe A, Wada T, Azuma M, Katada C, Koizumi W. Different clinical characteristics associated with acute bleeding and delayed bleeding after endoscopic submucosal dissection in patients with early gastric cancer. *Surg Endosc* 2017; **31**: 4542-4550 [PMID: 28378078 DOI: 10.1007/s00464-017-5513-1]

11 **Hashimoto M**, Hatta W, Tsuji Y, Yoshio T, Yabuuchi Y, Hoteya S, Doyama H, Nagami Y, Hikichi T, Kobayashi M, Morita Y, Sumiyoshi T, Iguchi M, Tomida H, Inoue T, Mikami T, Hasatani K, Nishikawa J, Matsumura T, Nebiki H, Nakamatsu D, Ohnita K, Suzuki H, Ueyama H, Hayashi Y, Sugimoto M, Fujishiro M, Masamune A, Ohira H; Collaborators. Rebleeding in patients with delayed bleeding after endoscopic submucosal dissection for early gastric cancer. *Dig Endosc* 2021; **33**: 1120-1130 [PMID: 33539035 DOI: 10.1111/den.13943]

12 **Kataoka Y**, Tsuji Y, Sakaguchi Y, Minatsuki C, Asada-Hirayama I, Niimi K, Ono S, Kodashima S, Yamamichi N, Fujishiro M, Koike K. Bleeding after endoscopic submucosal dissection: Risk factors and preventive methods. *World J Gastroenterol* 2016; **22**: 5927-5935 [PMID: 27468187 DOI: 10.3748/wjg.v22.i26.5927]

13 **Hatta W**, Tsuji Y, Yoshio T, Kakushima N, Hoteya S, Doyama H, Nagami Y, Hikichi T, Kobayashi M, Morita Y, Sumiyoshi T, Iguchi M, Tomida H, Inoue T, Koike T, Mikami T, Hasatani K, Nishikawa J, Matsumura T, Nebiki H, Nakamatsu D, Ohnita K, Suzuki H, Ueyama H, Hayashi Y, Sugimoto M, Yamaguchi S, Michida T, Yada T, Asahina Y, Narasaka T, Kuribasyashi S, Kiyotoki S, Mabe K, Nakamura T, Nakaya N, Fujishiro M, Masamune A. Prediction model of bleeding after endoscopic submucosal dissection for early gastric cancer: BEST-J score. *Gut* 2021; **70**: 476-484 [PMID: 32499390 DOI: 10.1136/gutjnl-2019-319926]

14 **Glissen Brown JR**, Waljee AK, Mori Y, Sharma P, Berzin TM. Charting a path forward for clinical research in artificial intelligence and gastroenterology. *Dig Endosc* 2022; **34**: 4-12 [PMID: 33715244 DOI: 10.1111/den.13974]

15 **Shung DL**, Au B, Taylor RA, Tay JK, Laursen SB, Stanley AJ, Dalton HR, Ngu J, Schultz M, Laine L. Validation of a Machine Learning Model That Outperforms Clinical Risk Scoring Systems for Upper Gastrointestinal Bleeding. *Gastroenterology* 2020; **158**: 160-167 [PMID: 31562847 DOI: 10.1053/j.gastro.2019.09.009]

16 **Wong GL**, Ma AJ, Deng H, Ching JY, Wong VW, Tse YK, Yip TC, Lau LH, Liu HH, Leung CM, Tsang SW, Chan CW, Lau JY, Yuen PC, Chan FK. Machine learning model to predict recurrent ulcer bleeding in patients with history of idiopathic gastroduodenal ulcer bleeding. *Aliment Pharmacol Ther* 2019; **49**: 912-918 [PMID: 30761584 DOI: 10.1111/apt.15145]

17 **Vaswani A**, Shazeer N, Parmar N, Uszkoreit J, Jones L, Gomez AN, Kaiser L, Polosukhin I. Attention is all you need. 31st Conference on Neural Information Processing Systems (NIPS 2017), Long Beach, CA, USA. [cited April 1, 2021] Available from: https://arxiv.org/pdf/1706.03762.pdf

18 **Jeon SW**, Jung MK, Cho CM, Tak WY, Kweon YO, Kim SK, Choi YH. Predictors of immediate bleeding during endoscopic submucosal dissection in gastric lesions. *Surg Endosc* 2009; **23**: 1974-1979 [PMID: 18553202 DOI: 10.1007/s00464-008-9988-7]

19 **Choe YH**, Jung DH, Park JC, Kim HY, Shin SK, Lee SK, Lee YC. Prediction model for bleeding after endoscopic submucosal dissection of gastric neoplasms from a high-volume center. *J Gastroenterol Hepatol* 2021; **36**: 2217-2223 [PMID: 33646614 DOI: 10.1111/jgh.15478]

20 **Nam HS**, Choi CW, Kim SJ, Kim HW, Kang DH, Park SB, Ryu DG. Risk factors for delayed bleeding by onset time after endoscopic submucosal dissection for gastric neoplasm. *Sci Rep* 2019; **9**: 2674 [PMID: 30804386 DOI: 10.1038/s41598-019-39381-1]

21 **Kim JW**, Kim HS, Park DH, Park YS, Jee MG, Baik SK, Kwon SO, Lee DK. Risk factors for delayed postendoscopic mucosal resection hemorrhage in patients with gastric tumor. *Eur J Gastroenterol Hepatol* 2007; **19**: 409-415 [PMID: 17413293 DOI: 10.1097/MEG.0b013e32801015be]

22 **Kim N**, Park YS, Cho SI, Lee HS, Choe G, Kim IW, Won YD, Park JH, Kim JS, Jung HC, Song IS. Prevalence and risk factors of atrophic gastritis and intestinal metaplasia in a Korean population without significant gastroduodenal disease. *Helicobacter* 2008; **13**: 245-255 [PMID: 18665932 DOI: 10.1111/j.1523-5378.2008.00604.x]

23 **Joo YE**, Park HK, Myung DS, Baik GH, Shin JE, Seo GS, Kim GH, Kim HU, Kim HY, Cho SI, Kim N. Prevalence and risk factors of atrophic gastritis and intestinal metaplasia: a nationwide multicenter prospective study in Korea. *Gut Liver* 2013; **7**: 303-310 [PMID: 23710311 DOI: 10.5009/gnl.2013.7.3.303]

24 **Chen YM**, Zhang JS, Duan XL. Changes of microvascular architecture, ultrastructure and permeability of rat jejunal villi at different ages. *World J Gastroenterol* 2003; **9**: 795-799 [PMID: 12679935 DOI: 10.3748/wjg.v9.i4.795]

25 **Lim JH**, Kim SG, Kim JW, Choi YJ, Kwon J, Kim JY, Lee YB, Choi J, Im JP, Kim JS, Jung HC, Song IS. Do antiplatelets increase the risk of bleeding after endoscopic submucosal dissection of gastric neoplasms? *Gastrointest Endosc* 2012; **75**: 719-727 [PMID: 22317881 DOI: 10.1016/j.gie.2011.11.034]

26 **Matsumura T**, Arai M, Maruoka D, Okimoto K, Minemura S, Ishigami H, Saito K, Nakagawa T, Katsuno T, Yokosuka O. Risk factors for early and delayed post-operative bleeding after endoscopic submucosal dissection of gastric neoplasms, including patients with continued use of antithrombotic agents. *BMC Gastroenterol* 2014; **14**: 172 [PMID: 25280756 DOI: 10.1186/1471-230X-14-172]

27 **Harada H**, Suehiro S, Murakami D, Nakahara R, Nagasaka T, Ujihara T, Sagami R, Katsuyama Y, Hayasaka K, Amano Y. Feasibility of gastric endoscopic submucosal dissection with continuous low-dose aspirin for patients receiving dual antiplatelet therapy. *World J Gastroenterol* 2019; **25**: 457-468 [PMID: 30700942 DOI: 10.3748/wjg.v25.i4.457]

28 **Sanomura Y**, Oka S, Tanaka S, Numata N, Higashiyama M, Kanao H, Yoshida S, Ueno Y, Chayama K. Continued use of low-dose aspirin does not increase the risk of bleeding during or after endoscopic submucosal dissection for early gastric cancer. *Gastric Cancer* 2014; **17**: 489-496 [PMID: 24142107 DOI: 10.1007/s10120-013-0305-3]

29 **Wu W**, Chen J, Ding Q, Yang D, Yu H, Lin J. Continued use of low-dose aspirin may increase risk of bleeding after

gastrointestinal endoscopic submucosal dissection: A meta-analysis. *Turk J Gastroenterol* 2017; **28**: 329-336 [PMID: 28797987 DOI: 10.5152/tjg.2017.16573]

30 **Oh S**, Kim SG, Kim J, Choi JM, Lim JH, Yang HJ, Park JY, Han SJ, Kim JL, Chung H, Jung HC. Continuous Use of Thienopyridine May Be as Safe as Low-Dose Aspirin in Endoscopic Resection of Gastric Tumors. *Gut Liver* 2018; **12**: 393-401 [PMID: 29429155 DOI: 10.5009/gnl17384]

31 **Numata N**, Oka S, Tanaka S, Higashiyama M, Sanomura Y, Yoshida S, Arihiro K, Chayama K. Clinical outcomes of endoscopic submucosal dissection for early gastric cancer in patients with chronic kidney disease. *J Gastroenterol Hepatol* 2013; **28**: 1632-1637 [PMID: 23808356 DOI: 10.1111/jgh.12320]

32 **Chung IK**, Lee JH, Lee SH, Kim SJ, Cho JY, Cho WY, Hwangbo Y, Keum BR, Park JJ, Chun HJ, Kim HJ, Kim JJ, Ji SR, Seol SY. Therapeutic outcomes in 1000 cases of endoscopic submucosal dissection for early gastric neoplasms: Korean ESD Study Group multicenter study. *Gastrointest Endosc* 2009; **69**: 1228-1235 [PMID: 19249769 DOI: 10.1016/j.gie.2008.09.027]

33 **ASGE Standards of Practice Committee**, Acosta RD, Abraham NS, Chandrasekhara V, Chathadi KV, Early DS, Eloubeidi MA, Evans JA, Faulx AL, Fisher DA, Fonkalsrud L, Hwang JH, Khashab MA, Lightdale JR, Muthusamy VR, Pasha SF, Saltzman JR, Shaukat A, Shergill AK, Wang A, Cash BD, DeWitt JM. The management of antithrombotic agents for patients undergoing GI endoscopy. *Gastrointest Endosc* 2016; **83**: 3-16 [PMID: 26621548 DOI: 10.1016/j.gie.2015.09.035]

34 **Chan FKL**, Goh KL, Reddy N, Fujimoto K, Ho KY, Hokimoto S, Jeong YH, Kitazono T, Lee HS, Mahachai V, Tsoi KKF, Wu MS, Yan BP, Sugano K. Management of patients on antithrombotic agents undergoing emergency and elective endoscopy: joint Asian Pacific Association of Gastroenterology (APAGE) and Asian Pacific Society for Digestive Endoscopy (APSDE) practice guidelines. *Gut* 2018; **67**: 405-417 [PMID: 29331946 DOI: 10.1136/gutjnl-2017-315131]

35 **Fujimoto K**, Fujishiro M, Kato M, Higuchi K, Iwakiri R, Sakamoto C, Uchiyama S, Kashiwagi A, Ogawa H, Murakami K, Mine T, Yoshino J, Kinoshita Y, Ichinose M, Matsui T; Japan Gastroenterological Endoscopy Society. Guidelines for gastroenterological endoscopy in patients undergoing antithrombotic treatment. *Dig Endosc* 2014; **26**: 1-14 [PMID: 24215155 DOI: 10.1111/den.12183]

36 **Veitch AM**, Vanbiervliet G, Gershlick AH, Boustiere C, Baglin TP, Smith LA, Radaelli F, Knight E, Gralnek IM, Hassan C, Dumonceau JM. Endoscopy in patients on antiplatelet or anticoagulant therapy, including direct oral anticoagulants: British Society of Gastroenterology (BSG) and European Society of Gastrointestinal Endoscopy (ESGE) guidelines. *Gut* 2016; **65**: 374-389 [PMID: 26873868 DOI: 10.1136/gutjnl-2015-311110]

37 **Lim H**, Gong EJ, Min BH, Kang SJ, Shin CM, Byeon JS, Choi M, Park CG, Cho JY, Lee ST, Kim HG, Chun HJ. Clinical Practice Guideline for the Management of Antithrombotic Agents in Patients Undergoing Gastrointestinal Endoscopy. *Clin Endosc* 2020; **53**: 663-677 [PMID: 33242928 DOI: 10.5946/ce.2020.192]

World Journal of Gastroenterology

Submit a Manuscript: https://www.f6publishing.com

World J Gastroenterol 2022 June 28; 28(24): 2733-2747

DOI: 10.3748/wjg.v28.i24.2733

ISSN 1007-9327 (print) ISSN 2219-2840 (online)

ORIGINAL ARTICLE

Retrospective Study

Radiomic analysis based on multi-phase magnetic resonance imaging to predict preoperatively microvascular invasion in hepatocellular carcinoma

Yue-Ming Li, Yue-Min Zhu, Lan-Mei Gao, Ze-Wen Han, Xiao-Jie Chen, Chuan Yan, Rong-Ping Ye, Dai-Rong Cao

Specialty type: Gastroenterology and hepatology

Provenance and peer review: Unsolicited article; Externally peer reviewed.

Peer-review model: Single blind

Peer-review report's scientific quality classification

Grade A (Excellent): 0
Grade B (Very good): B
Grade C (Good): C, C, C
Grade D (Fair): 0
Grade E (Poor): 0

P-Reviewer: Li L, New Zealand; Shomura M, Japan; Suda T, Japan

Received: December 24, 2021
Peer-review started: December 24, 2021
First decision: March 10, 2022
Revised: March 20, 2022
Accepted: May 12, 2022
Article in press: May 12, 2022
Published online: June 28, 2022

Yue-Ming Li, Yue-Min Zhu, Lan-Mei Gao, Ze-Wen Han, Xiao-Jie Chen, Chuan Yan, Rong-Ping Ye, Dai-Rong Cao, Department of Radiology, The First Affiliated Hospital of Fujian Medical University, Fuzhou 350005, Fujian Province, China

Yue-Ming Li, Key Laboratory of Radiation Biology (Fujian Medical University), Fujian Province University, Fuzhou 350005, Fujian Province, China

Corresponding author: Dai-Rong Cao, MD, Chief Doctor, Department of Radiology, The First Affiliated Hospital of Fujian Medical University, No. 20 Chazhong Road, Fuzhou 350005, Fujian Province, China. 3502505836@qq.com

Abstract

BACKGROUND

The prognosis of hepatocellular carcinoma (HCC) remains poor and relapse occurs in more than half of patients within 2 years after hepatectomy. In terms of recent studies, microvascular invasion (MVI) is one of the potential predictors of recurrence. Accurate preoperative prediction of MVI is potentially beneficial to the optimization of treatment planning.

AIM

To develop a radiomic analysis model based on pre-operative magnetic resonance imaging (MRI) data to predict MVI in HCC.

METHODS

A total of 113 patients recruited to this study have been diagnosed as having HCC with histological confirmation, among whom 73 were found to have MVI and 40 were not. All the patients received preoperative examination by Gd-enhanced MRI and then curative hepatectomy. We manually delineated the tumor lesion on the largest cross-sectional area of the tumor and the adjacent two images on MRI, namely, the regions of interest. Quantitative analyses included most discriminant factors (MDFs) developed using linear discriminant analysis algorithm and histogram analysis with MaZda software. Independent significant variables of clinical and radiological features and MDFs for the prediction of MVI were estimated and a discriminant model was established by univariate and

multivariate logistic regression analysis. Prediction ability of the above-mentioned parameters or model was then evaluated by receiver operating characteristic (ROC) curve analysis. Five-fold cross-validation was also applied *via* R software.

RESULTS

The area under the ROC curve (AUC) of the MDF (0.77-0.85) outperformed that of histogram parameters (0.51-0.74). After multivariate analysis, MDF values of the arterial and portal venous phase, and peritumoral hypointensity in the hepatobiliary phase were identified to be independent predictors of MVI ($P < 0.05$). The AUC value of the model was 0.939 [95% confidence interval (CI): 0.893-0.984, standard error: 0.023]. The result of internal five-fold cross-validation (AUC: 0.912, 95%CI: 0.841-0.959, standard error: 0.0298) also showed favorable predictive efficacy.

CONCLUSION

Noninvasive MRI radiomic model based on MDF values and imaging biomarkers may be useful to make preoperative prediction of MVI in patients with primary HCC.

Key Words: Hepatocellular carcinoma; Microvascular invasion; Magnetic resonance imaging; Radiomic analysis; Imaging biomarkers

Core Tip: We developed a radiomic analysis model based on pre-operative magnetic resonance imaging data to predict microvascular invasion (MVI) in hepatocellular carcinoma (HCC). Quantitative analyses included most discriminant factors (MDFs) developed using the linear discriminant analysis algorithm and histogram analysis with MaZda software. The area under the receiver operating characteristic curve value of the model and the result of internal five-fold cross-validation showed favorable predictive efficacy. Noninvasive radiomic model based on MDF values and imaging biomarkers may be useful to make preoperative prediction of MVI in patients with primary HCC.

Citation: Li YM, Zhu YM, Gao LM, Han ZW, Chen XJ, Yan C, Ye RP, Cao DR. Radiomic analysis based on multi-phase magnetic resonance imaging to predict preoperatively microvascular invasion in hepatocellular carcinoma. *World J Gastroenterol* 2022; 28(24): 2733-2747

URL: https://www.wjgnet.com/1007-9327/full/v28/i24/2733.htm

DOI: https://dx.doi.org/10.3748/wjg.v28.i24.2733

INTRODUCTION

As important therapies for hepatocellular carcinoma (HCC), liver resection and transplantation are widely applied in clinic and the techniques have great advances. However, the prognosis remains poor and relapse occurs in more than half patients within 2 years after hepatectomy[1]. In terms of recent studies, microvascular invasion (MVI) is one of the potential predictors of recurrence[2,3]. MVI, only seen under the microscope, is defined as the appearance of tumor cells in smaller vessels inside the liver which include small portal vein and small lymphatic vessels or hepatic artery[4,5]. And MVI can be classified as four subclasses varying from M0 to M3, and higher grade usually indicates higher invasiveness of HCC and poorer survival rate[6]. Nonetheless, MVI is diagnosed by post-surgery histological result at present, which is the gold standard. The accurate prediction of MVI before operation can help achieve the anatomic resection with expanding resection margin even for a small tumor[7]. Thus, accurate preoperative prediction of MVI is potentially beneficial to the optimization of treatment planning[3,8].

There have been some studies to preoperatively predict MVI in terms of serum markers, radiological features, or imaging techniques[9-11]. For example, albumin was independently associated with MVI [9]. Besides, non-smooth tumor margins had strong diagnostic power and were of great importance for MVI assessment[10]. Moreover, gadolinium ethoxybenzyl-diethylenetriaminepentaacetic acid (Gd-EOB-DTPA), a special hepatocellular parenchymal contrast agent for magnetic resonance imaging (MRI), was valuable for MVI prediction as well[11,12]. However, the levels of serum markers are instable and likely to be affected by other diseases, and the imaging characteristics are evaluated subjectively and lack of conformance between observers. Thus, a more reliable biomarker is needed for preoperative prediction of MVI.

Quantitative analysis may have advantages over subjective analysis in reflecting valuable microscopic image features. Radiomic analysis can quantify the spatial variations in gray-level patterns, image spectral properties, and pixel interrelationships, which therefore has attracted great interest[13-15]. Using automation algorithms based on big data and with the advantages of noninvasiveness, radiomics analysis provides a powerful tool for modern medicine, and it can broadly combine multiple biomarkers and then guide clinical decision-making for patients suspected with cancer[16]. Various machine-learning methods have been used for radiomic analysis for MVI prediction, such as support vector machine and random forest[17,18]. To the best of our knowledge, there is not yet radiomics study based on linear discriminant analysis (LDA) algorithm to predict MVI. Additionally, even without spatial information, histogram analysis alone can indicate a gray-level distribution and is used for MVI prediction[19,20].

Our aim was to identify the histogram parameters alone that are predictive for MVI, and determined the prediction capacity of LDA radiomic models based on multiple phases in pre-operative Gd-enhanced MRI alone or combined with the image features for detecting MVI.

MATERIALS AND METHODS

Patients

Patients who underwent Gd-enhanced MRI examination before surgery were consecutively recruited between June 2019 and November 2021. The inclusion criteria were: (1) Solitary HCC lesion which was resectable or multiple HCC lesions appearing within one liver lobe; (2) No macroscopic vascular invasion; (3) Received the examination of Gd-enhanced MRI of the liver [with or without hepatobiliary phase (HBP)] within 1 mo before surgery; (4) Received curative hepatectomy; and (5) Verification of MVI by pathological evidence. The exclusion criteria were as follows: (1) Other anti-tumor therapies had been performed before surgery; (2) Pathological or clinical information was incomplete; (3) Imaging was not enough for analysis as a result of motion artifact; and (4) MRI performed in a different 3.0T MR machine. A total of 113 patients (91 men and 22 women; age ranging from 29–88 years, median age 58 years old) were included. According to pathologic results, HCC patients were allocated into MVI-positive (MVI+) and MVI-negative (MVI-) groups. The inclusion and exclusion criteria are shown in the flow diagram (Figure 1). This single-center retrospective cohort study was approved by the Institutional Review Board (No. [2019]283), and the requirement for informed consent was waived.

MRI examination

A 3.0T MR machine (MAGNETOM Verio; Siemens, Healthcare, Erlangen, Germany) with a dedicated phased-array body coil was used for MRI. The standard abdominal MRI protocol included: (1) Axial T2-weighted fat-suppressed turbo-spin-echo: Repetition time (TR)/echo time (TE), 4700/79 msec, slice thickness, 5 mm, slice gap, 1 mm, FOV, 21 mm × 38 mm; (2) In-phase and out-of-phase axial T1-weighted imaging (T1WI): TR/TE, 133/2.5 msec (in-phase), 6.2 msec (out-phase), slice thickness, 5 mm, slice gap, 1 mm, FOV, 21 mm × 38 mm; (3) Diffusion-weighted imaging (b = 50, 800 sec/mm^2) performed using a free-breathing single-shot echo-planar technique, TR/TE, 9965/73 msec, slice thickness, 5 mm, slice gap, 1 mm, FOV, 21 mm × 38 mm. The MRI system automatically calculated the corresponding ADC maps; and (4) Contrast enhanced MRI: A 3D gradient echo sequence with volumetric interpolated breath-hold examination was performed before and after injection of gadobenate dimeglumine (MultiHance; Bracco) at a dose of 0.2 mL/kg and at a rate of 2 mL/sec followed by a 20 mL saline flush with the following parameters: TR/TE, 3.9/1.4 msec, slice thickness 3 mm, slice gap, 0.6 mm, FOV, 25 mm × 38 mm. Hepatic arterial phase (AP), portal venous phase (PVP), equilibrium phase (EP), and HBP images were obtained at 20–30 sec, 70–80 sec, 180 sec, and 90 min after contrast medium injection, respectively.

Radiomic analysis

MaZda software (version 4.6.0, available at http://www.eletel.p.lodz.pl/mazda/) was used for radiomic analysis[21], and Digital Imaging Transformation and Communications in Medicine (DICOM) format was needed for compatibility with MaZda software. Images (MVI+ and MVI-) were loaded into the MaZda software; then, regions of interest (ROIs) were segmented manually by one radiologist, on the largest cross-sectional area and adjacent two images of the tumor or largest lesion (in the case of multiple lesions), which also included cystic necrotic regions. To delineate the tumor, the reference was based on HBP or T2-weighted imaging (T2WI) (in the case of artifact) images which were first segmented. Subsequently, the ROI was overlaid onto other phase images as required. If the respiratory movement caused the change of tumor location, the ROI was finely adjusted.

Radiomic analysis was performed with the MaZda package after loading all segmented tumor T2WI and T1WI + Gd images; within each ROI, 101 features were generated. Six different statistical image descriptors including gradient features, histogram features, gray level co-occurrence matrix, gray level run-length matrix, wavelet transform, and autoregressive model were used to create these radiomic features[21,22]. In each ROI, gray-level was normalized to minimize the effect of brightness and contrast

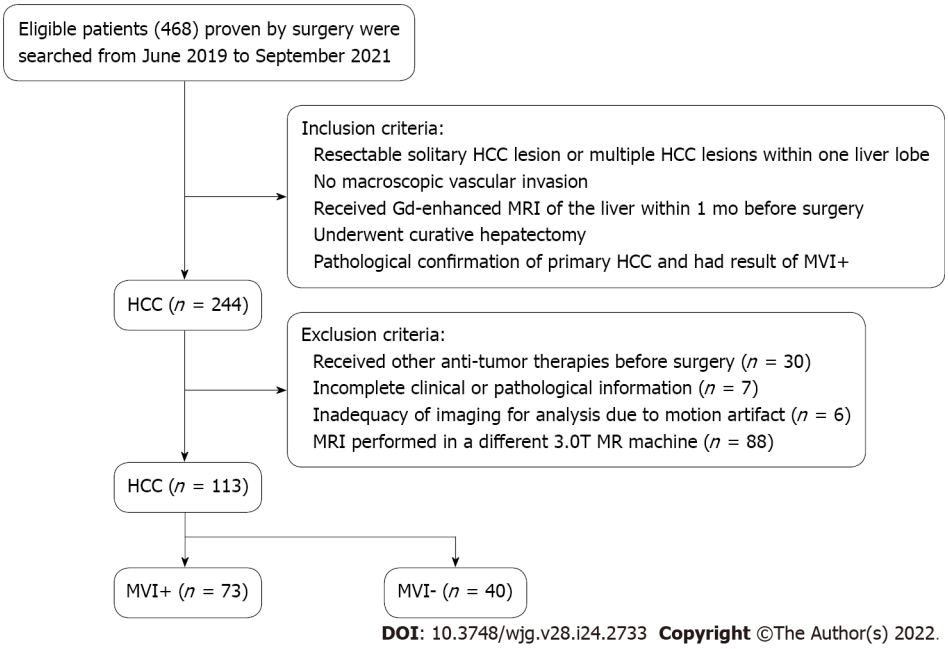

Figure 1 Flowchart of study selection process. HCC: Hepatocellular carcinoma; MVI: Microvascular invasion.

variation by image intensities in the range μ ± 3σ (μ, gray-level mean; σ, standard deviation), and the range was quantized to 6 bits/pixel[23,24].

Dimension reduction is necessary because it is impractical for clinicians to analyze all radiomic features on each patient and curse of dimensionality may happen in the case of too many features. Thus, the useful features were selected among 101 features in each sequence using algorithms, *i.e.*, mutual information (MI), Fisher coefficient (Fisher), and probability of classification error and average correlation coefficients (POE + ACC). These algorithms were used to select 30 highest discriminative power features in each sequence for further analysis. The statistical B11 radiomic analysis package (a plug-in of Mazda software) was used for analyzing these 30 features. A LDA model with the lowest misclassification rate was used to calculate the most discriminant factor (MDF)[25], which served as a comprehensive variable for discrimination and represented a linear transformation of these input 30 features that achieved the maximum separation for samples the between MVI+ and MVI- groups and the minimum separation of samples within each group. Hence, there were six MDFs, *i.e.*, MDF_{T1WI}, MDF_{T2WI}, MDF_{AP}, DMF_{PVP}, MDF_{EP}, and MDF_{HBP}.

The values of the nine histogram features (mean, variance, skewness, kurtosis, percent 1%, percent 10%, percent 50%, percent 90% and percent 99%) previously described (*i.e.*, one of six different statistical image descriptors used for radiomic analysis) were separately saved in addition for the comparison with MDF values. All characteristics of radiomic analysis were generated as presented in Figures 2 and 3.

Analysis of semantic features

In each case, an optimal window setting was adjusted to evaluate the preoperative MR images in the Picture Archiving and Communication System. The imaging features for each HCC were evaluated by two abdominal radiologists independently based on the following criteria: (1) Arterial rim enhancement, defined based on the image with irregular ring-like enhancement with relatively hypovascular central areas in the AP[26,27]; (2) Arterial peritumoral enhancement, defined based on the detectable crescent or polygonal shaped enhancement outside the tumor margin, which broadly contact with the tumor border in the AP, changing to isointense with liver parenchyma background in the delayed phase [28]; (3) Tumor margin, also defined as smooth margin, with the representative image being nodular tumors with smooth contour, or non-smooth margin presenting as non-nodular tumors with irregular margin that had surrounding budding portion in the transverse and coronal HBP images[10,28]; (4) Radiological capsule, presenting as peripheral edge of smooth hyperenhancement in the portal venous or EP[28,29]; (5) Tumor hypointensity in the HBP, shown as lower SI than that of the surrounding liver [12,30]; and (6) Peritumoral hypointensity in the HBP, defined as wedge-shaped or flame-like hypointense area of hepatic parenchyma located outside of the tumor margin in the HBP[31]. Two radiologists assessed the features of the HCC images or the largest lesion (in the case of multiple lesions). The final decision was based on their consensus.

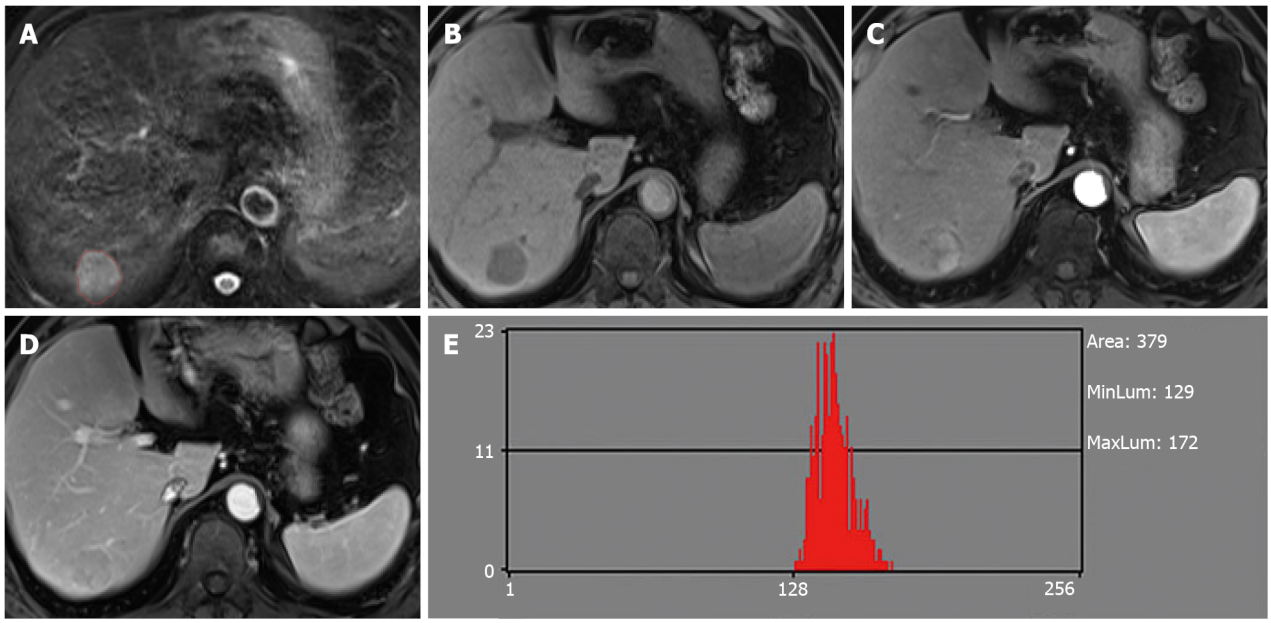

DOI: 10.3748/wjg.v28.i24.2733

Figure 2 Hepatocellular carcinoma without microvascular invasion in a 60-year-old man. A: The lesion showed slightly high signal intensity on T2-weighted imaging (T2WI) and was first regions of interest segmented; B: T1WI showed hypointensity; C: Hyper-enhancement in the arterial phase; D: The lesion showed wash-out in the portal venous phase; E: Histogram map derived from the portal venous phase.

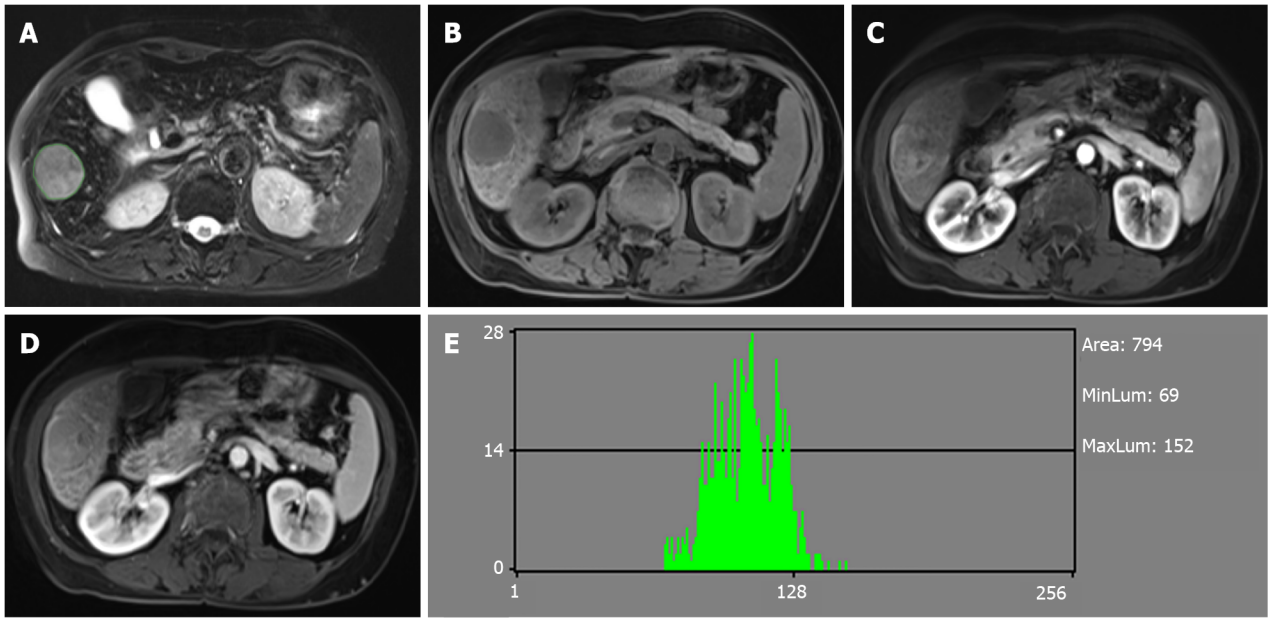

DOI: 10.3748/wjg.v28.i24.2733

Figure 3 Hepatocellular carcinoma with microvascular invasion in a 68-year-old woman. A: The lesion also showed slightly high signal intensity on T2-weighted imaging (T2WI) and was segmented; B: T1WI showed hypointensity; C: Hyper-enhancement in the arterial phase; D: The lesion showed wash-out in the portal venous phase; E: Histogram map derived from the portal venous phase indicating that the parameter of histogram was significantly different between the two groups.

Histopathological analysis

The tumor size, number, and capsule condition were collected and analyzed. The histological type, differentiation grade, lymphocyte infiltration, satellite nodules, MVI status, and chronic liver disease were compared[32]. The definition of MVI was the presence of tumor emboli in an endothelial cells-lined vascular space. The experienced pathologists reported the histopathological results after reviewing the clinical and imaging files.

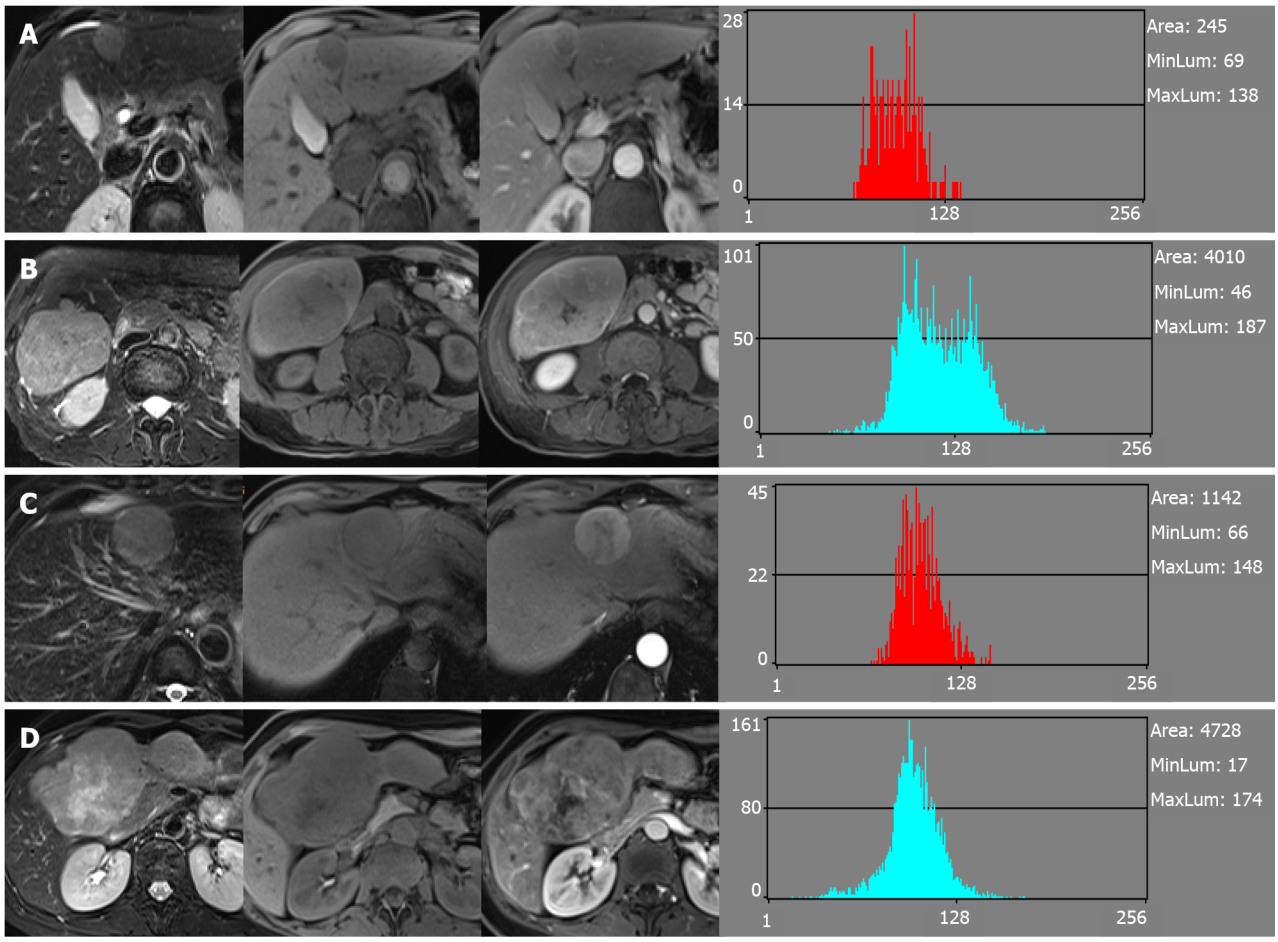

DOI: 10.3748/wjg.v28.i24.2733

Figure 4 Similar histogram features but different most discriminant factors. A: Hepatocellular carcinoma without microvascular invasion and the feature derived from the portal venous phase (PVP); B: Hepatocellular carcinoma with microvascular invasion and features derived from the PVP. Case B showed similar histogram features but different most discriminant factors (MDF) compared with case A; C: Hepatocellular carcinoma without microvascular invasion and features derived from the arterial phase (AP); D: Hepatocellular carcinoma with microvascular invasion and features derived from the AP. Case D showed similar histogram features but different MDF compared with case C.

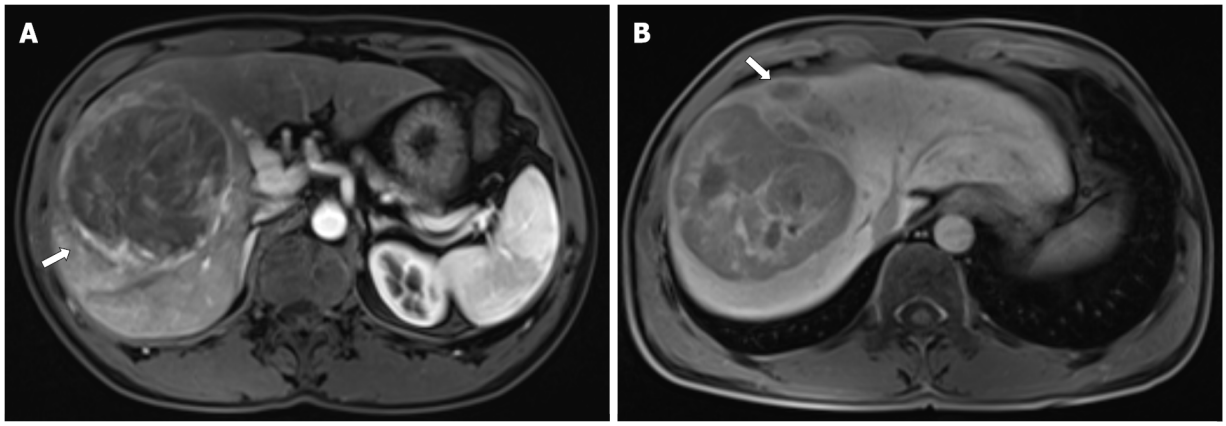

DOI: 10.3748/wjg.v28.i24.2733

Figure 5 Hepatocellular carcinoma with microvascular invasion in a 47-year-old man. A: Gd-enhanced arterial phase magnetic resonance imaging showed arterial rim enhancement (arrow); B: Hepatobiliary phase image showing peritumoral hypointensity (arrow).

Statistical analysis

SPSS for Windows (version 25.0) and Medcalc (Version 15.2.2) were used to generate the receiver operating characteristic (ROC) curves and compare the diagnostic performance for identifying MVI. The

Table 1 Comparison of patient characteristics according to microvascular invasion

Characteristic	MVI+ (*n* = 73)	MVI- (*n* = 40)	*P* value
Age (yr)[1]	56.82 ± 13.38	57.50 ± 11.98	0.790
Gender, *n* (%)			0.374
Male	57 (78.1)	34 (85.0)	
Female	16 (21.9)	6 (15.0)	
Tumor number, *n* (%)			0.152
1	58 (79.5)	36 (90.0)	
≥ 2	15 (20.5)	4 (10.0)	
AFP, *n* (%)			0.023
≤ 20	23 (31.5)	23 (57.5)	
20-400	22 (30.1)	9 (22.5)	
> 400	28 (38.4)	8 (20.0)	
HBsAg, *n* (%)			0.267
Negative	13 (17.8)	4 (10.0)	
Positive	60 (82.2)	36 (90.0)	
Pathologic grade, *n* (%)			0.042
Well	0 (0.0)	1 (2.5)	
Moderate	39 (53.4)	28 (70.0)	
Poor	34 (46.6)	11 (27.5)	
Location, *n* (%)			0.891
Left lobe	21 (28.8)	13 (32.5)	
Right lobe	51 (69.9)	27 (67.5)	
Caudate lobe	1 (1.3)	0 (0.0)	

[1]Data are the mean ± SD.

AFP: Alpha-fetoprotein; HBsAg: Hepatitis B surface antigen; MVI: Microvascular invasion.

areas under the ROC curve (AUCs) were used to assess the predictive efficacy and the optimal cutoff values from the maximum Youden's index were calculated, as well as the corresponding sensitivity and specificity for discriminating between MVI+ and MVI-. Univariate and multivariate logistic regression analyses were performed to confirm the significant variables related to MVI including clinical factors, imaging features, and MDFs in different sequences, and then build a discriminant model. Multivariate logistic regression analysis was performed using forward stepwise elimination method to identify the independent predictors. The prediction ability of significant MDF and the discriminant model was evaluated by AUC. Five-fold cross-validation was performed using the "caret" package, and nomogram was used as a graphical representation using the "rms" package (R software version 4.0.2, http://www.r-project.org). Student's *t*-test or Mann-Whitney U test was used to compare the continuous variables. Fisher's exact test or Pearson's chi-squared test was used to compare the categorical variables. $P < 0.05$ indicated statistical significance.

RESULTS

Patient characteristics

The patients were divided into two groups according to the histopathological results: MVI+ group and the MVI- group. Among 113 HCCs, 73 had MVI (4 patients had no HBP images), while 40 had no MVI (4 patients had no HBP images). The patients' clinical and radiological characteristics are listed in Tables 1 and 2, respectively. There were statistically significant differences in alpha-fetoprotein (AFP), pathologic grade, maximum tumor diameter (MTD), arterial rim enhancement, tumor margin, and peritumoral hypointensity in the HBP between the MVI+ and MVI- groups ($P < 0.050$).

Table 2 Comparison of different imaging features according to microvascular invasion

MRI feature	MVI+ (*n* = 73)	MVI- (*n* = 40)	*P* value
MTD (cm)[1]	7.23 ± 4.30	3.80 ± 2.43	< 0.001
Arterial rim enhancement (%)			0.002
Absent	37 (50.7)	32 (80)	
Present	36 (49.3)	8 (20)	
Arterial peritumoral enhancement (%)			0.134
Absent	53 (72.6)	34 (85)	
Present	20 (27.4)	6 (15)	
Tumor margin (%)			0.004
Smooth	36 (49.3)	31 (77.5)	
Non-smooth	37 (50.7)	9 (22.5)	
Radiological capsule (%)			0.303
Absent	19 (26.0)	7 (17.5)	
Present	54 (74.0)	33 (82.5)	
Tumor hypointensity in the HBP (%)			0.336
Absent	2 (2.9)	3 (8.3)	
Present	67 (97.1)	33 (91.7)	
Peritumoral hypointensity in the HBP (%)			0.016
Absent	17 (24.6)	34 (94.4)	
Present	52 (75.4)	2 (5.6)	

[1]Data are the mean ± SD.

There were eight patients who had no HBP images. HBP: Hepatobiliary phase; MVI: Microvascular invasion; MTD: Maximum tumor diameter; MRI: Magnetic resonance imaging.

Radiomic analysis

For the MVI+ and MVI- patients, the values of MDFs resulting from the LDA model under B11 analysis were significantly different between the two groups ($P < 0.001$). The analysis of MDF values with ROCs generated an AUC of 0.82 [95% confidence interval (CI): 0.77-0.87] for T1WI; 0.77 (95%CI: 0.72-0.83) for T2WI; 0.84 (95%CI: 0.80-0.88) for AP; 0.85 (95%CI: 0.81-0.90) for PVP; 0.84 (95%CI: 0.79-0.88) for EP; and 0.83 (95%CI: 0.78-0.87) for HBP images. Cutoff values of -1.38×10^{-3} (T1WI), 4.73×10^{-3} (T2WI), 1.97×10^{-2} (AP), 4.17×10^{-3} (PVP), 2.25×10^{-2} (EP), and 4.30×10^{-4} (HBP) were obtained with corresponding high sensitivities and specificities (T1WI: 78% and 78%; T2WI: 59% and 80%; AP: 87% and 66%; PVP: 67% and 90%; EP: 68% and 85%; HBP: 76% and 79%, respectively). The predictive power (AUC) of MDFs derived from the radiomics analysis was better than that of all other histogram parameters (T1WI: 0.52-0.68; T2WI: 0.53-0.70; AP: 0.54-0.69; PVP: 0.50-0.74; EP: 0.51-0.74; HBP: 0.52-0.65) (Tables 3 and 4). The MRI images of four MVI+ and MVI- cases in the AP and PVP are presented, which show similar histogram features but different MDFs (Figure 4 and Supplementary Table 1).

Association of MDFs and patient characteristics with microvascular invasion

We excluded the patients who had no HBP images. MDF values were derived from the largest cross-sectional area of images for univariate analysis. Univariate analysis showed that MDF_{T1WI} greater than -1.38×10^{-3} [odds ratio (OR) = 11.2000, 95%CI: 4.346-28.861; $P < 0.001$], MDF_{T2WI} greater than 4.73×10^{-3} (OR = 6.066, 95%CI: 2.334-15.765; $P < 0.001$), MDF_{AP} greater than 1.97×10^{-2} (OR = 8.552, 95%CI: 2.967-24.650; $P < 0.001$), MDF_{PVP} less than 4.17×10^{-3} (OR = 0.050, 95%CI: 0.017-0.143; $P < 0.001$), MDF_{EP} less than 2.25×10^{-2} (OR = 0.095, 95%CI: 0.037-0.244; $P < 0.001$), and MDF_{HBP} greater than 4.30×10^{-4} (OR = 8.800, 95%CI: 3.222-24.032; $P < 0.001$) were important risk factors related to the presence of MVI. Among patient characteristics, univariate analysis showed that MTD (OR = 1.351, 95%CI: 1.146–1.593; $P < 0.001$), AFP level (OR = 3.818, 95%CI: 1.357–10.605; $P = 0.028$), arterial rim enhancement (present *vs* absent, OR = 5.683, 95%CI: 1.977–16.340; $P = 0.001$), tumor margin (non-smooth *vs* smooth, OR = 4.024, 95%CI: 1.555–10.414; $P = 0.004$), and peritumoral hypointensity in the HBP (present *vs* absent, OR = 52.000, 95%CI: 11.287–239.569; $P < 0.001$) were significant risk factors associated with the presence of MVI

Table 3 Receiver operating characteristic results of radiomic analysis based on most discriminant factors in arterial phase and histogram parameters to discriminate between microvascular invasion+ and microvascular invasion- groups

	MVI (-)	MVI (+)	AUC	Sensitivity	Specificity	*P* value	Cut-off value
MDF	(-4.80 ± 6.14) × 10^{-2}	(2.63 ± 4.74) × 10^{-2}	0.84 (0.80-0.88)	87%	66%	< 0.001	1.97 × 10^{-2}
Histogram parameters							
Mean	(1.27 ± 0.28) × 10^{2}	(1.09 ± 0.26) × 10^{2}	0.68 (0.63-0.74)	78%	52%	< 0.001	1.06 × 10^{2}
Variance	(5.28 ± 4.24) × 10^{2}	(4.57 ± 3.21) × 10^{2}	0.54 (0.48-0.61)	68%	45%	0.204	3.32 × 10^{2}
Skewness	(-9.71 ± 58.46) × 10^{-2}	(2.52 ± 5.79) × 10^{-1}	0.68 (0.62-0.74)	76%	58%	< 0.001	1.30 × 10^{-1}
Kurtosis	(-5.24 ± 91.73) × 10^{-2}	(4.06 ± 11.19) × 10^{-1}	0.60 (0.53-0.66)	90%	25%	0.004	-5.96 × 10^{-1}
Perc.01%	(0.80 ± 0.20) × 10^{2}	(0.68 ± 0.20) × 10^{2}	0.68 (0.62-0.74)	78%	50%	< 0.001	64.5
Perc.10%	(0.99 ± 0.23) × 10^{2}	(0.84 ± 0.22) × 10^{2}	0.68 (0.62-0.74)	96%	32%	< 0.001	69.5
Perc.50%	(1.28 ± 0.30) × 10^{2}	(1.08 ± 0.27) × 10^{2}	0.69 (0.63-0.74)	76%	47%	< 0.001	105.5
Perc.90%	(1.54 ± 0.34) × 10^{2}	(1.35 ± 0.31) × 10^{2}	0.65 (0.59-0.71)	57%	70%	< 0.001	148.5
Perc.99%	(1.73 ± 0.39) × 10^{2}	(1.57 ± 0.35) × 10^{2}	0.62 (0.55-0.68)	48%	74%	< 0.001	177.5

AUC: Area under the receiver operating characteristic curve; MDF: Most discriminant factor; MVI: Microvascular invasion.

Table 4 Receiver operating characteristic results of radiomic analysis based on most discriminant factors in portal venous phase and histogram parameters to discriminate between microvascular invasion+ and microvascular invasion- groups

	MVI (-)	MVI (+)	AUC	Sensitivity	Specificity	*P* value	Cut-off value
MDF	(7.84 ± 9.26) × 10^{-3}	(-4.30 ± 7.00) × 10^{-3}	0.85 (0.81-0.90)	67%	90%	< 0.001	4.17 × 10^{-3}
Histogram parameters							
Mean	(1.24 ± 0.24) × 10^{2}	(1.08 ± 0.24) × 10^{2}	0.69 (0.63-0.75)	78%	54%	< 0.001	106.6
Variance	(3.07 ± 4.11) × 10^{2}	(4.30 ± 3.59) × 10^{2}	0.67 (0.61-0.74)	80%	50%	< 0.001	165.9
Skewness	(1.93 ± 6.11) × 10^{-1}	(1.87 ± 5.85) × 10^{-1}	0.50 (0.44-0.57)	16%	88%	0.09	7.76 × 10^{-1}
Kurtosis	(0.60 ± 1.20)	(0.62 ± 1.19)	0.51 (0.44-0.57)	57%	51%	0.787	1.62 × 10^{-1}
Perc.01%	(91.84 ± 30.33)	(67.16 ± 24.85)	0.74 (0.68-0.80)	50%	90%	< 0.001	101.5
Perc.10%	(1.06 ± 0.29) × 10^{2}	(0.84 ± 0.25) × 10^{2}	0.72 (0.67-0.78)	56%	81%	< 0.001	107.5
Perc.50%	(1.25 ± 0.24) × 10^{2}	(1.07 ± 0.24) × 10^{2}	0.69 (0.64-0.75)	78%	55%	< 0.001	106.5
Perc.90%	(1.44 ± 0.27) × 10^{2}	(1.32 ± 0.27) × 10^{2}	0.62 (0.56-0.68)	63%	61%	< 0.001	137.5
Perc.99%	(1.61 ± 0.31) × 10^{2}	(1.56 ± 0.34) × 10^{2}	0.55 (0.49-0.61)	35%	77%	0.179	176.5

AUC: Area under the receiver operating characteristic curve; MDF: Most discriminant factor; MVI: Microvascular invasion.

(Table 5).

Multivariate analysis of MDF values and patient characteristics with microvascular invasion

Multivariate analysis of the above 11 significant parameters showed that only MDF_{AP} (> 1.97 × 10^{-2} *vs* ≤ 1.97 × 10^{-2}, OR = 7.654, 95%CI: 1.860-31.501; P = 0.005), MDF_{PVP} (> 4.17 × 10^{-3} *vs* ≤ 4.17 × 10^{-3}, OR = 0.182, 95%CI: 0.047-0.705; P = 0.014), and peritumoral hypointensity in the HBP (present *vs* absent, OR = 37.098, 95%CI: 6.861-200.581; P < 0.001) were independent predictors related to the presence of MVI (Figure 5).

Table 5 Univariate analysis of risk factors for most discriminant factors and patient characteristic

Variable	OR	95%CI	*P* value
MDF_{T1}	11.200	4.346-28.861	< 0.001[a]
MDF_{T2}	6.066	2.334-15.765	< 0.001[a]
MDF_{AP}	8.552	2.967-24.650	< 0.001[a]
MDF_{PVP}	0.050	0.017-0.143	< 0.001[a]
MDF_{EP}	0.095	0.037-0.244	< 0.001[a]
MDF_{HBP}	8.800	3.222-24.032	< 0.001[a]
MTD	1.351	1.146-1.593	< 0.001[a]
AFP	3.818	1.375-10.605	0.028[a]
Pathologic grade			0.105
Arterial rim enhancement	5.683	1.977-16.340	0.001[a]
Arterial peritumoral enhancement			0.215
Tumor margin	4.024	1.555-10.414	0.004[a]
Radiological capsule			0.275
Tumor hypointensity in HBP			0.215
Peritumoral hypointensity in HBP	52.000	11.287-239.569	< 0.001[a]

[a]*P* < 0.05, statistically significant results from logistic regression analysis. Variables with [a]*P* < 0.05 in univariate logistic regression analysis were applied to a multivariate logistic regression analysis.

MDF: Most discriminant factor; AFP: Alpha-fetoprotein; AP: Arterial phase; CI: Confidence interval; EP: Equilibrium phase; HBP: Hepatobiliary phase; MTD: Maximum tumor diameter; OR: Odds ratio; PVP: Portal venous phase.

The risk scores for individual patients based on the final discriminant model were calculated using the following formula: Logit (P) = −4.612 + 3.614 × peritumoral hypointensity on HBP (absent = 0, present = 1) + 2.035 × MDF_{AP} (≤ 1.97×10^{-2} *vs* > 1.97×10^{-2}, ≤ 1.97×10^{-2} = 0, > 1.97×10^{-2} = 1) - 1.876 × MDF_{PVP} (≤ 4.17×10^{-3} *vs* > 4.17×10^{-3}, ≤ 4.17×10^{-3} = 0, > 4.17×10^{-3} = 1). The probabilities of MVI were calculated by the formula [P = e Logit (P)/1 + e Logit (P)].

The AUC of the final model was 0.939 (95%CI: 0.893-0.984; standard error: 0.023) and the optimal cutoff value was 0.595881 ≈ 0.60 (specificity: 89%; sensitivity: 90%; Youden's index: 0.788) (Figure 6A). The result of internal five-fold cross-validation (AUC: 0.912; 95%CI: 0.841-0.959; standard error: 0.0298) also showed favorable predictive efficacy (Figure 6A). The independent predictive factors were integrated into a nomogram by the multivariate logistic regression analysis (Figure 6B).

Comparison of area under the receiver operating characteristic curve values of MDF values and imaging features

We generated the ROC curves of MDF_{AP} and $MDF_{PVP,}$ respectively, which were independent predictors. The ROC curves of imaging features which were significantly different were also generated alone. The results were compared using the Delong test. The MDF_{AP} and MDF_{PVP} had significantly higher AUCs than MTDs, arterial rim enhancement, and tumor margin ($P < 0.05$; Supplementary Table 2). However, there were no differences in AUCs among MDF_{AP}, MDF_{PVP}, and peritumoral hypointensity in the HBP ($P > 0.05$; Supplementary Table 1). Comparison of ROC curves is shown in Figure 6C.

DISCUSSION

MVI indicates the invasiveness of HCC and poor prognosis[2,3]. Therefore, the pre-operative prediction of MVI is an important factor for assessing long-term patient survival and treatment optimization. The quantification of MRI images by radiomic analysis can characterize the heterogeneity of tumor and has demonstrated previous success in reflecting histological subtype[33,34]. In the present study, through the analysis of the top 30 parameters in each sequence, an overall discriminator, MDF, was generated with the LDA model, providing better prediction ability for MVI than the histogram features.

Our study showed a high sensitivity of MDF values from radiomic analysis on preoperative Gd-enhanced MRI images and/or specificity in distinguishing between MVI+ and MVI-. The AUCs of MDF values of six sequences, all of which were more than 0.75, outperformed those of all histogram

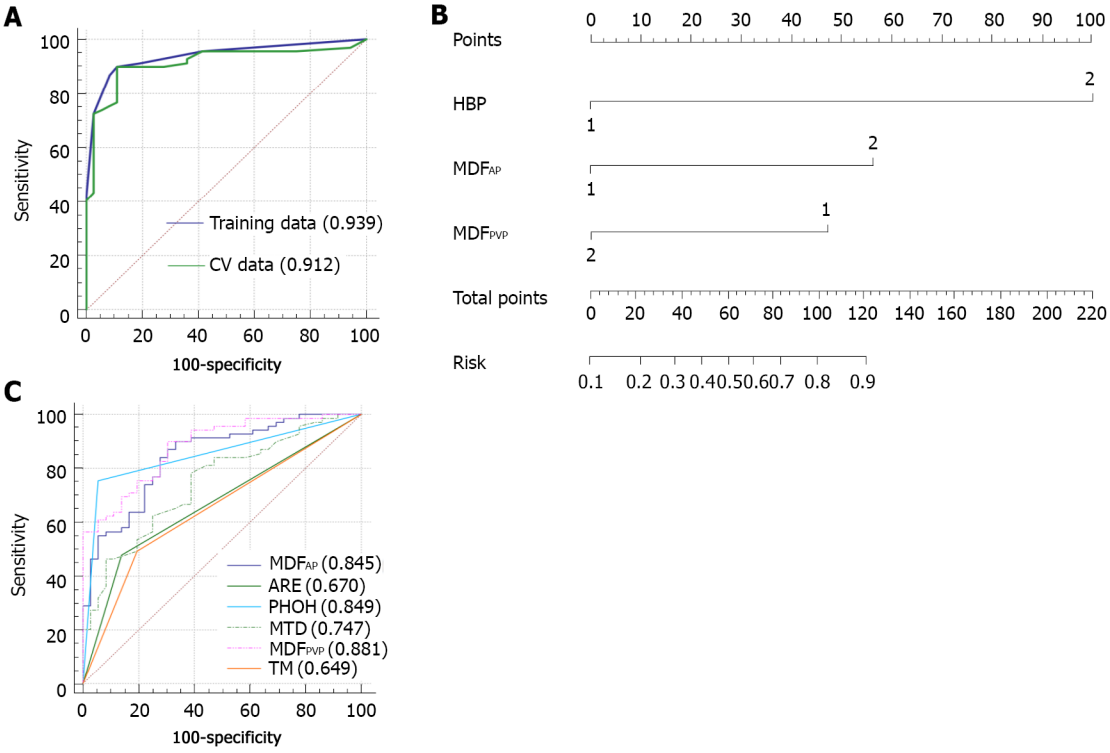

DOI: 10.3748/wjg.v28.i24.2733

Figure 6 Area under the receiver operating characteristic curve of the final model. A: Receiver operating characteristic (ROC) curves of the selected model and the ROC curve of the 5-fold cross-validation; B: Nomogram of the integrated model. Hepatobiliary phase (HBP) means peritumoral hypointensity in the HBP, most discriminant factor (MDF)$_{AP}$ means the MDF of the arterial phase, and MDF$_{PVP}$ means the MDF of the portal venous phase; C: Comparison of ROC curves for prediction of microvascular invasion. The area under the ROC curve (AUC) was largest for the MDF$_{PVP}$ alone (AUC = 0.881). ARE: Arterial rim enhancement; MTD: Maximum tumor diameter; PHOH: Peritumoral hypointensity in the HBP; TM: Tumor margin.

parameters and imaging features. The MDF values of AP and PVP images had significantly higher AUCs than most of imaging features. MDF values could provide additional information useful for clinical management decisions. Moreover, MaZda software can be easily used for general clinicians without additional requirement of expertise, easily serving as a potential powerful tool in preoperative prediction of MVI.

LDA has been used in radiomics studies recently[35]. Han *et al*[35] found that LDA and support vector machine achieved optimal performance when compared with multiple machine learning methods[35]. In our study, among the LDA models based on various sequences, MDF$_{AP}$ and MDF$_{PVP}$ were significant independent factors for the prediction of MVI, and showed satisfactory predictive efficacy with an AUC greater than 0.80. Histogram parameters have been used in quantitative analysis of MVI in clinical studies[19,20]. Li *et al*[19] performed histogram analysis of intravoxel incoherent motion and the best parameter provided a sensitivity of 81% and specificity of 85%[19]. It was based on whole tumor volume, but only 41 patients were enrolled. Wang *et al*[20] used computational quantitative measures based on the maximum cross-sectional area to predict MVI of small HCC, but only in HBP images[20]; the AUC, sensitivity, and specificity were 0.91, 0.87, and 0.80, respectively. In our study, the radiomic analysis-based MDF outperformed each individual histogram parameter in predicting the presence of MVI. Therefore, we considered that MDFs on the basis of LDA model that contained more comprehensive information could evaluate the Gd-enhanced MR images and determine MVI status better than histogram analysis alone.

Multivariate analysis of the 11 risk factors identified in the univariate analysis found that only peritumoral hypointensity in HCCs in the HBP, MDF$_{PVP}$, and MDF$_{AP}$ were independent predictors of MVI. Pathologically, MVI is usually found in the small portal vein and hepatic artery[4]. It may be detected in the small liver lymphatic vessels. But it is mostly found in small branches of the portal vein. This may explain why the MDF$_{PVP}$ and MDF$_{AP}$ were independent predictors of MDF values in the model that predicted MVI. The MDF$_{PVP}$ whose OR was less than 1 may be a protective factor, which means that the higher the MDF$_{PVP}$, the less possible the presence of MVI. MVI may affect the biological functions of the canalicular transporter multidrug resistance-associated protein 2 or the organic anion transporting peptides, both of which lead to the elimination of gadoxetate disodium. That may be the reason why peritumoral hypointensity appeared in HCCs in the HBP[12]. The OR of peritumoral hypointensity in the HBP was quite high, which may result from relatively small sample size.

It has been reported that MR findings including arterial peritumoral enhancement and non-smooth tumor margin were independent predictors associated with the presence of MVI or indicated the association between the hypointensity of HCCs in HBP images and a higher frequency of MVI[12,17], which is not consistent with our study. One possible reason for the inconsistence may be the differences between study populations, as all patients enrolled in that study had a single HCC with a diameter ≤ 5 cm. The inherent and technical inconsistencies between the observers in two studies may also account for the incompatible results. Arterial rim enhancement can predict biological characters of HCCs, including MVI, rapid progression, and early recurrence[26,36]. Our study showed that rim enhancement in the AP was not an independent predictor of MVI, and the reason may be that rim enhancement in AP is uncommon in HCC but more often seen in mass-forming cholangiocarcinoma or metastasis[37].

There are some limitations in this study. First, a selection bias may exist due to the retrospective study. Second, the radiomic analysis was performed only on the largest cross-sectional area and two adjacent images of the tumor. There may be information loss compared to whole tumors. In spite of this, our results showed excellent discriminative efficacy between the MVI+ and MVI- groups. Third, different MVI grading indicates a decreasing gradient of overall survival and time to early recurrence, which was not analyzed in the MVI+ group due to the small sample size. Finally, this study was performed at only one institution, causing the sample size small relative to the number of variables. Further multicenter, prospective studies are needed to validate the results of this study.

CONCLUSION

In conclusion, radiomic analysis based on preoperative Gd-enhanced MR images may be feasible for predicting MVI of HCC. Upon the application of MRI findings and radiomic variables in our model, the diagnostic prediction of MVI showed a high specificity and sensitivity, indicating that this method is a useful tool for clinicians in treatment decision-making.

ARTICLE HIGHLIGHTS

Research background

The prognosis of hepatocellular carcinoma (HCC) remains poor and relapse occurs in more than half of the patients within 2 years after hepatectomy. Microvascular invasion (MVI) is one of the potential predictors of recurrence. MVI is defined as the appearance of tumor cells in smaller vessels inside the liver which include small portal vein, and small lymphatic vessels or hepatic arteries. Accurate preoperative prediction of MVI is potentially beneficial to the optimization of treatment planning.

Research motivation

There have been some studies to preoperatively predict MVI in terms of serum markers, radiological features, or imaging techniques. However, the levels of serum markers are instable and likely to be affected by other diseases, and the imaging characteristics are evaluated subjectively and lack of conformance between observers. Thus, a more reliable biomarker is needed for preoperative prediction of MVI.

Research objectives

The aim of this study was to develop a radiomic analysis model based on pre-operative magnetic resonance imaging (MRI) data to predict MVI in HCC.

Research methods

A total of 113 patients recruited to this study have been diagnosed as having HCC with histological confirmation, among whom, 73 were found to have MVI and 40 were not. All the patients received preoperative examination by Gd-enhanced MRI and then curative hepatectomy. We manually delineated the tumor lesion on the largest cross-sectional area of the tumor and the two adjacent images on MRI. Quantitative analyses included most discriminant factors (MDFs) developed using a linear discriminant analysis algorithm and histogram analysis *via* MaZda software. Independent significant variables of clinical and radiological features and MDFs for the prediction of MVI were estimated and a discriminant model was established by univariate and multivariate logistic regression analysis. Prediction ability of the above-mentioned parameters or model was then evaluated by receiver operating characteristic (ROC) curve analysis, and five-fold cross-validation was applied *via* R software.

Research results

The area under the ROC curve of the MDF (0.77-0.85) outperformed the histogram parameters (0.51-0.74). After multivariate analysis, MDF values of the arterial and portal venous phase, and peritumoral

hypointensity in the hepatobiliary phase were identified to be independent predictors of MVI ($P < 0.05$). The area under the ROC curve (AUC) value of the model was 0.939. The result of internal five-fold cross-validation (AUC: 0.912) also showed favorable predictive efficacy.

Research conclusions

Noninvasive MRI radiomic model based on MDF values and imaging biomarkers may be useful to make preoperative prediction of MVI in patients with primary HCC.

Research perspectives

We believe that noninvasive radiomic models based on pre-operative MRI data have potential to be widely used in clinical fields.

ACKNOWLEDGEMENTS

We thank the radiographers at the First Affiliated Hospital of Fujian Medical University for scanning the patients and data collections in this study.

FOOTNOTES

Author contributions: Li YM, Zhu YM, and Cao DR worked out the conceptualization; Li YM, Cao DR, and Zhu YM did the methodology; Zhu YM and Yan C analyzed, collected, and interpreted the data; Li YM and Cao DR contributed to study supervision; all authors edited and reviewed the manuscript, and have read and approved the final manuscript.

Supported by Joint Funds for the Innovation of Science and Technology, Fujian Province (CN), No. 2019Y9125.

Institutional review board statement: This study was reviewed and approved by the Ethics Committee of the First Affiliated Hospital of Fujian Medical University.

Informed consent statement: This study was approved by the institutional review board of our institution. The requirement for written informed consent was waived for this retrospective study.

Conflict-of-interest statement: The authors declare that the research was conducted in the absence of any commercial or financial relationships that could be construed as a potential conflict of interest.

Data sharing statement: No additional data are available.

Country/Territory of origin: China

ORCID number: Yue-Ming Li 0000-0002-3669-568X; Yue-Min Zhu 0000-0001-9630-0160; Lan-Mei Gao 0000-0002-6032-6884; Ze-Wen Han 0000-0002-0146-8583; Xiao-Jie Chen 0000-0003-4521-3803; Chuan Yan 0000-0003-4106-8995; Rong-Ping Ye 0000-0001-7867-9752; Dai-Rong Cao 0000-0002-0051-3143.

S-Editor: Fan JR
L-Editor: Wang TQ
P-Editor: Fan JR

REFERENCES

1 **Llovet JM**, Kelley RK, Villanueva A, Singal AG, Pikarsky E, Roayaie S, Lencioni R, Koike K, Zucman-Rossi J, Finn RS. Hepatocellular carcinoma. *Nat Rev Dis Primers* 2021; **7**: 6 [PMID: 33479224 DOI: 10.1038/s41572-020-00240-3]
2 **Zhang X**, Li J, Shen F, Lau WY. Significance of presence of microvascular invasion in specimens obtained after surgical treatment of hepatocellular carcinoma. *J Gastroenterol Hepatol* 2018; **33**: 347-354 [PMID: 28589639 DOI: 10.1111/jgh.13843]
3 **Erstad DJ**, Tanabe KK. Prognostic and Therapeutic Implications of Microvascular Invasion in Hepatocellular Carcinoma. *Ann Surg Oncol* 2019; **26**: 1474-1493 [PMID: 30788629 DOI: 10.1245/s10434-019-07227-9]

4 **Gouw AS**, Balabaud C, Kusano H, Todo S, Ichida T, Kojiro M. Markers for microvascular invasion in hepatocellular carcinoma: where do we stand? *Liver Transpl* 2011; **17** Suppl 2: S72-S80 [PMID: 21714066 DOI: 10.1002/lt.22368]

5 **European Association for the Study of the Liver**. EASL Clinical Practice Guidelines: Management of hepatocellular carcinoma. *J Hepatol* 2018; **69**: 182-236 [PMID: 29628281 DOI: 10.1016/j.jhep.2018.03.019]

6 **Feng LH**, Dong H, Lau WY, Yu H, Zhu YY, Zhao Y, Lin YX, Chen J, Wu MC, Cong WM. Novel microvascular invasion-based prognostic nomograms to predict survival outcomes in patients after R0 resection for hepatocellular carcinoma. *J Cancer Res Clin Oncol* 2017; **143**: 293-303 [PMID: 27743138 DOI: 10.1007/s00432-016-2286-1]

7 **Han J**, Li ZL, Xing H, Wu H, Zhu P, Lau WY, Zhou YH, Gu WM, Wang H, Chen TH, Zeng YY, Wu MC, Shen F, Yang T. The impact of resection margin and microvascular invasion on long-term prognosis after curative resection of hepatocellular carcinoma: a multi-institutional study. *HPB (Oxford)* 2019; **21**: 962-971 [PMID: 30718183 DOI: 10.1016/j.hpb.2018.11.005]

8 **Lei Z**, Li J, Wu D, Xia Y, Wang Q, Si A, Wang K, Wan X, Lau WY, Wu M, Shen F. Nomogram for Preoperative Estimation of Microvascular Invasion Risk in Hepatitis B Virus-Related Hepatocellular Carcinoma Within the Milan Criteria. *JAMA Surg* 2016; **151**: 356-363 [PMID: 26579636 DOI: 10.1001/jamasurg.2015.4257]

9 **Zheng J**, Seier K, Gonen M, Balachandran VP, Kingham TP, D'Angelica MI, Allen PJ, Jarnagin WR, DeMatteo RP. Utility of Serum Inflammatory Markers for Predicting Microvascular Invasion and Survival for Patients with Hepatocellular Carcinoma. *Ann Surg Oncol* 2017; **24**: 3706-3714 [PMID: 28840521 DOI: 10.1245/s10434-017-6060-7]

10 **Hu H**, Zheng Q, Huang Y, Huang XW, Lai ZC, Liu J, Xie X, Feng ST, Wang W, Lu M. A non-smooth tumor margin on preoperative imaging assesses microvascular invasion of hepatocellular carcinoma: A systematic review and meta-analysis. *Sci Rep* 2017; **7**: 15375 [PMID: 29133822 DOI: 10.1038/s41598-017-15491-6]

11 **Huang M**, Liao B, Xu P, Cai H, Huang K, Dong Z, Xu L, Peng Z, Luo Y, Zheng K, Peng B, Li ZP, Feng ST. Prediction of Microvascular Invasion in Hepatocellular Carcinoma: Preoperative Gd-EOB-DTPA-Dynamic Enhanced MRI and Histopathological Correlation. *Contrast Media Mol Imaging* 2018; **2018**: 9674565 [PMID: 29606926 DOI: 10.1155/2018/9674565]

12 **Lee S**, Kim SH, Lee JE, Sinn DH, Park CK. Preoperative gadoxetic acid-enhanced MRI for predicting microvascular invasion in patients with single hepatocellular carcinoma. *J Hepatol* 2017; **67**: 526-534 [PMID: 28483680 DOI: 10.1016/j.jhep.2017.04.024]

13 **Chamming's F**, Ueno Y, Ferré R, Kao E, Jannot AS, Chong J, Omeroglu A, Mesurolle B, Reinhold C, Gallix B. Features from Computerized Texture Analysis of Breast Cancers at Pretreatment MR Imaging Are Associated with Response to Neoadjuvant Chemotherapy. *Radiology* 2018; **286**: 412-420 [PMID: 28980886 DOI: 10.1148/radiol.2017170143]

14 **Yang L**, Gu D, Wei J, Yang C, Rao S, Wang W, Chen C, Ding Y, Tian J, Zeng M. A Radiomics Nomogram for Preoperative Prediction of Microvascular Invasion in Hepatocellular Carcinoma. *Liver Cancer* 2019; **8**: 373-386 [PMID: 31768346 DOI: 10.1159/000494099]

15 **He B**, Dong D, She Y, Zhou C, Fang M, Zhu Y, Zhang H, Huang Z, Jiang T, Tian J, Chen C. Predicting response to immunotherapy in advanced non-small-cell lung cancer using tumor mutational burden radiomic biomarker. *J Immunother Cancer* 2020; **8** [PMID: 32636239 DOI: 10.1136/jitc-2020-000550]

16 **Lambin P**, Leijenaar RTH, Deist TM, Peerlings J, de Jong EEC, van Timmeren J, Sanduleanu S, Larue RTHM, Even AJG, Jochems A, van Wijk Y, Woodruff H, van Soest J, Lustberg T, Roelofs E, van Elmpt W, Dekker A, Mottaghy FM, Wildberger JE, Walsh S. Radiomics: the bridge between medical imaging and personalized medicine. *Nat Rev Clin Oncol* 2017; **14**: 749-762 [PMID: 28975929 DOI: 10.1038/nrclinonc.2017.141]

17 **Xu X**, Zhang HL, Liu QP, Sun SW, Zhang J, Zhu FP, Yang G, Yan X, Zhang YD, Liu XS. Radiomic analysis of contrast-enhanced CT predicts microvascular invasion and outcome in hepatocellular carcinoma. *J Hepatol* 2019; **70**: 1133-1144 [PMID: 30876945 DOI: 10.1016/j.jhep.2019.02.023]

18 **Chong HH**, Yang L, Sheng RF, Yu YL, Wu DJ, Rao SX, Yang C, Zeng MS. Multi-scale and multi-parametric radiomics of gadoxetate disodium-enhanced MRI predicts microvascular invasion and outcome in patients with solitary hepatocellular carcinoma ≤ 5 cm. *Eur Radiol* 2021; **31**: 4824-4838 [PMID: 33447861 DOI: 10.1007/s00330-020-07601-2]

19 **Li H**, Zhang J, Zheng Z, Guo Y, Chen M, Xie C, Zhang Z, Mei Y, Feng Y, Xu Y. Preoperative histogram analysis of intravoxel incoherent motion (IVIM) for predicting microvascular invasion in patients with single hepatocellular carcinoma. *Eur J Radiol* 2018; **105**: 65-71 [PMID: 30017300 DOI: 10.1016/j.ejrad.2018.05.032]

20 **Wang X**, Zhang Z, Zhou X, Zhang Y, Zhou J, Tang S, Liu Y, Zhou Y. Computational quantitative measures of Gd-EOB-DTPA enhanced MRI hepatobiliary phase images can predict microvascular invasion of small HCC. *Eur J Radiol* 2020; **133**: 109361 [PMID: 33120240 DOI: 10.1016/j.ejrad.2020.109361]

21 **Szczypiński PM**, Strzelecki M, Materka A, Klepaczko A. MaZda--a software package for image texture analysis. *Comput Methods Programs Biomed* 2009; **94**: 66-76 [PMID: 18922598 DOI: 10.1016/j.cmpb.2008.08.005]

22 **Strzelecki M**, Szczypinski P, Materka A, Klepaczko A. A software tool for automatic classification and segmentation of 2D/3D medical images. *Nucl Instrum Methods Phys Res* 2013; **702**: 137-140 [DOI: 10.1016/j.nima.2012.09.006]

23 **Yan PF**, Yan L, Hu TT, Xiao DD, Zhang Z, Zhao HY, Feng J. The Potential Value of Preoperative MRI Texture and Shape Analysis in Grading Meningiomas: A Preliminary Investigation. *Transl Oncol* 2017; **10**: 570-577 [PMID: 28654820 DOI: 10.1016/j.tranon.2017.04.006]

24 **Vallières M**, Freeman CR, Skamene SR, El Naqa I. A radiomics model from joint FDG-PET and MRI texture features for the prediction of lung metastases in soft-tissue sarcomas of the extremities. *Phys Med Biol* 2015; **60**: 5471-5496 [PMID: 26119045 DOI: 10.1088/0031-9155/60/14/5471]

25 **Brown AM**, Nagala S, McLean MA, Lu Y, Scoffings D, Apte A, Gonen M, Stambuk HE, Shaha AR, Tuttle RM, Deasy JO, Priest AN, Jani P, Shukla-Dave A, Griffiths J. Multi-institutional validation of a novel textural analysis tool for preoperative stratification of suspected thyroid tumors on diffusion-weighted MRI. *Magn Reson Med* 2016; **75**: 1708-1716 [PMID: 25995019 DOI: 10.1002/mrm.25743]

26 **Rhee H**, An C, Kim HY, Yoo JE, Park YN, Kim MJ. Hepatocellular Carcinoma with Irregular Rim-Like Arterial Phase Hyperenhancement: More Aggressive Pathologic Features. *Liver Cancer* 2019; **8**: 24-40 [PMID: 30815393 DOI: 10.1159/000488540]

27 **Kawamura Y**, Ikeda K, Hirakawa M, Yatsuji H, Sezaki H, Hosaka T, Akuta N, Kobayashi M, Saitoh S, Suzuki F, Suzuki Y, Arase Y, Kumada H. New classification of dynamic computed tomography images predictive of malignant characteristics of hepatocellular carcinoma. *Hepatol Res* 2010; **40**: 1006-1014 [PMID: 20887336 DOI: 10.1111/j.1872-034X.2010.00703.x]

28 **Kim H**, Park MS, Choi JY, Park YN, Kim MJ, Kim KS, Choi JS, Han KH, Kim E, Kim KW. Can microvessel invasion of hepatocellular carcinoma be predicted by pre-operative MRI? *Eur Radiol* 2009; **19**: 1744-1751 [PMID: 19247666 DOI: 10.1007/s00330-009-1331-8]

29 **Choi JY**, Lee JM, Sirlin CB. CT and MR imaging diagnosis and staging of hepatocellular carcinoma: part II. Extracellular agents, hepatobiliary agents, and ancillary imaging features. *Radiology* 2014; **273**: 30-50 [PMID: 25247563 DOI: 10.1148/radiol.14132362]

30 **Kitao A**, Matsui O, Yoneda N, Kozaka K, Kobayashi S, Koda W, Gabata T, Yamashita T, Kaneko S, Nakanuma Y, Kita R, Arii S. Hypervascular hepatocellular carcinoma: correlation between biologic features and signal intensity on gadoxetic acid-enhanced MR images. *Radiology* 2012; **265**: 780-789 [PMID: 23175543 DOI: 10.1148/radiol.12120226]

31 **Kim KA**, Kim MJ, Jeon HM, Kim KS, Choi JS, Ahn SH, Cha SJ, Chung YE. Prediction of microvascular invasion of hepatocellular carcinoma: usefulness of peritumoral hypointensity seen on gadoxetate disodium-enhanced hepatobiliary phase images. *J Magn Reson Imaging* 2012; **35**: 629-634 [PMID: 22069244 DOI: 10.1002/jmri.22876]

32 **Roayaie S**, Blume IN, Thung SN, Guido M, Fiel MI, Hiotis S, Labow DM, Llovet JM, Schwartz ME. A system of classifying microvascular invasion to predict outcome after resection in patients with hepatocellular carcinoma. *Gastroenterology* 2009; **137**: 850-855 [PMID: 19524573 DOI: 10.1053/j.gastro.2009.06.003]

33 **Li Y**, Yan C, Weng S, Shi Z, Sun H, Chen J, Xu X, Ye R, Hong J. Texture analysis of multi-phase MRI images to detect expression of Ki67 in hepatocellular carcinoma. *Clin Radiol* 2019; **74**: 813.e19-813.e27 [PMID: 31362887 DOI: 10.1016/j.crad.2019.06.024]

34 **Zhang S**, Chiang GC, Magge RS, Fine HA, Ramakrishna R, Chang EW, Pulisetty T, Wang Y, Zhu W, Kovanlikaya I. Texture analysis on conventional MRI images accurately predicts early malignant transformation of low-grade gliomas. *Eur Radiol* 2019; **29**: 2751-2759 [PMID: 30617484 DOI: 10.1007/s00330-018-5921-1]

35 **Han Y**, Ma Y, Wu Z, Zhang F, Zheng D, Liu X, Tao L, Liang Z, Yang Z, Li X, Huang J, Guo X. Histologic subtype classification of non-small cell lung cancer using PET/CT images. *Eur J Nucl Med Mol Imaging* 2021; **48**: 350-360 [PMID: 32776232 DOI: 10.1007/s00259-020-04771-5]

36 **Kierans AS**, Leonardou P, Hayashi P, Brubaker LM, Elazzazi M, Shaikh F, Semelka RC. MRI findings of rapidly progressive hepatocellular carcinoma. *Magn Reson Imaging* 2010; **28**: 790-796 [PMID: 20427139 DOI: 10.1016/j.mri.2010.03.005]

37 **Zou X**, Luo Y, Morelli JN, Hu X, Shen Y, Hu D. Differentiation of hepatocellular carcinoma from intrahepatic cholangiocarcinoma and combined hepatocellular-cholangiocarcinoma in high-risk patients matched to MR field strength: diagnostic performance of LI-RADS version 2018. *Abdom Radiol (NY)* 2021; **46**: 3168-3178 [PMID: 33660040 DOI: 10.1007/s00261-021-02996-y]

World Journal of Gastroenterology

Submit a Manuscript: https://www.f6publishing.com

World J Gastroenterol 2022 June 28; 28(24): 2748-2757

DOI: 10.3748/wjg.v28.i24.2748

ISSN 1007-9327 (print) ISSN 2219-2840 (online)

ORIGINAL ARTICLE

Retrospective Study

Brown slits for colorectal adenoma crypts on conventional magnifying endoscopy with narrow band imaging using the X1 system

Osamu Toyoshima, Toshihiro Nishizawa, Shuntaro Yoshida, Hidenobu Watanabe, Nariaki Odawara, Kosuke Sakitani, Toru Arano, Hirotoshi Takiyama, Hideyuki Kobayashi, Hirofumi Kogure, Mitsuhiro Fujishiro

Specialty type: Gastroenterology and hepatology

Provenance and peer review: Unsolicited article; Externally peer reviewed.

Peer-review model: Single blind

Peer-review report's scientific quality classification

Grade A (Excellent): 0
Grade B (Very good): B, B
Grade C (Good): C
Grade D (Fair): 0
Grade E (Poor): 0

P-Reviewer: Duan Z, China; Shafaee Z, United States; Sharaf MM, Syria
A-Editor: Sahin TT

Received: January 16, 2022
Peer-review started: January 16, 2022
First decision: March 8, 2022
Revised: March 14, 2022
Accepted: May 14, 2022
Article in press: May 14, 2022
Published online: June 28, 2022

Osamu Toyoshima, Toshihiro Nishizawa, Shuntaro Yoshida, Nariaki Odawara, Kosuke Sakitani, Toru Arano, Department of Gastroenterology, Toyoshima Endoscopy Clinic, Tokyo 157-0066, Japan

Toshihiro Nishizawa, Department of Gastroenterology and Hepatology, International University of Health and Welfare, Narita Hospital, Chiba 286-8520, Japan

Hidenobu Watanabe, Department of Pathology, Pathology and Cytology Laboratory Japan, Tokyo 166-0003, Japan

Nariaki Odawara, Hirofumi Kogure, Mitsuhiro Fujishiro, Department of Gastroenterology, Graduate School of Medicine, The University of Tokyo, Tokyo 113-8655, Japan

Kosuke Sakitani, Department of Gastroenterology, Sakitani Endoscopy Clinic, Chiba 275-0026, Japan

Toru Arano, Department of Gastroenterology, The Fraternity Memorial Hospital, Tokyo 130-8587, Japan

Hirotoshi Takiyama, Department of Surgical Oncology, The University of Tokyo, Tokyo 113-8655, Japan

Hideyuki Kobayashi, Department of Internal Medicine, Umegaoka Ekimae Clinic, Tokyo 154-0022, Japan

Corresponding author: Toshihiro Nishizawa, MD, PhD, Professor, Department of Gastroenterology and Hepatology, International University of Health and Welfare, Narita Hospital, 852 Hatakeda, Chiba 286-8520, Japan. nisizawa@kf7.so-net.ne.jp

Abstract

BACKGROUND

Accurate diagnosis of colorectal premalignant polyps, including adenomas, is vital in clinical practice.

AIM

To investigate the diagnostic yields of novel findings of brown slits for adenomas.

METHODS
Patients who underwent colonoscopy at the Toyoshima Endoscopy Clinic were enrolled. Polyps sized ≥ 5 mm suspected of adenomas or clinically significant serrated polyps were included in the study. We defined the surface structures of colorectal polyps, which were brown curves inside and along the tubular glands identified using a combination of a new X1 system (Olympus Corporation) and a conventional magnifying colonoscope with non-staining narrow band imaging (NBI), as brown slits. The brown slits corresponded to slit-like lumens on endocytoscopy and histological crypt openings of an adenoma. We evaluated the diagnostic performance of brown slits for adenoma.

RESULTS
A total of 108 Lesions from 62 patients were eligible. The average age was 60.4 years and 41.9% were male. The mean polyp size was 7.45 ± 2.83 mm. Fifty-seven lesions were positive for brown slits. Histopathological diagnosis comprised 59 low-grade tubular adenomas, 16 sessile serrated lesions, and 33 hyperplastic polyps. Among 59 adenomas, 56 (94.9%) were positive for brown slits. Among 16 sessile serrated lesions, 0 (0%) was positive for brown slits. Among 33 hyperplastic polyps, 1 (3.0%) was positive for brown slits. The sensitivity, specificity, and accuracy of brown slits for adenoma were 94.9%, 98.0%, and 96.3%, respectively. The positive predictive value and negative predictive value of brown slits for adenoma were also excellent for 98.2%, and 94.1%, respectively.

CONCLUSION
Brown slits on conventional magnifying endoscopy with non-staining NBI using the X1 system were useful for diagnosing colorectal adenoma. The new endoscopy system could be examined using new standards.

Key Words: Adenoma; Colonoscopy; Narrow band imaging; Magnifying endoscopy; X1; Serrated polyp; Colorectal neoplasm; Endocytoscopy

Core Tip: We defined the polyp's surface structure observed on conventional magnifying endoscopy with non-staining narrow band imaging using the X1 system as brown slits. The brown slits corresponded to slit-like lumens on endocytoscopy and histological crypt openings of an adenoma. Brown slits were useful for diagnosing colorectal adenoma.

Citation: Toyoshima O, Nishizawa T, Yoshida S, Watanabe H, Odawara N, Sakitani K, Arano T, Takiyama H, Kobayashi H, Kogure H, Fujishiro M. Brown slits for colorectal adenoma crypts on conventional magnifying endoscopy with narrow band imaging using the X1 system. *World J Gastroenterol* 2022; 28(24): 2748-2757
URL: https://www.wjgnet.com/1007-9327/full/v28/i24/2748.htm
DOI: https://dx.doi.org/10.3748/wjg.v28.i24.2748

INTRODUCTION

Colorectal adenoma is a premalignant neoplasm composed of a dysplastic epithelium. Removal of adenomas reduces the risk of colorectal adenocarcinoma[1,2]. Colorectal adenomas are found in ≥ 40% of proper colonoscopies, given that an accurate diagnosis of adenoma is crucial in routine endoscopic practice[3-6]. Colorectal serrated polyps are precursors with different molecular pathways and biological behaviors from adenomas[2,7,8]. Clinically significant serrated polyps (CSSPs), comprising all sessile serrated lesions (SSLs), all traditional serrated adenomas (TSAs), hyperplastic polyps ≥ 10 mm in size anywhere in the colorectum, and hyperplastic polyps ≥ 5 mm in size between the cecum and descending colon are recommended to be endoscopically removed[9-12]. The number, size, grade of dysplasia, and histological subtype of premalignant polyps, including both adenomas and serrated polyps, are the best determinants of the long-term risk of advanced neoplasia and inform surveillance decision-making[7,13-16].

Magnification, dye sprays, and modified light wavelengths, such as narrow band imaging (NBI) and blue laser imaging (BLI), are used to diagnose premalignant polyps better. The criteria for conventional magnifying endoscopy include pit pattern diagnosis using chromoendoscopy[17] and the Japan NBI expert team (JNET) classification using NBI and BLI[18-20]. The standards for ultra-high magnifying

endocytoscopy (EC) are as follows: EC classification, which evaluates the glandular structure and cellular atypia after double staining with methylene blue and crystal violet[21-24], and EC vascular classification, which evaluates the microvessels using NBI[25,26]. Slit-like lumens and microvessels with clear margins showing a network are good indicators of adenoma in EC, whereas narrow serrated lumens and obscure microvessels predict hyperplastic polyps. Sasajima *et al*[21] and Mori *et al*[23] have elucidated that long tubular pits (slit-like lumens) on EC are histologically equivalent to the crypt opening using the horizontal and vertical sections of specimens, respectively.

In 2020, a novel endoscopic system, which is a set of an EVIS X1 Video System Center (CV-1500) and a 4K ultra-high definition 32-inch liquid crystal display (LCD) monitor (OEV321UH), was released by Olympus Corporation, Tokyo, Japan. When using the same scope, this system has higher image quality and higher magnification than the previous generation's Olympus system, which is a set of EVIS Elite Video System Center (CV-290) and a high-definition 26-inch LCD monitor (OEV262H). For example, the magnifications of conventional magnifying endoscopes of Olympus' CF-HQ290Z and PCF-H290Z were 80 × and 110 ×, respectively, using the Elite system, while the magnifications increased to 95 × and 170 ×, respectively, using the X1 system. Given this, we hypothesized that the new X1 system allows conventional magnifying endoscopy to visualize the structures that could only be observed with EC, and to improve polyp diagnosis. Using a combination of the X1 system and the conventional magnifying endoscope with non-staining NBI, we identified the findings corresponding to the slit-like lumens, which present the crypts of adenoma. Then, we defined the findings as "brown slits" (Figure 1A and B).

To the best of our knowledge, there are no studies in which conventional magnifying endoscopy has verified the evidence accumulated by EC. Therefore, we focused on brown slits detected on conventional magnifying endoscopy using the X1 system and investigated their performance for adenoma diagnosis.

MATERIALS AND METHODS

Study design and overview

This retrospective study was conducted at the Toyoshima Endoscopy Clinic, a representative outpatient endoscopy-specialized clinic in Japan. This study was conducted in accordance with the ethical guidelines for medical studies in Japan. Written informed consent to use clinical information was obtained from the patients before colonoscopy. The study design was described in a protocol prepared by the Toyoshima Endoscopy Clinic and the Sakitani Endoscopy Clinic, and was approved by the Certified Institutional Review Board, Yoyogi Mental Clinic on July 16, 2021 (approval No. RKK227). We published this study's protocol on our institute's website (www.ichou.com) so that patients could opt out of the study if desired. All clinical investigations were performed in accordance with the ethical guidelines of the Declaration of Helsinki.

Study subjects

We enrolled patients who underwent colonoscopy at the Toyoshima Endoscopy Clinic in May and June 2021. Polyps sized ≥ 5 mm suspected of adenomas or CSSPs were included in this study[23,27,28]. The exclusion criteria were ulcerative colitis, poor bowel preparation, lesions for which endoscopic imaging could not be obtained, and lesions for which the specimen could not be collected. We also excluded histologically diagnosed adenocarcinomas, TSAs, and normal mucosa.

Brown slits for adenoma

Figure 1 shows typical images of a tubular adenoma observed using a combination of the conventional magnifying endoscope (CF-HQ290Z) and the X1 system, at full zoom magnification with NBI and WLI with or without indigo carmine spraying. Brown slits inside and along the tubular glands surrounded by microvessels were identified (pink curves in Figure 1B). We defined this brown pattern as a brown slit. The brown slit was additionally defined as having a length longer than the width of the tubular gland (approximately 100 μm). The brown slits were visible as faint and pale red slits on WLI (Figure 1C). Indigo carmine accumulated in the crypt openings that corresponded to brown slits (Figure 1A, B and D).

Figure 2 shows representative images of a tubular adenoma using a combination of the endocytoscope (CF-H290EC, Olympus Corporation) and the X1 system. To obtain a fully zoomed image with 790× magnification with a focusing depth of 35 μm, the endoscopist softly contacted the lesion with the endoscope lens[26]. On ultra-high magnifying observation with NBI, slits with a mixture of brown and white colors inside and along the tubular glands were visualized (Figure 2D, blue arrows). This tubular structure corresponded to a slit-like lumen for staining EC[22-25]. The microvessels were clearly identified surrounding the tubular gland and showed a vessel network[25]. On ultra-high magnifying observation with white light imaging (WLI), although microvessels were obscure, slits with a mixture of red and white colors were seen similar to the slits on NBI observation (Figure 2B, blue arrows). We could recognize tubular glands surrounded by the microvessels and brown and pale red slits inside and

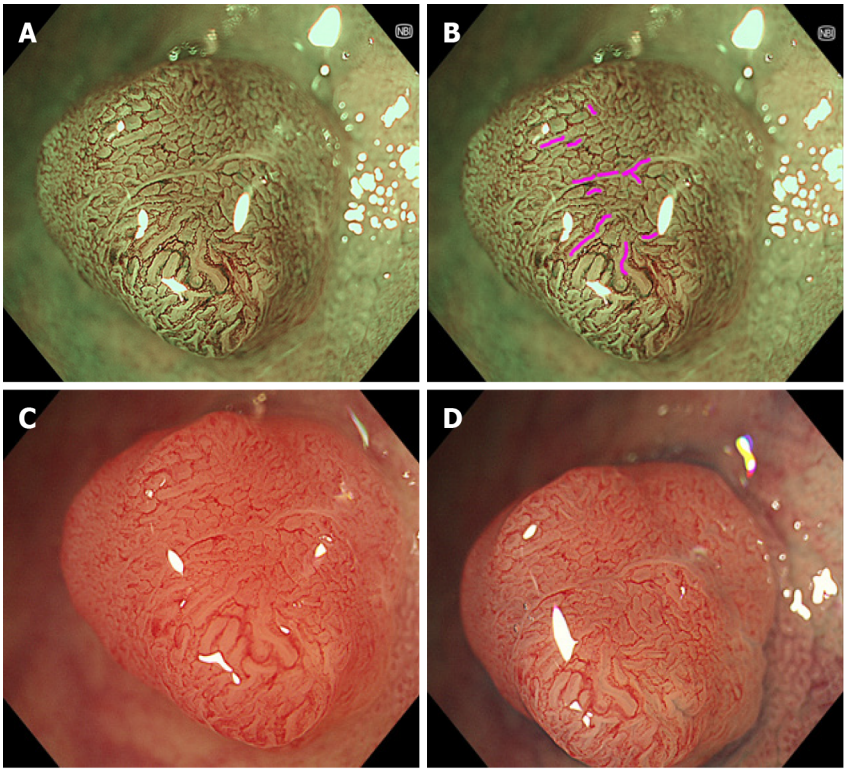

DOI: 10.3748/wjg.v28.i24.2748

Figure 1 Representative images of "brown slits" in a low-grade tubular adenoma using conventional magnifying endoscopy. A set of a conventional magnifying endoscope (CF-HQ290Z), X1 system, and 4K 32-inch monitor was used. A, B: Full-zoom (95 ×) magnification, narrow band imaging. Brown slits were observed inside and along the tubular glands surrounded by the microvessels; C: Full-zoom magnifying, white-light imaging observation without indigo carmine spraying showed faint and pale red slits inside and along the tubular glands; D: Full-zoom magnifying, white light imaging with indigo carmine spraying showed indigo carmine accumulated in the site corresponding to the brown slits.

along the tubular glands with NBI and WLI, respectively, when we observed with approximately 100 × magnification, which was similar to the full zoom of conventional magnifying endoscopy (Figure 2A and C, pink arrows).

The correspondence between EC and histology is presented in Figure 3. Variably shaped tubular glands (surrounded by white and red curves in Figures 3A and B, respectively) with homogeneous widths of approximately 100 μm were observed. The crypts (blue arrows in Figure 3A and B) were detected as brown and white slits inside and along the tubular glands on EC. The microvessels (yellow arrows in Figure 3) were observed in the intervening part (black arrows in Figure 3). The size and position of the crypt, intervening part, and microvessels were consistent between EC and histology.

From the above, the brown slits on conventional magnifying endoscopy with NBI corresponded to slit-like lumens on EC and crypt openings on histology.

Colonoscopy

Brown slits were diagnosed in real-time during colonoscopy. Before the colonoscopy, the endoscopists discussed and obtained consensus for the brown slits while viewing the images on non-magnifying, conventional magnifying, and ultra-high magnifying observation. Two expert endoscopists conducted all colonoscopies. An endoscopic set of the X1 system and CF-HQ290Z or PCF-H290Z was used. Colonoscopes without a magnifying function and those with an autofocus function were excluded. The optical enhancement of the NBI was set in mode A8. When a lesion was detected, the surface was washed to remove mucus and dye, and a non-magnifying observation was conducted. Subsequently, the endoscopists focused on and diagnosed brown slits at almost full zoom. The polyp was observed without indigo carmine staining. Location, size, and morphology according to the Paris classification, the presence or absence of brown slits, and endoscopic polyp diagnosis were recorded. The colonoscopists classified each polyp as an adenoma, SSL, or hyperplastic polyp. The lesion size was calibrated by comparison with closed cups of biopsy forceps (approximately 2.5 mm).

Before examination, patients underwent bowel preparation with 2 L of polyethylene glycol solution or 1.8 L of isotonic magnesium citrate. If necessary, additional magnesium citrate or polyethylene glycol was provided. Patients were sedated using midazolam and pethidine hydrochloride. Scopolamine butylbromide or glucagon was intravenously administered to suppress bowel peristalsis. The polyps were resected using snear polypectomy with or without submucosal saline injection.

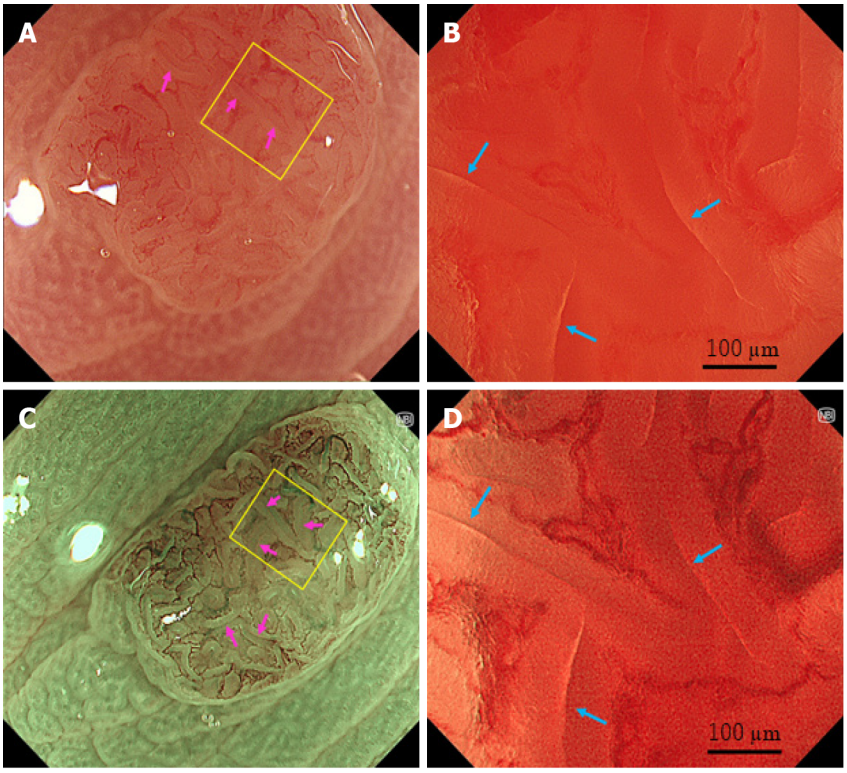

DOI: 10.3748/wjg.v28.i24.2748 **Copyright** ©The Author(s) 2022.

Figure 2 Representative images of "slit-like lumens" and "brown slits" in a low-grade tubular adenoma using endocytoscopy. A set of an endocytoscope (CF-H290EC), X1 system, and 4K 32-inch monitor was used. A, B: White light imaging observation; C, D: Narrow band imaging observation; A, C: Conventional (100 ×) magnifying observation. The yellow box represents the site for full-zoom observation; B, D: Full-zoom (790 ×) magnifying observation; D: Slit-like lumens were observed (blue arrows). The microvessels were clearly observed surrounding the slit-like lumen and showed a vessel network; C: A "brown slit" sign was observed (pink arrows); B: Slit-like lumens were obscurely observed (blue arrows).

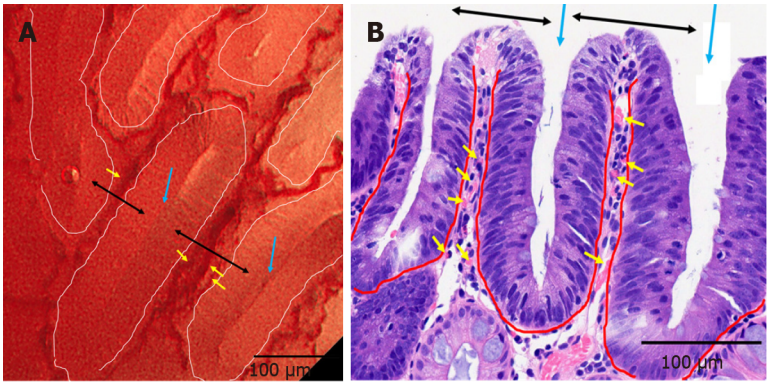

DOI: 10.3748/wjg.v28.i24.2748 **Copyright** ©The Author(s) 2022.

Figure 3 Correspondence between endocytoscopy and histology in a low-grade tubular adenoma. A: A set of an endocytoscope (CF-H290EC), X1 system, and 4K 32-inch monitor was used. Full-zoom magnifying, narrow band imaging observation. Variably shaped tubular glands (surrounded by white curves) with homogeneous widths of about 100 μm. The crypts (blue arrows) are detected as brown and white slits inside and along the tubular glands. The microvessels (yellow arrows) are identified in the intervening part (black arrows); B: Vertical sections stained with hematoxylin-eosin. The tubular glands (surrounded by red curves), crypts (blue arrows), intervening parts (black arrows), and microvessels (yellow arrows) are seen in endocytoscopy.

Pathology

Fixed specimens were subjected to histological examination. The reference standard was histopathology using standard hematoxylin-eosin staining. All lesions were diagnosed according to World Health Organization criteria[2] by a gastrointestinal pathologist. The pathologist classified each polyp as a tubular adenoma, villous adenoma, adenocarcinoma, SSL, TSA, microvesicular hyperplastic polyp (MVHP), goblet cell-rich hyperplastic polyp (GCHP), or normal mucosa.

Statistical analysis

The diagnostic performance of brown slits for colorectal adenoma was calculated using BellCurve for Excel (version 3.21; Social Survey Research Information Co., Ltd., Tokyo, Japan).

RESULTS

Of the 115 Lesions in 64 patients who met the criteria, 1 adenocarcinoma in situ, 1 TSA, 4 normal mucosae, and 1 lost specimen were excluded. A total of 108 Lesions in 62 patients were enrolled. Table 1 shows the characteristics of the study participants (mean age, 60.4 years; males, 41.9%). Of the lesions, the mean polyp size was 7.45 mm (range, 5–15 mm), and 57 and 51 were positive and negative for "brown slit" signs, respectively. Histopathological diagnosis of the polyps comprised 59 low-grade tubular adenomas, 16 SSLs, 27 MVHPs, and 6 GCHPs.

Table 2 presents the number of lesions in the brown slits. The diagnostic performance of brown slits for colorectal adenomas is shown in Table 3. The sensitivity, specificity, accuracy, positive predictive value, and negative predictive value were excellent for 94.9%, 98.0%, 96.3%, 98.2%, and 94.1%, respectively.

DISCUSSION

We defined the polyp's surface structure observed on conventional magnifying endoscopy with non-staining NBI using the X1 system as brown slits. The brown slits corresponded to the slit-like lumens detected on EC and to the histological crypt opening of the tubular gland of the adenoma. This study elucidated that the brown slits were highly accurate for differentiation between colorectal adenomas and serrated polyps with a sensitivity, specificity, and accuracy of 94.6%, 98.3%, and 96.5%, respectively. Kudo *et al*[22] reported that the sensitivity, specificity, and accuracy of slit-like lumens were 82.5%, 100%, and 83.9%, respectively, when comparing colorectal adenoma and hyperplastic polyps. The strength of the brown slits is not only the high diagnostic performance, but also the convenience of identification using a conventional magnifying endoscope with non-staining NBI. Kudo *et al*[25] reported that obtaining a clear ultra-high magnification view using EC was difficult and long. Thus, brown slits are simple and meaningful in daily practice.

Compared with EC, conventional magnifying endoscopy has advantages, such as not requiring contact, thereby reducing bleeding or tissue damage; easy focusing; and high familiarity. Additionally, CF-HQ290Z (4700000 yen: $ 40941) and PCF-H290Z (4500000 yen: $ 39199) are cheaper than CF-H290EC (7900000 yen: $ 68817). In the future, it would be beneficial if the accumulating evidence with the EC could be applied with conventional magnifying endoscopy.

JNET types 1 and 2A correspond to histological classifications of hyperplastic polyp/SSL and low-grade intramucosal neoplasia, respectively. JNET classification was comprehensively judged with two scales: surface pattern and vessel pattern[18,19]. Kobayashi *et al*[19] reported that the sensitivity, specificity, and accuracy of JNET 2A for low-grade intramucosal neoplasia were 91.4%, 75.1%, and 89.1%, respectively. Because the brown slit sign is based only on the surface pattern, it may be simpler and easier than the JNET classification.

The reasons why the set of X1 system allowed the visualization of the brown slits, which accurately predicted adenomas, were considered as follows: compared to the Elite system, the X1 system has a higher magnification and image quality due to 4K resolution, additional amber color LED, and a new noise reduction system. We previously reported that the new 290 series endoscopic system had advantages in polyp detection and procedure over the previous 260 series model[29]. Improvements of the endoscopic system may increase the visibility of the polyp findings.

The present study had some limitations. The slit-like lumens and a normal pit-like structure on staining EC distinguish low-grade adenoma from advanced neoplasia and allow DISCARD strategy[13,24,30]. Fused gland formations on EC staining can predict the histological grade of differentiation and risk factors for lymph node metastasis in T1 colorectal adenocarcinoma[31]. EC with NBI can examine the diameter and caliber variation of tumor microvessels that are associated with the depth of cancer invasion[32]. EC with NBI also possibly differentiates diminutive hyperplastic polyps from adenomas based on the microvessel pattern[26]. However, the present study excluded carcinomas, TSAs, and diminutive polyps. Furthermore, there were no villous adenomas. Validation of these EC-based evidence by applying conventional magnifying endoscopy in the future is desirable. Second, this was a retrospective study that was limited to single-center expert endoscopists. Prospective analysis at multiple centers, including non-experts, is needed. Third, the NBI mode and 290 series endoscopes were used in this study. Verification using other image-enhancing modalities, such as BLI[20], linked color imaging (LCI, Fujifilm Corporation)[33], texture and color enhancement imaging (TXI, Olympus Corporation), and using new colonoscopes, such as CF-EZ1500D and CF-XZ1200 (Olympus Corporation), are warranted. Fourth, the diagnostic efficacy of brown slit sign has not been proven to be

Table 1 Characteristics of study subjects

Patient (*n*)	62
Age [mean ± SD (range), yr]	60.4 ± 12.8, (40-89)
Sex (male)	41.9%
Polyp (*n*)	108
Location (cecum/ascending/transverse/descending/sigmoid/rectum, *n*)	13/20/38/7/25/5
Morphology (0-Is/0-IIa, *n*)	13/95
Size [mean ± SD (range), mm]	7.45 (2.83, 5-15)
Brown slits (positive/negative, n)	57/51
Endoscopic diagnosis (adenoma/SSL/hyperplastic polyp, *n*)	59/30/19
Histopathological diagnosis (adenoma/SSL/MVHP/GCHP, *n*)	59[1]/16/27/6
Endoscopist (1/2, *n*)	75/33
Endoscope (CF-HQ290Z/PCF-H290Z, *n*)	60/48

[1]All adenomas were tubular, low grade.
SD: Standard deviation; SSL: Sessile serrated lesion; MVHP: Microvesicular hyperplastic polyp; GCHP: Goblet cell-rich hyperplastic polyp.

Table 2 Number of colorectal lesions for brown slits

	Adenoma[1]	SSL	MVHP	GCHP
Positive	56	0	1	0
Negative	3	16	26	6

[1]All adenomas were tubular, low grade.
SSL: Sessile serrated lesion; MVHP: Microvesicular hyperplastic polyp; GCHP: Goblet cell-rich hyperplastic polyp.

Table 3 Diagnostic performance of brown slits for colorectal adenoma

Sensitivity	**94.9 (85.9-98.9)**
Specificity	98.0 (89.1-99.9)
Accuracy	96.3 (90.8-99.0)
Positive predictive value	98.2 (90.6-100)
Negative predictive value	94.1 (83.8-98.8)

Data are presented as percentage (95% confidence interval).

equivalent to that of the JNET classification, although the brown slit sign may be simpler and easier than the JNET classification. The comparison of the diagnostic efficacy between brown slit sign and the JNET classification is future issue.

CONCLUSION

Brown slits on conventional magnifying NBI endoscopy using the X1 system were useful for diagnosing colorectal adenoma. The new endoscopy system could be examined using new standards.

ARTICLE HIGHLIGHTS

Research background

Accurate diagnosis of colorectal premalignant polyps, including adenomas, is vital in clinical practice.

Research motivation

Using a combination of the X1 system and the conventional magnifying endoscope with non-staining narrow band imaging (NBI), we identified the findings corresponding to the slit-like lumens, which present the crypts of adenoma.

Research objectives

The authors investigated the diagnostic yields of novel findings of brown slits for adenomas.

Research methods

Patients who underwent colonoscopy at the Toyoshima Endoscopy Clinic were enrolled. Polyps sized ≥ 5 mm suspected of adenomas or clinically significant serrated polyps were included in the study. We defined the surface structures of colorectal polyps, which were brown curves inside and along the tubular glands identified using a combination of a new X1 system (Olympus Corporation) and a conventional magnifying colonoscope with non-staining NBI, as brown slits. The brown slits corresponded to slit-like lumens on endocytoscopy and histological crypt openings of an adenoma. We evaluated the diagnostic performance of brown slits for adenoma.

Research results

A total of 108 Lesions from 62 patients were eligible. The average age was 60.4 years and 41.9% were male. The mean polyp size was 7.45 mm. Fifty-seven lesions were positive for brown slits. Histopathological diagnosis comprised 59 low-grade tubular adenomas, 16 sessile serrated lesions, and 33 hyperplastic polyps. The sensitivity, specificity, and accuracy of brown slits for adenoma were 94.9%, 98.0%, and 96.3%, respectively.

Research conclusions

Brown slits on conventional magnifying endoscopy with non-staining NBI using the X1 system were useful for diagnosing colorectal adenoma.

Research perspectives

The new endoscopy system could be examined using new standards.

FOOTNOTES

Author contributions: Toyoshima O contributed to the study design, endoscopic diagnosis, writing the article, statistical analysis, and final manuscript approval; Nishizawa T contributed to study design, editing of article, and final manuscript approval; Yoshida S contributed to study design, endoscopic diagnosis, critical review, and final manuscript approval; Watanabe H contributed to study design, histological diagnosis, and final manuscript approval; Odawara N, Sakitani K, Arano T, Takiyama H, Kobayashi H, Kogure H and Fujishiro M contributed to critical review and final manuscript approval.

Institutional review board statement: This study was approved by the Certificated Review Board, Yoyogi Mental Clinic on July 16, 2021 (approval No. RKK227).

Conflict-of-interest statement: All authors have no any conflicts of interest.

Data sharing statement: No additional data are available.

Country/Territory of origin: Japan

ORCID number: Osamu Toyoshima 0000-0002-6953-6079; Toshihiro Nishizawa 0000-0003-4876-3384; Shuntaro Yoshida 0000-0002-9437-9132; Hidenobu Watanabe 0000-0002-7871-4738; Nariaki Odawara 0000-0002-9839-4700; Kosuke Sakitani 0000-0002-4537-6023; Toru Arano 0000-0003-3205-6669; Hirotoshi Takiyama 0000-0001-9994-4666; Hideyuki Kobayashi 0000-0002-3344-6848; Hirofumi Kogure 0000-0002-2355-7309; Mitsuhiro Fujishiro 0000-0002-4074-1140.

S-Editor: Ma YJ
L-Editor: A
P-Editor: Ma YJ

REFERENCES

1 **Nishihara R**, Wu K, Lochhead P, Morikawa T, Liao X, Qian ZR, Inamura K, Kim SA, Kuchiba A, Yamauchi M, Imamura Y, Willett WC, Rosner BA, Fuchs CS, Giovannucci E, Ogino S, Chan AT. Long-term colorectal-cancer incidence and mortality after lower endoscopy. *N Engl J Med* 2013; **369**: 1095-1105 [PMID: 24047059 DOI: 10.1056/NEJMoa1301969]
2 **Nagtegaal I**, Arends MJ, Odeze RD, Lam AK. Tumours of the colon and rectum. Lyon (France), 2019
3 **Hilsden RJ**, Rose SM, Dube C, Rostom A, Bridges R, McGregor SE, Brenner DR, Heitman SJ. Defining and Applying Locally Relevant Benchmarks for the Adenoma Detection Rate. *Am J Gastroenterol* 2019; **114**: 1315-1321 [PMID: 30848731 DOI: 10.14309/ajg.0000000000000120]
4 **Kaminski MF**, Wieszczy P, Rupinski M, Wojciechowska U, Didkowska J, Kraszewska E, Kobiela J, Franczyk R, Rupinska M, Kocot B, Chaber-Ciopinska A, Pachlewski J, Polkowski M, Regula J. Increased Rate of Adenoma Detection Associates With Reduced Risk of Colorectal Cancer and Death. *Gastroenterology* 2017; **153**: 98-105 [PMID: 28428142 DOI: 10.1053/j.gastro.2017.04.006]
5 **Toyoshima O**, Nishizawa T, Yoshida S, Sekiba K, Kataoka Y, Hata K, Watanabe H, Tsuji Y, Koike K. Expert endoscopists with high adenoma detection rates frequently detect diminutive adenomas in proximal colon. *Endosc Int Open* 2020; **8**: E775-E782 [PMID: 32490163 DOI: 10.1055/a-1136-9971]
6 **Toyoshima O**, Yoshida S, Nishizawa T, Yamakawa T, Arano T, Isomura Y, Kanazawa T, Ando H, Tsuji Y, Koike K. Simple feedback of colonoscopy performance improved the number of adenomas per colonoscopy and serrated polyp detection rate. *Endosc Int Open* 2021; **9**: E1032-E1038 [PMID: 34222627 DOI: 10.1055/a-1393-5469]
7 **East JE**, Atkin WS, Bateman AC, Clark SK, Dolwani S, Ket SN, Leedham SJ, Phull PS, Rutter MD, Shepherd NA, Tomlinson I, Rees CJ. British Society of Gastroenterology position statement on serrated polyps in the colon and rectum. *Gut* 2017; **66**: 1181-1196 [PMID: 28450390 DOI: 10.1136/gutjnl-2017-314005]
8 **Nagtegaal ID**, Odze RD, Klimstra D, Paradis V, Rugge M, Schirmacher P, Washington KM, Carneiro F, Cree IA; WHO Classification of Tumours Editorial Board. The 2019 WHO classification of tumours of the digestive system. *Histopathology* 2020; **76**: 182-188 [PMID: 31433515 DOI: 10.1111/his.13975]
9 **Rex DK**, Ahnen DJ, Baron JA, Batts KP, Burke CA, Burt RW, Goldblum JR, Guillem JG, Kahi CJ, Kalady MF, O'Brien MJ, Odze RD, Ogino S, Parry S, Snover DC, Torlakovic EE, Wise PE, Young J, Church J. Serrated lesions of the colorectum: review and recommendations from an expert panel. *Am J Gastroenterol* 2012; **107**: 1315-29; quiz 1314, 1330 [PMID: 22710576 DOI: 10.1038/ajg.2012.161]
10 **Anderson JC**, Butterly LF, Weiss JE, Robinson CM. Providing data for serrated polyp detection rate benchmarks: an analysis of the New Hampshire Colonoscopy Registry. *Gastrointest Endosc* 2017; **85**: 1188-1194 [PMID: 28153571 DOI: 10.1016/j.gie.2017.01.020]
11 **Li D**, Woolfrey J, Jiang SF, Jensen CD, Zhao WK, Kakar S, Santamaria M, Rumore G, Armstrong MA, Postlethwaite D, Corley DA, Levin TR. Diagnosis and predictors of sessile serrated adenoma after educational training in a large, community-based, integrated healthcare setting. *Gastrointest Endosc* 2018; **87**: 755-765.e1 [PMID: 28843582 DOI: 10.1016/j.gie.2017.08.012]
12 **Klair JS**, Ashat M, Johnson D, Arora S, Onteddu N, Machain Palacio JG, Samuel R, Bilal M, Buddam A, Gupta A, Gunderson A, Guturu P, Soota K, Chandra S, Murali AR. Serrated polyp detection rate and advanced adenoma detection rate from a US multicenter cohort. *Endoscopy* 2020; **52**: 61-67 [PMID: 31739370 DOI: 10.1055/a-1031-5672]
13 **Rees CJ**, Rajasekhar PT, Wilson A, Close H, Rutter MD, Saunders BP, East JE, Maier R, Moorghen M, Muhammad U, Hancock H, Jayaprakash A, MacDonald C, Ramadas A, Dhar A, Mason JM. Narrow band imaging optical diagnosis of small colorectal polyps in routine clinical practice: the Detect Inspect Characterise Resect and Discard 2 (DISCARD 2) study. *Gut* 2017; **66**: 887-895 [PMID: 27196576 DOI: 10.1136/gutjnl-2015-310584]
14 **Rutter MD**, East J, Rees CJ, Cripps N, Docherty J, Dolwani S, Kaye PV, Monahan KJ, Novelli MR, Plumb A, Saunders BP, Thomas-Gibson S, Tolan DJM, Whyte S, Bonnington S, Scope A, Wong R, Hibbert B, Marsh J, Moores B, Cross A, Sharp L. British Society of Gastroenterology/Association of Coloproctology of Great Britain and Ireland/Public Health England post-polypectomy and post-colorectal cancer resection surveillance guidelines. *Gut* 2020; **69**: 201-223 [PMID: 31776230 DOI: 10.1136/gutjnl-2019-319858]
15 **Gupta S**, Lieberman D, Anderson JC, Burke CA, Dominitz JA, Kaltenbach T, Robertson DJ, Shaukat A, Syngal S, Rex DK. Recommendations for Follow-Up After Colonoscopy and Polypectomy: A Consensus Update by the US Multi-Society Task Force on Colorectal Cancer. *Gastrointest Endosc* 2020; **91**: 463-485.e5 [PMID: 32044106 DOI: 10.1016/j.gie.2020.01.014]
16 **Li D**, Liu L, Fevrier HB, Alexeeff SE, Doherty AR, Raju M, Amsden LB, Lee JK, Levin TR, Corley DA, Herrinton LJ. Increased Risk of Colorectal Cancer in Individuals With a History of Serrated Polyps. *Gastroenterology* 2020; **159**: 502-511.e2 [PMID: 32277950 DOI: 10.1053/j.gastro.2020.04.004]
17 **Kudo S**, Rubio CA, Teixeira CR, Kashida H, Kogure E. Pit pattern in colorectal neoplasia: endoscopic magnifying view. *Endoscopy* 2001; **33**: 367-373 [PMID: 11315901 DOI: 10.1055/s-2004-826104]
18 **Sano Y**, Tanaka S, Kudo SE, Saito S, Matsuda T, Wada Y, Fujii T, Ikematsu H, Uraoka T, Kobayashi N, Nakamura H, Hotta K, Horimatsu T, Sakamoto N, Fu KI, Tsuruta O, Kawano H, Kashida H, Takeuchi Y, Machida H, Kusaka T, Yoshida N, Hirata I, Terai T, Yamano HO, Kaneko K, Nakajima T, Sakamoto T, Yamaguchi Y, Tamai N, Nakano N, Hayashi N, Oka S, Iwatate M, Ishikawa H, Murakami Y, Yoshida S, Saito Y. Narrow-band imaging (NBI) magnifying endoscopic classification of colorectal tumors proposed by the Japan NBI Expert Team. *Dig Endosc* 2016; **28**: 526-533 [PMID:

26927367 DOI: 10.1111/den.12644]
19 **Kobayashi S**, Yamada M, Takamaru H, Sakamoto T, Matsuda T, Sekine S, Igarashi Y, Saito Y. Diagnostic yield of the Japan NBI Expert Team (JNET) classification for endoscopic diagnosis of superficial colorectal neoplasms in a large-scale clinical practice database. *United European Gastroenterol J* 2019; **7**: 914-923 [PMID: 31428416 DOI: 10.1177/2050640619845987]
20 **Ito R**, Ikematsu H, Murano T, Shinmura K, Kojima M, Kumahara K, Furue Y, Sunakawa H, Minamide T, Sato D, Yamamoto Y, Takashima K, Yoda Y, Hori K, Yano T. Diagnostic ability of Japan Narrow-Band Imaging Expert Team classification for colorectal lesions by magnifying endoscopy with blue laser imaging versus narrow-band imaging. *Endosc Int Open* 2021; **9**: E271-E277 [PMID: 33553592 DOI: 10.1055/a-1324-3083]
21 **Sasajima K**, Kudo SE, Inoue H, Takeuchi T, Kashida H, Hidaka E, Kawachi H, Sakashita M, Tanaka J, Shiokawa A. Real-time in vivo virtual histology of colorectal lesions when using the endocytoscopy system. *Gastrointest Endosc* 2006; **63**: 1010-1017 [PMID: 16733118 DOI: 10.1016/j.gie.2006.01.021]
22 **Kudo SE**, Wakamura K, Ikehara N, Mori Y, Inoue H, Hamatani S. Diagnosis of colorectal lesions with a novel endocytoscopic classification - a pilot study. *Endoscopy* 2011; **43**: 869-875 [PMID: 21837586 DOI: 10.1055/s-0030-1256663]
23 **Mori Y**, Kudo S, Ikehara N, Wakamura K, Wada Y, Kutsukawa M, Misawa M, Kudo T, Kobayashi Y, Miyachi H, Yamamura F, Ohtsuka K, Inoue H, Hamatani S. Comprehensive diagnostic ability of endocytoscopy compared with biopsy for colorectal neoplasms: a prospective randomized noninferiority trial. *Endoscopy* 2013; **45**: 98-105 [PMID: 23307149 DOI: 10.1055/s-0032-1325932]
24 **Kudo T**, Suzuki K, Mori Y, Misawa M, Ichimasa K, Takeda K, Nakamura H, Maeda Y, Ogawa Y, Hayashi T, Wakamura K, Ishida F, Inoue H, Kudo SE. Endocytoscopy for the differential diagnosis of colorectal low-grade adenoma: a novel possibility for the "resect and discard" strategy. *Gastrointest Endosc* 2020; **91**: 676-683 [PMID: 31785276 DOI: 10.1016/j.gie.2019.11.029]
25 **Kudo SE**, Misawa M, Wada Y, Nakamura H, Kataoka S, Maeda Y, Toyoshima N, Hayashi S, Kutsukawa M, Oikawa H, Mori Y, Ogata N, Kudo T, Hisayuki T, Hayashi T, Wakamura K, Miyachi H, Ishida F, Inoue H. Endocytoscopic microvasculature evaluation is a reliable new diagnostic method for colorectal lesions (with video). *Gastrointest Endosc* 2015; **82**: 912-923 [PMID: 26071058 DOI: 10.1016/j.gie.2015.04.039]
26 **Kataoka S**, Kudo SE, Misawa M, Nakamura H, Takeda K, Toyoshima N, Mori Y, Ogata N, Kudo T, Hisayuki T, Hayashi T, Wakamura K, Baba T, Ishida F. Endocytoscopy with NBI has the potential to correctly diagnose diminutive colorectal polyps that are difficult to diagnose using conventional NBI. *Endosc Int Open* 2020; **8**: E360-E367 [PMID: 32118108 DOI: 10.1055/a-1068-9228]
27 **Ponugoti P**, Rastogi A, Kaltenbach T, MacPhail ME, Sullivan AW, Thygesen JC, Broadley HM, Rex DK. Disagreement between high confidence endoscopic adenoma prediction and histopathological diagnosis in colonic lesions ≤ 3 mm in size. *Endoscopy* 2019; **51**: 221-226 [PMID: 30722072 DOI: 10.1055/a-0831-2348]
28 **Nishizawa T**, Yoshida S, Toyoshima A, Yamada T, Sakaguchi Y, Irako T, Ebinuma H, Kanai T, Koike K, Toyoshima O. Endoscopic diagnosis for colorectal sessile serrated lesions. *World J Gastroenterol* 2021; **27**: 1321-1329 [PMID: 33833485 DOI: 10.3748/wjg.v27.i13.1321]
29 **Toyoshima O**, Yoshida S, Nishizawa T, Yamakawa T, Sakitani K, Hata K, Takahashi Y, Fujishiro M, Watanabe H, Koike K. CF290 for pancolonic chromoendoscopy improved sessile serrated polyp detection and procedure time: a propensity score-matching study. *Endosc Int Open* 2019; **7**: E987-E993 [PMID: 31367679 DOI: 10.1055/a-0953-1909]
30 **Ignjatovic A**, East JE, Suzuki N, Vance M, Guenther T, Saunders BP. Optical diagnosis of small colorectal polyps at routine colonoscopy (Detect InSpect ChAracterise Resect and Discard; DISCARD trial): a prospective cohort study. *Lancet Oncol* 2009; **10**: 1171-1178 [PMID: 19910250 DOI: 10.1016/S1470-2045(09)70329-8]
31 **Sako T**, Kudo SE, Miyachi H, Wakamura K, Igarashi K, Misawa M, Mori Y, Kudo T, Hayashi T, Katagiri A, Ishida F, Azuma T, Inoue H, Hamatani S. A novel ability of endocytoscopy to diagnose histological grade of differentiation in T1 colorectal carcinomas. *Endoscopy* 2018; **50**: 69-74 [PMID: 28962043 DOI: 10.1055/s-0043-117403]
32 **Takeda K**, Kudo SE, Misawa M, Mori Y, Kudo T, Kodama K, Wakamura K, Miyachi H, Hidaka E, Ishida F, Inoue H. Comparison of the endocytoscopic and clinicopathologic features of colorectal neoplasms. *Endosc Int Open* 2016; **4**: E397-E402 [PMID: 27547815 DOI: 10.1055/s-0042-101753]
33 **Paggi S**, Radaelli F, Senore C, Maselli R, Amato A, Andrisani G, Di Matteo F, Cecinato P, Grillo S, Sereni G, Sassatelli R, Manfredi G, Alicante S, Buscarini E, Canova D, Milan L, Pallini P, Iwatate M, Rondonotti E, Repici A, Hassan C. Linked-color imaging versus white-light colonoscopy in an organized colorectal cancer screening program. *Gastrointest Endosc* 2020; **92**: 723-730 [PMID: 32502550 DOI: 10.1016/j.gie.2020.05.044]

World Journal of Gastroenterology

Submit a Manuscript: https://www.f6publishing.com

World J Gastroenterol 2022 June 28; 28(24): 2758-2774

DOI: 10.3748/wjg.v28.i24.2758

ISSN 1007-9327 (print) ISSN 2219-2840 (online)

ORIGINAL ARTICLE

Observational Study

Usefulness of serum C-reactive protein and calprotectin for the early detection of colorectal anastomotic leakage: A prospective observational study

Nuno J G Rama, Marlene C C Lages, Maria Pedro S Guarino, Óscar Lourenço, Patrícia C Motta Lima, Diana Parente, Cândida S G Silva, Ricardo Castro, Ana Bento, Anabela Rocha, Fernando Castro-Pocas, João Pimentel

Specialty type: Surgery

Provenance and peer review: Unsolicited article; Externally peer reviewed.

Peer-review model: Single blind

Peer-review report's scientific quality classification

Grade A (Excellent): 0
Grade B (Very good): B
Grade C (Good): C
Grade D (Fair): D
Grade E (Poor): 0

P-Reviewer: Fiori E, Italy; Kayano H, Japan; Yan T, China

Received: January 13, 2022
Peer-review started: January 13, 2022
First decision: March 8, 2022
Revised: March 22, 2022
Accepted: May 14, 2022
Article in press: May 14, 2022
Published online: June 28, 2022

Nuno J G Rama, Patrícia C Motta Lima, Diana Parente, Colorectal Surgical Division, Leiria Hospital Centre, Leiria 2410-021, Portugal

Nuno J G Rama, Anabela Rocha, Fernando Castro-Pocas, Abel Salazar Biomedical Institute (ICBAS), University of Oporto, Oporto 4099-002, Portugal

Nuno J G Rama, Marlene C C Lages, Maria Pedro S Guarino, Cândida S G Silva, Center for Innovative Care and Health Technology (ciTechCare), Polytechnic of Leiria, Leiria 2410-541, Portugal

Óscar Lourenço, Faculty of Economics, CeBER, University of Coimbra, Coimbra 3000-137, Portugal

Ricardo Castro, Ana Bento, Clinical Pathology Division, Leiria Hospital Centre, Leiria 2410-541, Portugal

Anabela Rocha, Surgical Division, Oporto Hospital Centre, Oporto 4099-001, Portugal

Fernando Castro-Pocas, Department of Gastroenterology, Santo António Hospital, Porto Hospital Center, Porto 4099-001, Portugal

Fernando Castro-Pocas, Institute of Biomedical Sciences Abel Salazar, University of Porto, Porto 4099-001, Portugal

João Pimentel, Faculty of Medicine, University of Coimbra, Coimbra 3004-531, Portugal

João Pimentel, Surgical Division, Montes Claros Hospital, Coimbra 3030-320, Portugal

Corresponding author: Nuno JG Rama, FEBS, MD, MHSc, Associate Professor, Research Assistant Professor, Surgeon, Colorectal Surgical Division, Leiria Hospital Centre, Rua das Olhalvas, Leiria 2410-021, Portugal. ramanuno@gmail.com

Abstract

BACKGROUND

Colorectal anastomotic leakage (CAL) is one of the most dreaded complications

after colorectal surgery, with an incidence that can be as high as 27%. This event is associated with increased morbidity and mortality; therefore, its early diagnosis is crucial to reduce clinical consequences and costs. Some biomarkers have been suggested as laboratory tools for the diagnosis of CAL.

AIM

To assess the usefulness of plasma C-reactive protein (CRP) and calprotectin (CLP) as early predictors of CAL.

METHODS

A prospective monocentric observational study was conducted including patients who underwent colorectal resection with anastomosis, from March 2017 to August 2019. Patients were divided into three groups: G1 – no complications; G2 – complications not related to CAL; and G3 – CAL. Five biomarkers were measured and analyzed in the first 5 postoperative days (PODs), namely white blood cell (WBC) count, eosinophil cell count (ECC), CRP, CLP, and procalcitonin (PCT). Clinical criteria, such as abdominal pain and clinical condition, were also assessed. The correlation between biomarkers and CAL was evaluated. Receiver operating characteristic (ROC) curve analysis was used to compare the accuracy of these biomarkers as predictors of CAL, and the area under the ROC curve (AUROC), specificity, sensitivity, positive predictive value, and negative predictive value (NPV) during this period were estimated.

RESULTS

In total, 25 of 396 patients developed CAL (6.3%), and the mean time for this diagnosis was 9.0 ± 6.8 d. Some operative characteristics, such as surgical approach, blood loss, intraoperative complications, and duration of the procedure, were notably related to the development of CAL. The length of hospital stay was markedly higher in the group that developed CAL compared with the group with complications other than CAL and the group with no complications (median of 21 d *vs* 13 d and 7 d respectively; $P < 0.001$). For abdominal pain, the best predictive performance was on POD4 and POD5, with the largest AUROC of 0.84 on POD4. Worsening of the clinical condition was associated with the diagnosis of CAL, presenting a higher predictive effect on POD5, with an AUROC of 0.9. WBC and ECC showed better predictive effects on POD5 (AUROC = 0.62 and 0.7, respectively). Those markers also presented a high NPV (94%-98%). PCT had the best predictive effect on POD5 (AUROC = 0.61), although it presented low accuracy. However, this biomarker revealed a high NPV on POD3, POD4, and POD5 (96%, 95%, and 96%, respectively). The mean CRP value on POD5 was significantly higher in the group that developed CAL compared with the group without complications (195.5 ± 139.9 mg/L *vs* 59.5 ± 43.4 mg/L; $P < 0.00001$). On POD5, CRP had a NPV of 98%. The mean CLP value on POD3 was significantly higher in G3 compared with G1 (5.26 ± 3.58 μg/mL *vs* 11.52 ± 6.81 μg/mL; $P < 0.00005$). On POD3, the combination of CLP and CRP values showed a high diagnostic accuracy (AUROC = 0.82), providing a 5.2 d reduction in the time to CAL diagnosis.

CONCLUSION

CRP and CLP are moderate predictors of CAL. However, the combination of these biomarkers presents an increased diagnostic accuracy, potentially decreasing the time to CAL diagnosis.

Key Words: Anastomotic leakage; Colorectal; Surgery; Biomarkers; C-reactive protein; Calprotectin

Core Tip: Colorectal anastomotic leakage (CAL) remains a serious postoperative complication. It is associated with high morbidity rates, affecting overall costs and patients' quality of life. Clinical criteria, imaging studies, and biomarkers have been considered to increase diagnostic accuracy. Plasma C-reactive protein, calprotectin, procalcitonin, white blood cell count, and eosinophil cell count have been proposed as predictors of anastomotic leakage. The combination of C-reactive protein and calprotectin after a minimal clinical suspicion of CAL has shown good diagnostic accuracy, allowing clinicians to reduce the time to CAL detection. Regression models can facilitate building a decision model, as the score proposed for the early detection of CAL.

Citation: Rama NJG, Lages MCC, Guarino MPS, Lourenço Ó, Motta Lima PC, Parente D, Silva CSG, Castro R, Bento A, Rocha A, Castro-Pocas F, Pimentel J. Usefulness of serum C-reactive protein and calprotectin for the early detection of colorectal anastomotic leakage: A prospective observational study. *World J Gastroenterol* 2022; 28(24): 2758-2774
URL: https://www.wjgnet.com/1007-9327/full/v28/i24/2758.htm
DOI: https://dx.doi.org/10.3748/wjg.v28.i24.2758

INTRODUCTION

Colorectal anastomotic leakage (CAL) is one of the most frequent complications after colorectal surgery, representing a dreaded issue for patients and surgeons. The reported incidence ranges from 0.2% to 27.2%, depending on the study nature, level of anastomosis, or pathology[1-5]. This occurrence is associated with increased morbidity, mortality, reoperation, and health care costs[6-9]. Thus, its clinical relevance should not be underestimated. It also has a negative impact on a patient's quality of life[2,4].

Early CAL detection is key to decreasing related morbidity and mortality; therefore, a prompt and timely diagnosis is crucial[5,10,11]. Initially, it is difficult to distinguish CAL from other postoperative abdominal complications. Surgeons should be aware of subtle clinical signs, and then order additional tests including serum biomarkers, proper imaging, or even early reoperation. Unfortunately, diagnosis is often delayed, because of a misleading clinical picture, non-systematic assessment, or inconclusive investigations[11-15]. Besides clinical parameters, several biomarkers (plasma or intraperitoneal), imaging methods such as abdominal computed tomography (CT) scan or water-soluble contrast enema, and scores have been proposed to reduce the time to diagnosis and to establish an appropriate management pathway[16-19].

Plasma C-reactive protein (CRP) has been proposed as an early predictor of postoperative infectious complications[16,20-23]. This biomarker is an acute phase protein, increasing between 6 h and 48 h after surgery, and returning to baseline if inflammation ceases. After this period, a high CRP level is associated with postoperative infectious complications, especially in patients with CAL[24-26]. On the other hand, calprotectin (CLP) is a useful biomarker of inflammation and infection[18,27]. Fecal CLP has been widely used as a marker of gastrointestinal inflammation. However, some authors suggest that high levels of serum CLP could be associated with septic intra-abdominal complications, such as early-stage CAL[18,28].

The aim of this study was to evaluate the utility of plasma CRP and CLP, individually or combined, to shorten the time to CAL diagnosis.

MATERIALS AND METHODS

Study design and population

This was a prospective observational, single-center study that included adults over 18-years-old who underwent urgent or elective colorectal resection, regardless of the surgical approach (open or laparoscopic), indication (benign or malignant), and option for a protective stoma. The study was conducted in the colorectal division of a non-academic hospital accredited by Joint Commission International® and included about 500000 inhabitants. The data were collected between March 1, 2017 and August 31, 2019. The local ethics committee approved the study, and potential participants provided written informed consent before inclusion.

Definitions

CAL was defined in accordance with the following criteria[29]: (1) Clinical: Enteric discharge from abdominal drain or wound, rectovaginal fistula, or anastomotic defect found by digital examination; (2) Radiological (CT): Extravasation of endoluminally administered contrast, intra-abdominal collection around the anastomosis, presacral abscess near the anastomosis or perianastomotic air, and free intra-abdominal air; and (3) Surgical findings (reoperation): Necrosis of the anastomosis or signs of peritonitis and anastomotic defect.

Faced with clinical deterioration and/or serum biomarker increase, patients underwent further imaging with abdominopelvic CT scan (and water-soluble contrast enema if colorectal anastomosis was present). Once diagnosed, anastomotic leakage was classified into two categories: (1) Minor: Patients with CAL and Clavien-Dindo grade I or II, requiring no active intervention (radiological or surgical intervention) (Grade A of the International Study Group of Rectal Cancer definition); and (2) Major: All other patients with CAL[30,31]. Definitions of other postoperative complications, such as pneumonia, urinary tract infection, paralytic ileus, and surgical wound infection, are available in Supplementary material 1A (Definitions).

Exclusion criteria

Patients were excluded from the study if they were younger than 18-year-old, pregnant, unable to give or not providing written informed consent, R0 resection with anastomosis not having been performed, or presence of inflammatory bowel disease.

Study protocol and variables

Prospective data were collected and recorded in an electronic database according to the study protocol (Supplementary material 1B – Study protocol). Five biomarkers were measured in the first 5 postoperative days (POD), including white blood cell (WBC) count, eosinophil cell count (ECC), CRP, CLP, and procalcitonin (PCT). Clinical criteria, such as abdominal pain and clinical condition, were also assessed. Blood samples were analyzed at the Leiria Hospital Centre laboratory, according to the techniques described in Supplementary material 1C (Laboratory). The 90-d follow-up included data of all postoperative complications, the length of hospital stay, and the readmission rate. Discharge criteria are available in the Supplementary material 1B (Study protocol). All patients received prophylactic antibiotic accordingly to hospital infection control committee protocol.

Statistical analysis

Data were analyzed by using standard descriptive statistics and graphical analysis. One-way analysis of variance was performed to compare the differences in mean biomarkers' values across the three relevant groups of patients (G1 – no complications; G2 – complications not related to CAL; and G3 – CAL). Chi-squared tests were conducted to assess the association between other categorical variables and the patients. Receiver operating characteristic (ROC) curve analysis was employed to evaluate each biomarker as an appropriate classifier to detect CAL early. The area under the receiver operating characteristic curve (AUROC) was used to establish the diagnostic performance of the studied biomarker. Liu's method was used to establish the threshold value of each biomarker, and its sensitivity (SS) and specificity (SP) were defined[32]. The negative likelihood ratio (NLR) and positive likelihood ratio (PLR), and the negative predictive value (NPV) and positive predictive value (PPV) were computed by combining the observed incidence of CAL with the estimated SS and SP at the optimum cut-off value.

The added value of combining two different biomarkers, observed on POD3 or POD5, as a classifier to predict early CAL was explored. Regression models (probit, logit, and complementary log-log) were used to analyze binary dependent variables, and the observed CAL status (0/1) in a pairwise manner of all biomarkers included in our study: WBC, ECC, CRP, PCT, and CLP. Several potential classifiers of CAL were built, applying a non-linear combination of two different biomarkers. To minimize overfitting, the "leave-one-out" methodology was adopted[33]. The AUROC graph was used to select the classifier (defined by the model and the combination of two biomarkers) with the best predictive diagnostic performance. Liu's method was adopted to select the cut-off value for CAL.

The expected reduction in time to CAL diagnosis obtained by using one biomarker or a pairwise combination of biomarkers was estimated. This was the difference between the observed and the expected mean time to CAL diagnosis, if a specific classifier is used. The expected time to CAL diagnosis was computed by using the following expression: $S \times d1 + [(1 - S) \times d2]$, where S is the SS of the classifier, d1 is the POD of the classifier yielding a positive cut-off value for CAL, and d2 is the day of diagnosis if the classifier provides a false-negative result (time to CAL diagnosis estimated in the dataset). The statistical methods of this study were reviewed by Óscar Lourenço from the Faculty of Economics, CeBER, University of Coimbra, Portugal. All data management and statistical analyses were conducted with Stata Statistical software (Release 16; StataCorp, College Station, TX, United States).

RESULTS

Patients and outcomes

During the study period, we included 458 consecutive patients who underwent colorectal resection, and 62 (13.5%) were ruled out [exclusion criteria (n = 31), no consent (n = 15), no anastomosis (n = 16)] as shown in Figure 1. Patient characteristics, divided into three groups (G1, G2, and G3, as previously defined), are shown in Table 1. Age, the Charlson Comorbidity Index, and American Society of Anesthesiologists grade seem to affect CAL onset.

Table 2 summarizes the main operative characteristics. Eighty-two percent of patients had a laparoscopic approach, and the most common procedures performed were right colectomy (n = 196; 49.5%) and sigmoid colectomy/rectosigmoid resection (n = 74; 18.7%). The surgical approach ($P < 0.001$), the volume of blood loss ($P < 0.001$), the occurrence of intraoperative complications ($P < 0.001$), and the duration of the procedure ($P = 0.011$) were significantly related to the development of CAL.

In this study, CAL developed in 25 of 396 patients (6.3%) and was more frequent in men than women (68% *vs* 32%). Twenty-three patients with CAL (92.0%) were diagnosed during the first hospital admission. The mean ± SD and median time for CAL detection were 9.0 ± 6.8 d and 8 d (interquartile range = 7), respectively. Anastomotic leak was significantly associated with a longer hospital stay

Table 1 Patient demographic and clinical characteristics

	Group 1, *n* = 277	Group 2, *n* = 94	Group 3, *n* = 25	*P* value
Age, mean ± SD	68.8 ± 11.3	72.2 ± 14.5	73.6 ± 13.6	0.02
Sex, *n* (%)				0.505
Male	161 (58.1)	59 (62.7)	17 (68.0)	
Female	116 (41.9)	35 (37.3)	8 (32.0)	
BMI, mean ± SD	26.8 ± 3.99	26.3 ± 4.05	26.0 ± 3.97	0.33
BMI, *n* (%)				0.33
17.5 < BMI < 25	95 (35.0)	32 (34.0)	12 (48.0)	
25 ≤ BMI < 30	129 (46.0)	51 (54.0)	9 (36.0)	
BMI ≥ 30	53 (19.0)	11 (12.0)	4 (16.0)	
CCI, mean ± SD	5.12 ± 1.83	5.55 ± 2.38	6.04 ± 2.15	0.03
Prior abdominal surgery, *n* (%)	77 (27.8)	32 (34.0)	9 (36.0)	0.41
Immunosuppression, *n* (%)	10 (3.6)	5 (5.3)	0 (0)	0.45
Preoperative diagnosis malignant, *n* (%)	272 (98.2)	90 (95.7)	24 (96.0)	0.38
ASA score, *n* (%)				0.018
I–II	187 (67.5)	47 (50.0)	13 (45.8)	
III–IV	90 (32.5)	47 (50.0)	12 (54.2)	

Group 1: No complications; Group 2: Complications not related to colorectal anastomotic leakage (CAL); Group 3: CAL. BMI: Body mass index; CCI: Charlson Comorbidity Index; ASA: American Society of Anesthesiologists.

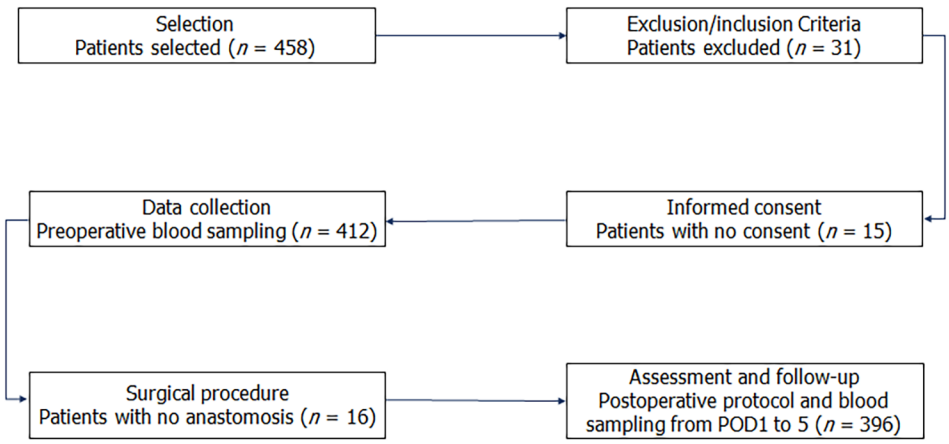

DOI: 10.3748/wjg.v28.i24.2758

Figure 1 Flow diagram of patients according to the study protocol. POD1: Postoperative day 1.

(median of 21 d *vs* 7 d and 13 d, in G1 and G2 patients, respectively; $P < 0.001$), the readmission rate (20% *vs* 6.4% and 5.4%), and the reoperation rate (12% *vs* 3.2% and 1.8%). Table 3 provides a summary of 90-d morbidity and mortality rates. Based on the Clavien-Dindo classification, grades III and IV complication were significantly higher in the G3 cohort (84.0% *vs* 17.0%; $P < 0.001$) (Table 4).

Table 5 outlines the intraoperative and postoperative details of patients with CAL (G3) based on the CAL classification (minor *vs* major). Seven patients (28.0%) were managed nonoperatively and two (8.0%) underwent radiologic drainage of intraabdominal collections. The remaining 16 patients (64.0%) required surgical intervention. Of the 16 reoperated patients, 10 (56%) had an anastomosis takedown with an end stoma and 6 (44%) received a defunctioning stoma. The 90-d mortality rate was 0.8%, representing 3 patients with CAL.

Table 2 Patients' operative characteristics

	Group 1, *n* = 277	Group 2, *n* = 94	Group 3, *n* = 25	*P* value
Type of surgery, *n* (%)				0.071
Elective	238 (86.0)	72 (76.6)	19 (75.0)	
Urgent	39 (14.0)	22 (23.4)	6 (25.0)	
Surgical approach, *n* (%)				< 0.001
Open	25 (9.0)	15 (16.0)	2 (8.0)	
Laparoscopic	238 (86.0)	72 (77.0)	15 (60.0)	
Conversion	14 (5.0)	7 (7.4)	8 (32.0)	
Procedure, *n* (%)				0.739
Right colectomy[1]	138 (49.8)	47 (50.0)	11 (44.0)	
Left colectomy	17 (6.1)	7 (7.4)	1 (4.0)	
Sigmoid/RS resection	55 (19.8)	15 (15.9)	4 (16.0)	
Low anterior resection	48 (17.3)	16 (17.0)	8 (32.0)	
Other	19 (6.8)	9 (9.6)	1 (4.0)	
Level of anastomosis, *n* (%)				0.66
Ileocolic	150 (54.1)	50 (53.2)	11 (44.0)	
Colocolic	23 (8.3)	5 (5.3)	1 (4.0)	
≥ 6 cm from AV	67 (24.2)	25 (26.6)	10 (40.0)	
< 6 cm from AV	37 (13.4)	14 (14.9)	3 (12.0)	
Covering stoma, *n* (%)	23 (8.3)	8 (8.51)	2 (8.0)	0.99
Blood loss, mean ± SD, mL	51.6 ± 36.6	58.8 ± 47.7	104.0 ± 191.1	< 0.001
Intraoperative complications, *n* (%)	3 (1.1)	5 (5.3)	4 (16.0)	< 0.001
Operative time in min, mean ± SD	141.9 (48.3)	146.2 (50.0)	172.8 (57.2)	0.011

[1]Included ileocecal resection/extended right-sided colectomy.

Group 1: No complications; Group 2: Complications not related to colorectal anastomotic leakage (CAL); Group 3: CAL. RS: Rectosigmoid; AV: Anal verge.

Clinical criteria – postoperative trend and predictive effect

Abdominal pain: Abdominal pain was markedly higher and persistent from POD3 onwards in G3 patients (Figure 2A). The AUROC for abdominal pain on POD3, POD4, and POD5 was 0.77, 0.84, and 0.83, respectively, as shown in Supplementary Table E (Supplementary material 2A) and Figure 3A. The predictive effect was higher on POD4 with an estimated AUROC of 0.84.

Clinical condition: The clinical condition was worse in G3 compared with G2 patients, and it was significantly different after POD3 (P = 0.001). The overall postoperative trend was a declining clinical condition, as shown in Figure 2B. The AUROC for the clinical condition on POD3, POD4, and POD5 was 0.62, 0.81, and 0.90, respectively, as shown in Supplementary Table E (Supplementary material 2A) and Figure 3B. The prediction effect was higher on POD5 with an estimated AUROC of 0.90.

Biomarkers – postoperative trend and predictive effect

WBC count and ECC: During the first five POD, WBC in G3 patients was higher than that in patients without CAL and was significantly different on POD2, POD4, and POD5 (P = 0.01 for each day). On the other hand, ECC was lower in G3 patients and significantly different on POD1 and POD5 (P = 0.04 and P = 0.01, respectively), as presented in Supplementary Figures 1 and 2 (Supplementary material 2B). Overall, the postoperative course showed a sustained trend for both blood cell counts, except for ECC on POD5. The AUROC for WBC and ECC from POD1 to POD5 is presented in Supplementary Figures 3 and 4, respectively (Supplementary material 2B). The predictive effects of blood cell count were better on POD5. On POD5, when ECC was greater than 250 cells/μL, the AUROC, SS, and SP were 0.70, 89.0%, and 43.0%, respectively, as shown in Table 6.

CRP, PCT, and CLP: The mean values of CRP, PCT, and CLP increased promptly after surgery in all

Table 3 Ninety-day postoperative morbidity and mortality

	Patients, *n* (%)	Length of hospital stay in d, mean ± SD
With complications	119 (30.0)	16.4 ± 9.91
With no complications	277 (70)	7.4 ± 2.10
Noninfectious complications	49 (41.2)	14.2 ± 6.93
Infectious complications		
Surgical wound	36 (30.3)	14.6 ± 8.34
Respiratory tract	10 (8.4)	16.1 ± 7.22
Urinary tract	11 (9.2)	16.2 ± 6.00
Anastomotic leakage classification		
Minor	7 (28)	28.0 ± 17.00
Major	18 (72)	22.4 ± 12.88
Postoperative mortality	3 (0.8)	NA

NA: Not applicable.

Table 4 Short-term outcomes by group

	Group 1, *n* = 277	Group 2, *n* = 94	Group 3, *n* = 25	*P* value
LOHS in d				< 0.001
mean ± SD	7.4 ± 2.1	14.3 ± 7.4	24.0 ± 14.0	
Median	7	13	21	
90-d morbidity, *n* (%)				< 0.001
Clavien-Dindo I	NA	64 (68.1)	0 (0)	
Clavien-Dindo II		14 (14.9)	4 (16.0)	
Clavien-Dindo III		8 (8.5)	16 (64.0)	
Clavien-Dindo IV		8 (8.5)	5 (20.0)	
Readmission, *n* (%)	15 (5.4)	6 (6.4)	5 (20.0)	0.019
Reoperation, *n* (%)	4 (1.1)	3 (3.2)	3 (12.0)	0.005
90-d mortality, *n* (%)	0 (0)	0 (0)	3 (12.0)	< 0.001

Group 1: No complications; Group 2: Complications not related to colorectal anastomotic leakage (CAL); Group 3: CAL. LOHS: Length of hospital stay; NA: Not applicable.

groups. CRP decreased in G1 patients and remained elevated in patients with a complicated postoperative course, but was significantly higher than in G3 patients. On POD5, the mean CRP level in G3 patients was significantly higher than that in G1 patients (195.5 ± 139.9 mg/L *vs* 59.5 ± 43.4 mg/L; $P < 0.00001$) (Figure 4A). Patients with major CAL had a higher mean CRP level than those with minor CAL (251.45 mg/dL *vs* 107.64 mg/dL; $P = 0.01$) (Table 5). On POD3, POD4, and POD5, the overall diagnostic accuracy of CRP to detect CAL was expressed by an AUROC of 0.76, 0.76, and 0.81, respectively (Figure 5A). On POD5, the optimum cut-off value of 96.8 mg/L was estimated, resulting in an SS and SP of 78%, an NPV of 98%, and a PPV of 19% (Table 6).

The PCT level tended to be stable from POD3 onwards. The mean values were higher in G3 patients than in patients without CAL, but without statistical significance [on POD5, 0.23 ± 0.08 ng/mL *vs* 0.22 ± 0.07 ng/mL; Supplementary Figure 5 (Supplementary material 2C)]. The AUROC on POD3, POD4, and POD5 was 0.57, 0.50, and 0.61, respectively, as shown in Supplementary Figure 6 (Supplementary material 2C). The best predictive effect was on POD5. When PCT was greater than 0.39 ng/mL, the SS and SP were 44.0% and 79.0%, respectively (Table 6).

Table 5 Intraoperative and postoperative details of patients with colorectal anastomotic leakage (minor *vs* major)

	Minor CAL, *n* = 7	Major CAL, *n* = 18	*P* value
Type of anastomosis, *n* (%)			0.52
Intrabdominal	3 (42.8)	9 (50.0)	
Pelvic	4 (57.2)	9 (50.0)	
Covering stoma, *n* (%)	1 (14.3)	1 (5.6)	0.47
Abdominal pain			
POD3	1.86	1.94	0.08
POD4	1.57	2.13	0.04
POD5	1.86	1.92	0.03
Clinical condition			
POD3	1	1.25	0.07
POD4	1.14	1.47	0.13
POD5	1.29	1.58	0.02
CRP levels in mg/L			
POD3	178.35	221.02	0.28
POD4	146.30	226.01	0.13
POD5	107.64	251.45	0.01
CLP levels in μg/mL			
POD3	2.75	12.99	< 0.001
POD4	3.34	10.60	0.01
POD5	2.52	10.96	0.004
CAL diagnosis in d, median	8	5.5	0.07
Diagnostic method, *n* (%)			0.12
Clinical	0 (0)	7 (38.9)	
Abdominopelvic CT	7 (100)	11 (61.1)	
CAL management, *n* (%)			< 0.001
Drainage	NA	2 (11.1)	
Reoperation		16 (88.9)	
LOHS in d, mean ± SD	28.0 ± 17.0	22.4 ± 12.9	0.38

CAL: Colorectal anastomotic leakage; POD: Postoperative day; CRP: C-reactive protein; CLP: Calprotectin; CT: Computed tomography; LOHS: Length of hospital stay; NA: Not applicable.

In the first 5 POD, the mean CLP value tended to follow the pattern of CRP, although it was not as pronounced (Figure 4B). The mean CLP value was significantly higher in G3 patients from POD2 onwards. On POD3, the mean values of G1 *vs* G3 patients were 5.26 ± 3.58 μg/mL *vs* 11.52 ± 6.81 μg/mL ($P < 0.00005$). On POD3, POD4, and POD5, the CLP AUROC was 0.78, 0.67, and 0.65, respectively, as presented in Table 6 and Figure 5B. On POD3, a cut-off value of 6.57 μg/mL yielded a sensitivity of 71.0% and a specificity of 72.0% (Table 6).

Finally, when we analyzed the best predictors (CRP and CLP) for major CAL, the AUROC of CRP was 0.74 and 0.88 for POD3 and POD5, respectively. CLP was a better predictor of CAL than CRP at POD3, with an AUROC of 0.92 (Figure 5C and D).

Combination of biomarkers: Tables 7 and 8 present the AUROC of several possible classifiers of CAL, built with the Probit model, on POD3 and POD5, respectively. The combination of CRP and CLP on POD3 showed the best performance, with an AUROC of 0.82 (Table 7). Of note, on POD5, the combination of CRP and ECC also generated good predictive performance (AUROC = 0.81). However, with the aim of early CAL diagnosis, we chose the combination of CRP and CLP on POD3. Thereafter, we determined the probability of CAL, based on the computed equation P (CAL) = F [-3.0842 + (0.094 ×

Table 6 Summary of the predictive performance of the studied plasma biomarkers

	AUROC	Cut-off value	SS	SP	NPV	PPV	PLR	NLR
WBC in g/L								
POD3	0.57	9.75	0.46	0.75	0.95	0.11	1.84	0.72
POD4	0.60	8.25	0.52	0.68	0.96	0.10	1.64	0.70
POD5	0.62	7.55	0.56	0.62	0.95	0.09	1.48	0.71
ECC in cells/μL								
POD3	0.59	150	0.50	0.59	0.95	0.08	1.23	0.84
POD4	0.54	150	0.33	0.71	0.94	0.07	1.14	0.94
POD5	0.70	250	0.89	0.43	0.98	0.10	1.55	0.26
CRP in mg/L								
POD3	0.76	175.90	0.64	0.83	0.97	0.20	3.77	0.44
POD4	0.76	152.40	0.62	0.89	0.97	0.27	5.40	0.43
POD5	0.81	96.80	0.78	0.78	0.98	0.19	3.48	0.29
PCT in ng/mL								
POD3	0.57	0.19	0.68	0.47	0.96	0.08	1.28	0.68
POD4	0.50	0.31	0.38	0.76	0.95	0.10	1.56	0.82
POD5	0.61	0.39	0.44	0.79	0.96	0.12	2.10	0.71
CLP in μg/mL								
POD3	0.78	6.57	0.71	0.72	0.97	0.15	2.55	0.40
POD4	0.67	8.34	0.56	0.86	0.97	0.21	3.89	0.51
POD5	0.65	6.98	0.58	0.80	0.97	0.16	2.84	0.52

AUROC: Area under the receiver operating characteristic curve; SS: Sensitivity; SP: Specificity; NPV: Negative predictive value; PPV: Positive predictive value; PLR: Positive likelihood ratio; NLR: Negative likelihood ratio; WBC: White blood cell count; POD: Postoperative day; ECC: Eosinophil cell count; CRP: C-reactive protein; PCT: Procalcitonin; CLP: Calprotectin.

Table 7 Area under the receiver operating characteristic curve of pairwise combination of biomarkers on postoperative day 3

	CLP	PCT	CRP	ECC
PCT	0.76			
CRP	0.82	0.72		
ECC	0.77	0.52	0.72	
WBC	0.74	0.53	0.72	0.54

CLP: Calprotectin; PCT: Procalcitonin; CRP: C-reactive protein; ECC: Eosinophil cell count; WBC: White blood cell count.

CLP_D3) + (0.0059 × CRP_D3)], where F is the cumulative standard normal distribution. Applying Liu's method, this classifier had an optimum cut-off point of 0.055, evidencing the existence of CAL above 0.055 on POD3, with an SS and SP of 86% and 75%, respectively. For hypothetical patient X on POD3 with CRP and CLP plasma levels of 137.4 mg/L and 8.75 μg/mL, respectively, the computed probability of CAL is high (score = 0.074). By adopting this classifier, the time to CAL diagnosis is estimated as 3.8 d [(0.86 × 3) + (0.14 × 9.0)], which represents a 5.2-d reduction compared with the baseline results.

Table 8 Area under the receiver operating characteristic curve of pairwise combination of biomarkers on postoperative day 5

	CLP	PCT	CRP	ECC
PCT	0.60			
CRP	0.78	0.79		
ECC	0.61	0.63	0.81	
WBC	0.57	0.60	0.78	0.67

CLP: Calprotectin; PCT: Procalcitonin; CRP: C-reactive protein; ECC: Eosinophil cell count; WBC: White blood cell count.

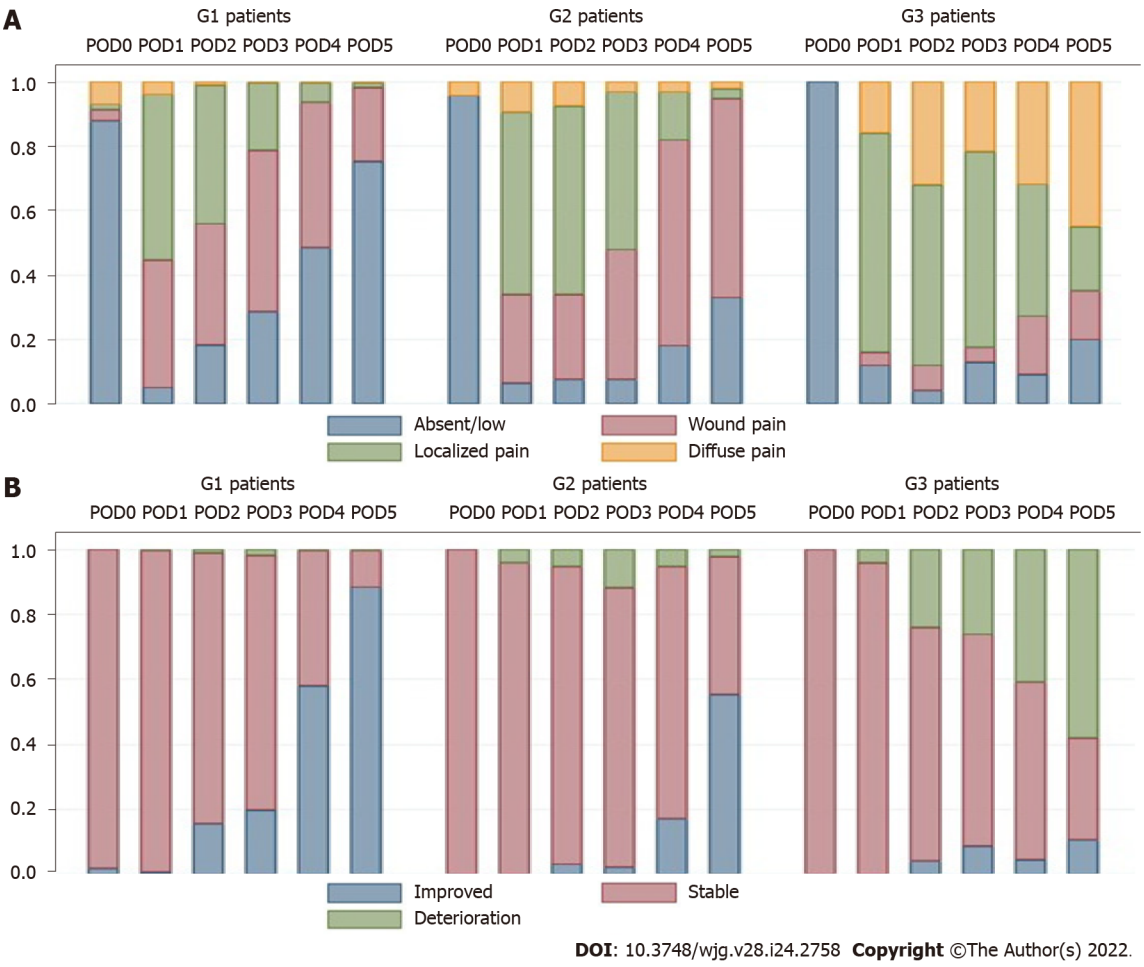

DOI: 10.3748/wjg.v28.i24.2758

Figure 2 Distribution of rates of abdominal pain (A) and clinical condition (B). G1: No complications; G2: Complications not related to colorectal anastomotic leakage; G3: CAL. POD: Postoperative day.

DISCUSSION

This study assessed the usefulness of biomarkers for the early detection of CAL. Clinical criteria demonstrated high diagnostic accuracy (AUROC > 0.8) on POD4 and POD5. Changes in the abdominal pain pattern and worsening of the clinical condition were associated with an increased risk of CAL diagnosis. Both clinical criteria seem to be an useful early markers for this condition, producing the best overall diagnostic accuracy of the parameters analyzed. Three large and well-conducted studies on the association between pain and postoperative complications are worth reporting. Boström *et al*[34] examined a cohort of 3084 patients and estimated that increased postoperative pain is associated with a high risk of CAL, being an independent marker and suggesting a need for further diagnostic measures. The other two studies had similar conclusions, although they were not exclusive for colorectal surgery [14,35]. A worse clinical condition and abdominal pain not localized to the wound are two of four modified Dutch leakage (DULK) score criteria, scoring 1 point each. Using a cut-off value of 1 point produced an overall SS and NPV of 97.0% and 99.5%, respectively[10]. We should bring the clinical

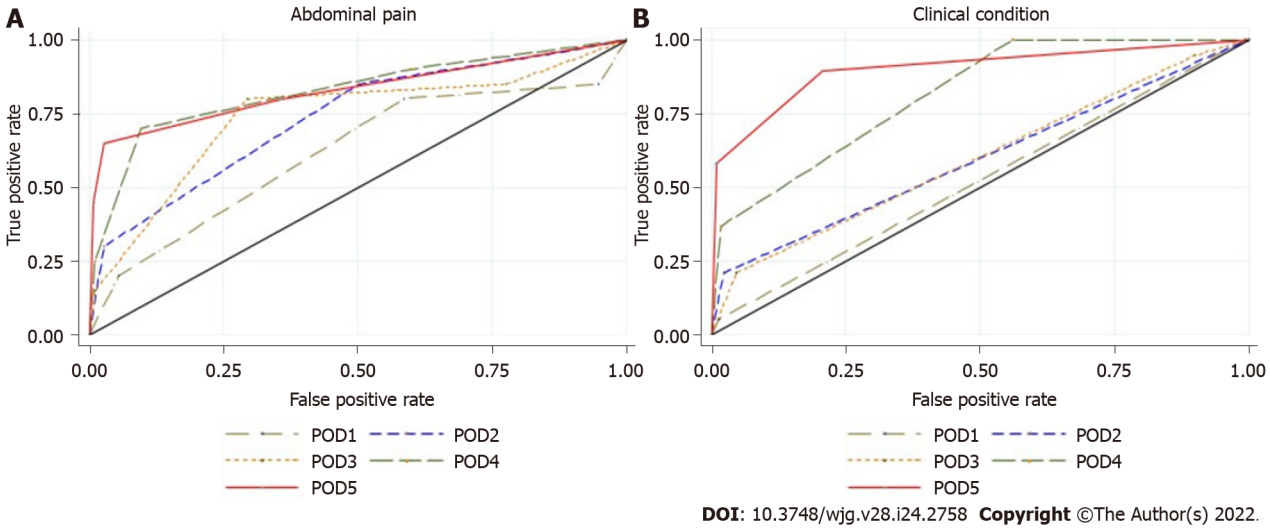

DOI: 10.3748/wjg.v28.i24.2758

Figure 3 Area under the receiver operating characteristic curve of colorectal anastomotic leakage for clinical criteria. A: Abdominal pain from postoperative day 1 to postoperative day 5; B: Clinical condition from postoperative day 1 to postoperative day 5. POD: Postoperative day.

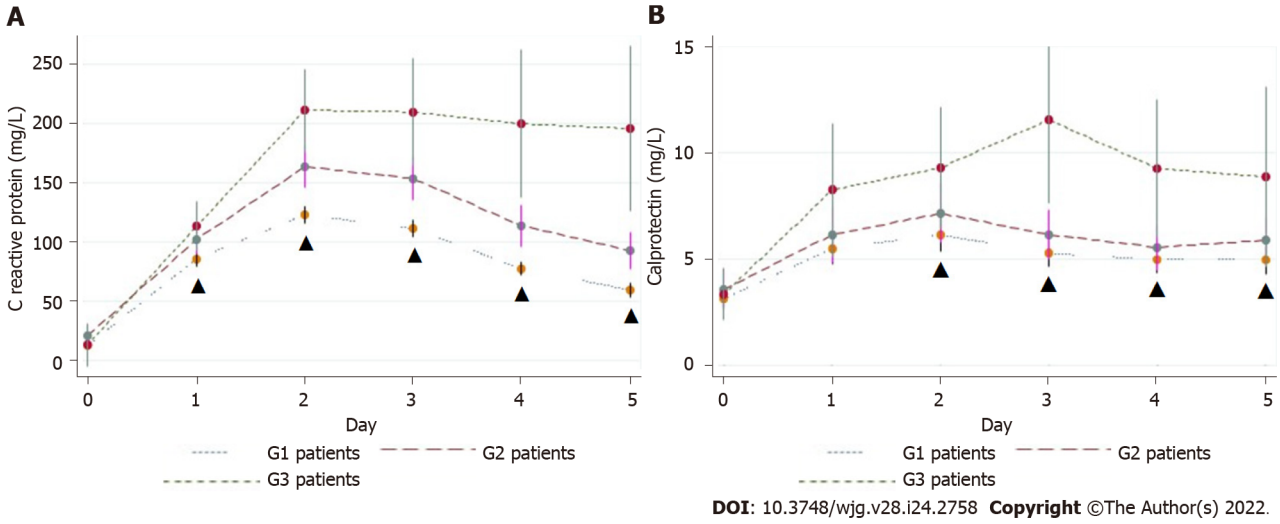

DOI: 10.3748/wjg.v28.i24.2758

Figure 4 C-reactive protein (A) and calprotectin (B) levels. Values are the mean ± SE. G1: No complications; G2: Complications not related to colorectal anastomotic leakage; G3: CAL; ▲ : *P* statistically significant ($P < 0.05$).

method to the forefront, being aware of the clinical signs of CAL. They are very helpful for the early diagnosis, as "red flags" for further investigation.

In our study, particularly on POD4 and POD5, WBC and ECC showed a distinct tendency in patients with and without CAL, with a high NPV (from 94%-98%) but low accuracy (AUROC from 0.54 to 0.70). In G3 patients, WBC plateaued after the acute inflammatory response, a phenomenon that was notably different from patients without CAL. In a large retrospective study, Warschkow *et al*[16] found that the WBC level contributed little to the early detection of septic complications, with a lower diagnostic accuracy than plasma CRP. In several other studies, researchers have estimated, from POD5 to POD7, an AUROC and SS ranging from 0.63 to 0.82 and from 58% to 74%, respectively[15,16,20,24,35].

Some researchers have proposed eosinopenia as a biomarker in this scenario. They concluded that it might help to identify several sepsis-related conditions, distinguished from other causes of systemic inflammatory response syndrome. It seems to be an interesting biomarker because of its widespread availability and low cost[36]. Shaaban *et al*[37] defined an optimum cut-off value of 50 cells/μL, which produced an SS, SP, and NPV of 81%, 65% and 80%, respectively. At hospital admission, ECC < 40 cells/μL is an independent prognostic factor for mortality[38,39]. Our study is original in assessing the usefulness of ECC for the early diagnosis of CAL. The mean ECC level showed a non-significant decline after POD4 in G3 patients, and a modest diagnostic accuracy (AUROC from 0.54 to 0.70) when compared with other biomarkers. Nevertheless, ECC could still be used in CAL diagnosis as a fast, simple, convenient, and inexpensive biomarker. It should be considered in the decision-making process

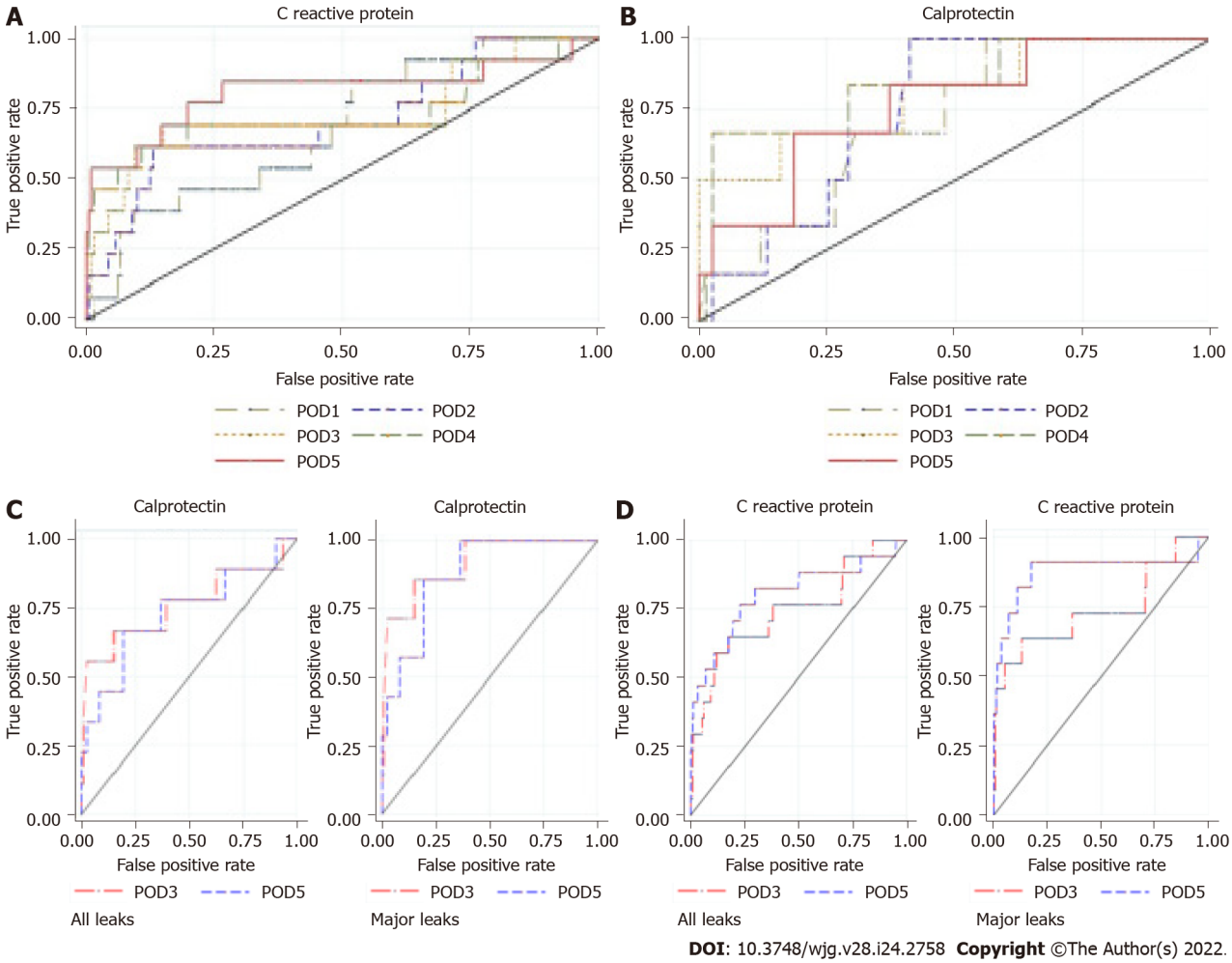

DOI: 10.3748/wjg.v28.i24.2758

Figure 5 Area under the receiver operating characteristic curve of colorectal anastomotic leakage. A: For C-reactive protein from postoperative day 1 to postoperative day 5; B: For calprotectin from postoperative day 1 to postoperative day 5; C: For calprotectin from postoperative day 3 to postoperative day 5; D: For C-reactive protein from postoperative day 3 to postoperative day 5. Left: All leaks; Right: Major leaks; POD: Postoperative day.

and future research[40].

The usefulness of CRP as a biomarker for early detection of CAL has been investigated by several groups[19,25,39,41,42]. In this study, the plasma CRP level exhibited a propensity to normalize from POD3 onwards in patients without CAL (G1 and G2). However, it remained steadily increased in G3 patients, with a markedly high mean value from POD1 to POD5. Yeung *et al*[43] performed the most comprehensive meta-analysis available in the literature, including nearly 7000 patients pooled from 23 studies. From POD1 to POD7, patients with CAL had a significantly higher mean CRP level compared with patients without CAL ($P < 0.001$)[43]. In this study, CRP was the best predictor for CAL on POD4 and POD5, with a maximum AUROC of 0.81 (cut-off value of 96.8 mg/L and an NPV of 98%) on POD5. Similar results have been published by other authors. Ortega-Deballon *et al*[26] estimated on POD4 an AUROC of 0.72 with a cut-off of 125 mg/L, yielding an SS and NPV of 81.8% and 95.8%, respectively. Garcia-Granero *et al*[25] reported that CRP level showed a good predictive ability for major CAL on POD5, with an AUROC of 0.85 (cut-off value of 135 mg/L and an NPV of 98%). In the Italian ColoRectal Anastomotic Leakage (iCral) multicentric prospective observational study, the CRP level was a good positive and excellent negative predictor of CAL, with an AUROC of 0.81 on POD6 (cut-off value of 81.5 mg/L), and an SS and NPV of 80.9% and 97.7%, respectively[41]. In the meta-analysis by Yeung *et al*[43], AUROC analysis established a threshold CRP level for CAL of 115 mg/L on POD5, with an SS and SP of 100%. All of these authors recommended CRP levels to predict CAL, and our group advocates a similar practice and suggests the use of this biomarker to expedite further investigation and treatment [25,26,41,43].

CLP, a sign of neutrophil activation, could be a promising early marker for excessive inflammatory response in major abdominal catastrophes, such as CAL. To date, only Reisinger *et al*[18] have studied the predictive value of CLP in CAL diagnosis. In G3 patients, the mean postoperative CLP level peaked on POD3 and was notably higher, persisting thereafter. On POD3, the AUROC (0.78) and SS (71%) were slightly higher than the CRP level, although they were lower than those obtained in the pioneering study by Reisinger *et al*[18] (0.92 and 86%, respectively). One possible explanation could be our compre-

hensive definition of CAL and the larger sample size. It remains unclear to what extent CLP level is an early predictor that is better than CRP for detecting CAL. As a neutrophil activation marker, CLP could be increased early after anastomotic failure, compared with CRP, which indicates a delayed systemic inflammatory response. Our study shows that CLP is worth evaluating for early diagnosis of CAL.

We demonstrated in the first 5 POD, the mean PCT values were marginally higher in G3 patients but with lower accuracy, SS, and SP than CRP and CLP levels. However, it had a high NPV (> 95%), making it an adequate and useful marker for early and safe discharge after colorectal surgery, considering the current enhanced recovery after surgery routine. In contrast to our study, Giaccaglia *et al*[17] estimated that on POD5, PCT had better accuracy than CRP (0.86 *vs* 0.81), as well as a high NPV (98.3%). A recent meta-analysis published by Su'a *et al*[44] determined a diagnostic accuracy of 0.88 on POD5 and an optimum cut-off value on POD3 and POD5 of 0.25 and 680 ng/mL, respectively. The NPV ranged from 95% to 100%. In agreement with these authors, we believe that PCT is a useful negative predictor for CAL; as a single test, however, it is worthless for CAL diagnosis.

We verified that, with the exception of plasma CRP on POD5 (AUROC > 0.80), each biomarker individually was a modest predictor of CAL[45]. The combination of two or more biomarkers has been considered in previous studies[17,18,41]. In this study, the combination of CRP and CLP values on POD3 increased diagnostic accuracy, shortening the mean CAL diagnosis by 5 d. This reduction would likely lead to reduced morbidity and mortality. Reisinger *et al*[18] confirmed a significant improvement in diagnostic accuracy (AUROC = 0.93) with the combination of CRP and CLP plasma levels on POD3, an SS of 100%, and an SP of 89.0%, decreasing the median time to diagnosis by 3 d. Furthermore, Giaccaglia *et al*[17] found that by adding PCT to CRP on POD5, the diagnostic accuracy markedly improved (AUROC = 0.90). Similarly, the iCral study demonstrated that the combination of CRP and PCT with a clinical score (DULK score) allowed the exclusion of CAL on POD2 (NPV = 99%)[41]. We believe that a user-friendly diagnostic tool, combining CLP and CRP levels by this mathematic model, would help the surgeon to diagnose CAL early. Consequently, this biomarkers' combination may be included in a standard postoperative surveillance program, as a warning tool for CAL. In the case of a "positive test", this protocol recommends abdominal and pelvic CT scan or early reoperation in case of imaging-dubious or -negative, to reduce the time to CAL detection and enable prompt management.

Strengths and limitations of the study

One strength of this study was its prospective design and independent data collection model, which minimized observer bias. Second, it was one of the largest monocentric sample size published to date. Based on the recent meta-analyses of Waterland *et al*[46] van Helsdingen *et al*[47], only two monocentric prospective studies have enrolled more than 400 patients. Furthermore, we analyzed five biomarkers, including plasma CLP, which was first studied by Reisinger *et al*[18]. Third, we chose a comprehensive definition of CAL, recently defined by van Helsdingen *et al*[29] to include all patients with CAL, minimizing selection bias. We did not exclude minor CAL from the cohort, which also affected the predictive effect of the analyzed biomarkers. In addition, to keep the biomarkers optimum cut-off values in AUROC analysis both standardized and reproducible, we adopted Liu's method. This method defines the optimum cut-off point as the point maximizing the product of SS and SP[48]. These reasons may explain some differences in biomarkers' diagnostic accuracy in this study. Fourth, we tried to adapt the study protocol to daily practice, making its enforcement easier in the future. Hence, we included all patients undergoing colorectal resection, even those with a diverting ostomy. In addition, clinicians were not blinded to the daily biomarkers' results and might use those data according to the study protocol. Finally, we proposed a predictive tool based on the combination of two biomarkers that improved CAL diagnostic accuracy. Adoption of this tool in daily practice might shorten the time to CAL diagnosis and management. Moreover, the data from this study provide information for the development of more complex mathematical predictive models, including machine learning methods.

This study had several limitations. First, the monocentric design may limit the external validity of the results. Second, our sample had some grade of heterogeneity, because the study population included benign and malignant disorders, elective and urgent procedures, and anastomosis within different levels of the colon and rectum. Third, we designed a phase I diagnostic study and estimated cut-off values for early CAL detection. However, we should change the direction of interpretation, running from the diagnostic test result toward the CAL diagnosis. To address this issue, we are performing a new multicentric prospective phase II diagnostic study, using the predictive tool and defined biomarkers cut-off values[49]. Fourth, plasma CLP measurement is expensive and these kits are not easily accessible in daily clinical practice. Finally, our study did not address the cost-effectiveness of biomarkers' measurement. It is crucial to estimate the economic burden of CAL, including the cost related to a delayed diagnosis, the high rate of false positives, and unjustified reoperations or frequent readmissions.

CONCLUSION

In conclusion, we found that clinical criteria have added value as a warning sign of CAL. On the other

hand, CRP and CLP levels are the best early predictors of CAL. Particularly relevant is the combination of CLP and CRP early during POD3, and its potential to markedly reduce the time to diagnosis of CAL. By reducing the time to CAL diagnosis, reduced morbidity and mortality are expected. Additional studies are needed to confirm the predictive ability of this model on early CAL detection and its utility in routine clinical care.

ARTICLE HIGHLIGHTS

Research background

Colorectal anastomotic leakage (CAL) is a major complication in abdominal surgery. Prompt diagnosis can reduce morbidity and mortality associated with this condition. Serum biomarkers have been proposed as predictors of CAL.

Research motivation

Biomarkers such as C-reactive protein (CRP) and white blood cell (WBC) count are frequently requested in the postoperative period of colorectal surgery. However, the usefulness of these and other biomarkers remains unclear.

Research objectives

To assess the role of CRP, WBC, eosinophil cell count, calprotectin (CLP), and procalcitonin in the first 5 postoperative days (PODs) after colorectal surgery, and thus, discuss in what order these biomarkers can be employed in clinical practice.

Research methods

From March 2017 to August 2019, we measured and analyzed five serum biomarkers daily in 396 patients who underwent colorectal surgery. The area under the receiver operating characteristic curve, specificity, sensitivity, positive predictive value (PPV), and negative predictive value (NPV) were used to estimate the best predictive diagnostic performance.

Research results

CRP had an NPV of 98% on POD5. The combination of CLP and CRP measurement presented a high diagnostic accuracy (AUCROC = 0.82) on POD3. We identified a reduction of 5.2 d to the diagnosis of CAL.

Research conclusions

The combination of CRP and CLP demonstrated good diagnostic accuracy. These tests can likely be used to reduce time to CAL detection.

Research perspectives

Further studies should test a warning index score built from selected predictive variables as biomarkers CRP and CLP.

FOOTNOTES

Author contributions: Rama NJM, Guarino MPS, and Lourenço Ó designed the study; Lages MCC, Castro R, Bento A, and Parente D coordinated the data collection process; Lourenço Ó and Silva CSG performed the data analyses; Rama NJM, Motta Lima PC and Guarino MPS prepared the manuscript; Rama NJM, Rocha A, Castro-Poças F, and Pimentel J revised the paper critically; All authors read and approved the final manuscript.

Supported by the Ministry of Health – Incentive Program for the Integration of Care and Valuation of Patients' Pathways in the National Health Service of Portugal.

Institutional review board statement: This study was conducted in accordance with the Declaration of Helsinki and was approved by the Local Ethical Committee of the Colorectal Referral Centre, after authorization obtained from the Portuguese Data Protection Authority. This study is registered with the number 9930/2016 and can be consulted at https://drive.google.com/file/d/1BiLxWlvcrqpX4KQrjW4F2codsOOywVF/view?usp=sharing.

Informed consent statement: Informed consent was obtained from all participants included in the study.

Conflict-of-interest statement: The authors have no conflicts of interest to declare.

Data sharing statement: For additional data, Dr. Nuno Rama can be contacted by e-mail at ramanuno@gmail.com.

STROBE statement: The authors have read the STROBE Statement – checklist of items, and the manuscript was prepared and revised according to the STROBE Statement – checklist of items.

Country/Territory of origin: Portugal

ORCID number: Nuno J G Rama 0000-0002-1572-2239; Marlene C C Lages 0000-0002-7389-6368; Maria Pedro S Guarino 0000-0001-6079-1105; Óscar Lourenço 0000-0002-3642-4919; Patrícia C Motta Lima 0000-0002-6427-8955; Diana Parente 0000-0003-0271-371X; Cândida S G Silva 0000-0002-7092-1169; Ricardo Castro 0000-0002-5110-0883; Ana Bento 0000-0002-3489-8774; Anabela Rocha 0000-0001-5000-5369; Fernando Castro-Pocas 0000-0002-2268-9107; João Pimentel 0000-0003-1908-8607.

S-Editor: Ma YJ
L-Editor: A
P-Editor: Ma YJ

REFERENCES

1 **Boccola MA**, Buettner PG, Rozen WM, Siu SK, Stevenson AR, Stitz R, Ho YH. Risk factors and outcomes for anastomotic leakage in colorectal surgery: a single-institution analysis of 1576 patients. *World J Surg* 2011; **35**: 186-195 [PMID: 20972678 DOI: 10.1007/s00268-010-0831-7]
2 **Trencheva K**, Morrissey KP, Wells M, Mancuso CA, Lee SW, Sonoda T, Michelassi F, Charlson ME, Milsom JW. Identifying important predictors for anastomotic leak after colon and rectal resection: prospective study on 616 patients. *Ann Surg* 2013; **257**: 108-113 [PMID: 22968068 DOI: 10.1097/SLA.0b013e318262a6cd]
3 **Pommergaard HC**, Gessler B, Burcharth J, Angenete E, Haglind E, Rosenberg J. Preoperative risk factors for anastomotic leakage after resection for colorectal cancer: a systematic review and meta-analysis. *Colorectal Dis* 2014; **16**: 662-671 [PMID: 24655784 DOI: 10.1111/codi.12618]
4 **McDermott FD**, Heeney A, Kelly ME, Steele RJ, Carlson GL, Winter DC. Systematic review of preoperative, intraoperative and postoperative risk factors for colorectal anastomotic leaks. *Br J Surg* 2015; **102**: 462-479 [PMID: 25703524 DOI: 10.1002/bjs.9697]
5 **Smith SR**, Pockney P, Holmes R, Doig F, Attia J, Holliday E, Carroll R, Draganic B. Biomarkers and anastomotic leakage in colorectal surgery: C-reactive protein trajectory is the gold standard. *ANZ J Surg* 2018; **88**: 440-444 [PMID: 28304142 DOI: 10.1111/ans.13937]
6 **Iancu C**, Mocan LC, Todea-Iancu D, Mocan T, Acalovschi I, Ionescu D, Zaharie FV, Osian G, Puia CI, Muntean V. Host-related predictive factors for anastomotic leakage following large bowel resections for colorectal cancer. *J Gastrointestin Liver Dis* 2008; **17**: 299-303 [PMID: 18836623]
7 **Cousin F**, Ortega-Deballon P, Bourredjem A, Doussot A, Giaccaglia V, Fournel I. Diagnostic Accuracy of Procalcitonin and C-reactive Protein for the Early Diagnosis of Intra-abdominal Infection After Elective Colorectal Surgery: A Meta-analysis. *Ann Surg* 2016; **264**: 252-256 [PMID: 27049766 DOI: 10.1097/SLA.0000000000001545]
8 **Watson AJ**, Krukowski ZH, Munro A. Salvage of large bowel anastomotic leaks. *Br J Surg* 1999; **86**: 499-500 [PMID: 10215823 DOI: 10.1046/j.1365-2168.1999.01096.x]
9 **Matthiessen P**, Henriksson M, Hallböök O, Grunditz E, Norén B, Arbman G. Increase of serum C-reactive protein is an early indicator of subsequent symptomatic anastomotic leakage after anterior resection. *Colorectal Dis* 2008; **10**: 75-80 [PMID: 17666099 DOI: 10.1111/j.1463-1318.2007.01300.x]
10 **den Dulk M**, Witvliet MJ, Kortram K, Neijenhuis PA, de Hingh IH, Engel AF, van de Velde CJ, de Brauw LM, Putter H, Brouwers MA, Steup WH. The DULK (Dutch leakage) and modified DULK score compared: actively seek the leak. *Colorectal Dis* 2013; **15**: e528-e533 [PMID: 24199233 DOI: 10.1111/codi.12379]
11 **Rojas-Machado SA**, Romero M, Arroyo A, Rojas-Machado A, López J, Calpena R. Anastomic leak in colorectal cancer surgery. Development of a diagnostic index (DIACOLE). *Int J Surg* 2016; **27**: 92-98 [PMID: 26827891 DOI: 10.1016/j.ijsu.2016.01.089]
12 **Doeksen A**, Tanis PJ, Vrouenraets BC, Lanschot van JJ, Tets van WF. Factors determining delay in relaparotomy for anastomotic leakage after colorectal resection. *World J Gastroenterol* 2007; **13**: 3721-3725 [PMID: 17659732 DOI: 10.3748/wjg.v13.i27.3721]
13 **Marres CCM**, van de Ven AWH, Leijssen LGJ, Verbeek PCM, Bemelman WA, Buskens CJ. Colorectal anastomotic leak: delay in reintervention after false-negative computed tomography scan is a reason for concern. *Tech Coloproctol* 2017; **21**: 709-714 [PMID: 28929306 DOI: 10.1007/s10151-017-1689-6]
14 **Regenbogen SE**, Mullard AJ, Peters N, Brooks S, Englesbe MJ, Campbell DA Jr, Hendren S. Hospital Analgesia Practices and Patient-reported Pain After Colorectal Resection. *Ann Surg* 2016; **264**: 1044-1050 [PMID: 26756749 DOI: 10.1097/sla.0000000000001541]
15 **Sutton CD**, Marshall LJ, Williams N, Berry DP, Thomas WM, Kelly MJ. Colo-rectal anastomotic leakage often

masquerades as a cardiac complication. *Colorectal Dis* 2004; **6**: 21-22 [PMID: 14692947 DOI: 10.1111/j.1463-1318.2004.00574.x]

16 **Warschkow R**, Tarantino I, Torzewski M, Näf F, Lange J, Steffen T. Diagnostic accuracy of C-reactive protein and white blood cell counts in the early detection of inflammatory complications after open resection of colorectal cancer: a retrospective study of 1,187 patients. *Int J Colorectal Dis* 2011; **26**: 1405-1413 [PMID: 21701807 DOI: 10.1007/s00384-011-1262-0]

17 **Giaccaglia V**, Salvi PF, Antonelli MS, Nigri G, Pirozzi F, Casagranda B, Giacca M, Corcione F, de Manzini N, Balducci G, Ramacciato G. Procalcitonin Reveals Early Dehiscence in Colorectal Surgery: The PREDICS Study. *Ann Surg* 2016; **263**: 967-972 [PMID: 26528879 DOI: 10.1097/SLA.0000000000001365]

18 **Reisinger KW**, Poeze M, Hulsewé KW, van Acker BA, van Bijnen AA, Hoofwijk AG, Stoot JH, Derikx JP. Accurate prediction of anastomotic leakage after colorectal surgery using plasma markers for intestinal damage and inflammation. *J Am Coll Surg* 2014; **219**: 744-751 [PMID: 25241234 DOI: 10.1016/j.jamcollsurg.2014.06.011]

19 **den Dulk M**, Noter SL, Hendriks ER, Brouwers MA, van der Vlies CH, Oostenbroek RJ, Menon AG, Steup WH, van de Velde CJ. Improved diagnosis and treatment of anastomotic leakage after colorectal surgery. *Eur J Surg Oncol* 2009; **35**: 420-426 [PMID: 18585889 DOI: 10.1016/j.ejso.2008.04.009]

20 **Welsch T**, Müller SA, Ulrich A, Kischlat A, Hinz U, Kienle P, Büchler MW, Schmidt J, Schmied BM. C-reactive protein as early predictor for infectious postoperative complications in rectal surgery. *Int J Colorectal Dis* 2007; **22**: 1499-1507 [PMID: 17639424 DOI: 10.1007/s00384-007-0354-3]

21 **Silvestre J**, Rebanda J, Lourenço C, Póvoa P. Diagnostic accuracy of C-reactive protein and procalcitonin in the early detection of infection after elective colorectal surgery - a pilot study. *BMC Infect Dis* 2014; **14**: 444 [PMID: 25132018 DOI: 10.1186/1471-2334-14-444]

22 **Kørner H**, Nielsen HJ, Søreide JA, Nedrebø BS, Søreide K, Knapp JC. Diagnostic accuracy of C-reactive protein for intraabdominal infections after colorectal resections. *J Gastrointest Surg* 2009; **13**: 1599-1606 [PMID: 19479312 DOI: 10.1007/s11605-009-0928-1]

23 **Facy O**, Paquette B, Orry D, Binquet C, Masson D, Bouvier A, Fournel I, Charles PE, Rat P, Ortega-Deballon P; IMACORS Study. Diagnostic Accuracy of Inflammatory Markers As Early Predictors of Infection After Elective Colorectal Surgery: Results From the IMACORS Study. *Ann Surg* 2016; **263**: 961-966 [PMID: 26135691 DOI: 10.1097/SLA.0000000000001303]

24 **Lagoutte N**, Facy O, Ravoire A, Chalumeau C, Jonval L, Rat P, Ortega-Deballon P. C-reactive protein and procalcitonin for the early detection of anastomotic leakage after elective colorectal surgery: pilot study in 100 patients. *J Visc Surg* 2012; **149**: e345-e349 [PMID: 23102916 DOI: 10.1016/j.jviscsurg.2012.09.003]

25 **Garcia-Granero A**, Frasson M, Flor-Lorente B, Blanco F, Puga R, Carratalá A, Garcia-Granero E. Procalcitonin and C-reactive protein as early predictors of anastomotic leak in colorectal surgery: a prospective observational study. *Dis Colon Rectum* 2013; **56**: 475-483 [PMID: 23478615 DOI: 10.1097/DCR.0b013e31826ce825]

26 **Ortega-Deballon P**, Radais F, Facy O, d'Athis P, Masson D, Charles PE, Cheynel N, Favre JP, Rat P. C-reactive protein is an early predictor of septic complications after elective colorectal surgery. *World J Surg* 2010; **34**: 808-814 [PMID: 20049435 DOI: 10.1007/s00268-009-0367-x]

27 **Cikot M**, Kones O, Gedikbası A, Kocatas A, Karabulut M, Temizgonul KB, Alis H. The marker C-reactive protein is helpful in monitoring the integrity of anastomosis: plasma calprotectin. *Am J Surg* 2016; **212**: 53-61 [PMID: 26606896 DOI: 10.1016/j.amjsurg.2015.06.018]

28 **Aadland E**, Fagerhol MK. Faecal calprotectin: a marker of inflammation throughout the intestinal tract. *Eur J Gastroenterol Hepatol* 2002; **14**: 823-825 [PMID: 12172400 DOI: 10.1097/00042737-200208000-00002]

29 **Rahbari NN**, Weitz J, Hohenberger W, Heald RJ, Moran B, Ulrich A, Holm T, Wong WD, Tiret E, Moriya Y, Laurberg S, den Dulk M, van de Velde C, Büchler MW. Definition and grading of anastomotic leakage following anterior resection of the rectum: a proposal by the International Study Group of Rectal Cancer. *Surgery* 2010; **147**: 339-351 [PMID: 20004450 DOI: 10.1016/j.surg.2009.10.012]

30 **Dindo D**, Demartines N, Clavien PA. Classification of surgical complications: a new proposal with evaluation in a cohort of 6336 patients and results of a survey. *Ann Surg* 2004; **240**: 205-213 [PMID: 15273542 DOI: 10.1097/01.sla.0000133083.54934.ae]

31 **Hand DJ**. Statistical Evaluation of Diagnostic Performance: Topics in ROC Analysis by Zou KH, Liu A, Bandos AI, Ohno-Machado L, Rockette HE. *Int Stat Rev* 2013; **81**: 335 [DOI: 10.1111/insr.12020_27]

32 **James G**, Witten D, Hastie T, Tibshira R. An introduction to statistical learning with applications in R. 1st ed. New York: Springer Science+Business Media, 2013

33 **Boström P**, Svensson J, Brorsson C, Rutegård M. Early postoperative pain as a marker of anastomotic leakage in colorectal cancer surgery. *Int J Colorectal Dis* 2021; **36**: 1955-1963 [PMID: 34272996 DOI: 10.1007/s00384-021-03984-w]

34 **van Boekel RLM**, Warlé MC, Nielen RGC, Vissers KCP, van der Sande R, Bronkhorst EM, Lerou JGC, Steegers MAH. Relationship Between Postoperative Pain and Overall 30-Day Complications in a Broad Surgical Population: An Observational Study. *Ann Surg* 2019; **269**: 856-865 [PMID: 29135493 DOI: 10.1097/SLA.0000000000002583]

35 **Garnacho-Montero J**, Huici-Moreno MJ, Gutiérrez-Pizarraya A, López I, Márquez-Vácaro JA, Macher H, Guerrero JM, Puppo-Moreno A. Prognostic and diagnostic value of eosinopenia, C-reactive protein, procalcitonin, and circulating cell-free DNA in critically ill patients admitted with suspicion of sepsis. *Crit Care* 2014; **18**: R116 [PMID: 24903083 DOI: 10.1186/cc13908]

36 **Shaaban H**, Daniel S, Sison R, Slim J, Perez G. Eosinopenia: Is it a good marker of sepsis in comparison to procalcitonin and C-reactive protein levels for patients admitted to a critical care unit in an urban hospital? *J Crit Care* 2010; **25**: 570-575 [PMID: 20435431 DOI: 10.1016/j.jcrc.2010.03.002]

37 **Abidi K**, Belayachi J, Derras Y, Khayari ME, Dendane T, Madani N, Khoudri I, Zeggwagh AA, Abouqal R. Eosinopenia, an early marker of increased mortality in critically ill medical patients. *Intensive Care Med* 2011; **37**: 1136-1142 [PMID: 21369810 DOI: 10.1007/s00134-011-2170-z]

38 **Terradas R**, Grau S, Blanch J, Riu M, Saballs P, Castells X, Horcajada JP, Knobel H. Eosinophil count and neutrophil-

lymphocyte count ratio as prognostic markers in patients with bacteremia: a retrospective cohort study. *PLoS One* 2012; **7**: e42860 [PMID: 22912753 DOI: 10.1371/journal.pone.0042860]

39 **Lin Y**, Rong J, Zhang Z. Silent existence of eosinopenia in sepsis: a systematic review and meta-analysis. *BMC Infect Dis* 2021; **21**: 471 [PMID: 34030641 DOI: 10.1186/s12879-021-06150-3]

40 **Italian ColoRectal Anastomotic Leakage (iCral) Study Group**. Anastomotic leakage after elective colorectal surgery: a prospective multicentre observational study on use of the Dutch leakage score, serum procalcitonin and serum C-reactive protein for diagnosis. *BJS Open* 2020; **4**: 499-507 [PMID: 32134216 DOI: 10.1002/bjs5.50269]

41 **Paliogiannis P**, Deidda S, Maslyankov S, Paycheva T, Farag A, Mashhour A, Misiakos E, Papakonstantinou D, Mik M, Losinska J, Scognamillo F, Sanna F, Feo CF, Porcu A, Xidas A, Zinellu A, Restivo A, Zorcolo L. C reactive protein to albumin ratio (CAR) as predictor of anastomotic leakage in colorectal surgery. *Surg Oncol* 2021; **38**: 101621 [PMID: 34126521 DOI: 10.1016/j.suronc.2021.101621]

42 **Yeung DE**, Peterknecht E, Hajibandeh S, Torrance AW. C-reactive protein can predict anastomotic leak in colorectal surgery: a systematic review and meta-analysis. *Int J Colorectal Dis* 2021; **36**: 1147-1162 [PMID: 33555423 DOI: 10.1007/s00384-021-03854-5]

43 **Su'a B**, Tutone S, MacFater W, Barazanchi A, Xia W, Zeng I, Hill AG. Diagnostic accuracy of procalcitonin for the early diagnosis of anastomotic leakage after colorectal surgery: a meta-analysis. *ANZ J Surg* 2020; **90**: 675-680 [PMID: 31230412 DOI: 10.1111/ans.15291]

44 **Mandrekar JN**. Receiver operating characteristic curve in diagnostic test assessment. *J Thorac Oncol* 2010; **5**: 1315-1316 [PMID: 20736804 DOI: 10.1097/JTO.0b013e3181ec173d]

45 **Mik M**, Dziki L, Berut M, Trzcinski R, Dziki A. Neutrophil to Lymphocyte Ratio and C-Reactive Protein as Two Predictive Tools of Anastomotic Leak in Colorectal Cancer Open Surgery. *Dig Surg* 2018; **35**: 77-84 [PMID: 28132052 DOI: 10.1159/000456081]

46 **Waterland P**, Ng J, Jones A, Broadley G, Nicol D, Patel H, Pandey S. Using CRP to predict anastomotic leakage after open and laparoscopic colorectal surgery: is there a difference? *Int J Colorectal Dis* 2016; **31**: 861-868 [PMID: 26951183 DOI: 10.1007/s00384-016-2547-0]

47 **van Helsdingen CP**, Jongen AC, de Jonge WJ, Bouvy ND, Derikx JP. Consensus on the definition of colorectal anastomotic leakage: A modified Delphi study. *World J Gastroenterol* 2020; **26**: 3293-3303 [PMID: 32684743 DOI: 10.3748/wjg.v26.i23.3293]

48 **Liu X**. Classification accuracy and cut point selection. *Stat Med* 2012; **31**: 2676-2686 [PMID: 22307964 DOI: 10.1002/sim.4509]

49 **Sackett DL**, Haynes RB. The architecture of diagnostic research. *BMJ* 2002; **324**: 539-541 [PMID: 11872558 DOI: 10.1136/bmj.324.7336.539]

World Journal of Gastroenterology

Submit a Manuscript: https://www.f6publishing.com

World J Gastroenterol 2022 June 28; 28(24): 2775-2777

DOI: 10.3748/wjg.v28.i24.2775

ISSN 1007-9327 (print) ISSN 2219-2840 (online)

LETTER TO THE EDITOR

Is long-term follow-up without surgical treatment a valid option for hepatic alveolar echinococcosis?

Yusufukadier Maimaitinijiati, Yuan Meng, Xiong Chen

Specialty type: Gastroenterology and hepatology

Provenance and peer review: Invited article; Externally peer reviewed.

Peer-review model: Single blind

Peer-review report's scientific quality classification

Grade A (Excellent): 0
Grade B (Very good): B
Grade C (Good): C
Grade D (Fair): 0
Grade E (Poor): 0

P-Reviewer: Aseni P, Italy; Augustin G, Croatia

Received: February 24, 2022
Peer-review started: February 24, 2022
First decision: April 5, 2022
Revised: April 13, 2022
Accepted: June 3, 2022
Article in press: June 3, 2022
Published online: June 28, 2022

Yusufukadier Maimaitinijiati, Yuan Meng, Xiong Chen, Department of Hepatobiliary Surgery, People's Hospital of Xinjiang Uyghur Autonomous Region, Urumqi 830001, Xinjiang Uyghur Autonomous Region, China

Yusufukadier Maimaitinijiati, School of Clinical Medicine, Medical College of Tsinghua University, Beijing 100084, China

Corresponding author: Xiong Chen, MD, Chief Doctor, Professor, Department of Hepatobiliary Surgery, People's Hospital of Xinjiang Uyghur Autonomous Region, No. 91 Tianchi Road, Tianshan District, Urumqi 830011, Xinjiang Uyghur Autonomous Region, China. 1512237458@qq.com

Abstract

We read the article titled, "Long-term follow-up of liver alveolar echinococcosis using echinococcosis multilocularis ultrasound classification," by Schuhbaur J with great interest. However, we found some worthwhile issues that we believe should be discussed with the authors, and have provided our comments in this letter. It would be valuable if the authors could provide further information about the clinical stages, follow-up time, and clinical outcomes of the patients.

Key Words: Alveolar echinococcosis; Albendazole; Surgical treatment; Ultrasound; Follow-up

Core Tip: Although many experts suggest that radical surgery combined with albendazole treatment is the optimal option for alveolar echinococcosis patients, no clear consensus has been reached on whether long-term treatment using albendazole alone without any surgical intervention can cure or control the disease. Therefore, some professional issues need to be clarified by discussion with peers, in order to benefit as many patients as possible.

Citation: Maimaitinijiati Y, Meng Y, Chen X. Is long-term follow-up without surgical treatment a valid option for hepatic alveolar echinococcosis? *World J Gastroenterol* 2022; 28(24): 2775-2777
URL: https://www.wjgnet.com/1007-9327/full/v28/i24/2775.htm
DOI: https://dx.doi.org/10.3748/wjg.v28.i24.2775

TO THE EDITOR

We read the article titled, "Long-term follow-up of liver alveolar echinococcosis using echinococcosis multilocularis ultrasound classification," by Schuhbaur *et al*[1] with great interest. In this significant study, the authors observed changes in sonomorphology during the follow-up of hepatic lesions using a sonomorphologic classification scheme. However, after reading the article carefully, we found some worthwhile issues that we would like to discuss with the authors.

Alveolar echinococcosis (AE) is an infectious zoonotic parasitic disease, which has been a major public health problem in its epidemic area[2]. In the large majority of cases, the liver is the first organ to be infested by the larvae. Hepatic AE often invades the surrounding vessels and adjacent organs in its advanced stages. The mortality rate within 10 years after diagnosis is more than 90% if the lesion is inadequately or not treated[3]. According to the World Health Organization Informal Working Group on Echinococcosis criteria[4], radical surgery combined with albendazole treatment is the optimal option for AE patients. In this article, the authors included 59 patients from Germany's national echinococcosis database, who were "considered" to have hepatic AE, and long-term follow-up using ultrasound was performed. However, they did not mention the clinical stages, specific follow-up time, and clinical prognosis of these patients. Hepatic AE is known as "parasitic cancer," due to its tumor-like characteristics with infiltration of vessels or biliary structures and distant metastasis. To date, no clear consensus has been reached on whether long-term treatment using albendazole alone without any surgical intervention can cure or control the disease. A 5-year analysis of two distinct cohorts in Bern, Switzerland and Besancon, France demonstrated that conservative treatment was less effective than surgical therapy[5]; however, longer follow-up results have not been available. Currently, "watch and wait" is not recommended unless complete inactivity of the AE lesion can be confirmed, in order to avoid delayed treatment resulting in adverse outcomes[6].

The authors' team proposed an ultrasonographic classification scheme for hepatic AE in 2015[7], which was used to follow 59 patients. However, we noted that the authors stated that all but 1 patient received antiparasitic drugs, but they also claimed that more than half of the patients (55.9%) were defined as "probable" hepatic AE. In such a case, the use of albendazole and other drugs with hepatotoxicity may cause unnecessary harm to patients. According to a recent study with long-term observation of 117 AE patients, about 44.4% experienced adverse reactions when taking albendazole, and severe liver toxicity occurred in 7.7% patients[8]. We believe that the authors should have provided a more detailed explanation about whether the use of albendazole is indeed necessary for these patients. The high rate of inoperable disease at diagnosis underscores the need for an early, definitive diagnosis. However, in cases that cannot be confirmed by conventional examination, supplementary tests such as serology and positron emission tomography (PET)/computed tomography (CT) may be useful.

Bresson-Hadni *et al*[9] suggested that "surgical resection, if feasible, is the gold standard for treatment." We also believe that early radical resection of the lesion should be considered in patients with hepatic AE, unless it is defined as unresectable. Based on the clinical guidelines and previous reports, the objectives for the treatment of hepatic AE should include the following: Completely removing the parasitic lesion, combined with 2 years of albendazole treatment after surgery; if this is not possible, reducing the proliferating potential of echinococcosis multilocularis by continuous administration of albendazole; and lesions that are massively calcified and/or negative by CT or PET may benefit from a "watch-and-wait" approach.

In summary, we admire the efforts of the authors in using ultrasound to assess sonomorphology changes over time in hepatic AE lesions. Nevertheless, it would be valuable if the authors could provide further information about the clinical stages, follow-up time, and clinical outcomes of the patients.

FOOTNOTES

Author contributions: Maimaitinijiati Y performed the research and wrote the letter; Meng Y and Chen X revised the letter.

Conflict-of-interest statement: All authors have no conflicts of interest to declare.

Country/Territory of origin: China

ORCID number: Yusufukadier Maimaitinijiati 0000-0003-2069-9202; Yuan Meng 0000-0002-2028-1175; Xiong Chen 0000-0002-2352-219X.

S-Editor: Liu X
L-Editor: A
P-Editor: Wang LL

REFERENCES

1 **Schuhbaur J**, Schweizer M, Philipp J, Schmidberger J, Schlingeloff P, Kratzer W. Long-term follow-up of liver alveolar echinococcosis using echinococcosis multilocularis ultrasound classification. *World J Gastroenterol* 2021; **27**: 6939-6950 [PMID: 34790016 DOI: 10.3748/wjg.v27.i40.6939]
2 **Torgerson PR**, Keller K, Magnotta M, Ragland N. The global burden of alveolar echinococcosis. *PLoS Negl Trop Dis* 2010; **4**: e722 [PMID: 20582310 DOI: 10.1371/journal.pntd.0000722]
3 **Vuitton DA**, Bresson-Hadni S. Alveolar echinococcosis: evaluation of therapeutic strategies. *Expert Opin Orphan D* 2014; **2**: 67-86 [DOI: 10.1517/21678707.2014.870033]
4 **Brunetti E**, Kern P, Vuitton DA; Writing Panel for the WHO-IWGE. Expert consensus for the diagnosis and treatment of cystic and alveolar echinococcosis in humans. *Acta Trop* 2010; **114**: 1-16 [PMID: 19931502 DOI: 10.1016/j.actatropica.2009.11.001]
5 **Beldi G**, Vuitton D, Lachenmayer A, Heyd B, Dufour JF, Richou C, Candinas D, Bresson-Hadni S. Is *ex vivo* liver resection and autotransplantation a valid alternative treatment for end-stage hepatic alveolar echinococcosis in Europe? *J Hepatol* 2019; **70**: 1030-1031 [PMID: 30718093 DOI: 10.1016/j.jhep.2018.12.011]
6 **Wen H**, Vuitton L, Tuxun T, Li J, Vuitton DA, Zhang W, McManus DP. Echinococcosis: Advances in the 21st Century. *Clin Microbiol Rev* 2019; **32** [PMID: 30760475 DOI: 10.1128/CMR.00075-18]
7 **Kratzer W**, Gruener B, Kaltenbach TE, Ansari-Bitzenberger S, Kern P, Fuchs M, Mason RA, Barth TF, Haenle MM, Hillenbrand A, Oeztuerk S, Graeter T. Proposal of an ultrasonographic classification for hepatic alveolar echinococcosis: Echinococcosis multilocularis Ulm classification-ultrasound. *World J Gastroenterol* 2015; **21**: 12392-12402 [PMID: 26604646 DOI: 10.3748/wjg.v21.i43.12392]
8 **Zavoikin VD**, Zelya OP, Tumolskaya NI. Clinical tolerance and efficacy of anti-parasitic treatment with albendazole in patients with alveolar echinococcosis: long-term follow-up observation in 117 patients. *Parasitol Res* 2021; **120**: 3603-3610 [PMID: 34432154 DOI: 10.1007/s00436-021-07297-3]
9 **Bresson-Hadni S**, Spahr L, Chappuis F. Hepatic Alveolar Echinococcosis. *Semin Liver Dis* 2021; **41**: 393-408 [PMID: 34161992 DOI: 10.1055/s-0041-1730925]

World Journal of Gastroenterology

Submit a Manuscript: https://www.f6publishing.com

World J Gastroenterol 2022 June 28; 28(24): 2778-2781

DOI: 10.3748/wjg.v28.i24.2778

ISSN 1007-9327 (print) ISSN 2219-2840 (online)

LETTER TO THE EDITOR

Using of artificial intelligence: Current and future applications in colorectal cancer screening

Georgios Zacharakis, Abdulaziz Almasoud

Specialty type: Gastroenterology and hepatology

Provenance and peer review: Unsolicited article; Externally peer reviewed.

Peer-review model: Single blind

Peer-review report's scientific quality classification

Grade A (Excellent): 0
Grade B (Very good): B, B
Grade C (Good): 0
Grade D (Fair): 0
Grade E (Poor): 0

P-Reviewer: Ozair A, India; Taheri S, Iran

Received: March 23, 2022
Peer-review started: March 23, 2022
First decision: April 25, 2022
Revised: April 26, 2022
Accepted: June 13, 2022
Article in press: June 13, 2022
Published online: June 28, 2022

Georgios Zacharakis, Division of Gastroenterology, Department of Internal Medicine, College of Medicine, Prince Sattam bin Abdulaziz University Hospital, Al Kharj 16277, Saudi Arabia

Abdulaziz Almasoud, Department of Gastroenterology and Hepatology, Prince Sultan Military Medical City, Riyadh 12233, Saudi Arabia

Corresponding author: Georgios Zacharakis, BSc, MSc, PhD, Professor, Division of Gastroenterology, Department of Internal Medicine, College of Medicine, Prince Sattam bin Abdulaziz University Hospital, Arrayan, Al Kharj 16277, Saudi Arabia.
g.zacharakis@psau.edu.sa

Abstract

Significant developments in colorectal cancer screening are underway and include new screening guidelines that incorporate considerations for patients aged 45 years, with unique features and new techniques at the forefront of screening. One of these new techniques is artificial intelligence which can increase adenoma detection rate and reduce the prevalence of colonic neoplasia.

Key Words: Basic concepts; Assessment of artificial intelligence in endoscopy; Current applications; Ethics; Safety challenge

Core Tip: Artificial intelligence (AI) is an integral part of endoscopy and health care in colorectal cancer screening because it has been shown to increase adenoma detection rates and reduce the prevalence of colonic neoplasia. It will soon provide an "optical biopsy" of polyps, assisting advanced therapeutic endoscopy-resection and 'discard– no pathology present. 'Innovations in AI have changed and improved the lives of gastroenterologists by examining quality monitoring *via* a single integrated system. The only boundaries of AI are clinical research trials and reimbursement.

Citation: Zacharakis G, Almasoud A. Using of artificial intelligence: Current and future applications in colorectal cancer screening. *World J Gastroenterol* 2022; 28(24): 2778-2781
URL: https://www.wjgnet.com/1007-9327/full/v28/i24/2778.htm
DOI: https://dx.doi.org/10.3748/wjg.v28.i24.2778

TO THE EDITOR

Artificial intelligence can increase adenoma detection rate in randomized control trials

Artificial intelligence (AI) has been shown to improve the adenoma detection rate (ADR) in colorectal cancer screening. It has been evaluated in multiple randomized controlled trials, showing that the withdrawal time does not vary at any polyp size, location, or morphology[1]. It also improves detection in serrated lesions; however, its usefulness is not clear for advanced adenomas, given that data are available from only three studies. A potential weakness of these studies is that they are largely confined to China and Italy. While the ADRs in China are low, ranging from 17% to 28%, in Italy, Repici *et al*[2] reported a rate of 40% to 55%. Studies conducted in the United States will be forthcoming.

AI in gastroenterology: Potential weaknesses

In this issue of the *World Journal of Gastroenterology*, a review article by Kröner *et al*[3] is entitled "Artificial intelligence in gastroenterology: a state-of-the-art review discussing the findings and a broad spectrum of clinical applications." The authors reviewed the literature highlighting the use of AI in current and future applications, especially in the detection of lesions and identification of pre-malignant or malignant lesions. However, we would like to mention that colonic disease detection of lesions using techniques such as polyp identification and classification are limited in number; these are not available in all AI systems, and clinical trial data from the USA are particularly limited[4]. Pentax Medical, Medronic, and EndoBrain provide only colonic polyp detection, and they lack the ability to classify the features of the CAD EYE system (Fujifilm) used in Europe and Japan[4]. Although the authors outlined the study limitations because of the lack of creating "universal datasets" and the lack of validating external in clinical settings and advise on future directions for research in this field, the important boundaries of AI are around clinical research trials, assessing AI in daily clinical practice, and around reimbursement and other ethical issues and safety challenges not highlighted here[3].

We would like to mention recent studies related to these important boundaries of AI use. It is expected that AI will compensate for human errors and the limits of human capabilities in performing real-time diagnostics of colonic lesions by providing accuracy, consistency, and greater diagnostic speed. However, Byrne *et al*[5] showed that 15% of polyps can not be classified. Therefore, further clinical trials are required to assess these benefits[5]. Whether endoscopic procedures become more efficient and of a higher quality when assisted by AI is yet to be proven. However, this new technology can mimic human behavior, identify colonic lesion precursors of colorectal cancer in at-risk patients[6], and can support medical decision-making[6].

Current endoscopy practices include the real-time administration of AI with computer vision to identify and delineate colonic lesions. This was achieved using an algorithm to diagnose and classify defined lesions. By applying machine learning (ML), the algorithm was trained using a large dataset of predefined polyp-containing video frames. These images include several key characteristics such as virtual chromoendoscopy, surface pit pattern morphology, microvascular pattern, high-magnification, and endocytoscopic appearance.

However, the promising applications of AI-assisted endoscopy raise several issues. Validation and quality control, video and image limitations, and annotation burden are primary areas of concern. Additionally, the data gathered has inherent biases due to a disproportionate representation of those with certain ethnicities, geographic and cultural inequities, and small segments of the population. Even if represented proportionately, inaccuracies can result in harmful consequences. Other contributors to bias included technical differences in colonoscopy techniques, bowel preparation, and colonoscopy equipment. The algorithm is as effective as the database.

Other issues with AI/ML are ethical and can be resolved by the careful and thorough regulation of data ownership and security. Data ownership could involve the patient, doctor, and/or the healthcare system, and the involvement of the Health Insurance Portability and Accountability Act, General Data Protection Regulation, industry, and science must be addressed. Finally, the endoscopist is responsible for the patient, not the computer.

The use of AI to demonstrate and characterize colonic lesions based on real-time signalling profiles is feasible. Video camera movement and tissue pathology captures a pair of frames, identifies recognized landmarks, and matches them by computing relative frames. Tissue classification was performed for all lesion types in real-time[7]. Its accuracy is evaluated by comparing it with the dual judgments of humans; however, few health professionals and patients wish to submit tissues for histological analyses [8].

Computer-assisted endoscopy has many clinical applications, including safety alerts, no-go zones, difficult notifications, staff notifications, and auto reports. Furthermore, AI supports decision-making by endoscopists, improves advanced therapeutic endoscopy and workflow, increases safety, reduces the need for manpower, and minimizes the need for humans to perform autonomous functions. Its limitations include physician resistance, limited video availability, data ownership, regulations, liability, privacy, lack of reimbursement, and cultural perceptions.

Currently, the fees for AI services are not standardized; however, there is an implementation cost. Given that better polyp detection results in more surveillance examinations, quality-based reimbursements could result in increased compensation. On the other hand, polyp diagnosis assisted by

AI has been shown to result in cost savings for the patient, particularly when the resultant strategy is "diagnose and leave without pathology"[9]. Overall, AI did not change the withdrawal timing and reduced the time required for endoscopic procedures. However, the cost and burden of these procedures remain unproven.

Real world testing needed

Evaluation of AI in healthcare requires real-world testing, including a minimal amount of randomized control trial data and a concentration of early stage research statistics such as ex vivo data, still images, and retrospective videos. Images should be carefully selected, and study designs should meet published standards such as preservation and incorporation of valuable endoscopic innovations, resect and discard criteria, and medical device approval by the US Food and Drug Administration. Furthermore, technical performance studies such as ML accuracy, system output accuracy, and usability, in addition to workflow studies such as effectiveness, efficiency, satisfaction, ease of use, learning ability, and utilization should be conducted. Additionally, health impact studies evaluating decision impact, patient outcomes, process outcomes, cost-effectiveness, care variability, and population impact should be conducted. Therefore, examination quality metrics are necessary, such as colonoscopy quality assessment *via* AI[10].

At this time, algorithms meet the preservation and incorporation of valuable endoscopic innovation criteria; however, multi-center trials have not been started. Experience is gained primarily from single-center studies conducted by expert endoscopists. Additionally, randomized controlled trials have not been performed, and magnifying scope technology is not available in some countries such as the USA[11]. Once these requirements are met, AI can become widely used in the daily practice of endoscopy, providing examination quality, polyp detection, polyp classification, and automatic reports. There are still a lot of unanswered questions and issues to be furthered discussed. However, we believe that the AI assisted colonoscopy, all in one integrated system, quality metrics of the colonoscopy exam, detection and classification of colonic lesions will play a key role in daily endoscopy clinical settings after 4-5 years.

FOOTNOTES

Author contributions: Zacharakis G and Almasoud A designed and performed the research and analyzed the data; Zacharakis G wrote the letter; Almasoud A revised the letter.

Conflict-of-interest statement: All authors declare no competing interests.

Country/Territory of origin: Saudi Arabia

ORCID number: Georgios Zacharakis 0000-0002-2859-9188; Abdulaziz Almasoud 0000-0003-2731-4395.

Corresponding Author's Membership in Professional Societies: SCFHS, 15RM0044572; Athens Medical Association, No. 055597.

S-Editor: Wang LL
L-Editor: A
P-Editor: Wang LL

REFERENCES

1 **Hassan C**, Spadaccini M, Iannone A, Maselli R, Jovani M, Chandrasekar VT, Antonelli G, Yu H, Areia M, Dinis-Ribeiro M, Bhandari P, Sharma P, Rex DK, Rösch T, Wallace M, Repici A. Performance of artificial intelligence in colonoscopy for adenoma and polyp detection: a systematic review and meta-analysis. *Gastrointest Endosc* 2021; **93**: 77-85.e6 [PMID: 32598963 DOI: 10.1016/j.gie.2020.06.059]

2 **Glissen Brown JR**, Mansour NM, Wang P, Chuchuca MA, Minchenberg SB, Chandnani M, Liu L, Gross SA, Sengupta N, Berzin TM. Deep Learning Computer-aided Polyp Detection Reduces Adenoma Miss Rate: A United States Multi-center Randomized Tandem Colonoscopy Study (CADeT-CS Trial). *Clin Gastroenterol Hepatol* 2021 [DOI: 10.1016/j.cgh.2021.09.009]

3 **Kröner PT**, Engels MM, Glicksberg BS, Johnson KW, Mzaik O, van Hooft JE, Wallace MB, El-Serag HB, Krittanawong C. Artificial intelligence in gastroenterology: A state-of-the-art review. *World J Gastroenterol* 2021; **27**: 6794-6824 [PMID:

34790008 DOI: 10.3748/wjg.v27.i40.6794]
4 **Mori Y**, Neumann H, Misawa M, Kudo SE, Bretthauer M. Artificial intelligence in colonoscopy - Now on the market. What's next? *J Gastroenterol Hepatol* 2021; **36**: 7-11 [PMID: 33179322 DOI: 10.1111/jgh.15339]
5 **Byrne MF**, Chapados N, Soudan F, Oertel C, Linares Pérez M, Kelly R, Iqbal N, Chandelier F, Rex DK. Real-time differentiation of adenomatous and hyperplastic diminutive colorectal polyps during analysis of unaltered videos of standard colonoscopy using a deep learning model. *Gut* 2019; **68**: 94-100 [PMID: 29066576 DOI: 10.1136/gutjnl-2017-314547]
6 **El Hajjar A**, Rey JF. Artificial intelligence in gastrointestinal endoscopy: general overview. *Chin Med J (Engl)* 2020; **133**: 326-334 [PMID: 31929362 DOI: 10.1097/CM9.0000000000000623]
7 **Marques KF**, Marques AF, Lopes MA, Beraldo RF, Lima TB, Sassaki LY. Artificial intelligence in colorectal cancer screening in patients with inflammatory bowel disease. *Artif Intell Gastrointest Endosc* 2022; **3**: 1-8 [DOI: 10.37126/aige.v3.i1.1]
8 **Kudo SE**, Mori Y, Misawa M, Takeda K, Kudo T, Itoh H, Oda M, Mori K. Artificial intelligence and colonoscopy: Current status and future perspectives. *Dig Endosc* 2019; **31**: 363-371 [PMID: 30624835 DOI: 10.1111/den.13340]
9 **Glover B**, Teare J, Patel N. The Status of Advanced Imaging Techniques for Optical Biopsy of Colonic Polyps. *Clin Transl Gastroenterol* 2020; **11**: e00130 [PMID: 32352708 DOI: 10.14309/ctg.0000000000000130]
10 **Mori Y**, Kudo SE, East JE, Rastogi A, Bretthauer M, Misawa M, Sekiguchi M, Matsuda T, Saito Y, Ikematsu H, Hotta K, Ohtsuka K, Kudo T, Mori K. Cost savings in colonoscopy with artificial intelligence-aided polyp diagnosis: an add-on analysis of a clinical trial (with video). *Gastrointest Endosc* 2020; **92**: 905-911.e1 [PMID: 32240683 DOI: 10.1016/j.gie.2020.03.3759]
11 **Thakkr S**, Carleton NM, Rao B, Syed A. Use of artificial intelligence-based analysis from live endosocpiesto optimize the quality of the colonoscopy exam in real time: proof of concept. *Gastroenterology* 2020; **158**: 1219-1221 [DOI: 10.1053/j.gastro.2019.12.035]

Published by **Baishideng Publishing Group Inc**
7041 Koll Center Parkway, Suite 160, Pleasanton, CA 94566, USA
Telephone: +1-925-3991568
E-mail: bpgoffice@wjgnet.com
Help Desk: https://www.f6publishing.com/helpdesk
https://www.wjgnet.com